LEABHARLANN CHOLÁISTE NA TRÍONÓIDE, BAILE ÁTHA CLIATH | TRINITY COLLEGE LIBRARY DUBLIN
Ollscoil Átha Cliath | The University of Dublin

Terms and Conditions of Use of Digitised Theses from Trinity College Library Dublin

Copyright statement

All material supplied by Trinity College Library is protected by copyright (under the Copyright and Related Rights Act, 2000 as amended) and other relevant Intellectual Property Rights. By accessing and using a Digitised Thesis from Trinity College Library you acknowledge that all Intellectual Property Rights in any Works supplied are the sole and exclusive property of the copyright and/or other IPR holder. Specific copyright holders may not be explicitly identified. Use of materials from other sources within a thesis should not be construed as a claim over them.

A non-exclusive, non-transferable licence is hereby granted to those using or reproducing, in whole or in part, the material for valid purposes, providing the copyright owners are acknowledged using the normal conventions. Where specific permission to use material is required, this is identified and such permission must be sought from the copyright holder or agency cited.

Liability statement

By using a Digitised Thesis, I accept that Trinity College Dublin bears no legal responsibility for the accuracy, legality or comprehensiveness of materials contained within the thesis, and that Trinity College Dublin accepts no liability for indirect, consequential, or incidental, damages or losses arising from use of the thesis for whatever reason. Information located in a thesis may be subject to specific use constraints, details of which may not be explicitly described. It is the responsibility of potential and actual users to be aware of such constraints and to abide by them. By making use of material from a digitised thesis, you accept these copyright and disclaimer provisions. Where it is brought to the attention of Trinity College Library that there may be a breach of copyright or other restraint, it is the policy to withdraw or take down access to a thesis while the issue is being resolved.

Access Agreement

By using a Digitised Thesis from Trinity College Library you are bound by the following Terms & Conditions. Please read them carefully.

I have read and I understand the following statement: All material supplied via a Digitised Thesis from Trinity College Library is protected by copyright and other intellectual property rights, and duplication or sale of all or part of any of a thesis is not permitted, except that material may be duplicated by you for your research use or for educational purposes in electronic or print form providing the copyright owners are acknowledged using the normal conventions. You must obtain permission for any other use. Electronic or print copies may not be offered, whether for sale or otherwise to anyone. This copy has been supplied on the understanding that it is copyright material and that no quotation from the thesis may be published without proper acknowledgement.

Intracellular and extracellular biomarkers predictive of response to anti-cancer treatments for breast and prostate cancer

A thesis submitted to the University of Dublin, Trinity College
towards a degree of Doctor of Philosophy

by

Claire Corcoran BSc. (Hons)

Based on research carried out under the supervision of
Assoc. Prof. Lorraine O'Driscoll

School of Pharmacy & Pharmaceutical Sciences,
Trinity Biomedical Sciences Insititute,
Trinity College Dublin



October 2013

TRINITY COLLEGE
1 4 APR 2014
LIBRARY DUBLIN

Thesis 10347

Declaration

I declare that this thesis has not been submitted as an exercise for a degree at this or any other university and it is entirely my own work. For research that has been carried out jointly or includes the published or unpublished work of others is duly acknowledged within the text of my work. I agree that the Trinity College Library may lend or copy this thesis upon request.

.

Signed: 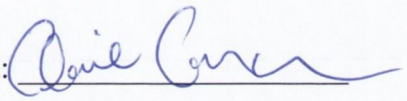

Acknowledgements

It is with great pleasure that I write this section of my PhD thesis. After 4 years of research, filled with many 'good science' days and some 'bad (or not-so-good) science' days, I never thought it would all eventually come to an end. There are many people I'd like to acknowledge who have helped me in different ways through the past few years and without them this PhD would not have be possible.

Firstly I would like to express my sincere appreciation to my supervisor Lorraine. Her endless support, guidance, encouragement and overall supervision throughout my PhD were immense, of which I am very grateful for.

I would also like to thank our senior member of the LOD group, Sweta, a never ending source of knowledge! On a professional level, Sweta was an excellent work colleague, team player and advisor but on a personal level, a great friend. To my partner in crime (and exosome isolation!) Keith, thanks for the help in the lab, but more importantly thanks for the laughs – much needed on those 'when science doesn't work' days ☺. To Susan, again thank you for your help whenever needed in my experiments but also for your positive energy and support when I needed it most (as well as the lend of those facemasks –when I definitely needed them most!). Thank you Sadhbh, our most recent PhD student to the group, thanks for the proof-reading, much appreciated! I'd like to thank some past members of the LOD group, particularly Post-doc's Anne and Serena who showed me the ropes in the first year of my PhD and MSc student Anna O'Brien for her help with some of the PC3 characterisation studies.

During the course of this PhD, I spent 3 months in the Dana Farber Cancer Institute in Boston. I'd like to take this opportunity to thank Dr. Irene Ghobrial for welcoming into her lab and all the lab members who made the experience an interesting and enjoyable one. I'd particularly like to thank Siobhan, a good friend and supplier of Barry's Tea!

The School of Pharmacy in Trinity has been an enjoyable place to work in mainly because of the staff and other post-grad students who worked there. I have made some great friends over the past few years, some of whom are friends for life. I will never forget the lads (including those of Pigeon and PILF decent!): Pat, Keith, Andy, Conor, Brian, Gary, Adrian, Tadhg, Shane, Jason, Vinny, Stefano, Cathal, Feri,Vilmar, Tao, Sid, Fran, Billy,

Mike, and The King. Of course I can't forget the girls either (including the excellent bakers!) both past and present who also may the School of Pharmacy a great place to work: Stephany, Susan, Sweta, Grainne, Katerina, Elena, Johanna, Serena, Svenja, Maria (x2!), Maire, Sadhbh, Agnes, Eva, Serena, Joanne, Edyta, Timea, Clare, Christine, Julia, Ines, Shu, Sara, Lili, Evelyn, Joanna, Orla, Shona, Deirdre, Yvonne. No doubts I may have forgotten a name or two but every single member of the department added to pleasant and welcoming atmosphere of the School of Pharmacy.

The endless support from my friends outside of the lab was great and I could not have completed this without them. I'd like to thank all my Castlebar friends, especially Leah and Zara who have been fantastic friends for most of my life, but have been enormous support during some tough times in the last few years. All my UCD Science Crew...where my science adventures began...though I don't see some of you as often as I would like, a skype chat on a tough day has always picked me up. Of the UCD Science heads that stayed in Dublin, I'd like to thank Audrey and Maeve...always were just a phone call away when I needed them most. Adam, (and Jess & Alex) thank you for making my time so enjoyable in Boston, I'll never forget it!

Thanks to all my housemates, past and present, particularly those who always had the kettle on ☺ and for all of you for putting up with my alarm constantly going off!

Finally and most importantly, I'd like to thank my family. Mum and Dad have been a huge source of support and encouragement throughout my entire education but especially through my toughest hurdle. From spoiling me when I came home for a visit to just listening to me when I had a problem I am forever grateful and proud to have them as my parents. To my brothers, Michael, Pádraic and Joe, you have constantly believed in me and thank you for all the support. My family have been the biggest influence in my life and for that I dedicate this PhD thesis to them.

Table of Contents

Declaration i

Acknowledgements ii

Summary 1

Abbreviations 2

CHAPTER 1 7

Introduction – Intracellular and extracellular biomarkers predictive of response to anti-cancer treatments for breast and prostate cancer 7

1 ABSTRACT 8

1.1 Incidence and diagnosis of breast and prostate cancer 9

1.1.1 Background 9

1.1.2 Current Diagnostic tools in breast cancer and prostate cancer 9

1.2 Current and emerging treatments for breast and prostate cancer 11

1.2.1 Targeted therapy in breast cancer 11

1.2.2 Treatment strategies for advanced Prostate Cancer 12

1.3 Chemoresistance – A common problem encountered in the treatment of both breast and prostate cancer 14

1.3.1 Receptor tyrosine kinases 15

1.3.2 Heat Shock proteins 17

1.3.3 Drug efflux pumps 18

1.3.4 Deregulation of apoptosis 20

1.4 miRNAs –biogenesis and functional relevance 22

1.4.1 Biogenesis of miRNAs 22

1.4.2 Mechansims of miRNA action 23

2.3.10 Phenotypic changes in HER2-overexpressing cells including motility, invasion and resistance to anoikis are also regulated, at least in part, by miR-630 80

2.3.11 Mechanism of Action for miR-630 84

2.3.12 The generation of stable miR-630 overexpressing and knockdown cell lines 87

2.3.13 Characterisation of stable miR-630 overexpressing and knockdown cell lines 89

2.3.14 miR-630 may also regulate Neuromedin U 92

2.4 DISCUSSION 93

2.5 CONCLUSIONS 99

CHAPTER 3 101

Neuromedin U: a potential predictive biomarker and a therapeutic target to overcome resistance to HER-tyrosine kinase inhibitors 101

3 ABSTRACT 102

3.1 INTRODUCTION 104

3.2 METHODS 106

3.2.1 Cell culture and treatments 106

3.2.2 Short-term drug exposure assays 107

3.2.3 RNA isolation from conditioned medium 107

3.2.4 NmU knockdown and overexpression 107

3.2.5 Proliferation assays 108

3.2.6 Assessing effects of NmU siRNAs with HER-targeted drugs 109

3.2.7 NmU peptide treatment and assessing affects with HER-targeted drugs 109

3.2.8 qPCR 110

2.2.8 Assessing effects of miR-630-regulated cellular response to HER-targeting drugs 57

2.2.9 Acid Phosphatase analysis- as used for proliferation and toxicity assays 57

2.2.10 Protein quantification and Immunoblotting 58

2.2.11 Cell motility –assessed using wound healing assays 59

2.2.12 Cell migration and invasion –assessed using transwell inserts 59

2.2.13 Anoikis assay 59

2.2.14 Generation of stable miR-630 knockdown and miR-630 precursor cells 60

2.2.15 Statistical and Bioinformatics analysis 64

2.3 RESULTS 65

2.3.1 Assessment yield and quality of RNA isolated for global miRNA profiling 65

2.3.2 Global miRNA profiling of SKBR3 sensitive cells and resistant variants 66

2.3.3 Identification and discovery of miRNAs from global miRNAs study ... 68

2.3.4 Validation of selected miRNAs from global miRNAs study 70

2.3.5 Changes in both intracellular and extracellular miR-630 levels are associated with acquired-resistance to lapatinib and trastuzumab 71

2.3.6 Changes in both intracellular and extracellular miR-630 levels are associated with acquired-resistance to neratinib and also innate-resistance to lapatinib/trastuzumab 73

2.3.7 miR-630 levels correspond to innate-resistance in a broad panel of HER2-overexpressing cell lines 75

2.3.8 miR-630 is decreased in tumour compared to peritumour breast cancer tissues 76

2.3.9 miR-630 regulates cellular response to HER-targeted drugs 77

1.5 The role of miRNAs in breast and prostate cancer 25

1.5.1 miRNAs as oncomirs or tumour suppressors 25

1.5.2 miRNAs implicated in cancer invasion and metastasis 28

1.5.3 miRNAs implicated in resistance to anti-cancer treatments 30

1.6 Extracellular biomarkers for cancer 31

1.6.1 Circulating miRNAs in Cancer 32

1.7 Exosomes and their relevance to cancer 34

1.8 Potential use of miRNAs as therapeutic agents or as therapeutic targets for treatment of cancer 37

1.9 Project aims 41

CHAPTER 2 43

Intracellular and extracellular miRNAs predictive of response to HER-targeted agents in the treatment of HER2-overexpressing breast cancer –A role for miR-630. 43

2 ABSTRACT 44

2.1 INTRODUCTION 46

2.2 METHODS 48

2.2.1 Cell Culture and Treatments 48

2.2.2 Conditioned Media collection and filtration 49

2.2.3 RNA Isolation and Quantification 49

2.2.4 Global miRNA profiling using Taqman Low Density Arrays 50

2.2.5 Validation- Quantitative Real Time Polymerase Chain Reaction (qPCR) 54

2.2.6 Assessment of miR-630 expression in patient derived breast tissue 56

2.2.7 microRNA inhibition or mimic transient transfection into cells 56

3.2.9 Immunoprecipitation 112

3.2.10 Immunoblotting and enzyme-linked immunosorbent assay 112

3.2.11 Wound-healing assay 113

3.2.12 Migration/invasion assay 113

3.2.13 Anoikis assay 114

3.2.14 Assessing potential clinical relevance of NmU in breast cancer 114

3.2.15 The generation of stable overexpression and stable knockdown cell lines for future in vivo studies 116

3.2.16 Detection of NmU in exosomes 118

3.2.17 Statistical analysis 118

3.3 RESULTS 119

3.3.1 Intracellular and extracellular NmU mRNA levels are associated with acquired-resistance to lapatinib. 119

3.3.2 Increased expression of NmU may be an early response to drug exposure 121

3.3.3 Induced NmU protein expression occurs in cells with acquired-resistance to other HER-targeted agents and is not restricted to lapatinib. 123

3.3.4 Endogenous NmU protein levels may be associated with innate sensitivity/resistance to HER-targeting drugs. 123

3.3.5 NmU expression is prognostic for poor outcome for breast cancer patients, particularly those with HER2-positive and luminal A subtypes 125

3.3.6 NmU affects sensitivity to lapatinib, trastuzumab, neratinib and afatinib. 127

3.3.7 NmU expression is also associated with other phenotypic characteristics including cell motility, invasion and resistance to anoikis 131

3.3.8 Proposed mechanism-of-action for NmU 134

3.3.9 Exogenous Nmu peptide treatment can increase resistance to HER-targeted therapies 137

3.3.10 The generation of stable overexpression and stable knockdown cell lines for future in vivo studies 139

3.3.11 NmU is detectable in exosomes 142

3.4 DISCUSSION 143

3.5 CONCLUSIONS 148

CHAPTER 4 149

Docetaxel-resistance in prostate cancer: evaluating associated phenotypic changes and potential for resistance transfer via exosomes 149

4 ABSTRACT 150

4.1 INTRODUCTION 151

4.2 METHODS 153

4.2.1 Cell culture and treatments 153

4.2.2 Establishment of docetaxel-resistant cell lines 153

4.2.3 Cytotoxicity assays 154

4.2.4 Cell proliferation assays 154

4.2.5 Cell motility –assessed using wound healing assays 154

4.2.6 Cell migration and invasion –assessed using transwell inserts 155

4.2.7 Anchorage-independent growth assays 155

4.2.8 Anoikis assays 156

4.2.9 Exosome isolation from conditioned medium 156

4.2.10 Transmission Electron Microscopy 157

4.2.11 Exosome isolation from serum specimens 157

4.2.12 Immunoblotting 158

4.2.13 Addition of exosomes to invasion, migration, proliferation and cytotoxicity assays 158

4.2.14 Statistical Analysis 159

4.3 RESULTS 160

4.3.1 Determining the extent of resistance to docetaxel and cross resistance to other anti-cancer agents 160

4.3.2 Docetaxel-resistant variants do not differ in morphology but showed different proliferation rates versus parent cell lines 161

4.3.3 Docetaxel-resistant variants have distinct motile and invasive phenotypes versus parent cell lines 162

4.3.4 Acquired docetaxel-resistance influences anchorage-independent survival and growth 164

4.3.5 Characterisation of exosomes derived from DU145 and 22Rv1 cell line variants 165

4.3.6 Exosomes secreted from prostate cancer cells can influence response to docetaxel but do not significantly alter proliferation, motility and invasion. 167

4.3.7 Exosomes are detected in serum from prostate cancer patients and can influence cellular proliferation, invasion and response to docetaxel ... 171

4.4 DISCUSSION 174

4.5 CONCLUSIONS 179

CHAPTER 5 181

miR-34a is an intracellular and exosomal predictive biomarker for response to docetaxel with clinical relevance to prostate cancer progression 181

5 ABSTRACT 182

5.1 INTRODUCTION 184

5.2 METHODS 186

5.1.1 Cell lines and cell culture 186

5.1.2 Exosome isolation from conditioned medium 186

5.1.3 Transmission Electron Microscopy 187

5.1.4 Immunoblotting 187

5.1.5 RNA isolation of cells and exosomes 187

5.1.6 Global miRNA profiling of cells and exosomes 188

5.1.7 Validation of selected miRNAs by qPCR 189

5.1.8 Assessment of miRNA expression in clinical specimens 190

5.1.9 miRNA inhibition/mimic manipulation in cells 190

5.1.10 Assessing effects of miR-34a – regulated cellular response to Docetaxel 191

5.1.11 Statistical Analysis 191

5.3 RESULTS 192

5.1.12 Characterisation of isolated exosomes 192

5.1.13 Yield and quality of cellular and exosomal RNA 193

5.1.14 miRNA profiling of docetaxel-resistant cells and corresponding exosomes 195

5.1.15 Selection of miRNAs for validation 198

5.1.16 The clinical relevance of selected miRNAs 203

5.1.17 Mechanism of action and functional relevance of miR-34a 207

5.4 DISCUSSION 209

5.5 CONCLUSIONS 213

CHAPTER 6 215

6 Discussion & Conclusion 215

6.1 Discussion & Conclusion 216

6.2 Future Directions....220

7 REFERENCES....224

APPENDIX I....253

A. Packaging and envelope plasmids for lentivirus production....254

B. Plasmids used for miR-630 knockdown and overexpression....256

C. Sequencing of miR-630 and scrambled plasmids....257

D. Generation of stable NmU-overexpressing cells....261

E. Generation of pcDNA3.1(+)zeo NmU construct....261

F. Stable knockdown of NmU by shRNAs....264

G. Survival analysis of miR-630 in ER+ breast cancer....265

APPENDIX II....267

Publications, Achievements & Presentations....267

A. Publications....268

B. Awards, Honors & Other....271

C. International and National conference presentations....272

Figures

Figure 1.1: Some examples of RTK signalling pathways. 16

Figure 1.2: Heat shock protein signalling in the regulation of proliferation and apoptosis. 18

Figure 1.3: Drug efflux via ABC-transporters 19

Figure 1.4: Example of molecular pathways initiating programmed cell death (Apoptosis). 21

Figure 1.5: The generation of miRNAs 23

Figure 1.6: Schematic representation of exosome formation and secretion 34

Figure 1.7: Example work plan for intracellular and extracellular miRNA analysis and the validation of miRNAs as biomarkers and/or potential new therapeutic targets. 40

Figure 2.1: Taqman Low Density Arrays 50

Figure 2.2: Schematic protocol for lentiviral production and infection. 63

Figure 2.3: Detection of miRNAs $<35C_T$ in cells and CM of SKB3 cell line variants. 66

Figure 2.4: Linear regression and hierarchical clustering of miRNA expression patterns 67

Figure 2.5: Identification of miRNAs increased with drug-resistance 68

Figure 2.6: Identification of miRNAs decreased with drug-resistance 69

Figure 2.7: miR-630 decreases with acquired-resistance to trastuzumab and lapatinib 72

Figure 2.8: miR-630 decreases with acquired-resistance to neratinib and innate-resistance. 74

Figure 2.9: Analysis of miR-630 in a broader panel of HER2 overexpressing cell lines. 75

Figure 2.10: Assessment of miR-630 in patient derived tissue. 76

Figure 2.11: Transient transfection of miR-630 inhibitor and mimic 77

Figure 2.12: Inhibition of miR-630 increases cell motility. 80

Figure 2.13: Inhibition of miR-630 increases migration, invasion and resistance to *anoikis*.....81

Figure 2.14: Mimicked expression of miR-630 increases cell motility. 82

Figure 2.15: Mimicked miR-630 decreases migration, invasion and resistance to *anoikis*.....83

Figure 2.16: Increased IGF1R, HER2 and EGFR with acquired lapatinib-resistance. 84

Figure 2.17: Inhibition of miR-630 increases IGF1R, HER2 and EGFR.....85

Figure 2.18: miR-630 mimic decreases IGF1R, HER and EGFR.....86

Figure 2.19: Generation of stable miR-630 overexpressing and knockdown cell lines. 88

Figure 2.20: Drug screen of stable miR-630 knockdown cells. 89

Figure 2.21: Drug screen of stable miR-630 overexpressing cells.....90

Figure 2.22: Proliferation and invasion of stable miR-630 cells.....91

Figure 2.23: miR-630 may regulate Neuromedin U.....92

Figure 2.24: Proposed model for outcome from manipulation of miR-630 in breast cancer cells. 98

Figure 3.1: Demonstration of qPCR amplification following DNAse treatment. 110

Figure 3.2: Acquired lapatinib-resistance in SKBR3 and HCC1954 cells.....119

Figure 3.3: NmU is increased with lapatinib-resistance in CM and cells. 120

Figure 3.4: Increased NmU with short-term lapatinib treatment.....121

Figure 3.5: Increased NmU with short-term treatment with trastuzumab, neratinib and afatinib. 122

Figure 3.6: NmU protein is increased with acquired- and innate-resistance to HER-targeted drugs. 124

Figure 3.7: NmU expression is prognostic for poor outcome for breast cancer patients.....126

Figure 3.8: NmU overexpression reduces sensitivity to HER-targeted agents. 128

Figure 3.9: NmU mRNA and protein expression following siRNA transfection. ...129

Figure 3.10: Overexpression of NmU increases cell motility. 131

Figure 3.11: Overexpression of NmU increases migration, invasion and resistance to *anoikis*. 132

Figure 3.12: NmU knockdown by siRNA decreases motility, migration, invasion and *anoikis* resistance. 133

Figure 3.13: NmU knockdown by siRNA decreases HER2 levels. 134

Figure 3.14: NmU partners with HSP27. 135

Figure 3.15: NmU also regulates phosphorylated EGFR and AKT. 136

Figure 3.16: Exogenous NmU peptide treatment can also alter protein expression. 137

Figure 3.17: Exogenous NmU treatment confers resistance to HER-targeted drugs. 138

Figure 3.18: Characterisation of HCC1954-LUC+ cells ovexpressing NmU. 140

Figure 3.19: NmU protein expression knockdown by shRNAs. 141

Figure 3.20: Analysis of NmU in exosomes. 142

Figure 3.21: Proposed mechanism of action for NmU. 146

Figure 4.1: Colony formation assay protocol. 155

Figure 4.2: Flow diagram summarising the protocol for exosome isolation 157

Figure 4.3: Cell morphology of cell line variants 161

Figure 4.4: Wound healing assays of docetaxel-resistant variants. 162

Figure 4.5:Transwell migration and invasion assays of docetaxel-resistant variants. 163

Figure 4.6: Anchorage independent growth of docetaxel-resistant variants. 164

Figure 4.7: Characterisation of cell derived exosomes. 166

Figure 4.8: Exosomes from DU145 and DU145RD do not alter motility or invasion of secondary cells. 167

Figure 4.9: Proliferation and toxicity assays in the presence of exosomes. 169

Figure 4.10: MDR-1/P-gp expression in cells and exosomes. 170

Figure 4.11: Isolation of exosomes from serum and assessment of effects on cells. 171

Figure 5.1: Confirmation of exosomes isolation from conditioned media isolates..192

Figure 5.2: Distribution of miRNA expression for cells and exosomes from all cell line variants....195

Figure 5.3: Linear regression analysis. 197

Figure 5.4: Hierachical cluster analysis....198

Figure 5.5: Identification of miRNAs decreased with docetaxel-resistance. 199

Figure 5.6: Identification of miRNAs increased with docetaxel-resistance. 200

Figure 5.7: Top miRNAs decreased with docetaxel-resistance....201

Figure 5.8: Volcano plots were used to demonstrate the spatial expression of all miRNAs assessed. 202

Figure 5.9: Clinical assessment of miR-34a. 205

Figure 5.10: Clinical assessment of miR-598, miR-148a and miR-146a. 206

Figure 5.11: miR-34a mechanism of action. 207

Figure 5.12: Effect of miR-34a on proliferation and response to docetaxel in 22Rv1 and 22Rv1RD cells. 208

Figure A.1: Vector map of packaging plasmid....254

Figure A.2: Vector map of evelope plasmid....255

Figure B.1: Vector map for miR-630 and scrambled inhibitor plasmids. 256

Figure B.2: Vector map for miR-630 and scrambled inhibitor plasmids. 256

Figure C.1: Alignment of miR-630 inhibitor plasmid sequence 257

Figure C.2: miR-630 inhibitor is specific for miR-630. 257

Figure C.3: Alignment of scrambled inhibitor plasmid sequence. 258

Figure C.4: Scrambled inhibitor is not specific for any transcript. 258

Figure C.5: Alignment of miR-630 precursor plasmid sequence. 259

Figure C.6: miR-630 precursor is matcbed to miR-630. 259

Figure C.7: Alignment of scrambled precursor plasmid sequence. 260

Figure C.8: Scrambled precursor is not matched for any transcript. 260

Figure D.1: Vector map for plasmid contruct used for NmU overexpression. 261

Figure E.1: Alignment and confirmation of pcDNA3.1 (+) ZEO construct. 262

Figure E.2: Alignment and confirmation of pcDNA3.1 (+) ZEO construct. 263

Figure F.1: Vector map for plasmid contruct used for NmU knockdown. 264

Figure G.1: Survival analysis of miR-630 in ER+ breast cancer. 265

Tables

Table 1.1: Examples of oncomirs in breast and prostate cancer. 26

Table 1.2: Examples of tumour suppressor miRNAs in breast and prostate cancer. .27

Table 1.3: Examples of metastasis-promoting or -suppressive miRNAs in breast and prostate cancer. 29

Table 1.4: Examples of miRNAs regulating resistance to anti-cancer treatments for breast and prostate cancer 30

Table 1.5: Examples miRNAs identified as potential circulating biomarkers 33

Table 1.6: Examples of studies assessing the effects of exosomes when applied to secondary cells. 36

Table 2.1: Volumes of components used for TLDA Reverse Transcription Reaction. 51

Table 2.2: Thermal cycling conditions used for TLDA Reverse Transcription Reaction 51

Table 2.3: Volumes of components used for the pre-amplification reaction. 52

Table 2.4: Thermal cycling conditions used for the pre-amplification reaction. 52

Table 2.5: Volumes of components used for RT Reaction for Taqman miRNA assays. 54

Table 2.6: Thermal cycling conditions used for RT Reaction for Taqman miRNA assays. 55

Table 2.7: Thermal cycling conditions used for real time PCR for Taqman miRNA assays. 55

Table 2.8: RNA yields and quality for cells and corresponding CM. 65

Table 2.9: miRNAs selected from TLDA analysis for validation by qPCR. 70

Table 2.10: Inhibition of miR-630 reduces sensitivity to HER-targeted drugs. 78

Table 2.11: Mimicked expression of miR-630 restores sensitivity to HER-targeted drugs. 79

Table 3.1: Volumes of components used for cDNA synthesis reaction 111

Table 3.2: Publically-available data sets used to assess NmU expression. 115

Table 3.3: NmU knockdown by siRNA can enhance sensitivity to HER-targeted drugs. 130

Table 3.4: Plasmid DNA isolated for stable NmU knockdown studie. 141

Table 4.1: Docetaxel-resistance and cross-resistance for prostate cancer cell line variants. 160

Table 4.2: Proliferation rates of docetaxel-resistant cell line variants. 161

Table 4.3: Assessment of serum derived exosomes in relation to docetaxel response. 173

Table 5.1: Exosomes quantities, RNA yields and quality as assessed by for cells and corresponding exosomes of the PC3 cell line variants. 193

Table 5.2: Exosome quantitites, RNA yields and quality as assessed for cells and corresponding exosomes of the DU145 cell line variants. 193

Table 5.3: RNA yields and quality as assessed for cells and corresponding exosomes of the 22Rv1 cell line variants. 194

Table 5.4: Percentage and distribution of microRNAs detected $<35C_T$ in all cell line variants. 196

Table 5.5: miRNAs selected for validation for qPCR. 203

Summary

Cancer remains one of the leading causes of death worldwide. Breast and prostate cancer are the most frequently diagnosed cancers among women and men, respectively. Despite some breakthroughs in their treatment, innate or acquired-resistance hinders the continued success of some treatments. Through the initial use of breast cancer cell lines with acquired- or innate-resistance to trastuzumab, lapatinib and later assessing neratinib and afatinib, this PhD investigated the mechanisms behind resistance to these therapies. Similarly, the mechanisms involved in regulating docetaxel-resistance in prostate cancer cell lines were also investigated. The second focus of this PhD involved testing the hypothesis that the extracellular environment may carry biomarkers representative of their cells of origin, thus offering the potential of identifying biomarkers in a minimally-invasive manner.

Global miRNA profiling of breast cancer cell lines and their corresponding conditioned medium identified miR-630 as one possible regulator of resistance to HER-targeted therapies, through its apparent regulation of IGF1R. Furthermore, this PhD describes the potential of Neuromedin U (NmU), a predicted target of miR-630, as another regulator of resistance, to these therapies through its chaperone protein, HSP27. Knockdown and overexpression studies identified that both miR-630 and NmU can regulate many phenotypic characteristics of cells including response to HER-targeted drugs, motility, invasion and *anoikis.* Initial characterisation of prostate cancer cell lines with acquired docetaxel-resistance demonstrated the multifaceted nature of the clinical problem. Furthermore, this PhD demonstrated that the prostate cancer cell line variants used in this study can secrete nano-sized vesicles, known as exosomes, which can modulate the transfer of drug- resistance to secondary cells, potentially via the transfer of molecules such as MDR-1/P-gp. Global miRNA profiling indentified miR-34a, as a potential regulator of docetaxel resistance, via its evident regulation of BCL-2. Interestingly, a strong correlation of miRNAs detected in cells and corresponding exosomes was identified. In conclusion, this PhD has identified several potential regulators of resistance to HER-targeted therapies for breast cancer and docetaxel treatment for prostate cancer. The support of our extracellular studies also highlights the importance of assessing biological fluids as a source for these biomarkers.

Abbreviations

630 K/D	miR-630 inhibitor
630 PRE	miR-630 precursor
ADC	Antibody Drug Conjugate
ADP	Adenosine Diphosphate
Ag	Aged Control
Ago2/EIF2C2	Argonaute RISC Catalytic Component 2
AIB1	Amplified in Breast Cancer 1
AKT	Protein Kinase B
ANGPTL1	Angiopoietin-like 1
ANKRD46	Ankyrin Repeat Domain 46
APAF1	Apoptotic Peptidase Activating Factor 1.
AR	Androgen Receptor
ATP	Adenosine Triphosphate
BAD	BCL2-associated Agonist of Cell Death
BAK	BCL2-Antagonist/Killer 1
BAX	BCL2-Associated X Protein
BCa	Breast Cancer
BCL2	B-Cell Lymphoma 2
BCL2L2	BCL2-Like 2
BCL-xl	BCL2-Like 1
BCR	Biochemical Recurrence
BID	BH3 Interacting Domain Death Agonist
BIK	BCL2-Interacting Killer (apoptosis-inducing)
BIM	BCL2-like 11 (apoptosis facilitator)
BOK	BCL2-related Ovarian Killer
BPH	Benign Prostatic Hyperplasia
BRCA-1	Breast Cancer 1, early onset
BRMS1	Breast Cancer Metastasis Suppressor 1
BSA	Bovine Serum Albumin
BTG2	B-Cell translocation gene 2
CD133	Prominin 1
CD44	CD44 molecule (Indian blood group)
CM	Conditioned Media
cMET	Met proto-oncogene
c-Myc	v-Myc avian myelocytomatosis viral oncogene homolog
CO_2	Carbon Dixoide
CPR	Complete Pathalogic Response
c-SRC	v-Src avian sarcoma (Schmidt-Ruppin A-2) viral oncogene homolog
CT	Cycle Threshold
CXCR4	Chemokine (C-X-C motif) Receptor 4

CYP17A1	17 α-hydroxylase/C17,20 lyase
Cyt. C	Cytochrome C
DHEA	Dehydroepiandrosterone
DMSO	Dimethyl Sulfoxide
DNA	Deoxyribonucleic acid
E2F1	E2F transcription factor 1
E2F2	E2F transcription factor 2
E2F3	E2F transcription factor 3
ECM	Extracellular Matrix
Egfl7	EGF-like domain 7
EGFR	Epidermal Growth Factor Receptor
eIF4E	Eukaryotic Translation Initiation Factor 4E
eIF6	Eukaryotic Translation Initiation Factor 6
ER	Estrogen Receptor
ERG	v-ets avian erythroblastosis virus e26 oncogene homolog
ERK	Mitogen-Activated Protein Kinase 1
EV	Extracellular Vesicle
EXO	Exosome
EXO1	Exonuclease 1
EZH2	Enhancer of Zeste Homolog 2
FAS	Fas cell surface death receptor
FFPE	Formalin Fixed Parafin Embedded (tissue)
FGFR	Fibroblast Growth Factor Receptor
FOXM1	Forkhead Box M1
FOXO1	Forkhead Box Protein O1
Fra-1	Fos-Related Antigen 1
GFP	Green Fluorescent Protein
GPX2	Glutathione Peroxidase-2
GRB2	Growth-Factor-Receptor-Bound-2
GRPC	G-Protein Coupled Receptor
GW182	Trinucleotide Repeat Containing 6A
HC	Healthy Control
HER2	Human Epidermal Growth Factor Receptor 2
HER3	Human Epidermal Growth Factor Receptor 3
HER4	Epidermal Growth Factor Receptor 4
HIF-1	HIF1A – Hypoxia Inducible Factor 1, alpha subunit
HIF-1α	Hypoxia Inducible Factor 1, alpha subunit
HSF1	Heat Shock Transcription Factor 1
HSP27	Heat Shock Protein 27
HSP70	Heat Shock Protein 70
HSP90	Heat Shock Protein 90
IGF1R	Insulin like Growth Factor Receptor 1

IL	Interleukin (IL)
IL24	e interleukin (IL) tumour suppressor genes 24
IL32	e interleukin (IL) tumour suppressor genes 32
JAK	Janus kinase
Ki-67	Antigen identified by monoclonal antibody Ki 67
KlF4	Kruppel-like Factor 4 (gut)
LAMC1	Laminin, Gamma 1 (formerly LAMB2)
LMTK3	Lemur Tyrosine Kinase 3
LR	Lapatinib-Resistant
MAPK	Mitogen Activated Protein Kinase
MARCKS	Myristoylated Alanine-Rich Protein Kinase C Substrate
mBCa	Metastatic Breast Cancer
mCherry/LUC+	mCherry and Luciferase expressing
MCL-1	Myeloid cell leukemia sequence 1 (BCL2-related)
MCM2	Minichromosome maintenance complex component 2
MDR-1	Multidrug-resistance protein 1
MED1	Mediator 1
MEK	MAPK-kinase
miR-34a	microRNA-34a
miR-630	microRNA-630
miRNA	microRNA
MMP2	Matrix Metallopeptidase 2
MnSOD	Manganese Superoxide Dismutase
mRNA	messenger RNA
mPCa	Metastatic Prostate Cancer
MRP-1	Multidrug-resistance-associated Protein 1
MVB	Multi-Vesicular Body
NF-kappaB	Nuclear Factor-kappaB
NmU	Neuromedin U
Notch-1	Notch gene homolog 1
NR	Neratinib-Resistant
N-RAS	Neuroblastoma RAS viral (v-ras) oncogene homolog
Oct-04	POU class 5 homeobox 1
p27Kip1	Cyclin-Dependent Kinase Inhibitor 1B
p53	Tumour protein p53
pAKT	Phosphorylated AKT
PBS	phosphate buffered saline
PCa	Prostate Cancer
PCAF	p300/CBP-associated factor
PCR	Polymerase Chain Reaction

PDC6I/Alix	Programmed Cell Death 6 Interacting Protein
PDCD4	Programmed cell death 4
P-gp	P-glycoprotein
PHB	Prohibitin
Pi	Phosphate group
PI3K	phosphatidylinositol 3-kinase
POL II/III	Polymerase I/IIII
Pre-miRNA	Precursor miRNAs
Pri-miRNA	Primary microRNA
qPCR	Quantitative Polymerase Chain Reaction
RAF	Raf Kinase, Effector of Ras
RAS	Rat Sarcoma viral oncogene
RECK	Reversion-inducing Cysteine-rich protein with Kazal motifs
RHOB	Ras Homolog family member B
RKIP	Raf Kinase Inhibitory Protein
RNA	Ribonucleic acid
RNA	Ribonucleic acid
ROCK1	Rho-associated,coiled-coil containing protein kinase 1
RT	Reverse Transcription
RTK	Receptor Tyrosine Kinase
RTKI	Receptor Tyrosine Kinase Inhibitor
RTKN	Rhotekin
SCR K/D	Scrambled inhibitor
SCR PRE	Scrambled precursor
SDF-1α	Stromal Cell-Derived Factor-1 alpha
SIRT1	Sirtuin 1
SOS	Son Of Sevenless
STAT	Signal-Transducer and Activator of Transcription protein
Stmn1	Stathmin1
tBID	Truncated form of Bid
TDM-1	Trastuzumab Emtansine
TIMP3	Tissue Inhibitor of Metalloproteinase 3
TLDA	Taqman Low Density Array
TNF	Tumour Necrosis Factor
TP53	Tumour Protein p53
TPM1	Tropomyosin 1
TR	Trastuzumab-Resistant
TRAIL	Tumour Necrosis Factor (ligand) Superfamily, member 10
TRBP/TARBP2P	TAR (HIV-1) RNA Binding Protein 2 pseudogene
TrxR2	Thioredoxin Reductase-2

TSG101	Tumour Susceptibility Gene 101
VEGF-A	Vascular Endothelial Growth Factor A
VIM	Vimentin
XRN1	5'-3' Exoribonuclease 1
ZBTB10	Zinc Finger And BTB Domain-Containing Protein 10
α-SMA	Alpha Smooth Muscle Actin
ΔNp63	Potein 63 transcript lacking trans activating (TA) domain

CHAPTER 1

Introduction – Intracellular and extracellular biomarkers predictive of response to anti-cancer treatments for breast and prostate cancer

Parts of this chapter are published in the following paper:

Intracellular and extracellular microRNAs in breast cancer

Claire Corcoran, Anne M. Friel, Michael J. Duffy, John Crown, Lorraine O'Driscoll

Clincial Chemistry, 2011 Jan *57(1), 18-32*

1 ABSTRACT

Cancer remains the second leading cause of death among men and women. Apart from basal and squamous cell skin cancers, breast cancer and prostate cancer are the most commonly diagnosed cancers among women and men in the US, respectively.

Diagnostic tools for breast cancer and prostate cancer are limited to a few established biomarkers, such as estrogen receptor (ER), progesterone receptor (PR), and Human epidermal growth factor receptor 2 (HER2) for breast cancer; and prostate specific antigen (PSA) for prostate cancer. However these biomarkers are arguably not adequate or ideal biomarkers for either breast cancer or prostate cancer.

Furthermore, resistance to anti-cancer treatments, such as trastuzumab (Genetech/Roche) and lapatinib (GlaxoSmithKline) for breast cancer and docetaxel (Sanofi Aventis) for prostate cancer, remains a major obstacle in the management of HER2-overexpressing breast cancer and castration-resistant prostate cancer (CRPC). Unfortunately there are no reliable methods of predicting sensitivity/resistance to anti-cancer agents.

In this chapter, the current and emerging treatments for breast and prostate cancer are described and how the acquisition of resistance to these therapies may be limiting their success. The relevance of microRNAs (miRNAs) as potential biomarkers for breast and prostate cancer and their ability to be assessed as extracellular and so minimally-invasive biomarkers is reviewed. Attention is also drawn to the potential of microRNAs (miRNAs) to be manipulated as therapeutic strategies or targets for disease. The rapidly evolving field of extracellular vesicles such as exosomes is also reviewed here, giving consideration to where these nano-sized vesicles may hold substantial bearing in the field of cancer.

1.1 Incidence and diagnosis of breast and prostate cancer

1.1.1 Background

Cancer remains the second leading cause of death among men and women worldwide surpassed only by heart disease [1]. Apart from basal and squamous cell skin cancers, breast cancer and prostate cancer are the most commonly diagnosed cancers among women and men in the US, respectively. According to the American Cancer Society (www.cancer.org), there is a 1 in 8 chance of a woman developing breast cancer at some stage during her lifetime. This disease is not restricted to women, as approximately 1% of all cases occur in men. Excluding non-melanoma skin cancer, according to the National Cancer Registry of Ireland (NCRI), breast cancer remains the most frequently diagnosed cancer in females with approximately 2767 cases per year [2]. If breast cancer is detected and treated at an early stage, successful outcomes can be achieved in some patients. Despite this, breast cancer continues to be an immense problem worldwide, with more than 1.4 million cases diagnosed in women annually, resulting in approximately 485 000 deaths per annum [1]; this number is predicted to increase in the future [3].

Similar to breast cancer, the occurrence of prostate cancer is frequent with 1 in 6 men diagnosed with prostate cancer in their lifetime. Specifically, in 2013 there is an estimated 238,590 (28% of total incident cases of cancer among men) cases of prostate cancer in the US contributing to approximately 29,720 mortalities [4]. Prostate cancer is not only an immense problem in the US; the NCRI reports that as many as 3014 cases of this disease are diagnosed in Ireland annually making it the leading cancer diagnosed in males (excluding non-melanoma skin cancers) [2].

1.1.2 Current Diagnostic tools in breast cancer and prostate cancer

As with many cancers, progress in early breast cancer detection has been inadequate [5] and methods for determining diagnosis and prognosis of breast cancer are still limited to invasive procedures, such as tissue biopsies for histological examination [6, 7]. Existing diagnostic tools for breast cancer, although important and necessary, have many limitations. For example, although mammography is currently considered the more reliable option for earliest diagnosis within certain age groups, associated problems have arisen due

to varied interpretation of results among radiologists and inconsistent rates of false-positive results [8]. For breast cancer, ER, PR and HER2 expressions are among a very limited number of diagnostic biomarkers that have been established as relevant for routine assessment [9]. Although these receptors have many merits as biomarkers, by their selective nature they arguably cannot be considered as adequate and ideal candidate biomarkers for all breast cancer patients. In terms of their use as biomarkers predictive of response to treatment, for instance, some patients with HER2-positive tumours do not respond to trastuzumab [10]. Possible suggestions for this include the intratumoural heterogeneity in the amplification of HER2 gene, expression of truncated forms of HER2 as well as activation of downstream signalling pathways [10]. On the contrary, reports of some patients described as having HER2-negative (no amplification nor overexpression) tumours indicate that this subset of patients may also benefit to this HER2-targeted monoclonal antibody [11].

The current strategy for diagnosis of prostate cancer involves measuring PSA levels, histopathological assessment of prostate biopsies (Gleason Grade) and digital rectal examination (DRE). PSA is generally found at low levels in the blood of adult males. Increased release of PSA into circulation has been associated with the onset of prostate cancer and, thus, its detection in serum has become a universal tool in screening for the disease; particularly in combination with DRE [12]. Despite this finding, the use of PSA as a prostate cancer biomarker has faced much controversy in recent years as elevated PSA levels have also been associated with benign prostatic hyperplasia and prostatic inflammation and/or infection. The major limitations of this biomarker, therefore, are that it cannot reliably distinguish between benign and malignant disease, or between low or high grade prostate cancers [13]. So the fact that PSA may be a prostate-specific rather than a cancer-specific biomarker has given rise to questions of its efficacy as an accurate tumour biomarker. Consequently the current limitations of PSA as a definitive biomarker for prostate cancer implies that a more consistent panel of biomarkers with potential of indicating invasive prostate cancer; disease progression; and predicting response to therapy is urgently needed.

1.2 Current and emerging treatments for breast and prostate cancer

1.2.1 Targeted therapy in breast cancer

While ER and PR status are important prognostic factors for breast cancer, the recent focus of research has broadened to include other tumour-specific targets such as HER2 [14]. The predominant emphasis of this thesis is on one of the subtypes of breast cancer, HER2-overpressing breast cancer. HER2-overexpression occurs in approximately 25% of breast cancer and is associated with poor prognosis [15, 16]. Investigations into the pathways involved in HER2-overexpression have led to the development of targeted therapeutics such as trastuzumab. Trastuzumab, is a recombinant humanised monoclonal antibody (mAb) targeting HER2 [17]. While trastuzumab has had success in some patients whose tumour overexpresses HER2, other patients fail to respond and develop resistance which inevitably leads to metastasis. In an effort to identify additional therapies for patients for whom trastuzumab is un-successful, receptor tyrosine kinase inhibitors (RTKIs) such as lapatinib have been developed. Lapatinib concurrently inhibits the epidermal growth factor receptor (EGFR, also known as ErBb1) and HER2 receptor which has been shown to block the activation of mitogen activated protein kinase (MAPK) and phosphatidylinositol 3-kinase (PI3K) signaling pathways, resulting in growth arrest and/or apoptosis in cell lines and xenograft models [18, 19]. Like trastuzumab, the use of lapatinib is complicated with the challenge of the development of drug-resistance [20-22]. Thus the quest to develop strategies that may overcome or avoid the emergence of this associated resistance is still ongoing.

Several new treatments for HER2-overexpressing breast cancer are currently in the pipeline, some of which are demonstrating promising results in phase II and III clinical trials. Pertuzumab (Genetech, Inc.), for example, is a humanized monoclonal antibody that prevents ligand induced heterodimerisation of HER2 and human epidermal growth factor receptor 3 (HER3) by its binding to the dimerisation domain II of HER2 [23]. Phase II clinical trials of pertuzumab with or without trastuzumab or docetaxel or both (Neosphere trial) demonstrated that the pertuzumab plus both trastuzumab and docetaxel patient group had a significantly improved pathological complete response rate compared to the other groups and that pertuzumab plus trastuzumab without docetaxel also eliminated tumours in

some patients [24]. Other Phase II (TRYPHAENA) and III (CLEOPATRA) trials have indicated successful results with the use of pertuzumab in combination with trastuzumab or other chemotherapy and the phase III (Aphinity) is currently underway [25]. More recently developed HER-targeting drugs include neratinib (Pfizer/Puma), an irreversible small molecule RTKI of EGFR/HER1, HER2 and epidermal growth factor receptor 4 (HER4) [26]. In advanced HER2-overexpressing breast cancers, including trastuzumab-refractory and trastuzumab-naïve patients, single-agent neratinib demonstrated some clinical benefits in both cohorts [27]. Phase II and III clinical trials of neratinib in combination with trastuzumab and/or classical chemotherapy are underway (www.clinicaltrials.gov Trial identifiers: NCT01008150; NCT01808573). Afatinib (Boehringer Ingelheim), another irreversible oral small molecule RTKI of EGFR/HER1, HER2 and HER4 has shown single-agent activity in a Phase II trial including trastuzumab-refractory HER2-positive metastatic breast cancers [28]. A phase II trial of afatinib (with vinorelbine versus venorelbine/trastuzumab) in HER2-positive metastatic breast cancer after trastuzumab progression is currently recruiting (www.clinicaltrials.gov Trial identifier: NCT01531764).

While the targeting of one or several HER family members with or without classical chemotherapy has demonstrated some success in the treatment of HER2-overexpressing breast cancer, another approach that has emerged in recent years is the use of antibody-drug conjugates (ADC). An ADC works by having the specificity of a monoclonal-antibody and the potency of a cytotoxic agent [29]. Trastuzumab emtansine (TDM-1) is an ADC that joins trastuzumab with the cytotoxic agent maytansinoid DM1 and is currently at late-stage trials for the use in HER2-overexpressing metastatic breast cancer [30]. While phase III trial (EMILIA) has provided strong evidence for the use of TDM-1 in a second line setting [31], other trials, including phase III (MARIANNE), are investigating it's use as a first- line treatment [25].

1.2.2 Treatment strategies for advanced Prostate Cancer

The nature of prostate cancer varies from aggressive to indolent; depending on the point of diagnosis it can be classified into several stages. In the case of localised prostate cancer, there are many treatments options available including radical prostatectomy, radiation therapy and cryotherapy [32]. Androgen-ablation is currently the treatment of choice for patients with advanced metastatic disease [33].

Unfortunately, many patients become resistant to hormonal manipulation and invariably develop a highly-aggressive androgen-independent disease, hormone-refractory prostate cancer (HRPC) [34, 35]. The term HRPC has also more recently been used interchangeably with the term castration-resistant prostate cancer (CRPC). CRPC refers to prostate cancer that has progressed despite castrate serum levels of testosterone [36] and is associated with significant morbidity and mortality [37]. The Prostate Cancer Working Group 2 (PCWG 2) have advised the preferred use of the term CRPC, rather than HRPC, for those patients who have progressed following castration as some of these patients may yet respond to second- and third-line hormonal therapies [38].

Docetaxel, which is currently the gold standard treatment for patients with CRPC, is a member of the taxane class of drugs and is a semi-synthetic analogue of the originally discovered paclitaxel. Docetaxel acts by inhibiting microtubule activity which is required for cells to undergo mitosis and other cellular functions [39]. When docetaxel binds tubulin α and β dimers it promotes their binding into stable tubules. This action consequently inhibits the disassembly of the microtubules, thus preventing mitotic activity and cell growth [39]. In addition to microtubule stabilisation and blocking of its dynamic events, docetaxel also inactivates the anti-apoptotic protein, B-cell lymphoma 2 (BCL-2) [40].

While docetaxel offers some improvement in overall survival of patients with CRPC in comparison to other anti-cancer agents, unfortunately relapse is almost inevitable which leaves patients with an extremely poor prognosis. Several other treatment options have demonstrated some clinical benefit for patients with disease progression following docetaxel treatment. Carbazitaxel is a second generation taxane that has been FDA approved for the use in metastatic CRPC patients who have failed docetaxel treatment [41]. A current Phase III trial (FIRSTANA), directly comparing carbazitaxel *versus* docetaxel as first line treatment is currently on going [42].

Abiraterone acetate (Janssen Biotech, Inc.) is the first FDA approved potent and tolerable androgen biosynthesis inhibitor which demonstrated a 4-month improvement in survival of docetaxel-resistant metastatic prostate cancer patients [43]. Aberaterone works by selectively and irreversibly inhibiting 17 α-hydroxylase/C17,20 lyase (CYP17A1), an enzyme responsible for the catalysing the conversion of 17-hydroxypregnenolone to the main androgen precursor dehydroepiandrosterone (DHEA) [44]. Recent reports have

indicated the benefit of aberaterone in a pre-chemotherapy setting for patients with metastatic CRPC [45]. Enzalutamide (Medivation, Inc., and Astellas, Inc.) is a second generation androgen receptor (AR) inhibitor that has also recently been approved for the use in patients with metastatic CRPC following docetaxel chemotherapy [46]. Enzalutamide acts by competitively inhibiting the binding of androgens to ARs in addition to preventing nuclear translocation of the ARs and their interaction with DNA [46]. A recent study however has suggested that resistance to this treatment is possible following chronic exposure of prostate cancer cells to enzalutamide [47].

1.3 Chemoresistance – A common problem encountered in the treatment of both breast and prostate cancer

While the treatment of HER2-overexpressing breast cancer as (discussed in Section 1.2.1) and advanced prostate cancer (Section 1.2.2) varies from targeted therapies such as trastuzumab and lapatinib to the use of cytotoxic drugs such as docetaxel, one of the key challenges that limits the success of these drugs is the innate or inevitable emergence of drug-resistance that occurs in many breast and prostate cancer patients. One of the main aims of the research presented in this thesis was to elucidate novel mechanisms of drug-resistance in breast cancer (Chapters 2 & 3) and prostate cancer (Chapters 4 & 5). Some proposed mechanisms and contributing factors reported to be associated with drug-resistance and aggressive disease in breast and prostate cancer are outlined in Sections 1.3.1-1.3.4.

1.3.1 Receptor tyrosine kinases

Receptor Tyrosine Kinases (RTKs) have been implicated in regulating many cellular functions, including differentiation, cell cycle, proliferation, cell motility, and cell death/survival. These cellular processes are instigated by the vital role of RTKs in signal transduction and subsequent effect on gene transcription in the nucleus [48]. An example of some of the important downstream signalling cascades activated by RTKs include the Ras-extracellular regulated kinase (ERK)-MAPK pathway, the PI3K-AKT (protein kinase B) pathway, and the Janus kinase/signal-transducer and activator of transcription protein (JAK/STAT) pathway are outlined in Figure 1.1. RTKs are sub-divided into 20 different families based on their specific structural features and homologous domains [49, 50]. One of the most widely documented and well characterised sub-family, the EGFR family, has been exploited by pharmaceutical companies as a therapeutic target for some current and emerging anti-cancer therapies. For example, trastuzumab, lapatinib, neratinib, afatinib, pertuzumab and TDM-1 as mentioned in Section 1.2.1 are currently used or being evaluated in the treatment of HER2-overexpressing breast cancer [23, 27, 28, 30, 51]. Recent evidence suggests that the deregulated expression of RTKs may be casually involved in the emergence of resistance to classical chemotherapy [52, 53]. Many RTK subfamily members have been implicated in regulating drug-resistance. These include insulin-like growth factor receptor 1 (IGF1R), whose aberrant expression has been associated with regulating response or resistance to classical chemotherapy [54-58]. EGFR [54], HER2 [59], fibroblast growth factor receptor (FGFR) [60, 61] met proto-oncogene (cMET) [62] are among many other RTKs whose deregulated expression can alter drug sensitivity/resistance. In Chapters 2 and 3 the relevance of some RTKs, including IGF1R, HER2 and EGFR, is discussed in relation to conferred resistance to HER-targeted therapies through mechanisms involving miR-630 (Chapter 2) and Neuromedin U (NmU) (Chapter 3).

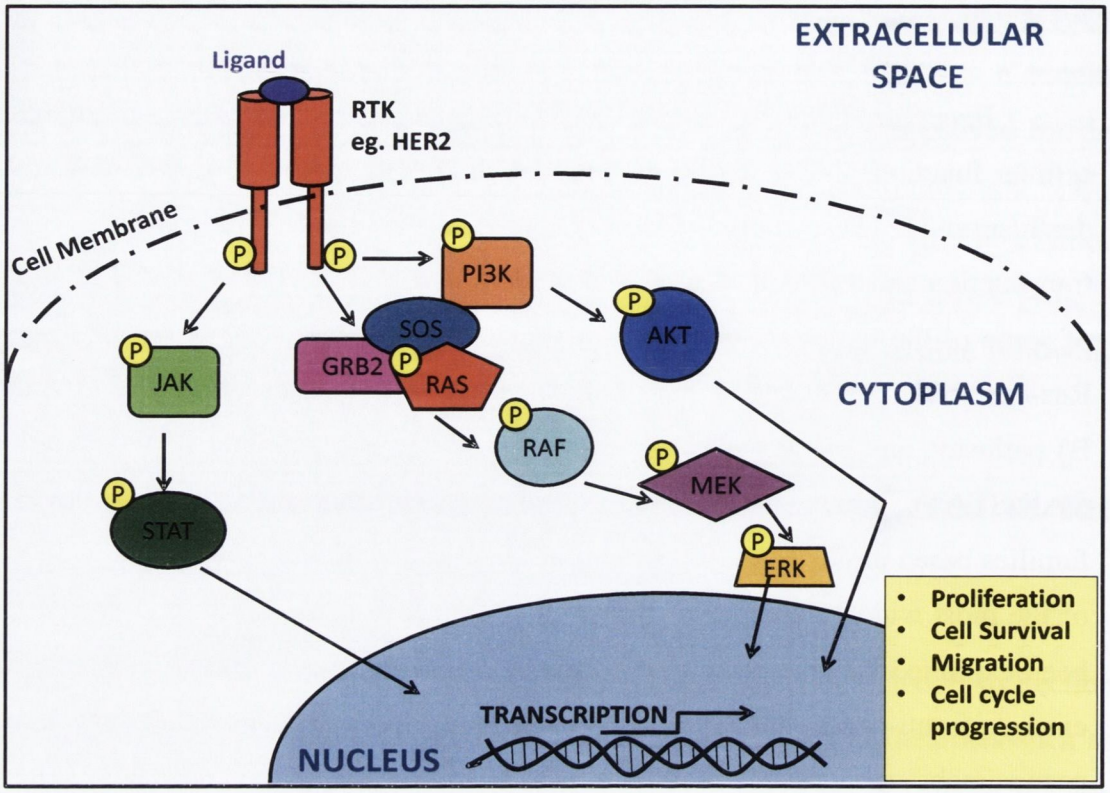

Figure 1.1: Some examples of RTK signalling pathways.

Adapted from Archer *et al.* [63]. Upon ligand binding with the RTK, the cytoplasmic RTK residues become phosophorylated (P) and activate downstream signalling pathways ultimately altering proliferation, cell survival, migration, *etc.* RTK: receptor tyrosine kinase; JAK: janus kinase; STAT: signal-transducer and activator of transcription protein; GRB2: growth factor receptor bound 2; SOS: son-of-sevenless; RAS: rat sarcoma viral oncogene; RAF: raf kinase, effector of Ras; MEK: MAPK-kinase; ERK: mitogen-activated protein kinase 1; PI3K: phosphatidylinositol 3-kinase; ATK: protein kinase B.

1.3.2 Heat Shock proteins

Heath shock proteins (HSP) are molecular chaperones that are implicated in aiding the correct folding of proteins in normal conditions and inducing cell response to stressful conditions [64]. As molecular chaperones, it is thought that the role of HSPs may protect cells from a variety of stressful conditions by partnering to other molecules ultimately aiding in assembly and folding of proteins as well as intracellular localisation, secretion, regulation and degradation of other proteins, failure of which may instigate many diseased states [64]. There are five major famies of HSPs: HSPA (Hsp70), HSPB (e.g. HSP27), HSPC (Hsp90), HSPD (Hsp60) and HSPH (eg. HSP110) [65]. In recent years several studies have indicated the altered expression of HSPs in drug-resistance. In studies not detailed in this thesis, we have demonstrated the altered expression of HSP70 and HSP90α can occur in multiple docetaxel-resistant cell lines [66]. HSP70 has also previously been associated with resistance to cisplatin and several other anti-cancer agents [67, 68]. Due to the important role that HSPs may play in drug-resistance, several inhibitors have been developed for use in combination with current drug treatments. Increased expression of HSP90 has frequently been associated with cancer and its poor prognosis, along with playing a protective role in cancer cells against the cytotoxic effects of anti-cancer drugs [69]. For this reason targeting HSP90 with specific inhibitors offers an attractive treatment option [70]. Another HSP that has been implicated with drug-resistance is HSP27. Through binding to HER2, HSP27 has been associated with increasing HER2 stability and consequently reducing cellular sensitivity to trastuzumab [71]. Elevated expression of HSP27 has also been implicated with increased cancer cell aggression in several cancer types [72-74]. In Chapter 3 the proposed mechanism of resistance to HER-targeted therapies and increased cancer cell aggression through regulation of NmU and its partner protein HSP27 is evaluated. A schematic diagram of the mechanism heat shock protein regulation is indicated in Figure 1.2.

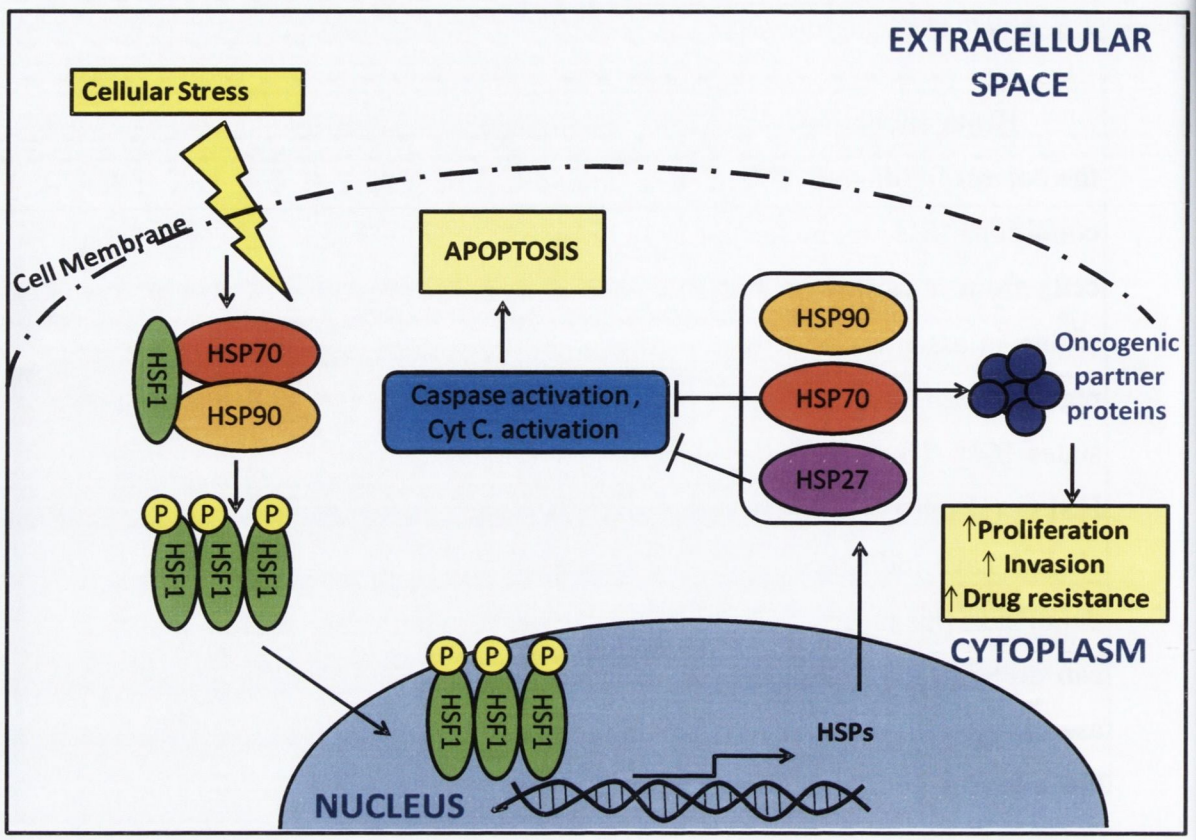

Figure 1.2: Heat shock protein signalling in the regulation of proliferation and apoptosis.
Adapted from Xi et al, [75]. HSF1: heat shock transcription factor 1; Cyt. C: Cytochrome C.

1.3.3 Drug efflux pumps

The therapeutic failure of taxanes in prostate cancer and targeted therapies for breast cancer may, at least in part, be attributed to multidrug-resistance (MDR) mechanisms protecting cancer cells against chemotherapeutic drugs. MDR is frequently attributed with the overexpression of one or several transporter proteins, located on the cell membrane, that act as drug efflux pumps [6, 76]. P-glycoprotein (MDR-1/P-gp), the gene product of multidrug-resistance protein 1 (MDR-1 (also known as ABCB1)) and multidrug-resistance-associated protein 1 (MRP-1 (also known as ABCC1)) are two members of the ATP-binding cassette (ABC) transporter family that have been broadly studied for their association with the efflux of some commonly used chemotherapeutic drugs. Several studies have demonstrated the association of MRP-1 with prostate cancer progression and subsequent chemoresistance to drugs such as doxorubicin and paclitaxel [77-80]. However, in general, taxanes are considered to be poor substrates of MRP-1 [6]. Reported expression of MDR-1/P-gp expression in prostate cancer has been somewhat varied [77, 81-83].

Although the mechanism of docetaxel-resistance in prostate cancer has yet to be fully elucidated, MDR-1/P-gp has been reported to convey docetaxel-resistance in both pancreatic cancer [84] and breast cancer [85]. In Chapter 4, the expression of MDR-1/P-gp induced in two out of three of our docetaxel-resistant cell lines is demonstrated. This indicates that, while this drug efflux pump may contribute to docetaxel-resistance, progression of prostate cancer to an advanced metastatic and chemoresistant stage may also rely on other different parameters. An example mechanism of how drug efflux pumps work is indicated in Figure 1.3.

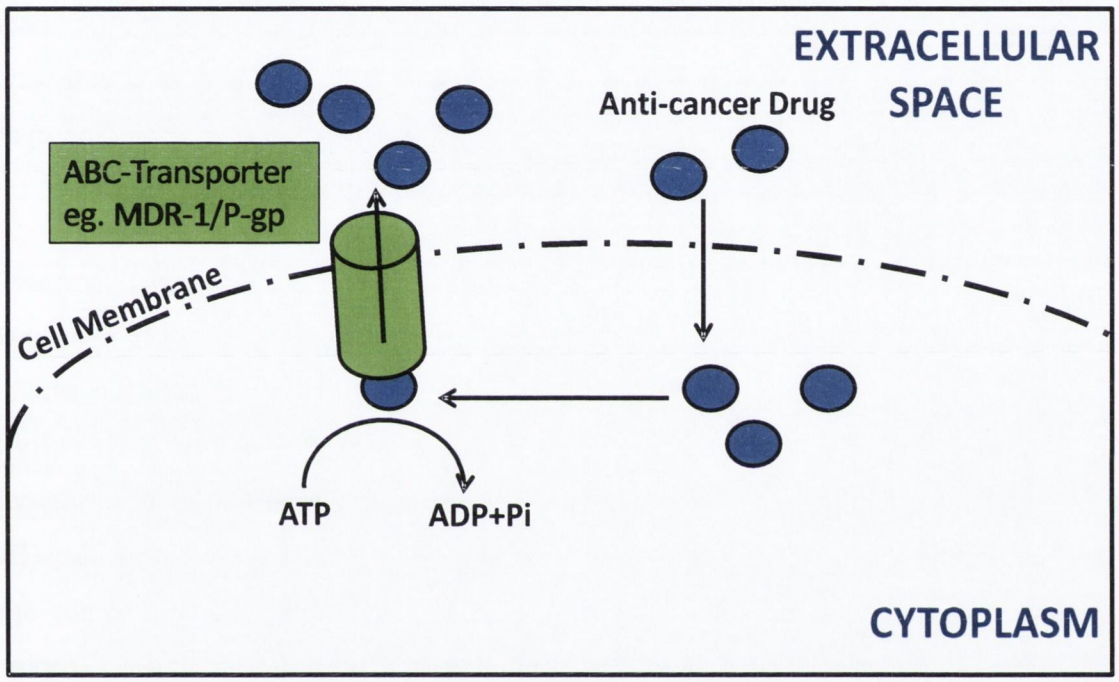

Figure 1.3: Drug efflux via ABC-transporters

(eg. Multidrug-resistance protein (MDR-1/P-gp). The energy required for ABC-transporters to efflux drugs is based on the conversion of ATP (Adenosine Triphosphate) to ADP (Adenosine Diphostate). Pi: Phosphate group.

1.3.4 Deregulation of apoptosis

Apoptosis is a form of programmed cell that maintains homeostasis within a cell. Irregular (reduced) apoptosis is often associated with the occurrence and progression of cancer as well as resistance to treatment [86]. Apoptosis may occur by the intrinsic or extrinsic pathways. The intrinsic pathway can be induced through the deregulation of mitochondrial functions, whereas the extrinsic pathway is associated with ligand binding of membrane-linked death receptors [87]. There are several key ligands that can activate death receptor systems to modulate the extrinsic apoptosis pathway including tumour necrosis factor (TNF), Fas cell surface death receptor (FAS) ligand and tumour necrosis factor (ligand) superfamily, member 10 (TRAIL). The intrinsic apoptotic pathway has several molecules that control its cascade of events. Caspases are a family of cysteine proteases that play a central role in the intrinsic apoptosis pathway [88].

Previous studies have indicated the regulation of chemoresistance by caspase 3 in breast cancer [89]. Reduced levels of caspase 3 were associated with resistance to doxorubicin and re-constituting caspase 3 expression in cells could enhance sensitivity [89]. Another group of key contributors in the intrinsic pathway is the BCL-2 family [86]. The BCL-2 family comprise of several pro-apoptotic proteins including BCL2-associated X protein (BAX), BCL2-antagonist/killer 1 (BAK), BCL2-related ovarian killer (BOK), BCL2-associated agonist of cell death (BAD), BH3 interacting domain death agonist (BID), BCL2-interacting killer (apoptosis-inducing) (BIK), BCL2-like 11 (apoptosis facilitator) (BIM), among others. Anti-apoptotic protein members of this family include B-cell CLL/lymphoma 2 (BCL-2), BCL2-like 1 (BCL-X_L), and myeloid cell leukemia sequence 1 (BCL2-related) (Mcl-1) [86]. In studies not detailed in this thesis, we have demonstrated the altered expression of some BCL-2 family members with docetaxel-resistance in PC3 prostate cancer cells including BCL-X_L, BID and BAX [90]. In Chapter 5, BCL-2 is reported as elevated with docetaxel-resistance in 22Rv1 cells and is apparently directly targeted by miR-34a. Altered BCL-2 expression has been associated with drug-resistance in several other cancer types [91-93]. An illustration of intrinisic and extrinsic apoptosis pathways is indicated in Figure 1.4.

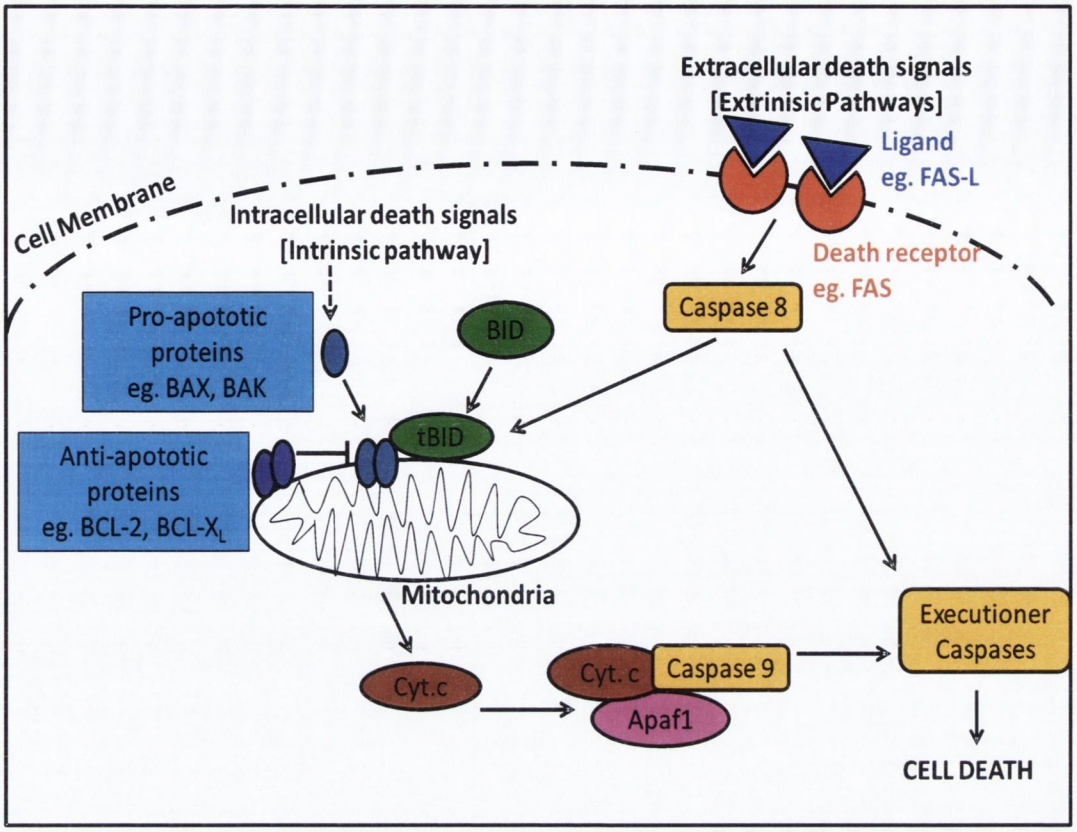

Figure 1.4: Example of molecular pathways initiating programmed cell death (Apoptosis).

Adapted from Vila and Przedborski [94]. FAS-L: Fas cell surface death receptor ligand; BID: BH3 interacting domain death agonist; tBID: truncated form of BID; BAX: BCL2-associated X protein; BAK: BCL2-antagonist/killer 1; BCL-2: B-Cell Lymphoma 2; BCL-XL: BCL-2-like 1; Cyt. C: cytochrome C; APAF1: apoptotic peptidase activating factor 1.

1.4 miRNAs –biogenesis and functional relevance

It has been reported that the miRNA profiling of several different tissues is far superior to mRNA characterisation with regards to their informative nature allowing for better prediction and more accurate classification of poorly-differentiated tumours of uncertain origin [95, 96]. In this thesis the relevance of miRNAs in relation to breast cancer (Chapter 2) and prostate cancer (Chapter 4) is reported. The mechanisms of how miRNAs are formed and what functional implications they hold that may ultimately lead to the regulation of diseases including cancer are discussed in Sections 1.4.1 and 1.4.2.

1.4.1 Biogenesis of miRNAs

Mature miRNAs are small (approximately 18–25 nucleotides long) non-protein coding RNAs. The first step in miRNA generation begins in the nucleus with a long primary miRNA, produced after miRNA gene transcription by RNA polymerase II (POL II) [97, 98] or, less commonly, by RNA polymerase III (POL III) [99]. The initial step involved in the processing of this primary miRNA (pri-miRNA) is mediated by the microprocessor complex. This complex is comprised of the double-stranded RNA-specific ribonuclease III–type endonuclease, Drosha, with its cofactor DGCR8, a double-stranded RNA-binding protein responsible for recognising the hairpin loop of the pri-miRNA and ensuring correct cleavage by Drosha. This step results in a hairpin-shaped precursor miRNA (pre-miRNA) of approximately 70 nucleotides in length [100-102]. This pre-miRNA is then transported across the nuclear envelope to the cytoplasm by the nuclear transport protein, termed exportin 5, where it is further modified by a second RNase enzyme, termed Dicer, which acts in conjunction with a double-stranded RNA-binding protein, TAR (HIV-1) RNA binding protein 2 pseudogene (TRBP/TARBP2P). In mammalian cells, TRBP recruits argonaute RISC catalytic component 2 protein (Ago2/EIF2C2); together Dicer, TRBP, and Ago2 form the RNA-induced silencing complex. Cleavage of the pre-miRNA by Dicer produces a mature miRNA/miRNA nucleotide duplex approximately 22 nucleotides in length, one strand of which will become the mature miRNA [101]. A schematic diagram of miRNA biogenesis is shown in Figure 1.5. The Ago2-bound mature miRNA is subsequently assembled into effector complexes termed miRNA-containing ribonucleoprotein particles. Within the silencing complex, miRNAs pair to the messages of protein-coding genes, usually through imperfect base

pairing within the 3′-UTR. The "seed" region (nucleotides 2–7) at the 5′ end of the miRNA is often sufficient for its specificity and functionality. The effect of a miRNA is generally negative regulation of gene expression, by acting post-transcriptionally. However, miRNAs have also been implicated in regulating mRNA stability (including degradation, by accelerating decapping and deadenylation) and compartmentalisation.

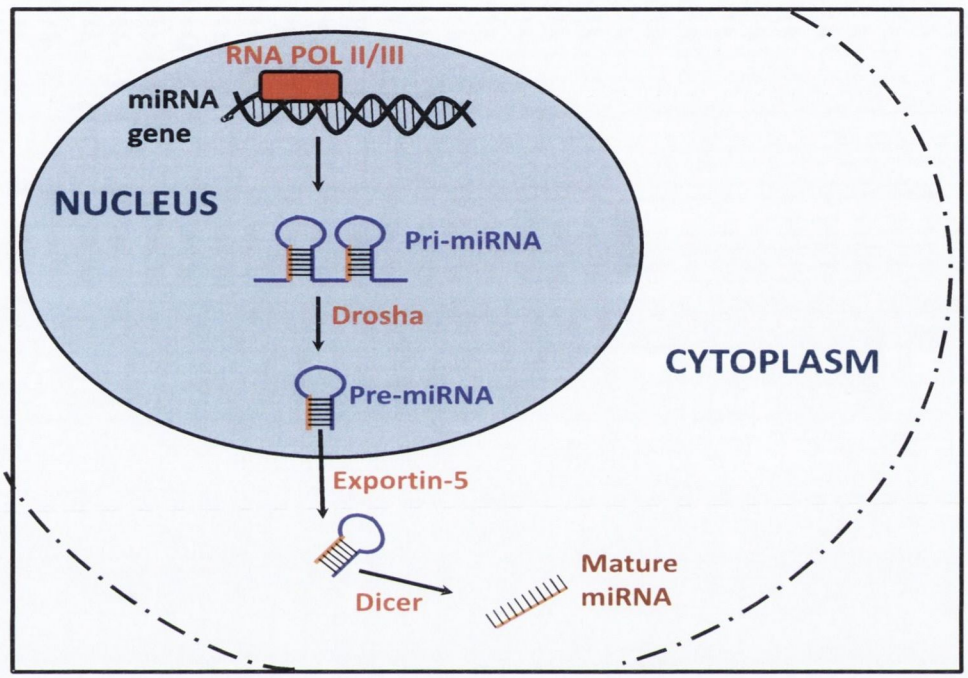

Figure 1.5: The generation of miRNAs

1.4.2 Mechansims of miRNA action

As previously detailed [98], several proposed models exist for the mechanism of translational repression, including miRNAs repressing translation at both pre-initiation and post-initiation stages. However, it still remains to be deciphered which of these model mechanisms are cause and consequence of translational repression. miRNAs that affect initiation steps are possibly involved in m^7G cap recognition, because only cap-dependent translation is effected by miRNA action. Argonaute proteins contain structural similarities to cap-binding protein, eukaryotic translation initiation factor 4E (eIF4E), and so it has been suggested that translational repression may occur owing to competition between argonaute proteins and eIF4E for binding to the cap structure. Argonaute proteins are also thought to recruit eukaryotic translation initiation factor 6 (eIF6), which binds to the large ribosomal subunit, preventing binding of the small subunit, thus inhibiting mRNA

translation. Post-initiation mechanisms of repression that affect both cap-dependent and cap-independent translation also exist. Polysome profile experiments indicate that, under conditions of translational repression, target mRNAs are fully loaded with ribosomes, a number of which are engaged in active translation, suggesting that translation initiation and elongation phases are not compromised. Two possible hypotheses have been proposed to explain these findings. The ribosome "drop-off" theory suggests that ribosomes engaged in translation of miRNA-associated mRNAs are prone to terminate translation prematurely. Alternatively, association of active ribosomes with repressed mRNAs may also be explained by the ability of the miRNA complex to recruit proteolytic enzymes to degrade the nascent polypeptide as it emerges from the ribosome. Conflicting evidence exists on the role of proteolytic enzymes in miRNA function, because targeting of reporter proteins and the use of proteinase inhibitors have generally shown no effect on translational repression.

Induction of mRNA decay is another mechanism by which miRNAs apply their actions. Argonaute proteins, miRNAs, and their repressed target mRNAs have been shown to accumulate in cytoplasmic foci called P-bodies, *i.e.* cytoplasmic processing bodies in mammalian cells. P-bodies are sites of translational repression and mRNA decay, are rich in factors associated with these processes, and are lacking in ribosomes or any other factors associated with translation initiation. It has been proposed that P-body proteins may participate in the formation of a repressive complex on the target mRNA that could eventually lead to mRNA aggregation into P-bodies. Within P-bodies, miRNA/mRNA-bound Ago protein recruits trinucleotide repeat containing 6A (GW182) protein, which subsequently recruits deadenylase enzyme CCR4:NOT1, which is followed by mRNA decapping by DCP1:DCP2 enzyme. Repressed mRNAs are then degraded by 5′ to 3′ exonuclease activity of XRN1 (5′-exoribonuclease 1). In addition to facilitating mRNA degradation, P-bodies may function as temporary storage sites for repressed mRNAs. Once protein synthesis has been stimulated, repressed mRNAs may re-enter translation.

The relevance of miRNAs rests on their involvement in, and subsequent effects on, many diverse biological functions. Since the discovery of miRNAs over 20 years ago [103], it has been estimated that miRNAs regulate more than 60% of all human protein-coding genes [104]. miRNAs have been implicated in the control of a wide range of essential biological activities, including cellular proliferation [105], differentiation [106],

and apoptosis [107]. Importantly, the association of miRNAs with cancer (see Section 1.5) has prompted additional functional classification of these short RNAs and their potential relevance in cancer diagnosis, prognosis prediction, and treatment.

1.5 The role of miRNAs in breast and prostate cancer

Since the initial association of miRNAs with carcinogenesis, demonstrated in B-cell chronic lymphocytic leukaemia [108], these short non-coding RNAs have been shown to have widespread aberrant expression in cancer biology with miRNA profiles identified for several cancers including breast cancer [109], prostate cancer [110], lung cancer [111, 112] and colon carcinoma [113]. miRNAs have been demonstrated to have both oncogeneic and tumour suppressive roles in cancer. Sections 1.5.1-1.5.3 outline some examples of miRNAs and their indicated roles in breast and prostate cancer

1.5.1 miRNAs as oncomirs or tumour suppressors

Oncogene miRNAs, now commonly termed oncomirs, may act by hindering the expression of tumour-suppressor genes and/or genes responsible for apoptosis and differentiation [114, 115]. Investigations to identify functional oncogenic role(s) for miRNAs have, for the most part, involved their individual manipulation in cell-line models and subsequent assessment of associated phenotypic changes. microRNA-21 (miR-21) is one of the most widely documented miRNAs in cancer with indications of an oncogenic role in carcinogenesis [116]. Table 1.1 summarizes some examples of miRNAs that have apparent oncogenic activity in breast cancer and prostate cancer.

In contrast to oncomirs, if the expression of a miRNA is lowered in cancer cells compared to normal cells, it is regarded as a tumour suppressor miRNA (oncosuppressor miRNA). Such miRNAs are associated with tumour suppressive activity, because they operate by negatively regulating (inhibiting) genes that promote tumourigenesis (oncogenes) and control cellular differentiation and/or apoptosis [114]. Accordingly, the dysfunction of an oncosuppressor miRNA may ultimately lead to the development of malignant cells [117]. Table 1.2 summarises some examples of such miRNAs, which support their role as tumour suppressors in breast and prostate cancer.

miRNA	Targets in Breast cancer	Models used	Targets in Prostate cancer	Models used
miR-21	PDCD4 [118, 119]	MCF-7 cells	BTG2 [120]	RWPE-1 cells
	ANKRD46 [121]	MCF-7, MDA-MB-231 cells; tissue specimens; Xenograft mouse model	RECK [122]	DU145 cells; tissue specimens
	BCL-2 [123]	MCF7 cells; Xenograft mouse model	MARCKS [124]	DU145 & PC3 cells
	TPM1 [125]	MCF7 cells		
	TIMP3 [126]	BCAP-37, MCF-7, MDA-MB-231, MDA-MD-435 cells; Tissue specimens		
miR-27a	ZBTB10 [127]	MDA-MB-231 cells	PHB [128]	LnCap cells
	ZBTB10 [129]	SKBR3 cells		
	FOXO1 [130]	MCF-7 cells	AR [131]	LnCap cells
miR-221/222	$p27^{Kip1}$ [132]	MDA-MB-231, BT-20, MDA-MB-468 cells; Xenograft mouse model	$p27^{Kip1}$ [133]	PC3, LnCap cells
	ERα [134]	MCF-7 cells	$p27^{Kip1}$ [135]	LnCap, PC3 cells;Xenograft mouse model

Table 1.1: Examples of oncomirs in breast and prostate cancer.

PDCD4: Programmed cell death 4; BTG2: B-Cell translocation gene 2; ANKRD46: ankyrin repeat domain 46; RECK: Reversion-inducing cysteine-rich protein with Kazal motifs; BCL-2: B-Cell Lymphoma 2; MARCKS: Myristoylated Alanine-Rich Protein Kinase C Substrate; TPM1: tropomyosin 1, TIMP3: tissue inhibitor of metalloproteinase 3; ZBTB10: Zinc Finger And BTB Domain-Containing Protein 10; PHB: Prohibitin; FOXO1: Forkhead Box Protein O1; AR: Andorgen receptor; $p27^{Kip1}$: Cyclin-Dependent Kinase Inhibitor 1B; ERα: Estrogen receptor-alpha

miRNA	Targets in Breast cancer	Models used	Targets in Prostate cancer	Models used
miR-145	N-RAS, VEGF-A [136]	MCF-7, MDA-MD-231 cells; tissue specimens; xenograft mouse model	ERG [137]	Vcap, LnCap, DU145 cells; tissue specimens
	TP53, ERα [138]	MCF-7, MCF-10A, MDA-MB-231 cells	CD133, CD44, Oct4, c-Myc,Klf4 [139]	PC3 cells
	RTKN [140]	MCF-7 cells	--- [141]	Tissue specimens
miR-205	HER3 [142]	SKBR3, MCF-7 cells	BCL-2 [143]	PC3, LnCap cells
	VEGF-A [144]	MCF-7, MDA-MB-231 cells; tissue specimens	MED1 [144]	LnCap, PrEC cells, tissue specimens
	Ki-67, p53 [145]	MCF-7 cells; Blood specimens,	ΔNp63 [146]	RPWE-1 cells, tissue specimens
	E2F1, LAMC1 [147]	MDA-MB-231, BT-459 cells; tissue specimens; xenograft mouse models	IL24, IL32 [148]	PC3 cells; tissue specimems
miR-17	AIB1 [149]	MCF-7 cells	MnSOD, GPX2, TrxR2 [150]	PC3 cells
	BRCA-1 [151]	MCF-7 cells	VIM [152]	P69, M2182, M2055, M12, F6 cells; xenograft mouse models
			PCAF [153]	RWPE-1, LnCap cells

Table 1.2: Examples of tumour suppressor miRNAs in breast and prostate cancer.

N-RAS: neuroblastoma RAS viral (v-ras) oncogene homolog;VEGF-A: Vascular endothelial growth factor A; ERG: the v-ets avian erythroblastosis virus e26 oncogene homolog; TP53: tumour protein p53; ERα: Estrogen receptor-alpha; CD133: prominin 1; CD44: CD44 molecule (Indian blood group); Oct4: POU class 5 homeobox 1; c-Myc: v-myc avian myelocytomatosis viral oncogene homolog; KlF4: Kruppel-like factor 4 (gut); RTKN: Rhotekin; HER3: Human epidermal growth factor receptor 3; BCL-2: B-cell lymphoma 2; VEGF-A: Vascular endothelial growth factor A; MED1: Mediator 1; Ki-67: antigen identified by monoclonal antibody Ki 67; p53: tumour protein p53; ΔNp63: Potein 63 transcript lacking transactivating (TA) domain; E2F1: E2F transcription factor 1; LAMC1: aminin, gamma 1 (formerly LAMB2); IL24: e interleukin (IL) tumour suppressor genes 24; IL32: e interleukin (IL) tumour suppressor genes 32; AIB1: amplified in breast cancer 1; MnSOD: manganese superoxide dismutase; GPX2: glutathione peroxidase-2; TrxR2: thioredoxin reductase-2; BRCA-1: breast cancer 1, early onset; VIM: Vimentin; PCAF: p300/CBP-associated factor

1.5.2 miRNAs implicated in cancer invasion and metastasis

Current management strategies for breast and prostate cancer are focused on early-stage detection, tumour resection, and neo-adjuvant or adjuvant treatment with or without hormone ablation, radiation, chemotherapy, and/or new targeted agents (generally a combination of these approaches). Despite advancements in the treatment of these diseases, both breast and prostate cancer still remain leading causes of cancer death. Metastasis is the primary reason for high cancer death rates. Hence, to successfully curtail this disease, there is an urgent need to define therapeutic agents that could effectively target cancer before it metastasises. As outlined in Section 1.5.1, recent research studies have established the presence of aberrant expression of miRNAs with the potential of either promoting or suppressing tumourigenesis in breast cancer compared to normal breast tissue. The possibility that miRNAs specifically contribute to metastasis has recently been explored. Table 1.3 below outlines several miRNAs that have been described as potentially promoting ("metastamirs") or suppressing metastasis for both breast and prostate cancer.

miRNA	Targets in Breast cancer	Role in breast Cancer metastasis	Targets in Prostate cancer	Role in prostate cancer metastasis
miR-373	CD44	Promoter [154]	CD44	Promoter [154, 155]
miR-520c	CD44	Promoter [154]	CD44	Promoter [154, 155]
miR-21	VIM, α-SMA, E-Cadherin, N-Cadherin, ANKRD46, RHOB, HER2, PDCD4	Promoter [121, 156-158]	BTG2, HIF-1α, VEGF-1, AKT, ERK, MARCKS	Promoter [118, 120, 124]
miR-34a	E2F3, CD44, SIRT1, Fra-1, BCL-2	Suppressor [159-161]	CD44, AR, Notch-1	Suppressor [162, 163]
miR-101	STMN1, EZH2	Suppressor [164, 165]	EZH2, RKIP	Suppressor [165, 166]
miR-31	BIM	Suppressor [167]	E2F1, E2F2, EXO1, FOXM1, MCM2	Suppressor [168, 169]
miR-146/146a	BRMS1, CXCR4	Suppressor [170, 171]	EGFR, MMP2, ROCK1	Suppressor [172, 173]
miR-126/126*	SDF-1α	Suppressor [174]	Egfl7	Suppressor [175]

Table 1.3: Examples of metastasis-promoting or -suppressive miRNAs in breast and prostate cancer. CD44: CD44 molecule (Indian blood group); VIM: Vimentin; α-SMA: alpha smooth muscle Actin ; ANKRD46: ankyrin repeat domain 46; RHOB: ras homolog family member B; HER2: Human epidermal growth factor receptor 2; PDCD4: Programmed cell death 4; BTG2: B-Cell translocation gene 2; HIF-1α: hypoxia inducible factor 1 -alpha subunit; VEGF-1: Vascular endothelial growth factor A ; AKT: protein kinase B; ERK: mitogen-activated protein kinase 1; MARCKS: Myristoylated Alanine-Rich Protein Kinase C Substrate; EGF3: E2F transcription factor 3; SIRT1: sirtuin 1; Fra-1: Fos-related antigen 1; BCL-2: B-Cell Lymphoma 2; AR: Androgen Receptor; Notch-1: Notch gene homolog 1; STMN1: Stathmin1; EZH2: Enhancer of zeste homolog 2; RKIP: Raf kinase inhibitory protein; BIM: BH3 interacting domain death agonist; E2F1: E2F transcription factor 1; E2F2: E2F transcription factor 2; EXO1: exonuclease 1; FOXM1: forkhead box M1; MCM2: minichromosome maintenance complex component 2; BRMS1: Breast cancer metastasis suppressor 1; CXCR4: chemokine (C-X-C motif) receptor 4; EGFR: Epidermeral growth factor receptor; MMP2: matrix metallopeptidase 2 ; ROCK 1: Rho-associated, coiled-coil containing protein kinase 1; SDF-1α: stromal cell-derived factor-1 alpha; Egfl7: EGF-like domain 7.

1.5.3 miRNAs implicated in resistance to anti-cancer treatments

Research to date has predominantly focused on the role of miRNAs in the emergence of cancer, acting as oncomirs or tumour suppressors. This later evolved to focusing on the role of miRNAs in regulating cancer progression and metastasis. Recent studies however have indicated that miRNAs may also play a significant part in regulating resistance to anti-cancer therapies, the findings of which are growing exponentially. In Chapters 2, the role of miR-630 regulating cell response to HER-targeted therapies in breast cancer is demonstrated. Furthermore, Chapter 5 indicates the potential relevance of miR-34a in regulating docetaxel-resistance in prostate cancer. The role of several other miRNAs in regulating anti-cancer treatments for both breast and prostate cancer are outlined in Table 4 below.

miRNA	Treatments for breast cancer	Role in resistance	Treatments for prostate cancer	Role in resistance
miR-21	cisplatin; doxorubicin; paclitaxel; trastuzumab; doxorubicin; radiation	Promoter [176-181]	castration; docetaxel	Promotor [182, 183]
miR-34a	docetaxel; doxorubicin; 3,6-dihydroxyflavone (3,6-DHF)	Promoter [184] Suppressor [185, 186]	camptothecin; paclitaxel	Suppressor [187, 188]
miR-200c	paclitaxel; cisplatin; doxorubicin; epirubicin; radiation; tamoxifen; fulvestrant; 5-fluorouracil	Suppressor [189-193]	docetaxel	Suppressor [194] Promoter [195]
miR-205	gefitinib; lapatinib	Suppressor [142]	docetaxel; cisplatin	Suppressor [194-196]
miR-31	radiation; doxorubicin	Suppressor [197]	docetaxel	Suppressor [196]
miR-210	Trastuzumab	Promoter [198]	Varied treatments - based on PSA response	Promoter [199]

Table 1.4: Examples of miRNAs regulating resistance to anti-cancer treatments for breast and prostate cancer

1.6 Extracellular biomarkers for cancer

The pursuit of minimally-invasive biomarkers is a challenging, but exciting, area of research. Clearly, such markers would need to be sensitive and specific enough to aid in the detection of cancer at an early stage, would monitor progression of the disease, and could predict the individual patient's response to treatment. Existing diagnostic tools for breast and prostate cancer, although important and necessary, have many limitations. For example, although mammography is currently considered the more reliable option for earliest diagnosis within certain age groups, associated problems have arisen due to varied interpretation of results among radiologists and inconsistent rates of false-positive result [8].

For breast cancer, ER, PR, and HER2 expression are among a very limited number of biomarkers that have been established as relevant for routine assessment [9]. Although these receptors have many merits as biomarkers, they are not as adequate and ideal candidate biomarkers for all breast cancer patients. For example, some patients with HER2-positive tumours do not respond to trastuzumab [10]. Even some of the diagnostic tools for prostate cancer used in the clinic, while considered the best options at present, they too have limitations. For example, while clinically useful, the main disadvantage of the digital rectal examination is the invasive and uncomfortable procedure associated with it. As indicated earlier in Section 1.1.2, the use of PSA, despite its initial advancement in prostate cancer diagnostics, also has limitations.

In addition to PSA for prostate cancer, several other circulating tumour protein biomarkers frequently used clinically, such as carcinoembryonic antigen and carbohydrate antigen 15-3, both of which have been noted to have low pre-operative diagnostic sensitivity, thus indicating their limited use for detecting early-stage breast cancer [200]. Over the past decade, certain mRNAs have been reported as circulating in serum/plasma from cancer patients [201, 202]. In fact, the feasibility of using whole-genome microarrays and subsequent qPCR as a means of identifying panels of extracellular mRNAs with potential as diagnostic and prognostic breast tumour biomarkers was initially demonstrated in our laboratory [201].

1.6.1 Circulating miRNAs in Cancer

Reports on the existence of circulating miRNAs associated with cancer have, emerged only within the past few years [203-206]. The stability of miRNAs, demonstrated to be well preserved in formalin-fixed paraffin-embedded tissue [207] prompted researchers to investigate whether such miRNAs exist in blood and other bodily fluids. In 2008, in the first report of miRNAs in serum, increased levels of tumour-associated miRNAs were identified in patients with diffuse large–B-cell lymphoma [208]. In our pilot global studies, in addition to circulating mRNAs [201], we observed that circulating miRNAs (including miR-141 and miR-195) were present at significantly higher levels ($p<$ 0.001) in serum from patients recently diagnosed with breast cancer compared with age- and sex-matched healthy volunteers (unpublished data). Since then, our group have identified a panel of miRNAs as potential biomarkers for lung cancer [206]. Several other very interesting studies have revealed associations between circulating miRNAs and the presence of cancers, including pancreatic [209], colorectal [210, 211], and breast cancer [212, 213]. In Chapter 2, the relevance of miR-630 in relation to breast cancer and associated resistance to HER-targeted therapies is demonstrated. In addition to this the altered expression in cells was reflected in medium conditioned by these cells indicating the potential of miR-630 as a circulating biomarker.

The concept of miRNAs existing in the systemic circulation extends beyond that of free miRNAs in plasma and serum, because miRNAs (as well as mRNAs and proteins) have been shown to exist in circulating extracellular vesicles [214, 215]. For example, exosomes (described further in section 1.6.2) , which are nano-sized extracellular vesicles, contain miRNAs and have been associated with cancers, including those of the lung [216], ovary [217] and breast [218] as well as glioblastoma [219]. Research of circulating miRNAs is evolving rapidly, however evidence from the studies outlined above indicates a positive correlation between these potentially non-invasive biomarkers and cancer diagnosis. Whether these miRNAs exist freely in the systemic circulation or are predominantly transported via tumour-secreted microvesicles remains somewhat unclear, given that evidence supporting both possibilities has been documented. Table 1.5 outlines some examples of miRNAs identitied with potential as circulating biomarkers for breast and prostate cancer.

miRNA	Breast Cancer	Conditions assessed	Sample type	Prostate Cancer	Conditions assessed	Sample type
miR-21	Increased [220]	68 BCa Vs 40 HC	Serum	Increased [221]	51 PCa (various stages) Vs 20 HC	Plasma
	Increased [222]	102 BCa (various stages) Vs 20 HC	Serum	Increased [223]	50 PCa (various stages) Vs 6 BPH	Plasma
	Increased [224]	100 BCa Vs 20 HC	Serum			
miR-210	Increased [225]	61 CTC(+) mBCa Vs 72 CTC(-) mBCa Vs 76 HC	Plasma	Increased [199]	25 PCa Vs 25 Healty Controls	Serum
	Increased [198]	18 HER2+ BCa - CPR to trastuzumab Vs 11 residual disease	Plasma	Increased [199]	CM from cells (LnCap, VCap) in Normoxic Vs Hypoxic conditions	Conditioned media
	Increased [198]	27 BCa Vs 28 HC	Plasma	Increased [199]	No PSA response Vs PSA response	Serum
miR-141	Increased [225]	61 CTC (+) mBCa Vs 72 CTC(-) mBCa Vs 76 HC	Plasma	Increased [225]	25 mPCa Vs 25 HC	Serum
				Increased [225]	25 mPCa Vs 25 HC	Serum
				Increased [226]	78 PCa (various grades) Vs 28 HC	Plasma (EVs)
				Increased [226]	16 mPCa Vs 55 primary disease	Plasma (Evs)
				Increased [226]	47 mPCa Vs 72 non-recurrant PCa	Serum (Evs)
miR-181a	Decreased [227]	152 BCa Vs 75 HC	Serum	Decreased [226]	78 PCa (various grades) Vs 28 HC	Plasma (EVs)
				Decreased [226]	16 mPCa Vs 55 primary disease	Plasma (EVs)

Table 1.5: Examples miRNAs identified as potential circulating biomarkers

HC: healthy controls; BCa: Breast Cancer; mBCa: metastatic breast cancer; CPR: Complete pathologic response; PCa: prostate cancer; mPCa: metastatic prostate cancer; BPH: Benign prostatic byperplasia; PSA: prostate specific antigen; EVs: Extracellular vesicles; CTC (+): positive for circulating tumour cells; CTC(-) negative for circulating tumour cells.

1.7 Exosomes and their relevance to cancer

The identification of circulating tumour biomarkers in a wide range of cancers (including breast and prostate cancer) has undoubtedly shown great promise for their application in a clinical setting. However, the profiling of new biomarkers in bodily fluids still remains a huge challenge in cancer research and is faced with several limitations including large sample variation and the fact that ~97% of body fluids comprises high-abundance proteins [228]. Studies in recent years have indicated that biomarkers in the extracellular environment may be encapsulated in extracellular vesicles (EVs). Exosomes are one type of extracellular vesicles that have been described as approximately 40-100nm diameter membrane bound vesicles of endocytic origin that are secreted by many cell types into the extracellular space [229]. Intracellular formation of exosomes occurs through the inward budding of endosomal membranes (endocytosis) [230] which results in vesicle-containing endosomes known as multivesicular bodies (MVBs). The term exosomes is derived when the MVBs fuse with the cell membrane and release their internal vesicles into the extracellular environment (exocytosis) [231] (See Figure 1.6).

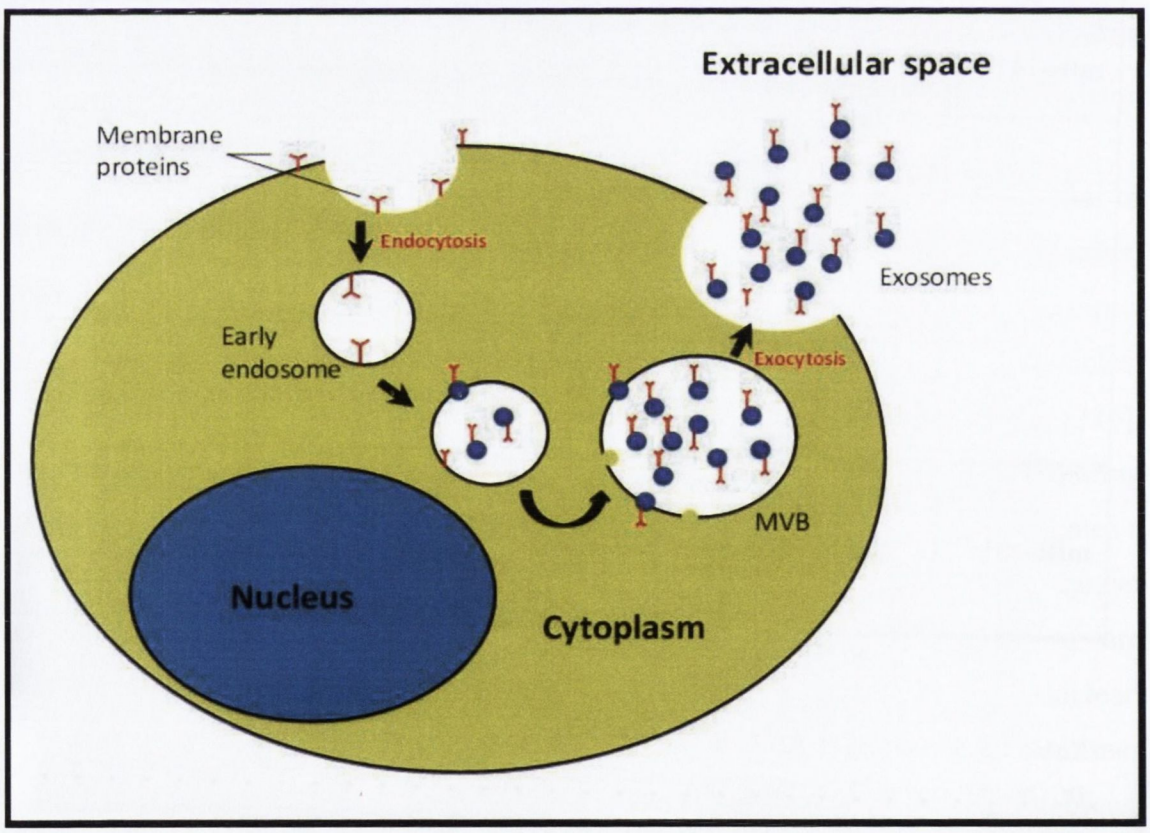

Figure 1.6: Schematic representation of exosome formation and secretion

Depending on their cell of origin, these small vesicles have been implicated with several different roles some of which suggest their association with diseased states such as cancer. Intercellular communication is one such role, through the ability of exosomes to promote signal transduction [232] and the transfer of membrane receptors, proteins, mRNA, and miRNAs [214] from one cell to another. Exosomes are also implicated in the delivery of toxic agents such as chemotherapeutic drugs into cells [233]. Tumour-derived exosomes have been found to promote cellular proliferation, as previously demonstrated in human U87 glioma cells [219] as well as tumour growth in mouse models of mammary carcinoma [234]. A correlation of exosomes production with invasiveness of various cancer cell lines (8701-BC, MCF-7, MDA-MB-231 and HT-1080) *in vitro* has also been observed [235]. Furthermore, exosomes derived from malignant mesothelioma cells have been associated with the suppression of immune response to IL-2 [236]. We have recently reported on the ability of exosomes to transfer phenotypic effects representative of their cells of origin to secondary cells, in both triple negative breast cancer [218] and prostate cancer (described further in Chapter 4) [237]. Some example studies, assessing the influences on phenotypic characteristics by exosomes when applied to secondary cells, as assessed by our group and others are outlined in Table 1.6. The mechanisms by which exosomes can elicit these phenotypic effects may be due to the transfer of proteins and RNAs between cells. We and others have reported on the content of exosomes [214, 219, 237, 238] and in Chapter 5 global miRNA profiling of cells and their corresponding exosomes in prostate cancer is examined.

Source of exosomes	Effect on secondary cells	Secondary cells used	Phenotypic change assessed
Hs578T Vs Hs578Ti8 cells	Promote [218]	HS578T, SKBR3, HCC1954, MDA-MB-231, and Endothelial cells	Proliferation, Invasion, Migration, Anoikis, Angiogenesis
TNBC Vs HC serum	Promote [218]	SKBR3	Invasion
22Rv1 Vs 22Rv1RD cells	Promote [237]	DU145, 22Rv1, LnCap	Docetaxel-resistance
DU145 Vs DU145RD cells	Promote [237]	DU145, 22Rv1, LnCap	Docetaxel-resistance
DU145 Vs DU145RD cells	No affect [237]	DU145, 22Rv1	Motility & invasion
Pca Vs HC serum	Promote [237]	DU145, 22Rv1	Invasion & proliferation
Pre-tx Vs Post-tx PCa serum	Promote [237]	DU145, 22Rv1	Docetaxel-resistance
Fetal Bovine Serum	Promote [239]	MDA-MB-231, MCF-10A, MDA-MB-435	Anchorage independent growth
NIH3T3neu Vs NIH3T3 WT cells	Promote [240]	SKBR3	Trastuzumab-resistance
SKBR3 cells	Promote [240]	SKBR3	Trastuzumab-resistance
exosomes expressing FasL from activated CD8(+) T cells from OT-I mice	No affect [241]	B16, 3LL cells	Proliferation & apoptoisis
exosomes expressing FasL from activated CD8(+) T cells from OT-I mice	Promote [241]	B16, 3LL cells	Invasion
SUM149 cells	Promote [242]	Breast cancer cells: SUM149	Migration
A172 cells	Promote [242]	Glioma Cells: A172	Migration
MDCK cells overexpressing amphiregulin	Promote [243]	Lung metastatic cells from breast cancer (MDA-MB-231 cells): LM2-4175	Migration
Human mesenchymal stem cells	Promote [243]	Breast cancer cells: MCF7	Migration

Table 1.6: Examples of studies assessing the effects of exosomes when applied to secondary cells.

1.8 Potential use of miRNAs as therapeutic agents or as therapeutic targets for treatment of cancer

The growing list of reports indicating the significance of miRNAs in diagnosis and prognosis of breast and prostate cancer has led to the advancement of research to explore the potential relevance of miRNAs as therapeutics. An attractive attribute of miRNAs is their ability to target gene networks at multiple levels [244]. This finding, together with the observations that miRNAs can either promote or suppress tumourigenesis and metastasis, and have been found to be associated with tumour subtype and with response to systemic therapy, has stimulated efforts to modulate miRNA expression to reduce tumour development and metastasis, improve response to treatment, and prevent resistance to therapy.

Several methods exist that may be used to adjust miRNA expression, depending on whether the objective is to inhibit the expression of oncogenic miRNA(s) or to increase the expression of tumour-suppressive miRNA(s). Antisense oligonucleotides or their chemically tailored analogs (known as locked nucleic acids) may be used to inactivate an oncogenic miRNA; targeting the precursors of mature miRNAs can also inhibit production [245]. Such modalities may be considered as part of a treatment regime that also includes other small molecule/monoclonal antibody-targeted agents or chemotherapy. Alternatively, to increase the expression of a tumour suppressing miRNA (as a miRNA replacement-therapy), viral or liposomal delivery methods are showing promise in achieving miRNA introduction [as reviewed in [246]]. However, alternate approaches such as repetitive administration of miRNAs and exploitation of antibody-mediated endocytosis are also being considered as optimal routes for the delivery of small RNA therapeutics.

Although the therapeutic delivery of any new molecular type involves challenges in getting acceptance to move from preclinical to clinical investigation, miRNAs have the advantage that much of the fundamental work in this field is already at an advanced stage with regard to the delivery of antisense and siRNA therapeutics. Major clinical advances are currently underway in the ribonucleic-acid–based arena. For example, a phase IIb trial with an siRNA molecule termed ALN-RSV01 (Alnylam) for the treatment of respiratory syncytial virus infections has just been completed indicating it to be well tolerated and

associated with decreased incidence of new and progressive Bronchiolitis Obliterans Syndrome (www.clinicaltrials.gov, Trial Identifier: NCT01617967). In relation to cancer, a number of other RNA molecules are currently in phase I /II clinical trials, e.g., FANG currently in Phase II (Gadalis, Inc.) for the treatment of ovarian cancer (www.clinicaltrials.gov, Trial Identifier: NCT01309230); SPC2996 (Santaris Pharm.) completed Phase I/II for the treatment of relapsed Chronic Lymphocytic Leukaemi (www.clinicaltrials.gov, Trial Identifier: NCT00285103); ALN-VSP02 (Alnylam) completed Phase I for the treatment of patients with advanced solid tumours with liver involvement (www.clinicaltrials.gov, Trial Identifier: NCT00882180).

Several of the studies outlined in Tables 1.1-1.4 have indicated the potential for altering expression of many other miRNAs as a means to identify their function and/or their potential therapeutic relevance. The inhibition of miR-21 expression in MCF-7 breast cancer cells is a prime example of how antisense oligonucleotides may be used to manipulate the expression of an oncogenic miRNA [123]. miR-21 expression, known to be increased in breast cancer, has also been implicated in the modulation of the tumour suppressor, PTEN (phosphatase and tensin) [247], as well as a number of other targets indicated in Tables 1.1 and 1.3. miR-21 therefore may be another attractive therapeutic target, because PTEN has been reported to be a regulator of sensitivity to trastuzumab [248]. This concept is further supported because suppression of miR-21 has been shown to sensitize breast cancer cells to several anti-cancer treatments as shown in Table 1.4. The fact that miR-21 holds relevance in other cancers, as well as to breast cancer, also indicates its potential as a therapeutic target with vast application. However, miR-21 is not the only miRNA whose manipulation may be of benefit in sensitizing cancer cells to anti-cancer therapy. For example, miR-205 introduction into such cells increases response to Gefitinib and Lapatinib in breast cancer. Furthermore, miR-205 can sensitise prostate cancer cells to docetaxela and cisplatin treatment. Collectively, these observations support the possibility that modulating (singly or multiply) miRNA expression—through administration of, for example, premirs (also known as miRNA mimics) or antimirs (also known as miRNA inhibitors)—may be of clinical benefit when combined with chemotherapy or more targeted therapies.

Of course, development of the optimal delivery solutions for miRNA therapeutics as anti-cancer agents has its own challenges (e.g., identifying cancer cell–specific antigens

against which to target antibodies for steering delivery), and this remains an important component in realising such a therapeutic approach. miRNAs have the advantage that siRNA delivery has at least paved the way for the acceptance of the therapeutic use of small RNA molecules. Undoubtedly the relevance and potential of RNA-based therapeutics has been realised by pharmaceutical and biotechnology companies with several miRNA-based therapeutics entering clinical trials for the potential treatment of diseases. For example, miR-122 antagonist, miravirsen (Santaris Pharma) has just completed phase II clinical trials for hepatitis C with no adverse effects indicated (www.clinicaltrials.gov, Trial Identifier: NCT01200420). MiRNA Therapeutics, Inc. have recently entered phase I clinical trials with their miR-34 mimic (MRX034) for the treatment of patients with primary liver cancer or those with liver metastasis from other cancers (www.clinicaltrials.gov, Trial Identifier: NCT01829971).

These are but a few examples of how the exploitation of miRNA expression may be applicable to the future treatment of cancer. Although research in this area looks promising, the transition from bench to bedside still faces several obstacles. Depsite growing progress to date, the functional validation of cancer–associated miRNAs is still at a relatively early stage. The identification of further clinically relevant miRNAs will undoubtedly be important. To fully comprehend the significance of these short RNAs, it is imperative that all human miRNAs, in addition to those currently known, are identified and characterised in full. Standardisation of techniques involved in miRNA analysis and comprehensive collaborative studies (such as those proposed in Figure 1.7), with due consideration given to technical issues (e.g., type and number of miRNAs to be examined, experimental conditions, test sensitivity, specificity) are necessary if miRNAs are to reach their full potential in the clinical setting [97].

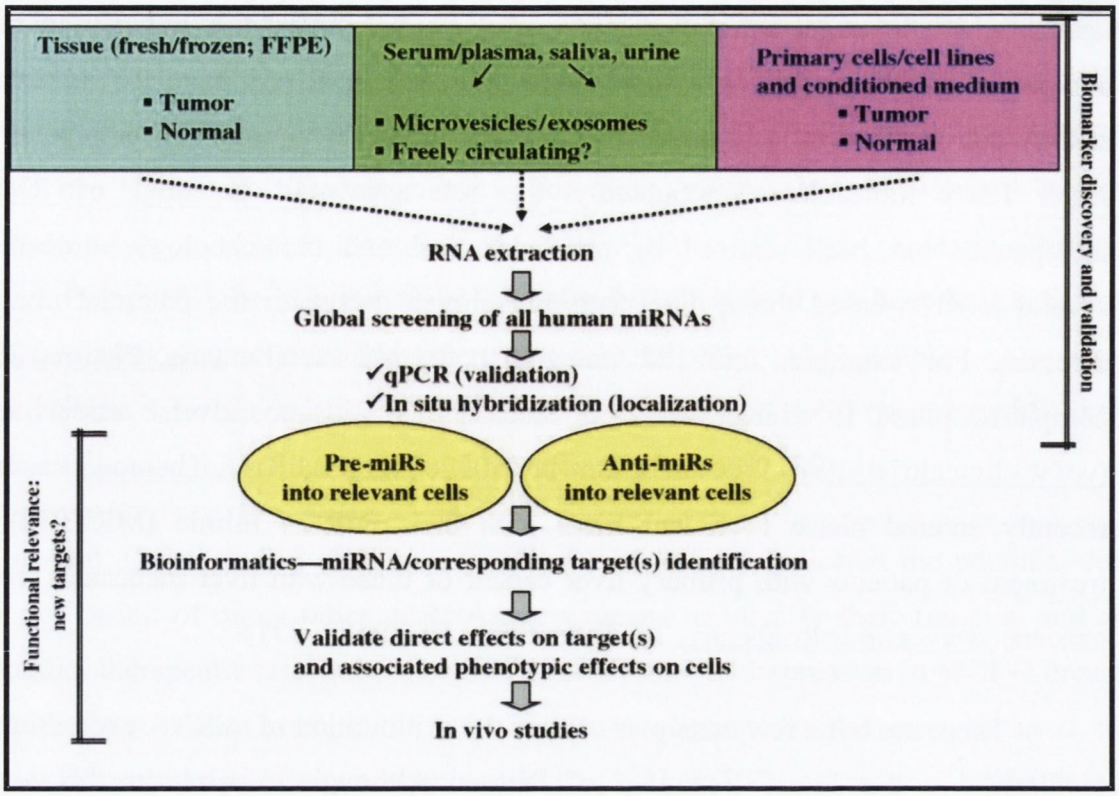

Figure 1.7: Example work plan for intracellular and extracellular miRNA analysis and the validation of miRNAs as biomarkers and/or potential new therapeutic targets.

Figure taken from Corcoran *et al.* [249].

1.9 **Project aims**

The primary aim of this study was to identify intracellular and extracelluar biomarkers predictive of response to anti-cancer therapies in HER2-overexpressing breast cancer and castration-resistant prostate cancer; some of which may also have relevance as new therapeutic targets.

- In relation to breast cancer, the initial aim of this study was to assess the presence and expression of miRNAs in the cells and conditioned media from the HER2-overexpressing breast cancer cell line SKBR3 and its trastuzumab (SKBR3-TR) and lapatinib (SKBR3-LR) resistant variants. Following global miRNA profiling and validation of key leads, the most interesting miRNA (miR-630) was then assessed in other lapatinib-resistant cells (HCC1954-LR), established in our laboratory, as well as neratinib-resistant variants (SKBR3-NR and HCC1954-NR).

  - Having identified miR-630 as a potential biomarker predictive of response to HER-targeted therapies, this study then aimed to perform functional analysis on miR-630 to confirm its role in HER2-overexpressing breast cancer.

  - Furthermore, this study aimed to identify the mechanism of action, as well as the clinical relevance, of miR-630.

  - One of the predicted mRNA targets of miR-630, Neuromedin U (NmU) was previously identified in our group as a potential regulator of resistance to HER-targeted therapies. Therefore, in collaboration with Dr. Sweta Rani (Post-Doctoral Research Fellow), the aim of this study was also to further explore the relevance of NmU in HER2-overexpressing breast cancer.

- In relation to prostate cancer, in order to assess docetaxel-resistance in castration-resistant prostate cancer and to identify biomarkers predictive of response to this treatment, an objective of this work was to develop docetaxel-resistant variants of two prostate cancer cell lines, DU145 and 22Rv1; to subsequently characterise these cells for cross-resistance (multiple drug-resistance) with other anti-cancer drugs; and to assess phenotypic characteristics of the cells. Docetaxel-resistant PC3 cells (a gift from Prof. William Watson- University College Dublin) were also included in this study.

  - This study also aimed to explore possible mechanisms of docetaxel-resistance;

  - To assess the secretion of and phenotypic effects of exosomes derived from the docetaxel-resistant cell line variants, on secondary cells.

  - To complete this body of work the final aim of this study was to perform intracellular and extracellular miRNA profiling of these docetaxel-resistant and sensitive prostate cancer cell lines and to identify key miRNAs relevant to docetaxel-resistance.

  - Where serum specimens were available or publically available datasets existed, this study also aimed to assess clinical relevance of exosomes and selected miRNAs in prostate cancer.

CHAPTER 2

Intracellular and extracellular miRNAs predictive of response to HER-targeted agents in the treatment of HER2-overexpressing breast cancer –A role for miR-630.

Parts of this chapter are included in the following paper submitted and currently under peer review:

miR-630 targets IGF1R to regulate response to HER-targeting drugs and overall cancer cell progression in HER2-overexpressing breast cancer

Claire Corcoran, Sweta Rani, Susan Breslin, Irene M. Ghobrial, John Crown, Lorraine O'Driscoll

2 ABSTRACT

Introduction: Primary or acquired-resistance limits the success of treatments for HER2-overexpressing breast cancer. microRNAs (miRNAs) have potential as diagnostic, prognostic and predictive biomarkers for such drugs, as well as replacement therapies.

Methods: Through global miRNA profiling, we investigated the levels of intra- and extracellular miRNAs in cells and conditioned media from breast cancer cell lines with acquired-resistance to HER-targeting drugs, trastuzumab and lapatinib, compared to their corresponding drug sensitive cell lines. We further assessed the relevance of one of these miRNAs, miR-630, in cells with acquired neratinib (Phase III drug)-resistance, and cells with innate-resistance to HER-targeting agents. To support the role of miR-630 in breast cancer, we examined the clinical relevance of this miRNA in breast cancer tumours *versus* matched peritumours. Transfection of miR-630 mimics and inhibitors was used to manipulate the expression of miR-630 to assess effects on response to HER-targeting drugs (lapatinib, neratinib and afatinib). Other phenotypic changes associated with cellular aggressiveness were evaluated by motility, invasion and *anoikis* assays. TargetScan prediction software and immunoblotting were used to assess proteins potentially regulated by miR-630, to understand its mechanism of action. Cells with stable miR-630 overexpression or knockdown were established, using lentiviral transduction; potentially for future potential *in vivo* studies.

Results: We demonstrated that introducing miR-630 into cells with innate- or acquired-resistance to HER-drugs significantly restored the efficacy of lapatinib, neratinib and afatinib; through a mechanism which we have determined to, at least partly, involve miR-630's regulation of IGF1R. Conversely, we demonstrated that blocking miR-630 induced resistance/insensitivity to these drugs. Cellular motility, invasion, and *anoikis* were also observed as significantly altered by miR-630 manipulation, whereby introducing miR-630 into cells reduced cellular aggression while inhibition of miR-630 induced a more aggressive cellular phenotype. Stable knockdown of miR-630 may elicit partial drug-resistance, increased proliferation and invasion.

Conclusion: Taken together, our findings suggest miR-630 as a regulator of cancer cell progression in HER2-overexpressing breast cancer, through targeting IGF1R. This

study suggests miR-630 as a diagnostic and predictive biomarker for response to HER-targeted drugs and indicates that the therapeutic addition of miR-630 may enhance and improve patients' response to HER-targeting drugs.

2.1 INTRODUCTION

Approximately a quarter of all breast cancers are associated with the HER2-overexpression [15]. Amplification of the HER2 gene has been associated with more aggressive disease and, prior to the development of HER-targeted therapies, had an overall poor prognosis [250]. Since the initial development of trastuzumab (Herceptin); the use of lapatinib (Tykerb) a small-molecule receptor tyrosine kinase inhibitor (RTKI) that dually targets human epidermal growth factor receptor 2 (HER2) and epidermal growth factor receptor (EGFR/HER1)) have vastly improved clinical benefit in recent years [19, 251]. Unfortunately, evidence of innate- or acquired-resistance to these drugs [20, 21, 252, 253] indicates that, despite their initial success in the treatment of HER2-overexpressing cancers, their use in the clinic is becoming somewhat compromised. Newer HER-targeting drugs including neratinib (HK1-272) and afatinib (BIBW 2992), both of which are irreversible oral small molecule RTKIs of target HER2, EGFR/HER1 and HER4, are producing promising results in clinical trials [27, 28]. Unfortunately, it is probable that these drugs will eventually be faced with similar problems due to resistance as that of their predecessors.

There is an urgent need to identify predictive biomarkers for HER-targeting drugs in order to improve patients' stratification and, subsequently, patients' outcome. microRNAs (miRNAs) are small (approximately 18–25 nucleotides long) non-protein coding RNAs that have been associated with regulating gene expression, typically at a post-translational level [249]. In general, miRNAs are considered as negative regulators of gene expression. For example, miRNAs acting as tumour suppressors are responsible for controlling the levels of genes promoting tumourigenesis and are often decreased in cancerous compared to normal cells [114].

In this study, global miRNA analysis was initially performed on acquired trastuzumab- and lapatinib-resistant SKBR3 cell lines compared to drug-sensitive age-matched parent cells in an effort to identify miRNAs that may regulate acquired drug-resistance. We also aimed to investigate the miRNA expression profiles in the extracellular environment (by evaluating the conditioned media) of the cells themselves as a means of identifying cell-derived miRNAs that may be used as potential minimally-invasive biomarkers. Advancing on the global profiling and associated data analysis, miR-630 was

identified as significantly decreased with drug-resistance and so chosen for further study. miR-630 has previously been reported to regulate cisplatin-induced cell death in both non-small cell lung cancer and head and neck cancer [254, 255]. In a separate study, inhibition of miR-630 in lung cancer cells was found to be associated with an increase in cellular migration and invasion [256]. Furthermore, the overexpression of miR-630 has recently been implicated in degradation of Insulin Growth Factor Receptor 1 (IGF1R) mRNA and protein levels and subsequent enhanced apoptosis in pancreatic cancer cells [257]. The relevance of further studying this target was confirmed by our finding that miR-630 was significantly decreased in breast cancer tissue compared to matched peritumour tissue. Subsequent studies were performed to investigate if manipulation of miR-630 can influence cellular response to HER-targeted agents, lapatinib, neratinib and afatinib and the mechanism behind miR-630's action. In addition, miR-630's effect on motility, invasion and *anoikis* assays was also assessed. Here we also report on preliminary findings performed on stable cell lines that may be used for future *in vivo* related studies.

2.2 METHODS

2.2.1 Cell Culture and Treatments

SKBR3, HCC1954, BT474, EFM-192A, MDA-MB-361, HCC1569, UACC812 and UACC893 cells, obtained from ATCC, were cultured in RPMI-1640 (Sigma-Aldrich, Cat #: R0883) with 10% FCS (PAA Cat. #: A15-151) and 1% L-glutamine (Sigma-Aldrich, Cat. #: G7513). MDA-MB-453, a gift from Dr. Kornelia Polyak (Dana Farber Cancer Institute) were cultured in McCoys 5A (Sigma-Aldrich, Cat. #: M8403) with 10% FCS and 1% L-glutamine. HEK293T cells were a gift from Dr. Irene Ghobrial (Dana Farber Cancer Institute) cultured in DMEM (Sigma-Aldrich, Cat. #: D5671), 10% FCS and 1% L-glutamine. All cells were grown in at 37°C/5% CO_2 with the exception of UACC812 and UACC893 cells which were grown in CO_2 deficient conditions. UACC812 and UACC893 cells were cultured in L15 media (Invitrogen, Cat. #: 1145049) with 10% FCS and 1% L-glutamine. Lapatinib-resistant SKBR3 and HCC1954 cells (SKBR3-LR and HCC1954-LR, respectively- developed by Dr. Sweta Rani, Post-Doctoral Research Fellow) were established by continuously exposing cells to lapatinib, starting with 5nM and increased stepwise to 250nM over 6 months. Similarly, neratinib-resistant cells (SKBR3-NR, HCC1954-NR developed by Susan Breslin) were established by continuously exposing cells to neratinib, increasing stepwise to 80nM (for SKBR3-NR) and 250nM (for HCC1954-NR) for over 4 months. SKBR3 trastuzumab-resistant variants (SKBR3-TR) were established through exposure to trastuzumab over a period of 6 months and were kindly provided by Dr. Norma O'Donovan (Molecular Therapeutics for Cancer Ireland, Dublin City University). For each drug-resistant cell line established, age-matched parent cells (SKBR3-Ag, HCC1954-Ag) were maintained in culture, in parallel, but were not exposed to drug. Working banks of all cell line variants were cryopreserved (freezing media at a final concentration of 5% Dimetyl Sulfoxide (DMSO, Sigma-Aldrich, Cat. #: D2650)) and stored in liquid nitrogen. All experiments on acquired-resistant cells and corresponding aged controls were performed within 10 passages in culture and were performed on cells that receieved no drug for a minimum of one week. Passage numbers used were approximately the following: SKBR3-LR/-Ag (p95-105); HCC1954-LR/-Ag (p74-84); SKBR3-NR/-Ag (p99-109); HCC1954-NR/-Ag (p70-80); SKBR3-TR/Ag- (p85-95). Cells were routinely tested for *Mycoplasma* contamination using the PCR Mycoplasma Test Kit 1/RT Variant B (Promocell, Cat. #: PK-CA91-3025B) and were

found to be negative. Lapatinib (Cat. #: SRP01210l), neratinib (Cat. #: SRP06000n) and afatinib (Cat. #: SRP037103a) were obtained from Sequoia Research Chemicals Ltd. (Pangbourne UK). Lapatinib, neratinib and afatinib were prepared in DMSO to a concentration of 10mM and stored in aliquots at -20°C. Working stocks of 10μM were prepared fresh every week as necessary and for each biological replicate of toxicity assays. Trastuzumab was provided by St. James's University Hospital, Dublin; prepared at 21mg/ml in Bacteriostatic Water for Injection and stored at 4°C. Working stocks of 1mg/ml were prepared fresh every week as necessary and for each biological replicate of toxicity assays

2.2.2 Conditioned Media collection and filtration

SKBR3 parent cells and variants SKBR3-TR and SKBR3-LR were seeded in 75cm^2 cell culture flasks (Costar, Cat. #: CLS430641) at 2x10^6 cells per flask with 10ml of culture medium. A minimum of triplicate flasks of each cell line cells were prepared. When cells were approximately 80% confluent, fresh medium was replaced on the cells and this medium was then "conditioned" for a further 48hrs. This conditioned medium (CM) was subsequently collected and passed through a 0.45μm filter (VWR, Cat. #: 4564). 250μl aliquots of filtered conditioned medium (CM) were added to TriReagent™ (Sigma-Aldrich, Cat. #:T9429) (750μl TriReagent + 250μl CM). These were incubated for 5-10mins on ice (to ensure complete dissociation of nucleoprotein complexes) prior to freezing and were subsequently stored at -80°C until required for analysis. The corresponding cultured cells were trypsinised, counted and centrifuged (130g for 5mins) to form a pellet. Following washing in Phosphate Buffered Saline (PBS) (Sigma-Aldrich, Cat. #:D8537) (X2 times), cell pellets were re-suspended in 1ml TriReagent™ and were, subsequently, incubated and stored as above.

2.2.3 RNA Isolation and Quantification

Total RNA was isolated from CM and pelleted cells by extracting with TriReagent™ with modifications/"optimisation" of the manufacturer's instructions, developed during the course of this study. In brief, 0.2ml of chloroform (Sigma-Aldrich, Cat. #:C4342) was added to each sample and this was shaken vigorously for 15secs, followed by incubation at room temperature for 15mins. This was then centrifuged at 12,000g for 15mins at 4°C, and the aqueous phase containing RNA (upper layer) was removed and transferred into a fresh

RNAse-free 1.5ml Eppendorf tube (Sigma-Aldrich, Cat. #:Z606340). Isopropanol (Sigma-Aldrich, Cat. #: I9516) (0.5ml) and glycogen (Sigma-Aldrich Cat. #:G8751) (final concentration 120µg/ml) were added, incubated at room temperature for 5-10mins and was stored at –20°C over-night, to ensure maximum RNA precipitation. Eppendorf tubes were then centrifuged at 12,000g for 30mins at 4°C to pellet the precipitated RNA. Taking care not to disturb the RNA pellet, supernatant was removed and the pellet was subsequently washed by the addition of 750µl of 75% ethanol (Sigma-Aldrich, Cat. #: E7418) and vortexing. Following centrifugation at 7,500g for 5mins at 4°C, supernatant was removed (this wash step was repeated). The RNA pellet was then allowed to air-dry for 5-10mins and subsequently was re-suspended in 10µl (for CM-derived RNA) and 30µl (for cell-derived RNA) of DEPC-treated H_20 (Ambion, Cat. #: AM9916). Quantity and quality of RNA isolated was assessed on the Nanodrop-ND 1000 spectrophotometer.

2.2.4 Global miRNA profiling using Taqman Low Density Arrays

The Applied Biosystems (ABI) Taqman microRNA Low Density Arrays (TLDA) (Life Technologies) were selected as the platform for microRNA profiling. Taqman array Human microArray A+B cards Set v2.0 (Life Technologies, Cat. # 4400238) of 2 arrays: TLDA panel A (377 functionally defined microRNAs) and TLDA panel B (290 microRNAs whose function were not yet completely defined) resulting in a total of 667 microRNA assays. RNA (400ng) was pooled from the cells of each replicate for each cell line and, seperately RNA (30ng) was pooled from the corresponding replicates of CM prior to performing reverse transcription for TLDAs (Figure 2.1).

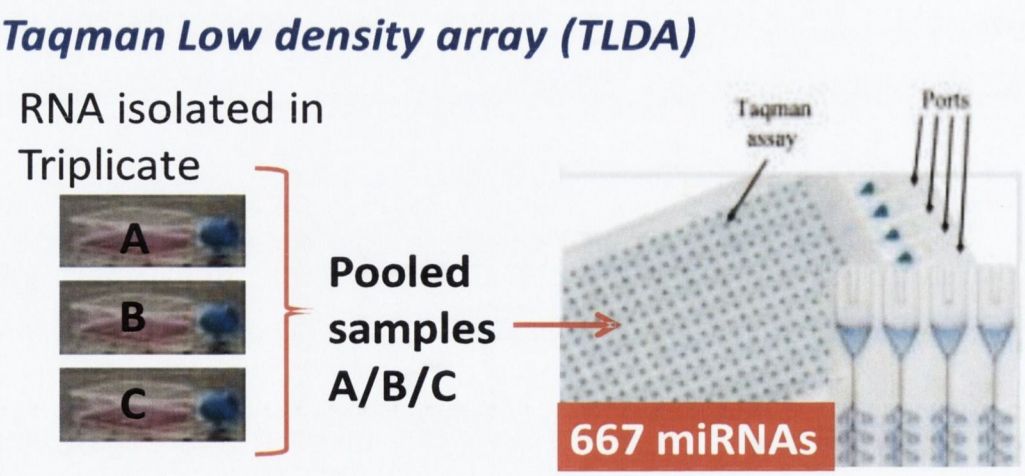

Figure 2.1: Taqman Low Density Arrays

2.2.4.1 Reverse transcription for TLDA

RNA reverse transcription to cDNA was performed according to the ABI microRNA TLDA Reverse Transcription (RT) Reaction protocol. In brief, the Megaplex Primer Pools, Human Pool Set v2.0 (Applied Biosystems, Cat. #:4400928) and TaqMan MicroRNA Reverse Transcription Kit components (Applied Biosystems, Cat. #: 4366595) were thawed on ice. Two RT master mixes per sample, one for each TLDA panel (panel A and panel B) were prepared as indicated in Table 2.1, with all volumes scaled for the number of reactions required.

MegaPlex RT primers (10x) (Applied Biosystems, Cat. #:4400928)	0.80µl
dNTPs with dTTP (100mM) (Applied Biosystems, Cat. #: 4366595)	0.20µl
MultiScribe ReverseTranscriptase (50U/µl) (Applied Biosystems, Cat. #: 4366595)	1.50µl
10x RT Buffer (Applied Biosystems, Cat. #: 4366595)	0.80µl
$MgCl_2$ (25mM) (Applied Biosystems, Cat. #:4400928)	0.90µl
RNase Inhibitor (20U/µl) (Applied Biosystems, Cat. #: 4366595)	0.10µl
nuclease-free water (Ambion, Cat. #: AM9916)	0.20µl

Table 2.1: Volumes of components used for TLDA Reverse Transcription Reaction.
All components except for water were part of either the Megaplex Primer Pools, Human Pool Set v2.0 (Applied Biosystems, Cat. #:4400928) or the TaqMan MicroRNA Reverse Transcription Kits (Applied Biosystems, Cat. #: 4366595).

Three µl of pooled RNA (equal volumes of aliquots from each biological replicate were pooled) were loaded into appropriate wells of a 96-well plate containing 4.5µl RT reaction mix and incubated on ice for 5mins. The thermal cycling conditions used in the ABI 9700 thermal cycler with maximum ramp speed are indicated in Table 2.2.

1x cycle	40x cycles	Hold	Hold	Hold
16°C, 2mins	42°C, 1min	50°C, 1sec	85°C, 5mins	4°C, forever

Table 2.2: Thermal cycling conditions used for TLDA Reverse Transcription Reaction

2.2.4.2 Pre-amplification reaction for RNA diluted from CM

Due to the low quantity of RNA isolated from the CM, a pre-amplification step was used before TLDAs were performed. The cDNA product (2.5µl per sample) was pre-amplified according to the ABI TLDA pre-amplification protocol. A total of 22.5µl of pre-amplification reaction mix was prepared as indicated in Table 2.3.

TaqMan PreAmp Master Mix (2x) (Invitrogen Cat. #:4391128)	12.5µl
Megaplex PreAmp Primers (10x) (Invitrogen, Cat. #:4400928)	2.5µl
Nuclease-free H_2O (Ambion, Cat. #: AM9916)	7.5µl

Table 2.3: Volumes of components used for the pre-amplification reaction.

This pre-amplification mix was added to the cDNA product, derived from Table 2.1, in a 96-well optical plate sealed with MicroAmp Clear Adhesive Film (Applied Biosystems, Cat. # 4306311). The plate was spun briefly and incubated on ice for 5 min. The pre-amplification was conducted in the ABI 9700 thermal cycler using standard ramp speed and following thermal cycling conditions indicated in Table 2.4.

Hold	Hold	Hold	12x cycles	12x cycles	Hold
95°C, 10 min	55°C, 2 min	72°C, 1 sec	95°C, 15 sec	60°C, 4 min	4°C, forever

Table 2.4: Thermal cycling conditions used for the pre-amplification reaction.

Following the pre-amplification reaction, the pre-amplification product 25µl was diluted with 75 µL of 0.1× TE pH 8.0 (Ambion, Cat. #AM9858)

2.2.4.3 Real Time Assay

TLDA TaqMan Real Time Assay was set up for each specimen and was prepared as follows: 450µl of TaqMan Universal PCR Master Mix-No AmpErase®UNG (2x) (Applied Biosystems, Cat. #4440048) was added to 9µl of diluted product following pre-amplification (in this case of CM samples – see section 2.2.4.2) or 6µl of cDNA product (in the case of cell samples) in a 1.5ml RNase-free microcentrifuge tube containing

441µl or 444µl of nuclease-free water, respectively. The reaction was mixed by inverting the tube 6 times and then briefly centrifuging. One hundred µl aliquots of the PCR reaction mix were loaded into each port of the TLDA array. The TLDA plate was centrifuged with 9 up-and-down ramp rates at 331g for 1 min and loaded into the 7900 HT Sequence Detection System using the 384-well TaqMan Low Density Array default thermal-cycling conditions.

2.2.4.4 TLDA Data analysis

TLDA were run in the 7900 HT Sequence Detection system. The ABI TaqMan SDS v2.3 software was utilised to obtain raw C_T (cycle threshold) values. Fold changes (of miRNAs detected for resistant variants (SKBR3-TR and SKBR3-LR) compared to age-matched parent cells (SKRB3-Ag)) were calculated by global mean normalisation as previously described [258]. Normalisation was performed as below:

ΔC_T =C_T cell line variant – mean C_T for all expressed (<35C_T) miRNAs for that variant

$\Delta\Delta C_T$= ΔC_T Resistant variant – ΔC_T parental

Where, C_T = Cycle threshold at which the miRNA was detected

Fold change = $2^{(-\Delta\Delta CT)}$

For example:

ΔC_T for SKRB3-Ag = 25.984 (C_T for miRNA for SKBR3-Ag) – 29.4 (mean C_T) = **1.164**

ΔC_T for SKBR3-LR = 31.524 (C_T for miRNA for SKBR3-LR) – 30.3 (mean C_T) =**-3.416**

$\Delta\Delta C_T$ for SKRB3-Ag = 1.164-1.164 = 0

$\Delta\Delta C_T$ for SKBR3-LR = -3.164 – 1.164 = 4.58

Fold change for SKBR3-Ag = $2^{(-\Delta\Delta CT)} = 2^{(0)} = 1$

Fold change for SKBR3-LR = $2^{(-\Delta\Delta CT)} = 2^{(-4.58)}$

0.0418 fold change ⇔ 1/0.0418 = 23.9 fold decreased

2.2.5 Validation- Quantitative Real Time Polymerase Chain Reaction (qPCR)

2.2.5.1 cDNA synthesis

qPCR was performed on individual biological replicates to validate the expression of selected miRNAs from TLDA analysis. Selection criteria was based on miRNAs that were differentially expressed in the resistant cell lines >1.2 fold compared to the sensitive parent cells; that had commonly expressed trends in cells and CM; novelty and relevance to literature. A cut off of 1.2 fold change among experimental conditions has been previously used in several microRNA profiling studies [259-261]. Synthesis of single stranded cDNA from total RNA samples (10ng for cells and 4µl CM-derived total RNA) was performed using the Taqman MicroRNA Reverse Transcription (RT) Kit (Applied Biosystems, Cat. #: 4366595) and according to the Applied Biosystems protocol. In brief, each 15µl reaction (per single RNA sample) consisting of the components of the Taqman MicroRNA Reverse Transcription Kit as outlined in Table 2.5 was prepared with the addition of 3µl RT Primer and 5µl (Cell -10ng) or 4µl (CM) total RNA. Volumes listed in Table 2.5 are for one reaction and were scaled to the number of desired RT reactions.

Reaction Mix	Cell sampl	CM samples
100mM dNTPs	0.15µl	0.15µl
MultiScribe Reverse Transcriptase	1µl	1µl
10X MultiScribe ReverseTranscriptase Buffer	1.50µl	1.50µl
RNase Inihibitor	0.19µl	0.19µl
nuclease-free water (Ambion, Cat. #: AM9916)	4.16µl	5.16µl
RNA	5µl	4µl

Table 2.5: Volumes of components used for RT Reaction for Taqman miRNA assays.
All components except for water were part of TaqMan MicroRNA Reverse Transcription Kit (Applied Biosystems, Cat. #: 4366595).

The reaction was mixed and dispensed into a single well (per reaction) of a MicroAmp Fast Optical 96-well Reaction Plate (Applied Biosystems, Cat. #: 4346907). The plate was sealed with MicroAmp clear adhesive film (Applied Biosystems, Cat. # 4306311) and incubated on ice for 5mins. The reverse transcription was conducted in the ABI 9700

thermal cycler using standard ramp speed and the thermal cycling conditions indicated in Table 2.6.

Hold	Hold	Hold	Hold
16°C, 30mins	42°C, 30mins	85°C, 5mins	4°C, forever

Table 2.6: Thermal cycling conditions used for RT Reaction for Taqman miRNA assays.

2.2.5.2 PCR Amplification

PCR amplification was performed according to the Applied Biosystems protocol for TaqMan MicroRNA Assays. In brief, each 20µl reaction (per single cDNA sample) consisted of 10µl TaqMan 2X Universal PCR Master Mix, No AmpErase UNG (Applied Biosystems, Cat. #: 4440048), 7.67µl Nuclease-free water (Ambion, Cat. #: AM9916), 1µl 20X Taqman microRNA Assay mix, 1.33µl RT product. The reaction was mixed and dispensed into a single well (per reaction) of a MicroAmp Fast Optical 96-well Reaction Plate (Applied Biosystems, Cat. #: 4346907). The plate was sealed with MicroAmp optical adhesive cover (Applied Biosystems, Cat. #: 4311971) and centrifuged briefly to spin down contents and eliminate any air bubbles. The PCR reaction was conducted in the ABI 9700 thermal cycler using standard ramp speed, 9600 emulation run mode and the thermal cycling conditions indicated in Table 2.7.

Hold	40x cycles	40x cycles
95°C, 10mins	95°C, 15sec	60°C , 1min

Table 2.7: Thermal cycling conditions used for real time PCR for Taqman miRNA assays.

Taqman miRNA assays (Applied Biosystems, Cat. #: 4427975) were used to quantify miR-572 (Assay ID #: 001614), miR-502-5p (Assay ID #: 001109), miR-487b (Assay ID #: 001285), miR-520f (Assay ID #: 001120), miR-616* (Assay ID #: 001589), miR-135a* (Assay ID #: 002232) and miR-630 (Assay ID #: 001563). miRNAs were quantified using the cycle threshold (C_T) adjusting to the levels of U6 snRNA (Assay ID #: 001973) used as an endogenous control.

2.2.6 Assessment of miR-630 expression in patient derived breast tissue

miR-630 expression in breast cancer [all breast tissue (n=56), HER2+ breast tissue (n=6) basal-like (n=7) and luminal (n=43)] was determined based on previous miRNA profiling of breast tumours and matched peritumours using a publically available data set (GSE40525) on Gene Expression Omnibus (GEO) (http://www.ncbi.nlm.nih.gov/geo/) [262]. miR-630 expression levels, p-values and Log fold change (Log FC) between groups were determined using the GEO2R analysis function.

2.2.7 microRNA inhibition or mimic transient transfection into cells

Drug sensitive SKBR3-Ag and HCC1954-Ag cells were transfected with 30nM of miR-630 inhibitor (Applied Biosystems, Cat. #: 4464084, ID: MH11552) or miRNA inhibitor negative control (Applied Biosystems, Cat. #: 4464076). To achieve this, cells were seeded in 24-well plates (in 500µl medium) at a density of $5x10^4$/well for SKBR3-Ag and $2.5x10^4$/well for HCC1954-Ag cells. Transfection was performed at the same time as seeding of the cells. Similarly, acquired- or innately-resistant SKBR3-LR ($5x10^4$/well), HCC1954-LR ($2.5x10^4$/well) and MDA-MB-453 ($5x10^4$/well) cells were transfected with 30nM miR-630 mimic (Applied Biosystems, Cat. #: 4464066, ID MH11552) or miRNA mimic negative control (Applied Biosystems, Cat. #: 4464058). Transfection was performed using lipofectamine 2000 (Invitrogen, Cat. #: 11668-027) and opti-MEM (Invitrogen, Cat. #:11058-021) following manufacturer's instructions. In brief, two master mixes were prepared and scaled up depending on the number of wells of cells to be transfected. Mix A contained: lipofectamine (1µl/well in a 24-well plate) and opti-MEM (50µl/well in a 24-well plate); Mix B contained: 30nM of the inhibitor or mimic in question and opti-MEM (50µl/well in a 24-well plate). Both mixtures were incubated for 5mins at room temperature before equal volume of Mix A was added to the Mix B. The combined transfection mixture was incubated for a further 20mins at room temperature before 100µl was added to each well in the 24-well plate. All functional assays were performed 48hrs post-transfection.

2.2.8 *Assessing effects of miR-630-regulated cellular response to HER-targeting drugs*

Following transfection with miR-630 inhibitor, miR-630 mimic or their relevant negative controls, cells were exposed to their approximate IC_{50} concentrations of lapatinib (as indicated Table 2.10 & 2.11) previously been determined by ourselves and/or others [263-266]. Fixed concentrations of neratinib and afatinib were also used (see Table 2.10 & 2.11). Following 72hrs incubation with the given drug, cell proliferation was assessed using acid phosphatase analysis.

2.2.9 *Acid Phosphatase analysis- as used for proliferation and toxicity assays*

Medium was removed from plates and cells were washed twice in PBS (Sigma-Aldrich, Cat. #: P8537). Sodium acetate buffer was prepared as follows:

-500 ml dH_2O
-4.1g sodium acetate (Sigma-Aldrich, Cat. #: S2889)
-500 µl of Triton X-100 (Sigma-Aldrich, Cat. #: T8787)
- pH to 5.5 with HCl (Sigma-Aldrich, Cat. #: H1758)

Immediately prior to use, p-nitrophenol phosphate (VWR, Cat. #: 27963.101) was added to sodium acetate buffer at a concentration of 0.027g of 10mM p-nitrophenol phosphate per 10ml buffer and was scaled up according to the number of plates required; allowing 10ml per plate. 200µL of freshly prepared substrate-containing buffer (10mM p-nitrophenyl phosphate in sodium acetate buffer) was added to each well (of a 24-well plate; 100µl would be added to wells of a 96-well plate). The plates were wrapped in aluminium foil and placed in the incubator ($37^{o}C/5\%$ CO_2) for approximately 1.5hrs. After incubation, the reaction was stopped by adding 1M NaOH (100µl per well of 24-well plate and 50µl per well of 96-well plate). The absorbance was read at 405nm on a FlouStar Optima microplate reader (BMG Labtech).

2.2.10 Protein quantification and Immunoblotting

Cell pellets were lysed using Cell Extraction Buffer (Invitrogen, Cat. #: FNN0011) with the addition of protease and phosphatase inhibitors as appropriate (Roche, Cat. #: 05892970001; Cat#: 04906837001). Cell/lysis buffer suspensions were incubated in ice for 30mins with vortexing every 10mins. Lysates were centrifuged at 13,000g for 15mins at 4°C and resulting supernatants (containing protein) was transferred to a fresh eppendorf tube. Protein was quantified using BioRad protein assay Dye Reagent (BioRad, Cat. #:500-0006). In brief, an aliquot of protein was diluted 1:10 (for concentrated protein) with water and 10µl of this protein was placed into the well of a 96-well plate (duplicate wells for each sample were set up). BSA standards were prepared ranging from 1mg/ml and serially diluted to 25µg/ml. BioRad Dye reagent was diluted 1:4 with water and 200µl of this solution was added to each well containing protein or standards. The plate was incubated at room temperature in the dark for 5mins before being read at 595nm a FlouStar Optima microplate reader (BMG Labtech).

Total cellular proteins 30µg for HER2 and EGFR; 50µg for IGF1R and 100µg for NmU were resolved on PAGEr Gold precast gels for protein electrophoresis (Lonza). The following percentage gels were used: 7.5% (Lonza, Cat. # 59513) for EGFR and HER2; 10% (Lonza, Cat. #: 59514) for IGF1R, and 12% (Lonza, Cat. #: 59515) for NmU. Proteins were transferred to PVDF membranes (Bio-Rad laboratories, Cat. #: 162-0177). Blots were incubated in blocking buffer [5% BSA (Sigma-Aldrich, Cat. #A9413) in PBS/0.1% Tween (Sigma-Aldrich, Cat. #: P2287)] at room temperature for 1hr. Primary antibodies were prepared in 5% BSA in PBS/0.1% Tween and diluted as follows: HER2 (Calbiochem, CAT. #: OP15; 1:500 dilution); EGFR (Cell Signalling, D38131; 1:1000 dilution); IGF1R (Santa Cruz, Cat. #: SC-713; 1:1000 dilution); NmU (Sigma-Aldrich, Cat. #: SAB1401542; 1:200 dilution); β-actin (Sigma-Aldrich, Cat. #: A5316; 1:1000 dilution). Membranes were incubated in primary antibodies over night at 4°C. Membranes were then incubated with appropriate horseradish peroxidase-conjugated secondary antibodies i.e. anti-mouse (Cell Signalling, Cat. #: 7074; 1:1000 dilution) or anti-rabbit (Cell Signalling, Cat. #: 7076; 1:1000 dilution) for 1hr at room temperature and proteins were visualized by chemiluminescence (Themofisher: Cat. #: 34080). Detection was performed with a Chemidoc exposure system (Bio-Rad Laboratories). Densitometry on the

bands of protein expression was performed using NIH ImageJ software and normalised to the loading control (β-actin).

2.2.11 Cell motility –assessed using wound healing assays

Transfected cells ($3x10^5$ cells/well for SKBR3 cell line variants and $2x10^5$/well for HCC1954 cell line variants) were seeded on 24-well plates and cultured for 24hrs to confluency. Monolayers were scratched with a 200µl pipette tip and the resulting wounded areas were photographed using CellA software and measured using NIH ImageJ software. Throughout the duration of monitoring wound closure, cells were maintained in low serum (0.1%) containing medium to reduce any influences due to proliferation. Medium was changed before each time point was photographed.

2.2.12 Cell migration and invasion –assessed using transwell inserts

Assays were performed using 8µm pore size 24-well Transwell chambers (Unitech, Cat. #: 353097). For invasion assays, the inserts were pre-coated with extracellular matrix (ECM) (Sigma-Aldrich, Cat. #: E1270). Migration and invasion assays were performed using transfected cells (HCC1954 variants, $5x10^4$/insert; SKBR3-Ag, $1x10^6$/insert; SKBR3-LR, $5x10^5$/insert) were seeded in the upper compartment and allowed to migrate for 48hrs (HCC1954 variants) and 72hrs (SKBR3 variants), respectively. Cells were seeded in low serum (0.1%) containing medium in the upper chamber and 10% serum-containing medium in the well below the insert. Cells in the upper chamber were physically removed using a cotton swab soaked in PBS and migrated/invaded cells were stained with crystal violet (Sigma-Aldrich, Cat. #: C6158). Staining was solubilized in 10% acetic acid and absorbance was measured at 595nm on a FlouStar Optima microplate reader (BMG Labtech).

2.2.13 Anoikis assay

Anoikis is a form of apoptosis induced by the loss of cell anchorage. For *anoikis* assays, plates were coated with poly(hydroxyethyl methacrylic) acid (poly-hema) (Sigma-Aldrich, Cat. #: P3932) made to 12mg/ml (in 95% ethanol), 200µl per well allowed and allowed to dry overnight in the laminar flow cabinet. A second coating was performed and allowed to dry overnight again. Before seeding cells, coated plates were washed twice with

PBS (Sigma-Aldrich Cat. #: D8537). As a control, plates were also set up and coated with just 95% ethanol. Transfected cells ($1x10^4$cells/well) were seeded onto a 24-well plate coated with poly-hema (Sigma-Aldrich, Cat. #: P3932) or 95% ethanol and were cultured for 48hrs. Alamar blue dye (100µl; Invitrogen Cat. #DAL1100) was added/well and absorbance read at 570nm on a FlouStar Optima microplate reader (BMG Labtech). Percentage cell death of cells grown on poly-hema was calculated against cells grown without poly-hema coating.

2.2.14 Generation of stable miR-630 knockdown and miR-630 precursor cells

2.2.14.1 Lentiviral transduction of mcherry/LUC

mCherry is a red fluorescent protein that can be visualised using confocal or fluorescence microscopy. Luciferase (LUC) is an enzyme that can catalyse the oxidation of luciferin and ATP to produce light that can be visualised for bioluminescence studies. Both mcherry and LUC can be used for *in vivo* imaging. SKBR3 cells overexpressing mcherry/LUC (SKBR3 mcherry/LUC+) were kindly provided Dr. Kornelia Polyak's group in DFCI. For lentiviral transduction of HCC1954 cells to overexpress mcherry/LUC+ initially (this virus was also provided by Dr. Polyak's group in DFCI and its use has also been previously been reported [267-269]), cells (HCC1954) were seeded into 6 well plates. When cells were approximately 70% confluent the virus was diluted 1:2 ratio with complete growth medium and 8µg/ml polybrene (Sigma-Aldrich, Cat. #: H9268) which was placed onto the cells. Following 48hrs incubation (37°C, 5% CO_2), virus was removed and replaced with regular growth medium containing the appropriate selection antibiotic [in this case 2µg/ml puromycin (Invitrogen Cat. #: A11118-03)]. Cells surviving following antibiotic selection were cultured for subsequent analysis and stocks were cryopreserved

2.2.14.2 Generation of lentiviruses for miR-630 inhibitor and precursor

The vector map information for all constructs used in this section is shown in Appendix I, Section A & B. A sample of the miR-630 and scrambled inhibitor and precursor plasmids were sent to Eurofins for sequencing using the primer walking service. The obtained sequence read outs were aligned with the expected sequences for each construct using MultiAlign software. Blast software was used to confirm that the miR-630 inhibitior and precursor constructs were matched to miR-630 and that the scrambled

constructs did not show similarity with any other transcript (Appendix I, Section C, Figure C.1-C.8).

HEK293T packaging cells were seeded at a density of $1x10^7$/ml into 10cm dishes in 10ml medium (DMEM containing 10% FBS). After 24hrs, when the cells were approximately 70% confluent, transfection was performed. A mixture of three transfection plasmids was prepared comprising of 3μg of packaging plasmid (pCMV-dR8.91; Appendix I, Figure A.1), 3μg envelope plasmid (VSV-G/pMD2.G; Appendix I, Figure A.2), 3μg of the plasmid interest [in this case all plasmids for the miR-630 study were purchased from Genecopeia: miR-630 precursor (Cat. #:HmiR0257-MR03, Appendix I, Figure B.1), scrambled precursor (Cat. #: CmiR0001-MR03; Appendix I, Figure B.1); miR-630 inhibitor (Cat. #: HmiR-AN0740-AM03; Appendix I, Figure B.2); and scrambled inhibitor (Cat. #:CmiR-AN0001-AM03; Appendix I, Figure B.2)] and opti-MEM (Invitrogen, Cat. #:11058-021) to a final volume of 90μl. A separate mix of lipofectamine 2000 (18μl) and opti-MEM to a final volume of 90μl was prepared. Both mixtures were incubated for 5mins and then the 3 plasmid mix was added dropwise to the diluted lipofectamine mix whilst flicking the tube. This mix was incubated for approximately 20mins at room temperature before adding dropwise to the plate of HEK293T packaging cells. The cells were incubated for 18hrs (37°C, 5% CO_2) after which medium was removed and replaced with high serum (30% FBS) containing medium for virus harvests. Cells were incubated for a further 24hrs and media now containing the lentivirus was harvested and stored at -80°C. For harvesting, medium containing the lentivirus was centrifuged at 500g for 10mins to remove any cell debris.

2.2.14.3 Lentiviral transduction of miR-630 inhibitor or precursor

Once the new HCC1954 mcherry/LUC+ and SKBR3 mcherry/LUC+ cells were established, these cell lines were subsequently transduced in a similar manner with either miR-630/scrambled inhibitor or miR-630/scrambled precursor (The sequences of the miR-630 and scrambled constructs are shown in Appendix I, Sections C, Figures C.1-C.8). The selection of miR-630/scrambled inhibitor cells was performed with the addition of 200μg of hygromycin (Invivogen, Cat. #:ant-hm-1) in growth medium. As the selection antibiotic for miR-630/scrambled precursor was the same as the mcherry/LUC+ (i.e. 2μg/ml puromycin), selection was therefore performed by cell sorting by flow cytometry to

identify cells positive for the reporter gene, green fluorescent protein (GFP). Cell sorting was performed by a research technician at the DFCI Flow Cytometry –Jimmy Fund Facility using the BD FACSAria II SORP UV cell sorter.

A model of the virus production and subsequent infection of cells is outlined in Figure 2.2.

2.2.14.4 Characterisation of new stable miR-630 cell lines

New stable cell lines were visualised for mcherry and GFP reporter genes as appropriate using the Nikon floursecent microscope. For GFP expressing cells, these were visualised using excitation wavelength at 395/475nm and emission wavelength at 507nm. Cells expressing mcherry were visualised using excitation wavelength at 587nm and emission at 610nm.

Cell lines were characterised for mir-630 expression by qPCR as described in Section 2.2.5. Proliferation and toxicity assays using acid phosphatase analysis as described in Section 2.2.9 were also performed. Drug concentrations, as used for transient transfection toxicity assays in Section 2.2.8, were used for these assays. Invasion using cell culture inserts, were performed as described in Section 2.2.12.

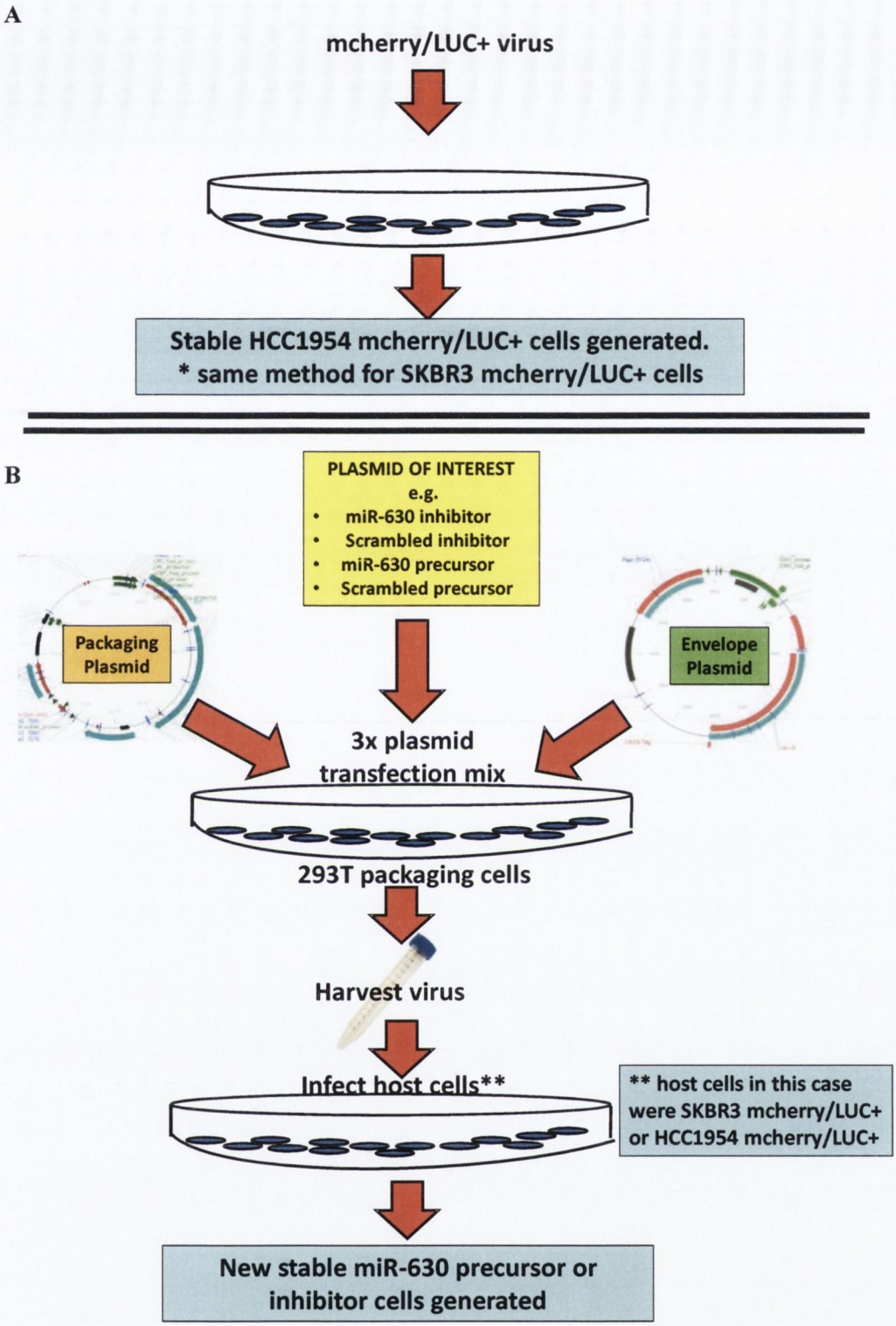

Figure 2.2: Schematic protocol for lentiviral production and infection.

(A) HCC1954 cells were infected with mcherry/LUC+ virus (gift from Dr. Kornelia Polyak's group, DFCI) and cells were selected 48hrs later with puromycin (2μg/ml). SKBR3 mcherry/LUC+ cells were generated in a similar manner. **(B)** Lentivirus for miR-630 or scrambled inhibitors and precursors were generated using a 3-plasmid transfection method of HEK293T packaging cells. Medium containing viruses were collected and used to infect the newly generated mcherry/LUC+ cells.

2.2.15 Statistical and Bioinformatics analysis

Online miRNA target prediction software (TargetScan Human Release 6.2) was used to identify proteins potentially regulated by miR-630. Statistical analysis was performed in Excel. P-values were generated using Student's T-tests, with $p<0.05$ considered as statistically significant. Where multiple cell lines were compared, the Anova statistical test adjusting the p-values using Tukey's Honest Significant Difference was performed. GraphPad Prism 5.0 was used for graph generation (Graph Pad Software Inc, La Jolla, USA). Linear regression analysis and the calculation of R^2 were performed on GraphPad and p-values were calculated based on deviation from zero. Hierarchical clustering was performed using DChip online software.

2.3 RESULTS

2.3.1 Assessment yield and quality of RNA isolated for global miRNA profiling

Prior to performing global miRNA profiling, the quantity and quality of RNA isolated were measured on the Nanodrop-ND 1000 spectrophotometer. Table 2.8 indicates the yields and the 260/280 ratios of RNA isolated from cell pellets and 250µl or their respective corresponding CM as used for the TLDAs.

Cell Samples	Total RNA (µg)	260/280	CM Samples	Total RNA (µg)	260/280
SKBR3-Ag A	56.40	1.97	SKBR3-Ag A	0.27	1.53
SKBR3-Ag B	58.41	1.98	SKBR3-Ag B	0.19	1.48
SKBR3-Ag C	63.23	1.97	SKBR3-Ag C	0.14	1.58
SKBR3-TR A	89.21	1.93	SKBR3-TR A	0.18	1.51
SKBR3-TR B	80.26	1.95	SKBR3-TR B	0.16	1.56
SKBR3-TR C	90.19	1.91	SKBR3-TR C	0.20	1.49
SKBR3-LR A	45.37	1.97	SKBR3-LR A	0.16	1.40
SKBR3-LR B	55.06	1.96	SKBR3-LR B	0.21	1.58
SKBR3-LR C	35.91	1.94	SKBR3-LR C	0.12	1.49

Table 2.8: RNA yields and quality for cells and corresponding CM.

RNA, as assessed by Nanodrop ND-1000 spectrophotmeter. Biological replicates are indicated by A, B and C. RNA from cells was resuspended in 30µl RNAse free water, whereas RNA from CM was resuspended in 10µl RNAse free water. Table indicated total RNA isolated per sample.

2.3.2 Global miRNA profiling of SKBR3 sensitive cells and resistant variants

As detailed in Section 2.2.4, global miRNA profiling of cells and conditioned media (CM) of the both trastuzumab- and lapatinib-resistant cell line variants (SKBR3-TR and SKBR3-LR) and their respective age-matched parent control cells (SKBR3-Ag) was performed for 667 miRNAs. All sets of samples were run on pooled biological triplicate. Taking a cut-off point of 35-cycle thresholds (C_T), miRNAs detected $<35C_T$ were considered as 'present' where as those with values $>35C_T$ were considered as 'undetected'. The distribution of miRNAs detected for all cell line variants is shown in Figure 2.3.

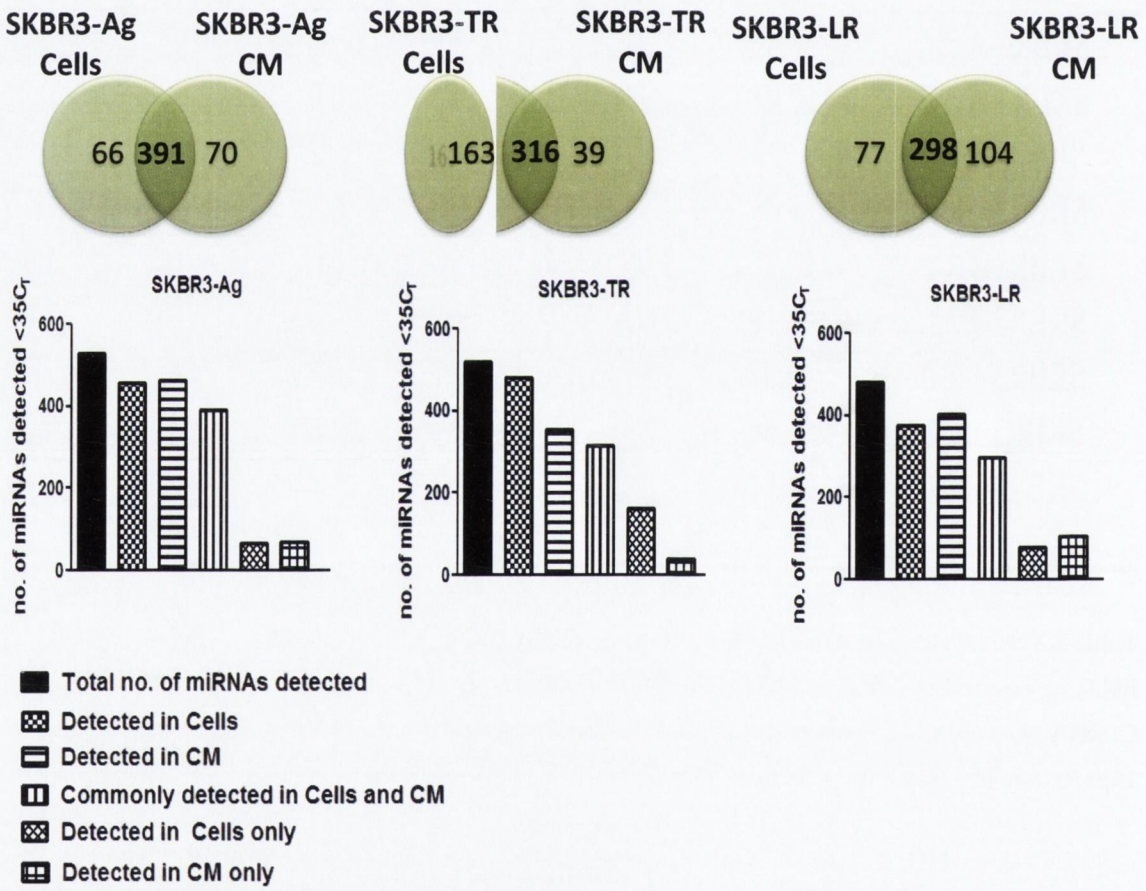

Figure 2.3: Detection of miRNAs $<35C_T$ in cells and CM of SKB3 cell line variants.

Venn diagrams and graphs illustrating the distribution of miRNAs detected in all cell line variants and their corresponding CM. Results represent analysis from single samples of pooled n=3 biological repeats.

Linear regression analysis on miRNAs detected at <35C_T in cells and CM indicated correlation for all cell line variants (Figure 2.4A) as SKBR3 (R^2=0.4037), SKBR3-TR (R^2=0.3159), SKBR3-LR (R^2=0.3367). Hierarchical clustering using normalised fold changes for both resistant cell line variants compared to parent cell lines (SKBR3-TR and SKBR3-LR) was performed. Clustering of miRNA profile in cells and corresponding CM was observed for both resistant variants (Figure 2.4B).

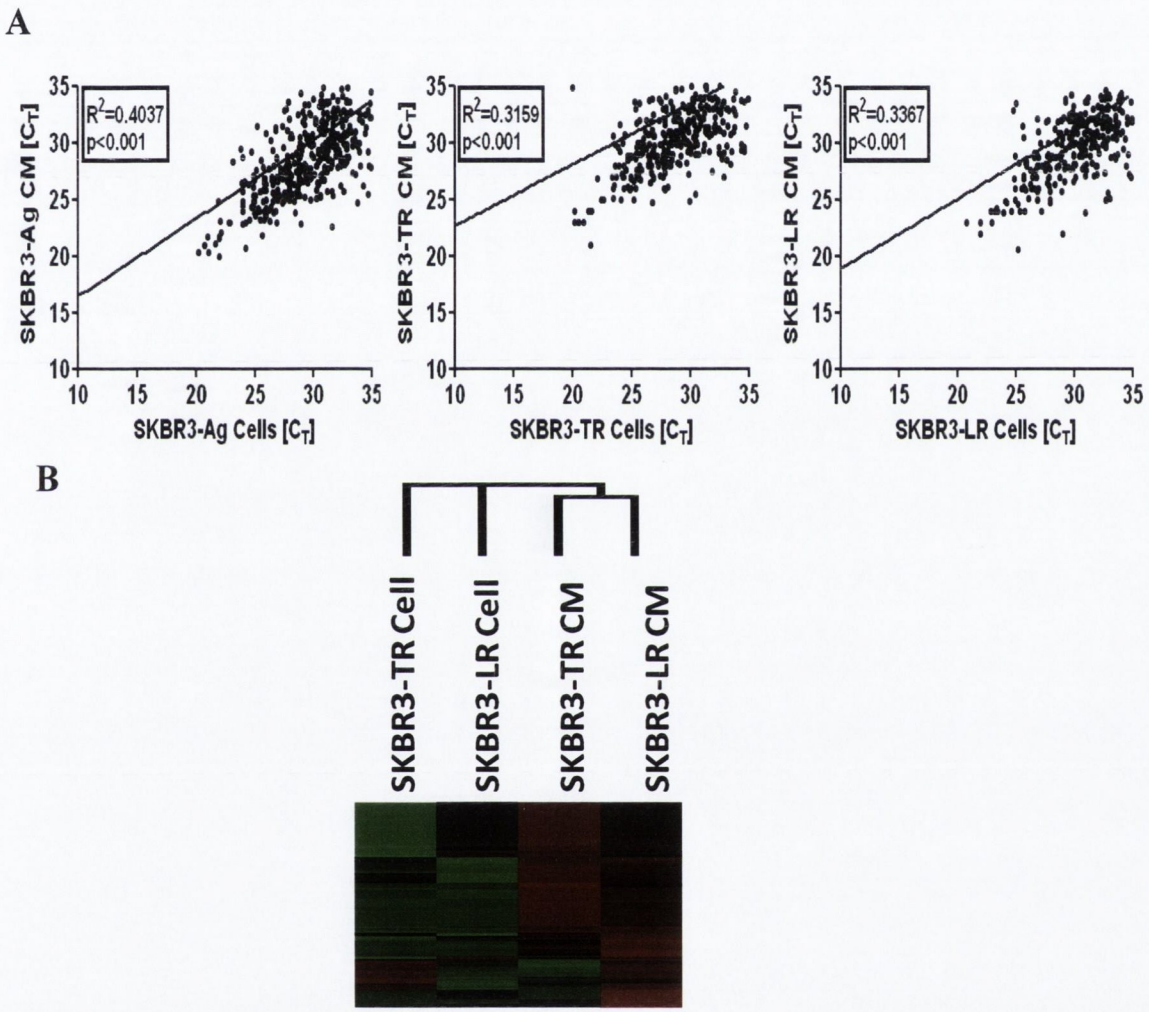

Figure 2.4: Linear regression and hierarchical clustering of miRNA expression patterns

(A) Linear regression analysis of SKBR3-Ag, SKBR3-TR and SKBR3-LR cell line variants comparing miRNAs detected by <35C_T in the cells and corresponding CM. **(B)** Hierarchical clustering (peformed using DChip software) of fold changes of miRNA expression in SKBR3-TR and SKBR3-LR compared to SKBR3-Ag for cells and CM, following global mean normalisation. Results represent analysis from single samples of pooled n=3 biological repeats

2.3.3 Identification and discovery of miRNAs from global miRNAs study

Following normalisation of the global miRNA profiling data to the mean C_T, analysis of deregulated miRNAs between cell line variants – within cells and CM - was performed using Venn diagrams to identify key miRNAs that may play an important role in resistance to trastuzumab and lapatinib. Taking a cut-off point of 1.2 fold up- or down-regulated expression in resistant cell line variants compared to their parent cell lines, a total of 127 miRNAs were detected as commonly increased in the SKBR3-TR and SKBR3-LR cells and 240 were commonly increased in corresponding CM of both cell line variants. On comparing these cellular miRNAs and those in CM, 55 were identified as being commonly up-regulated in both cells and CM of SKBR3-TR and SKBR3-LR (Figure 2.5).

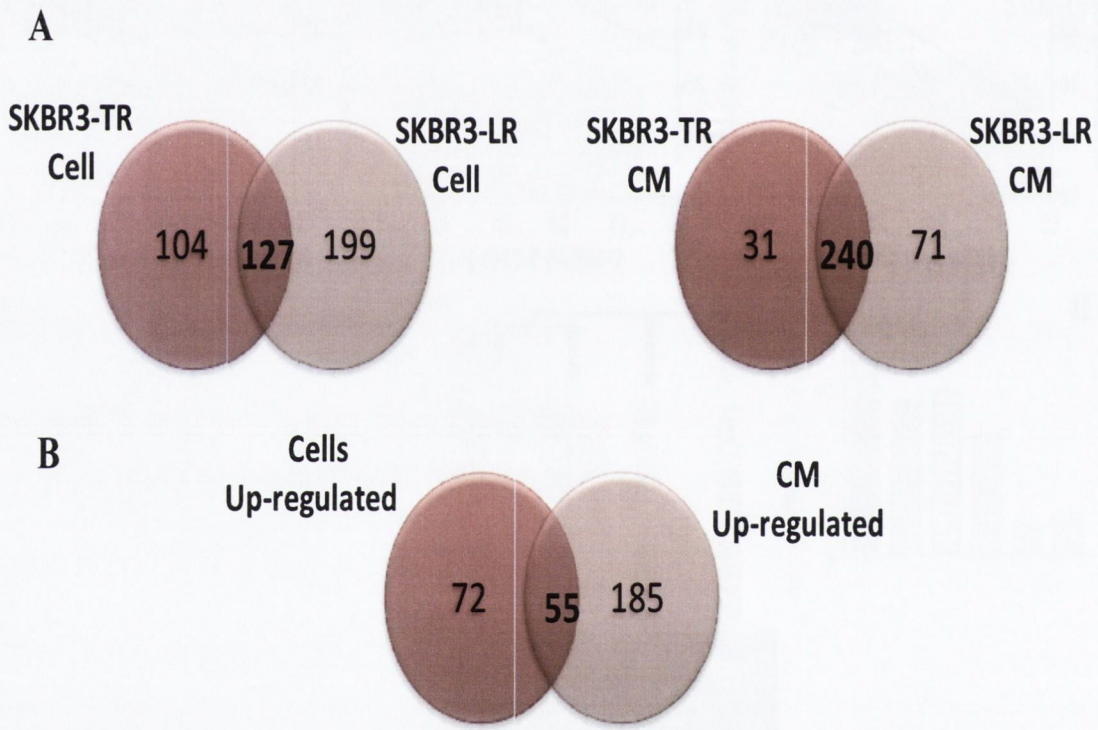

Figure 2.5: Identification of miRNAs increased with drug-resistance

(A) Venn diagrams illustrating the miRNAs commonly increased in cells and corresponding CM from SKBR3-TR and SKBR3-LR resistant variants compared to SKBR3-Ag. **(B)** The miRNAs commonly observed to be increased in SKBR3-TR and SKBR3-LR cells was compared to that of the corresponding CM. Results represent analysis from single samples of pooled n=3 biological repeats.

Of the miRNAs calculated as greater than 1.2 fold decreased, a total of 137 miRNAs were detected as commonly decreased in the cells SKBR3-TR and SKBR3-LR and 252 were commonly decreased in corresponding CM of both cell line variants. On comparing these cellular miRNAs and those in CM, 69 were identified as being commonly down-regulated in both cells and CM of SKBR3-TR and SKBR3-LR (Figure 6)

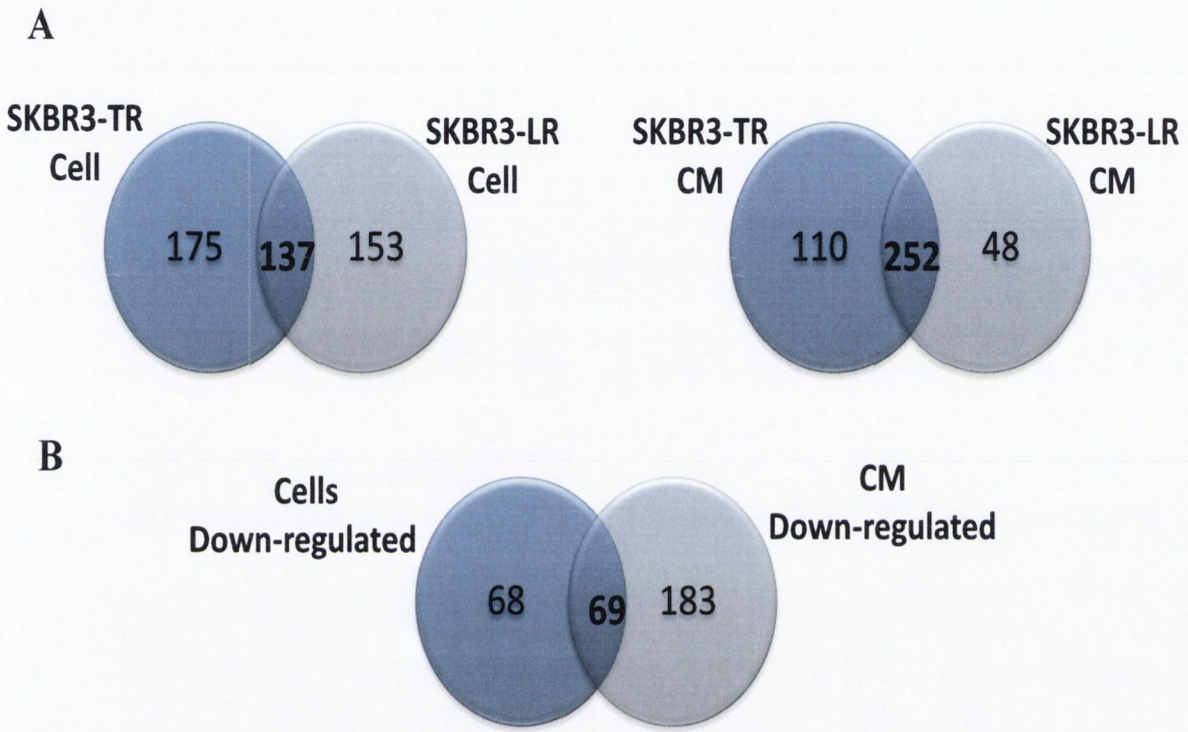

Figure 2.6: Identification of miRNAs decreased with drug-resistance

(A) Venn diagrams illustrating the miRNAs commonly decreased in cells and corresponding CM from SKBR3-TR and SKBR3-LR resistant variants compared to SKBR3-Ag. **(B)** The miRNAs commonly observed to be decreased in SKBR3-TR and SKBR3-LR cells was compared to that of the corresponding CM. Results represent analysis from single samples of pooled n=3 biological repeats.

2.3.4 *Validation of selected miRNAs from global miRNAs study*

A total of 7 miRNAs were selected for validation by qPCR (Table 2.9 and Figure 2.7). The selection criteria was based of those miRNAs that were 1.2 fold up- or down-regulated in both resistant cell line variants (SKBR3-TR and SKBR3-LR) with a similar aberrant expression in the cells and corresponding CM. Two up-regulated miRNAs (miR-572, and miR-502-5p) and three down-regulated miRNAs (miR-487b, miR-520f and, miR-630) were selected for validation. Other miRNAs (miR-616*) previously demonstrated in our group as aberrantly expressed in lung cancer [206] was also selected for validation along with one "best guess" from literature (miR-135a*). The expression levels of these selected miRNAs after qPCR are shown in Table 2.9, with miR-630 demonstrated in Figure 2.7 as it was selected for further analysis based on the best validated results.

miR-572	Cell Fold change (Mean±SEM)	P-value	miR-572	CM Fold Change (Mean±SEM)	P-value
SKBR3-TR	1.16 ± 0.23	0.537	SKBR3-TR	1.09 ± 0.19	0.645
SKBR3-LR	1.5± 0.31	0.181	SKBR3-LR	-1.29 ± 0.07	0.035
miR-502-5p	**Cell Fold change (Mean±SEM)**	**P-value**	**miR-502-5p**	**CM Fold Change (Mean±SEM)**	**P-value**
SKBR3-TR	1.24 ± 0.36	0.544	SKBR3-TR	1.39 ± 0.97	0.706
SKBR3-LR	1.96± 0.22	0.012	SKBR3-LR	3.44 ± 1.49	0.177
miR-487b	**Cell Fold change (Mean±SEM)**	**P-value**	**miR-487b**	**CM Fold Change (Mean±SEM)**	**P-value**
SKBR3-TR	-2.52 ± 0.39	0.001	SKBR3-TR	-0.28± 1.41	0.414
SKBR3-LR	-0.45± 1.15	0.278	SKBR3-LR	-2.26± 0.3	0.000
miR-520f	**Cell Fold change (Mean±SEM)**	**P-value**	**miR-520f**	**CM Fold Change (Mean±SEM)**	**P-value**
SKBR3-TR	-3.57 ± 0.89	0.007	SKBR3-TR	26.43± 23.53	0.341
SKBR3-LR	-2.67± 0.31	0.000	SKBR3-LR	1.79± 6.59	0.910
miR-616*	**Cell Fold change (Mean±SEM)**	**P-value**	**miR-616***	**CM Fold Change (Mean±SEM)**	**P-value**
SKBR3-TR	-0.50±0.85	0.154	SKBR3-TR	-5.53±1.24	0.006
SKBR3-LR	1.72±0.29	0.067	SKBR3-LR	1.26±0.14	0.126
miR-135a*	**Cell Fold change (Mean±SEM)**	**P-value**	**miR-135a***	**CM Fold Change (Mean±SEM)**	**P-value**
SKBR3-TR	-3.65±2.63	0.152	SKBR3-TR	-1.33±0.06	0.000
SKBR3-LR	-1.33±0.10	0.000	SKBR3-LR	-1.29±1.29	0.152
miR-630	**Cell Fold change (Mean±SEM)**	**P-value**	**miR-630**	**CM Fold Change (Mean±SEM)**	**P-value**
SKBR3-TR	-1.3±0.1	0.040	SKBR3-TR	-1.2±0.1	0.027
SKBR3-LR	-3.8±1.5	0.010	SKBR3-LR	-12.8±8.1	0.000

Table 2.9: miRNAs selected from TLDA analysis for validation by qPCR.

Fold change for SKBR3-TR and SKBR3-LR were calculated against SKBR3-Ag which was set at an arbitrary fold change of 1.

2.3.5 Changes in both intracellular and extracellular miR-630 levels are associated with acquired-resistance to lapatinib and trastuzumab

miR-630 demonstrated the most consistent aberrant expression in both the cells and CM of SKBR3-TR and SKBR3-LR compared to SKBR3-Ag (Figure 2.7). The levels of miR-630, detected by qPCR, was slight but significantly decreased in SKBR3-TR cells (1.3±0.1 fold; $p<0.05$) and corresponding CM (1.2±0.1 fold; $p<0.05$) compared to SKBR3-Ag (Figure 2.7A). Furthermore, decreased levels of miR-630 was also observed in SKBR3-LR cells (3.8±1.5 fold; $p<0.01$) and corresponding CM (12.8 ±8.1 fold; $p<0.001$) (Figure 2.7B). In addition, this miRNA was further assessed in the cells and CM of lapatinib-resistant HCC1954 cell line variant (HCC1954-LR) which established that miR-630 is significantly decreased in HCC1954-LR cells (8.9±4.7 fold; $p<0.001$) and corresponding CM (5.0 ±1.2; $p<0.001$) (Figure 2.7C).

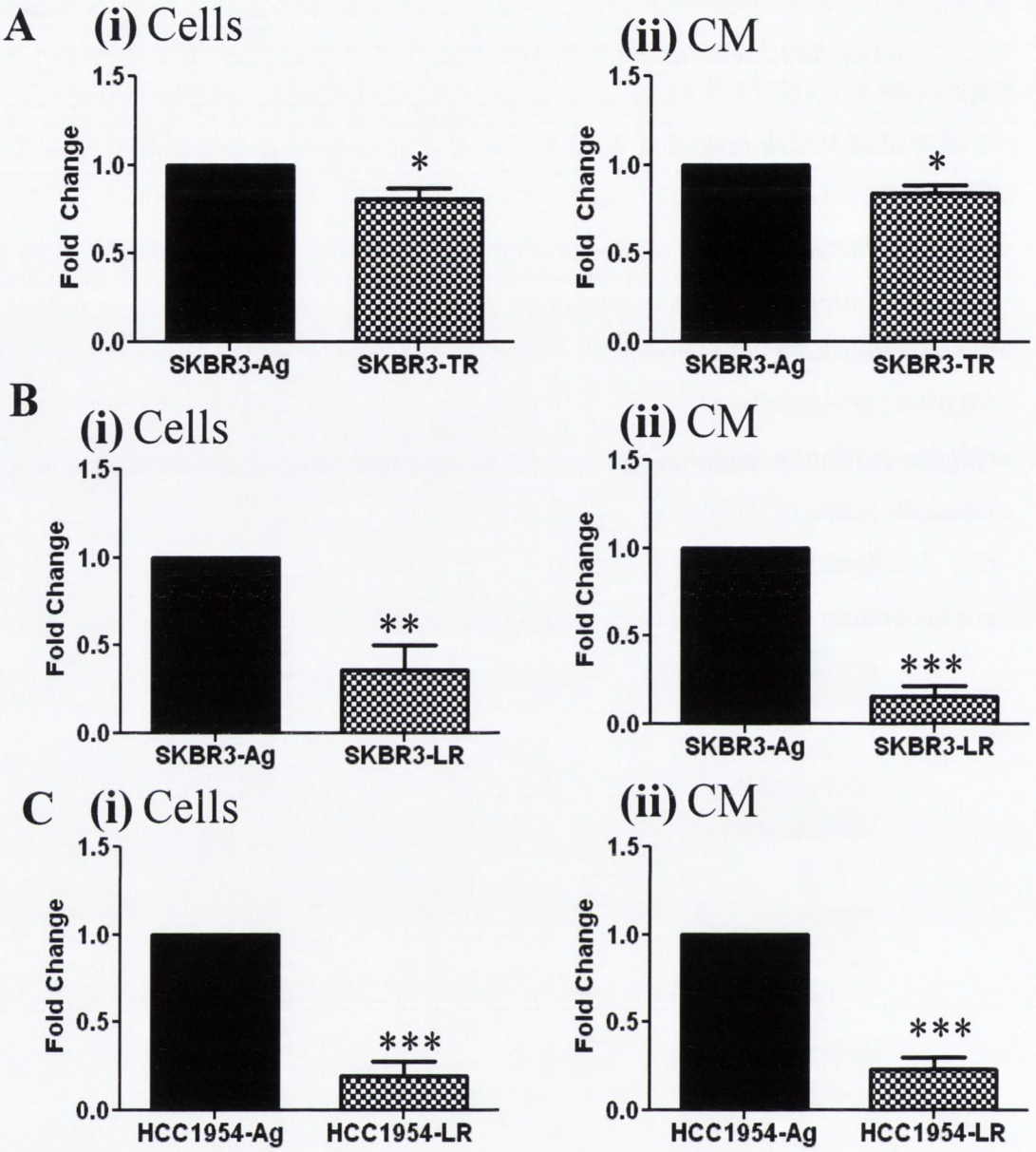

Figure 2.7: miR-630 decreases with acquired-resistance to trastuzumab and lapatinib

(A) miR-630 expression, assessed by qPCR, was slightly, but significantly, decreased in cells with acquired trastuzumab-resistance **(i)** SKBR3-TR compared to their age-matched controls (SKBR3-Ag). **(B-C)** miR-630 expression was also significantly decreased in cells with acquired-resistance to lapatinib **(i)** SKBR3-LR and HCC1954-LR, respectively) compared to their respective age-matched controls (SKBR3-Ag and HCC1954-Ag). **(A-C (ii))** Extracellular levels of miR-630 were also assessed in the corresponding conditioned medium of these cells and trends followed that of the cells. All results represent biological repeats n=3±SEM, where * $p < 0.05$, ** $p < 0.01$, *** $p < 0.001$.

2.3.6 *Changes in both intracellular and extracellular miR-630 levels are associated with acquired-resistance to neratinib and also innate-resistance to lapatinib/trastuzumab*

As the expression levels of miR-630 were substantially decreased in lapatinib-resistant cells (SKBR3-LR and HCC1954-LR) and showed a slight decrease in trastuzumab-resistant cells (SKBR3-TR), we elected to further assess whether decreased miR-630 may be associated with resistance to other HER-targeted therapies. For this we used cells that had acquired-resistance to neratinib (SKBR3-NR and HCC1954-NR). Here we observed that miR-630 was significantly decreased in the cells (3.3±1.0 fold; $p<0.01$) and CM (20.3± 11.3 fold, $p<0.001$) of SKBR3-NR compared SKBR3-Ag (Figure 2.8A). Similarly, miR-630 was significantly decreased in cells (1.7±0.2 fold; $p<0.01$) and CM (4.9±1.1 fold; $p<0.001$) of HCC1954-NR compared to HCC1954-Ag (Figure 2.8B).

Our analysis to this point demonstrated that miR-630 is associated with acquired-resistance to some HER-targeting drugs; our next investigation was to examine whether this observation may also be associated with innate-resistance to HER-targeting drugs. SKBR3 cells have previously been termed as innately-sensitive to both trastuzumab and lapatinib, whereas MDA-MB-453 have been characterised as innately-resistant to these drugs [265]. In this instance we demonstrate that miR-630 is significantly decreased (6.8±4.2 fold; $p<0.05$) in MDA-MB-453 cells compared to SKBR3 and a similar trend was observed for the corresponding CM (2.1±0.7 fold; $p=0.07$) (Figure 2.8C).

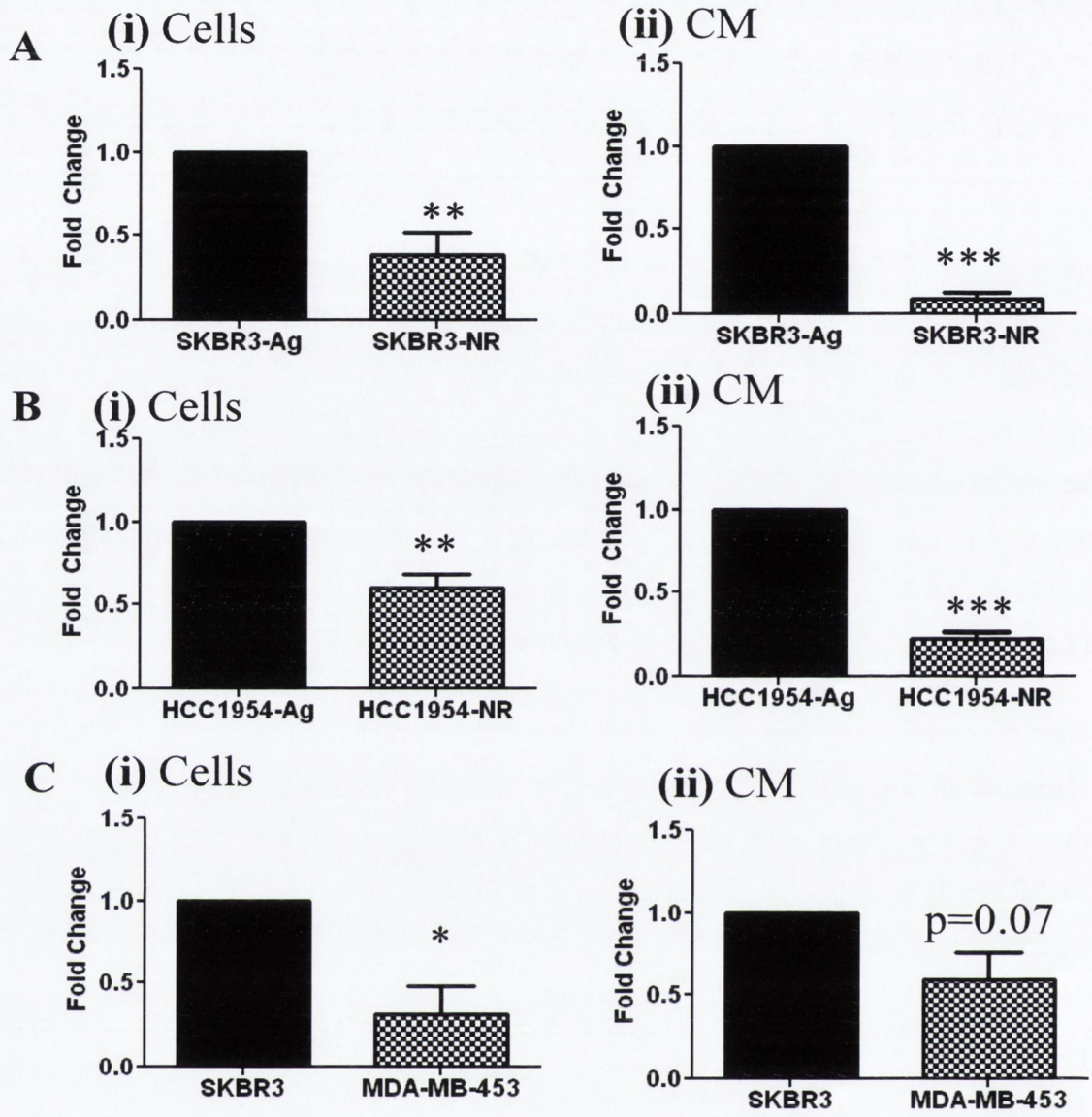

Figure 2.8: miR-630 decreases with acquired-resistance to neratinib and innate-resistance.

(A-B) miR-630 expression was significantly decreased in cells with acquired neratinib-resistance **((i)** SKBR3-NR and HCC1954-NR) compared to their respective age-matched controls (SKBR3-Ag and HCC1954-Ag). **(C (i))** miR-630 expression was also significantly decreased in cells with innate-resistance to lapatinib and trastuzumab (MDA-MB-453) compared to cells with innate sensitivity to both these drugs (SKBR3). **(A-C (ii))** Extracellular expression of miR-630 was also assessed in the corresponding conditioned medium of these cells and trends followed that of the cells. All results represent biological repeats n=3±SEM, where * $p < 0.05$, ** $p < 0.01$, *** $p < 0.001$.

2.3.7 *miR-630 levels correspond to innate-resistance in a broad panel of HER2-overexpressing cell lines*

To further explore the observation shown in Figure 2.8C whereby miR-630 was found to be at higher levels in SKBR3 cells (which are innately-sensitive to lapatinib) compared to innately-resistant MDA-MB-453 cells, we elected to perform qPCR analysis on a panel of available HER2-overexpressing cell lines that were deemed either innately-sensitive or innately-resistant to lapatinib by O'Brien *et al.* [265]. Innate-resistance was defined as an IC_{50} > 1μM for lapatinib. Here the expression of miR-630 for all cells assessed was compared to the cell line with the lowest IC_{50} for lapatinib i.e. BT474, which was given an arbitrary value of 1 (Figure 2.9). For all cell lines assessed, which had higher IC_{50} values compared to BT474, there was a significant ($p<0.001$) decrease in miR-630 levels. Specifically, miR-630 was decreased by 4.8±1.1 fold (for SKBR3); 5.0±1.3 fold (for EFM-192A); 3.7±0.7 fold (for HCC1954); 5.1±0.2 fold (for UACC812); 22.7±12.2 fold (for UACC893); 8.5±1.5 (for HCC1569); 6.9±1.3 fold (for MDA-MB-453) and 7.0±1.9 fold (for MDA-MB-361). Furthermore, grouping innately-sensitive SKBR3, EFM-192A, HCC1954 and UACC812 together there was on average a 4.6±0.4 fold decrease in miR-630 compared to BT474 while grouping innately-resistant UACC893, HCC1569, MDA-MB-453 and MDA-MB-361 demonstrated a further significant ($p<0.001$) decrease (11.3±4.4 fold) in miR-630 levels.

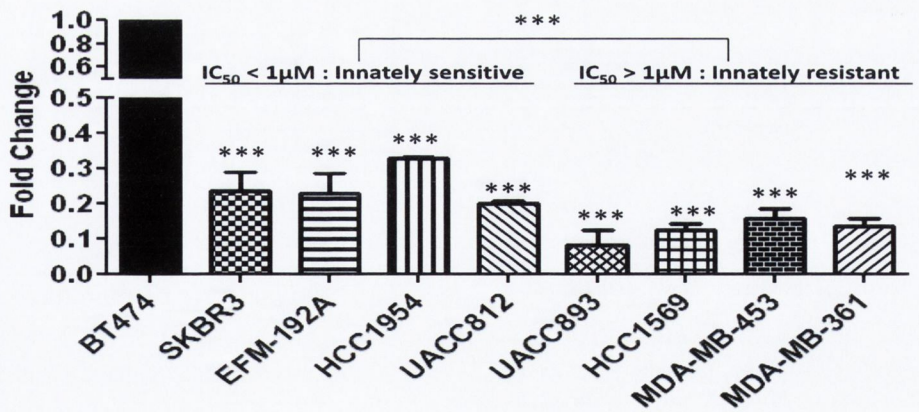

Figure 2.9: Analysis of miR-630 in a broader panel of HER2 overexpressing cell lines.

When normalised to the cells with the lowest IC_{50} for lapatinib (BT474), miR-630 was significantly decreased in all cells that had higher IC_{50}'s for lapatinib than BT474. When grouped together, cells with innate-resistance to lapatinib compared to cells with innate sensitivity had significantly decreased miR-630 expression. All results represent biological repeats and assessed by Anova statistical test. n=3±SEM, where *** $p<0.001$.

2.3.8 miR-630 is decreased in tumour compared to peritumour breast cancer tissues

Before progressing further with our analysis of miR-630, we next decided to assess the clinical relevance of miR-630. For this, as outlined in Section 2.2.6, we analysed a publically available dataset on the gene expression omnibus (GSE40525) comprised of breast tumour tissue and matched peritumour tissue from all breast cancers (n=56), HER2+ (n=6), basal-like (n=7) and luminal (n=43). Here we found the miR-630 was significantly decreased ($p<0.001$) in all breast cancer tissues compared to matched peritumours (Figure 2.10A). Assessing the subtypes individually, there was also a significant decrease observed for miR-630 levels in HER2+ ($p<0.05$), basal like ($p<0.01$) and luminal ($p<0.001$) breast tumours compared to their respective matched peritumours (Figure 2.10B-D).

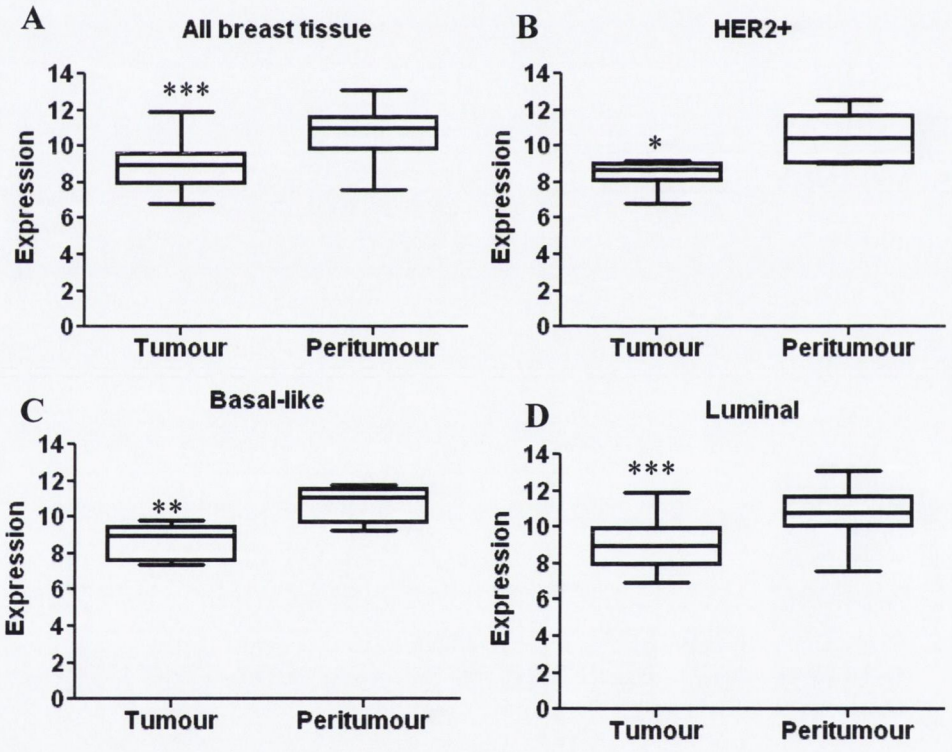

Figure 2.10: Assessment of miR-630 in patient derived tissue.

Using a publically-available data set (GSE40525) on Gene Expression Omnibus (GEO) the expression of miR-630 was determined in breast cancer tumour tissues compared to matched peritumour. **(A)** miR-630 was significantly decreased in all breast tumours (n=56), and also in each subtype assessed **(B)** HER2+ (n=6); **(C)** Basal-like (n=7); **(D)** Luminal (n=43) compared with miR-630 levels in peritumour tissue. *$p<0.05$, **$p<0.01$, ***$p<0.001$.

2.3.9 miR-630 regulates cellular response to HER-targeted drugs

Having established that reduced miR-630 expression levels are associated with both innate- and acquired-resistance to HER-targeting drugs, and that this miRNA holds clinical relevance in breast cancer tumour tissues, we next progressed to establishing if miR-630 holds a functional role in drug-resistance. miR-630 was only slightly decreased in trastuzumab-resistant cells; functional studies therefore focused on lapatinib and neratinib. To establish if the role miR-630 is specific to lapatinib and neratinib alone or more generally associated with HER-targeting drugs, we also included afatinib in our subsequent analyses. The expression of miR-630 following transient transfection with inhibitors and mimics are shown in Figure 2.11. Specifically, miR-630 inhibitors induced a 7.8±3.2 (SKRB3-Ag) and 3±0.6 fold (HCC1954-Ag) decrease in miR-630 levels compared to negative control (NC) inhibitor (Figure 2.11A). The miR-630 mimic induced a 655.7±152.3 (SKBR3-LR) and 4657.7±1305.6 (HCC1954-LR) increase in miR-630 levels compared to NC mimic (Figure 2.11B).

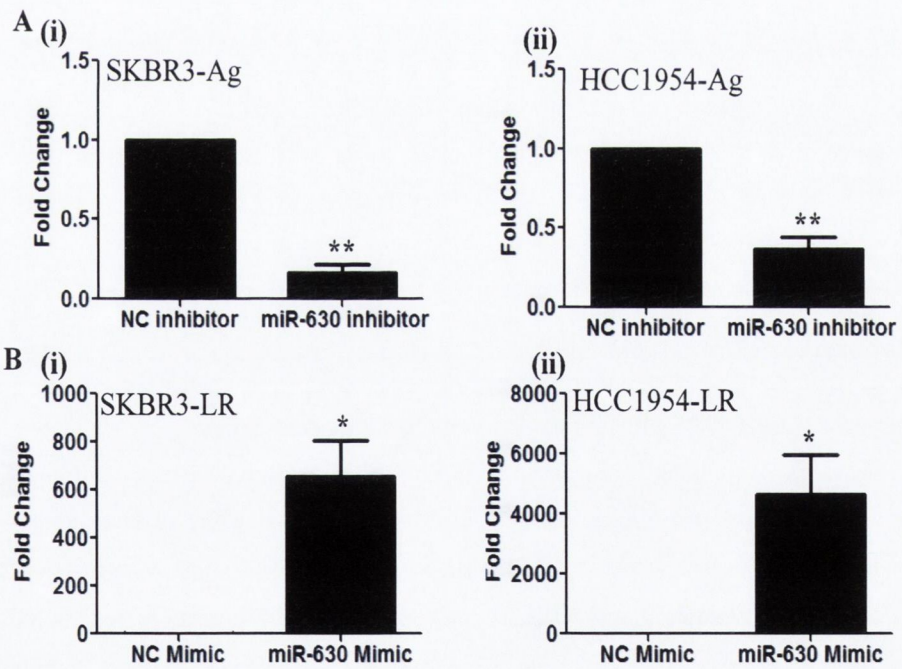

Figure 2.11: Transient transfection of miR-630 inhibitor and mimic

Following transfection with miR-630 inhibitor or a negative control (NC) inhibitor **(A)** Levels of miR-630 inhibition was assessed by qPCR in **(i)** SKBR3-Ag cells and **(ii)** HCC1954-Ag. **(B)** Similarly, levels of miR-630 overexpression were confirmed by qPCR in **(i)** SKBR3-LR and **(ii)** HCC1954-LR cells. Results represent n=3±SEM, where *$p<0.05$, **$p<0.01$.

Inhibition of miR-630 (in sensitive parent cells) or its mimicked expression (in acquired lapatinib-resistant or innately-resistant cells) our studies identified a correlation between miR-630 expression and cellular response to all 3 HER-targeting drugs tested *i.e.* lapatinib, neratinib and afatinib (Table 2.10 and 2.11). Specifically, inhibition of miR-630 in SKBR3-Ag and HCC1954-Ag increased resistance to lapatinib by 13-22%, neratinib by 8-15% and afatinib by 11-14% compared to NC inhibitor (Table 2.10). Furthermore, mimicked expression of miR-630 in acquired-lapatinib-resistant SKBR3-LR and HCC1954-LR and innately-resistant MDA-MB-453 increased sensitivity to lapatinib by 9-31%, neratinib by 4-17% and afatinib by 9-25% compared to NC mimic (Table 2.11).

Drug	Drug Conc.	Cell Line	% Cell Viability Drug + NC Inhibitor	% Cell Viability Drug + miR-630 Inhibitor	% Resistance induced by miR-630 inhibitor	p-value
Lapatinib	0.05 μM	SKBR3-Ag	50.0±9.6	63.6±9.1	**13.6±0.8**	0.002
Lapatinib	0.7 μM	HCC1954-Ag	40.8±3.6	63.7± 4.8	**22.9±6.7**	0.039
Neratinib	0.005 μM	SKBR3-Ag	34.7±6.4	43.2±7.4	**8.6±1.6**	0.017
Neratinib	0.005 μM	HCC1954-Ag	43.2±2.3	58.2±2.4	**15.1±3.0**	0.019
Afatinib	0.005 μM	SKBR3-Ag	47.7±5.2	62.3±4.6	**14.6±1.7**	0.002
Afatinib	0.005 μM	HCC1954-Ag	70.4±8.3	82.1±9.0	**11.7±2.3**	0.019

Table 2.10: **Inhibition of miR-630 reduces sensitivity to HER-targeted drugs.**

The percentage cell viability following treatment with HER-targeted drugs in the presence of negative control inhibitor (NC inhibitor) compared to the percentage cell viability following the same treatment but in the presence of miR-630 inhibitor. Percentage resistance induced in the presence of a fixed concentration of given drug, is the difference between cell viability with miR-630 inhibitor compared to NC inhibitor. Response to treatment shown here was assessed using the acid phosphatase method. Results represent n=3±SEM; p-values are indicated on the Table.

Drug	Drug Conc.	Cell Line	% Cell Viability Drug + NC Mimic	%Cell Viability Drug + miR-630 mimic	% Anti proliferative benefit with miR-630 Mimic	p-value
Lapatinib	3 μM	SKBR3-LR	40.2±5.1	9.2±2.3	**31.0±4.0**	0.008
Lapatinib	5 μM	HCC1954-LR	27.6±6.3	17.8±4.5	**9.7±2.3**	0.026
Lapatinib	6 μM	MDA-MB-453	19.0±0.9	9.9±0.9	**9.1±1.6**	0.015
Neratinib	0.5 μM	SKBR3-LR	23.9±6.4	9.7±2.3	**14.2±4.1**	0.037
Neratinib	0.5 μM	HCC1954-LR	26.3±4.6	22.3±4.7	**3.9±0.1**	0.000
Neratinib	0.5 μM	MDA-MB-453	45.3±7.5	28.3±3.0	**17.0±4.9**	0.037
Afatinib	0.5 μM	SKBR3-LR	32.6±9.3	7.2±2.4	**25.4±6.9**	0.033
Afatinib	0.5 μM	HCC1954-LR	30.5±7.0	20.7±6.5	**9.8±0.5**	0.001
Afatinib	0.5 μM	MDA-MB-453	50.6±8.3	31.4±10.4	**19.2±2.3**	0.007

Table 2.11: Mimicked expression of miR-630 restores sensitivity to HER-targeted drugs.

This table summarises the percentage cell viability following treatment with HER-targeted drugs in the presence of a negative control mimic (NC mimic) compared to the percentage cell viability following drug treatment in the presence of miR-630 mimic. The illustrated percentage anti-proliferative benefit induced is the difference between cell viability with miR-630 mimic compared to NC mimic. Response to treatment shown here was assessed using the acid phosphatase method. Results represent n=3±SEM, p-values are indicated on the Table

2.3.10 Phenotypic changes in HER2-overexpressing cells including motility, invasion and resistance to anoikis are also regulated, at least in part, by miR-630

Assessing wound healing ability of cells (as described in Section 2.2.11) demonstrated that the inhibition of miR-630 was associated with significantly ($p<0.05$) increased motility of HCC1954-Ag by 19.8±6.9% and SKBR3-Ag by 13.2±3.2%, compared to their respective negative controls after 72hrs (Figure 2.12).

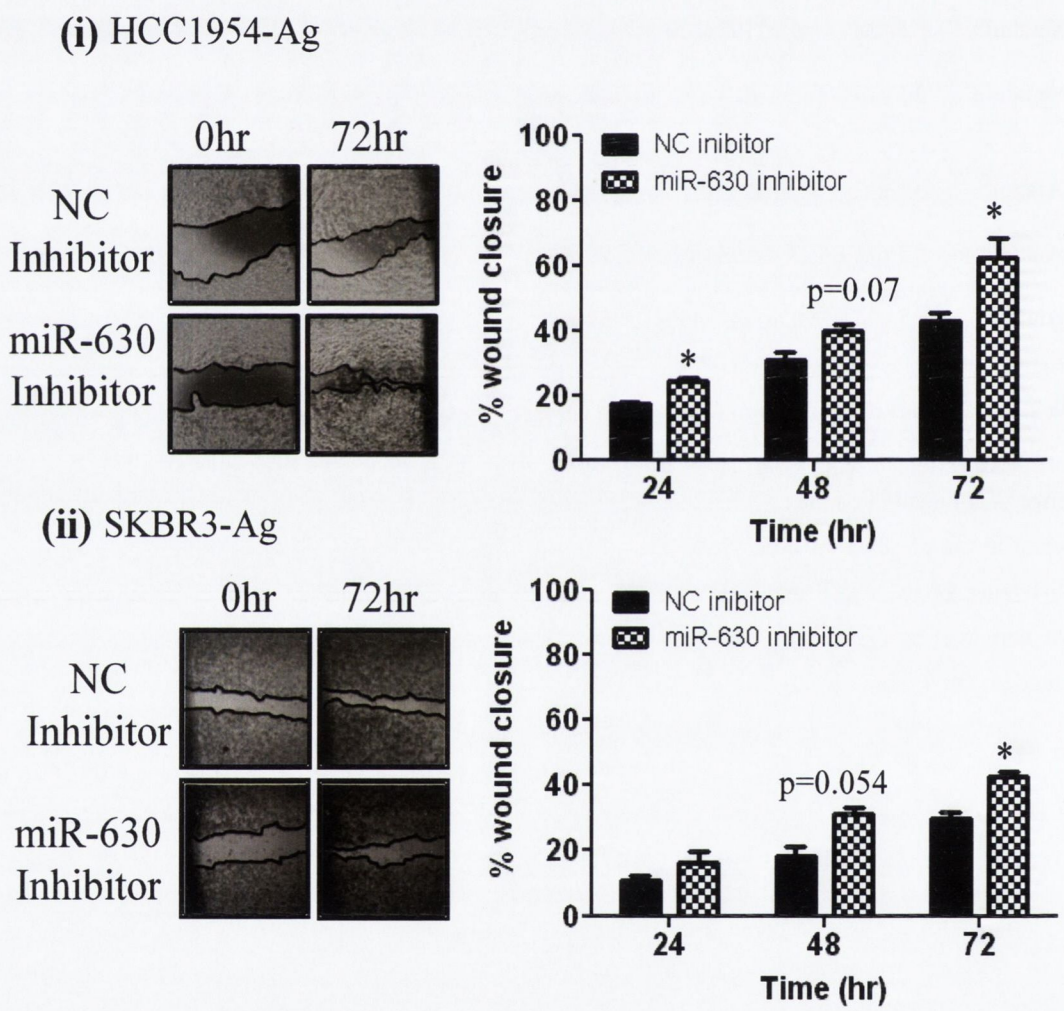

Figure 2.12: Inhibition of miR-630 increases cell motility.

Following transfection with miR-630 inhibitor or a negative control (NC) inhibitor in **(i)** HCC1954-Ag and **(ii)** SKBR3-Ag motility, assessed by wound-healing assay, was found to be significantly changed as a consequence of miR-630 inhibition. Results represent n=3±SEM, where * $p<0.05$

Furthermore, miR-630 inhibition was associated with significantly ($p<0.05$) increased migration through transwells for (i) HCC1954-Ag by 20.6±4.3% and (ii) SKBR3-Ag by 32.0±6.6% compared to NC inhibitor (Figure 2.13A). Invasion through extracellular matrix-coated transwells was also increased by miR-630 inhibition, specifically for (i) HCC1954-Ag by 29.7±3.2 ($p<0.01$) and for (ii) SKBR3-Ag by 13.0±4.4 ($p<0.05$) (Figure 2.13B). The percentage cell death due to anoikis was significantly ($p<0.05$) decreased following miR-630 inhibition for (i) HCC1954-Ag by 3.9±1.6 fold and (ii) SKBR3-Ag by 7.0±2.5 fold (Figure 2.13C).

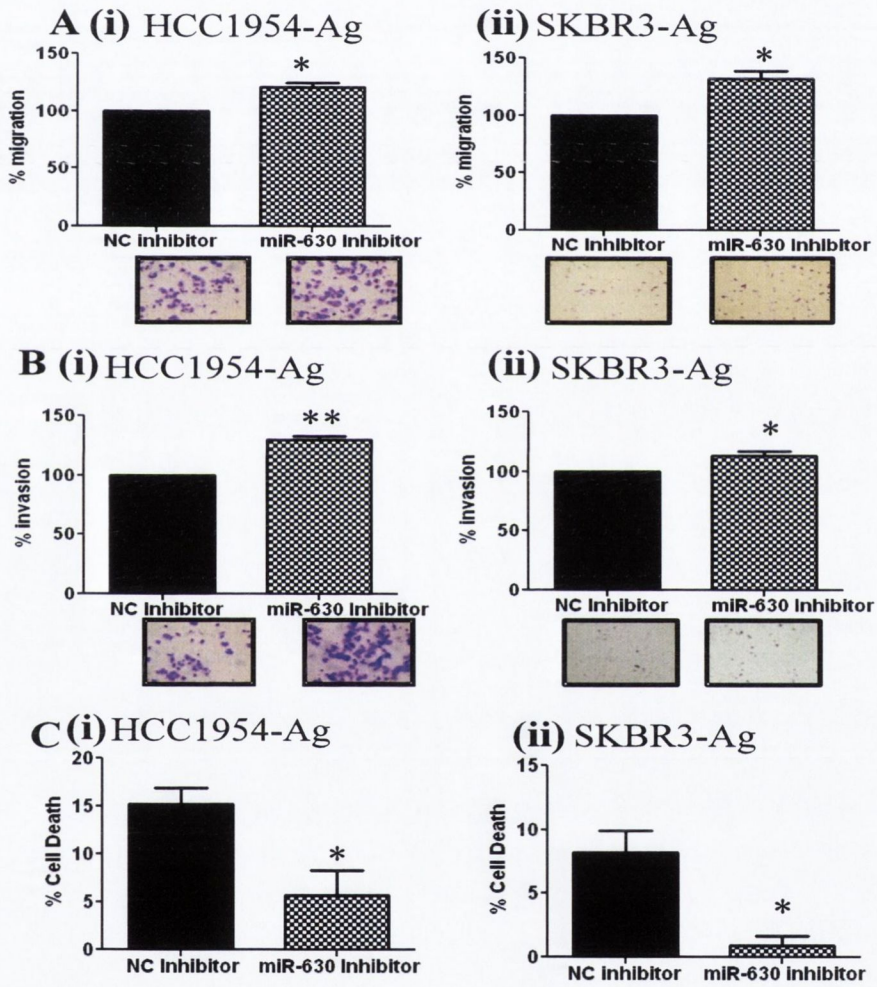

Figure 2.13: Inhibition of miR-630 increases migration, invasion and resistance to *anoikis*.
Following transfection with miR-630 inhibitor or a negative control (NC) inhibitor in **(i)** HCC1954-Ag and **(ii)** SKBR3-Ag; **(A)** migration, through transwells and **(B)** invasion, through ECM-coated transwells; **(C)** *anoikis*, assessed using poly(hydroxyethyl methacrylic) acid coated plates, was found to be significantly changed as a consequence of miR-630 inhibition. *Anoikis* assays shown here was assessed using alamar blue. Results represent n=3±SEM, where * $p<0.05$, ** $p<0.01$.

On the contrary to the results in Figures 2.12, mimicked expression of miR-630 in drug-resistant HCC1954-LR and SKBR3-LR, was associated with significantly decreased motility for (i) HCC1954-LR by 32.9±1.8% ($p<0.001$) and (ii) SKBR3-LR by 32.3±5.6% ($p<0.05$) compared to their respective negative controls after 72hrs (Figure 2.14)

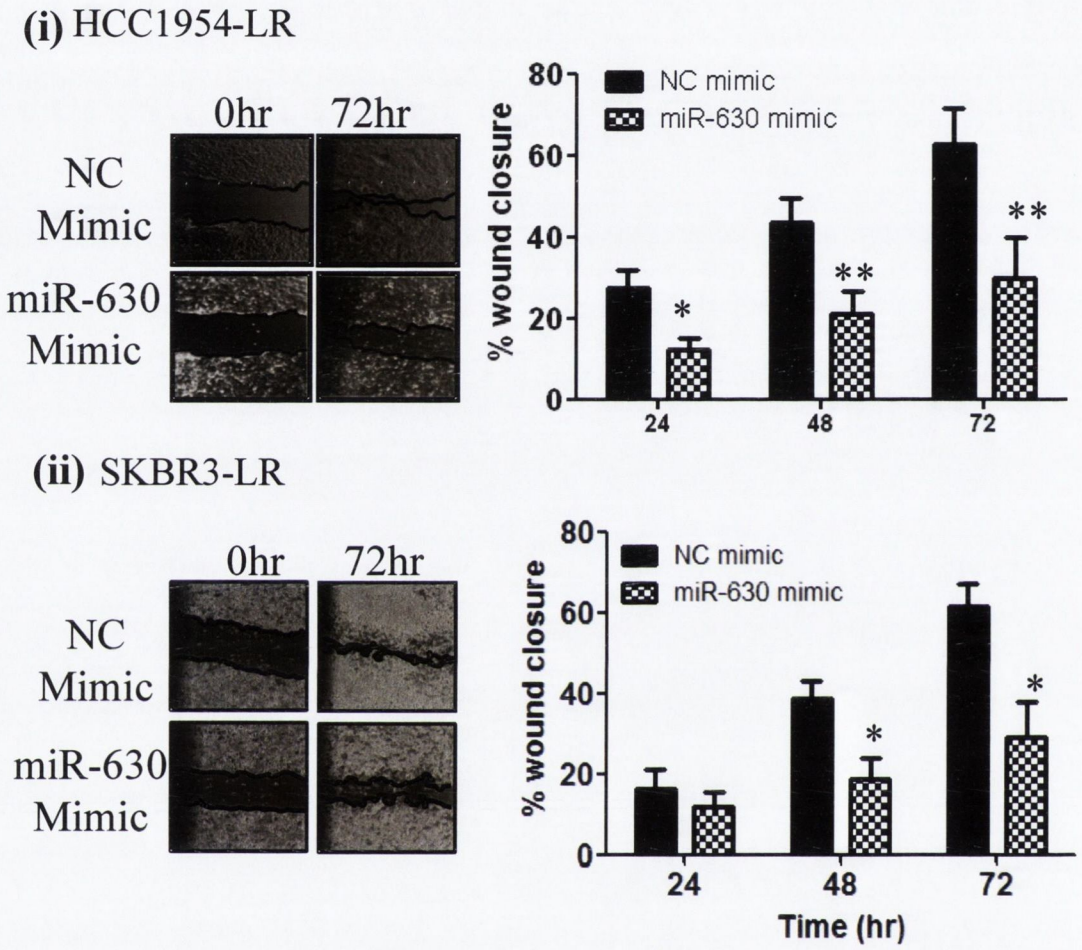

Figure 2.14: Mimicked expression of miR-630 increases cell motility.

Following transfection with miR-630 mimic or a negative control (NC) mimic in (i) HCC1954-LR and (ii) SKBR3-LR motility, assessed by wound-healing assay, was found to be significantly changed as a consequence of miR-630 inhibition. Results represent n=3±SEM, where * $p<0.05$ ** $p<0.01$

Similarly, mimicked expression of miR-630 in cells was associated with significantly ($p<0.05$) decreased migration through transwells for (i) HCC1954-LR by 32.0±6.8% and (ii) SKBR3-LR by 16.6±1.7% (Figure 2.15A). Invasion through extracellular matrix-coated transwells was also significantly ($p<0.05$) decreased for (i) HCC1954-LR by 31.4±7.9% and (ii) SKBR3-LR by 17.2±4.0% (Figure 2.15B). A significantly increased percentage cell death due to *anoikis* was observed following miR-630 mimicked expression for (i) HCC1954-LR by 1.8±0.1 fold ($p<0.01$) and (ii) SKBR3-LR by 1.9±0.4 fold ($p<0.05$) (Figure 2.15C).

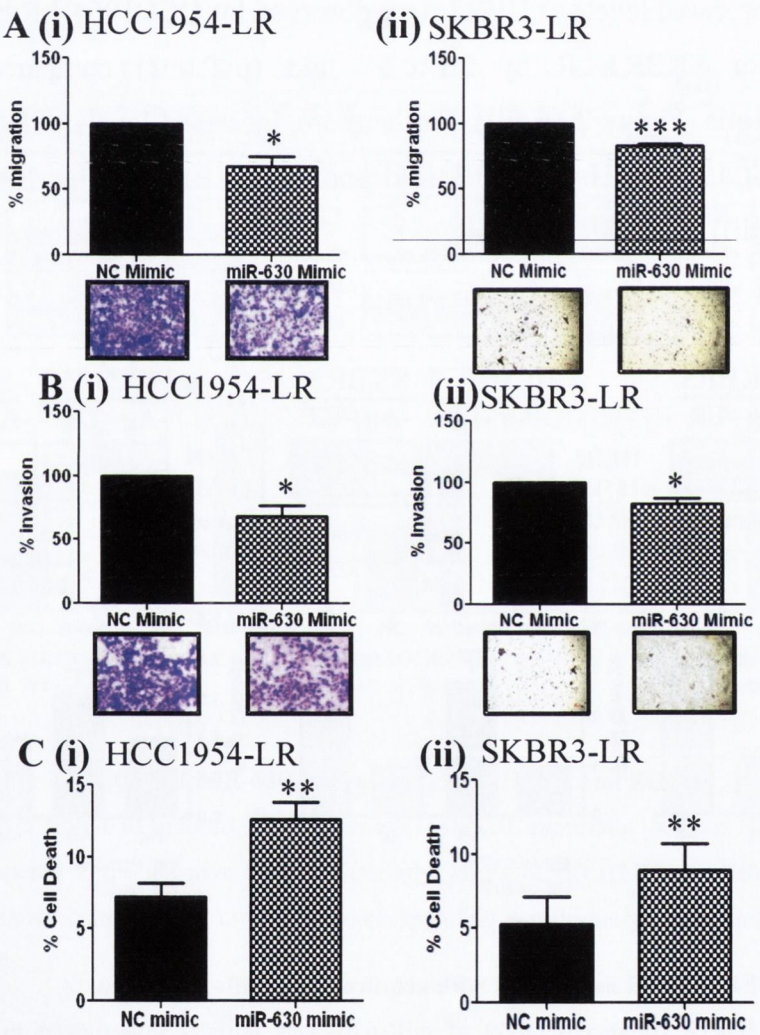

Figure 2.15: Mimicked miR-630 decreases migration, invasion and resistance to *anoikis*.

Following transfection with miR-630 inhibitor or a negative control (NC) inhibitor in **(i)** HCC1954-LR and **(ii)** SKBR3-LR **(A)** migration, through transwells and **(B)** invasion, through ECM-coated transwells; **(C)** *anoikis* was found to be significantly changed as a consequence of miR-630 inhibition. *Anoikis* assays shown here was assessed using alamar blue . Results represent n=3±SEM, where * $p<0.05$, ** $p<0.01$.

2.3.11 Mechanism of Action for miR-630

Through the use of target prediction software (TargetScan Human Release 6.2), IGF1R was predicted to be regulated by miR-630. Initially the levels of IGF1R in our acquired lapatinib-resistant cells (HCC1954-LR and SKBR3-LR) were assessed. Here, a significant increase in IGF1R levels were observed in HCC1954-LR by 1.5±0.1 fold ($p<0.001$) and in SKBR3-LR by 2.3±0.3 fold ($p<0.01$) compared to their corresponding parent cells (Figure 2.16 (i)). As HER2 and EGFR are the targets for all 3 drugs assessed, we also determined the protein levels of these specific targets using immunoblotting, as described in Section 2.2.10. Significantly increased levels of HER2 were observed for HCC1954-LR by 2.7±0.6 fold ($p<0.05$) and for SKBR3-LR by 2.1±0.01 fold ($p<0.001$) compared to the corresponding parent cells (Figure 2.16 (ii)). Furthermore, increased levels of EGFR were also observed for HCC1954-LR by 1.6±0.3 fold and for SKBR3-LR by 1.9±0.3 fold ($p<0.05$) (Figure 2.16(iii))

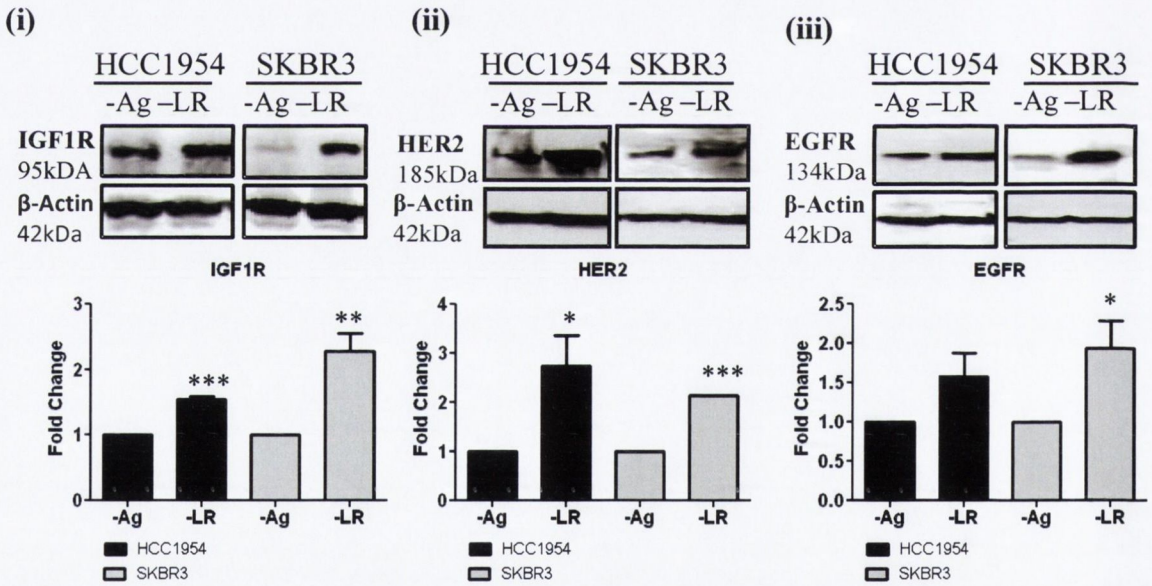

Figure 2.16: Increased IGF1R, HER2 and EGFR with acquired lapatinib-resistance.

The innate expression of IGF1R (predicted target of miR-630) was initially investigated in cells with acquired-resistance to lapatinib. **(i)** IGF1R was significantly increased in HCC1954-LR and SKBR3-LR compared to age-match parent cells (HCC1954-Ag and SKBR3-Ag respectively). **(ii-iii)** Furthermore, targets of the drugs assessed in this study (HER2 and EGFR) were also found to be increased in HCC1954-LR and SKBR3-LR compared to age-matched parent cells (HCC1954-Ag and SKBR3-Ag respectively). Representative immunoblots, n=3±SEM (corresponding densitometry below blots), where *$p<0.05$, ** $p<0.01$ *** $p<0.001$

We next investigated if manipulation of miR-630 could alter the levels of predicted target IGF1R as well as HER2 and EGFR. Here we observed that after inhibiting miR-630 in parent cells HCC1954-Ag and SKBR3-Ag, there was a significant increase of IGF1R protein levels in HCC1954-Ag by 1.3±0.05 fold ($p<0.05$) and in SKBR3-Ag by 1.4±0.05 fold ($p<0.01$) compared to the NC inhibitor transfected cells (Figure 2.17 (i)). Furthermore, inhibition of miR-630 was associated with increased levels of HER2 in HCC1954 by 2.1±0.1 fold ($p<0.01$) and SKBR3 by 1.3±0.02 fold ($p<0.05$) (Figure 2.17 (ii)). EGFR was also increased upon miR-630 inhibition in HCC1954 by 1.5±0.2 ($p<0.05$) fold and SKBR3 by 1.7±0.2 fold ($p<0.05$) (Figure 2.17 (iii)).

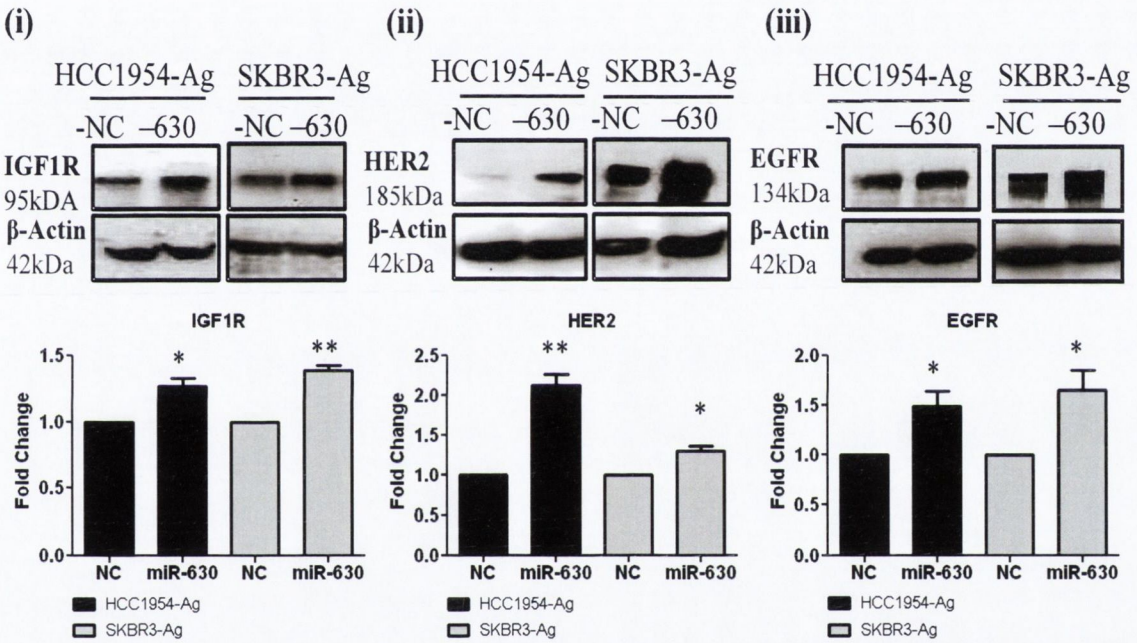

Figure 2.17: Inhibition of miR-630 increases IGF1R, HER2 and EGFR.

Inhibition of miR-630 induced an increase in **(i)** IGF1R expression in both HCC1954-Ag and SKBR3-Ag cells compared to the negative control. Similarly, levels of **(ii)** HER2 and **(iii)** EGFR were also increased. Representative immunoblots, n=3±SEM (corresponding densitometry below blots), where * $p<0.05$, ** $p<0.01$

In contrast to the findings of miR-630 inhibition, mimicked expression of miR-630 in lapatinib-resistant HCC1954-LR and SKBR3-LR was associated with decreased levels of IGF1R, HER2 and EGFR (Figure 2.18). Specifically, miR-630 mimic transfected cells demonstrated a 2.9±0.9 fold decrease for HCC1954-LR ($p<0.05$) and a 1.9±0.4 fold decreased for SKBR3-LR ($p<0.05$) compared to NC mimic transfected cells (Figure 2.18 (i). The levels of HER were decreased in HCC1954-LR by 1.9±0.4 fold ($p<0.05$) and SKBR3-LR by 2.6±0.3 fold upon miR-630 mimicked expression (Figure 2.18 (ii)). Additionally, EGFR was also decreased in HCC1954-LR by 4.6±2.3 fold ($p<0.05$) and SKBR3-LR by1.5±0.3 fold ($p<0.05$) (Figure 2.18 (iii)).

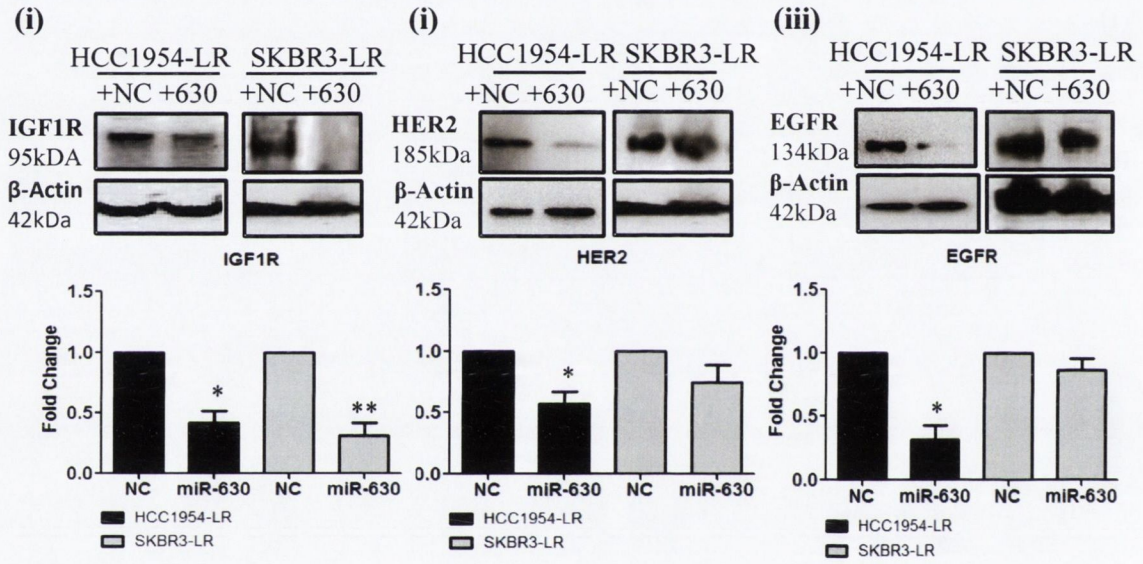

Figure 2.18: miR-630 mimic decreases IGF1R, HER and EGFR.

Mimicked expression of miR-630 induced a decrease in **(i)** IGF1R expression in both HCC1954-LR and SKBR3-LR cells compared to the negative control. Similarly, levels of **(ii)** HER2 and **(iii)** EGFR were also decreased. Representative immunoblots, n=3±SEM (corresponding densitometry below blots), where * $p<0.05$, ** $p<0.01$

2.3.12 The generation of stable miR-630 overexpressing and knockdown cell lines

The assessment of the functional relevance of miR-630 to this point was performed on cell lines through transient inhibition or overexpression of miR-630. In order to further examine the potential of miR-630 and its relevance for using as an *in vivo* model, we decided to establish cell lines that had stable knockdown or overexpression of miR-630. The generation of these stable cell lines were performed by lentiviral transduction (as detailed in Sections 2.2.14), a method adopted during a period spent in the Dana Farber Cancer Institute (DFCI). Prior to establishing these cell lines, it was necessary to have cell lines that expressed the Luciferase gene (LUC) so that it would be possible to visualise *in vivo* tumour growth via bioluminescence. The mcherry/LUC+ virus was kindly provided by Kornelia Polyak's group in DFCI which was used to establish HCC1954 mcherry/LUC+ cells. Previously established SKBR3 mcherry/LUC+ cells were also a gift provided by Prof. Polyak's group.

SKBR3 mcherry/LUC+ (Figure 2.19A) and HCC1954 mcherry/LUC+ (Figure 2.19B) cells were both subsequently infected with viruses containing either an inhibitor for the miR-630 mature miRNA or miR-630 precursor sequence. Scrambled inhibitors and precursors were used to establish relevant controls for the stable cell lines. After 48hrs, successful infection of cells was visualised under a fluorescence microscope (Figure 2.19A & 2.19B). The miR-630 precursor and scrambled precursors expressed green fluorescent protein (GFP) as a reporter gene. Detection of GFP in the cells infected with either scrambled or miR-630 precursors demonstrated successful infection. SKBR3 mcherry/LUC+ and HCC1954 mcherry/LUC+ Cells that were not infected with any virus were also photographed as a control. As expected, GFP was not detected in these cells, nor was it detected in cells that were infected with miR-630 inhibitor or scrambled inhibitor. As the selection antibiotic for these precursors (puromycin) was also the same as that used for mcherry/LUC, GFP+ cells were therefore sorted by flow cytometry. All infected cells, including the non-infected cells, had a basal level of mcherry expression (as the cell lines used were already mcherry/LUC+). Since mcherry was the reporter gene for miR-630 inhibitor and the scrambled inhibitor, inhibitor infected cells tended to have a higher level of mcherry expression although flow cytometry would not be suitable to sort these cells. Therefore selection of these cells was performed using hygromycin (since these cells already expressed mcherry, selected for with puromycin) (Figure 2.19A & 2.19B).

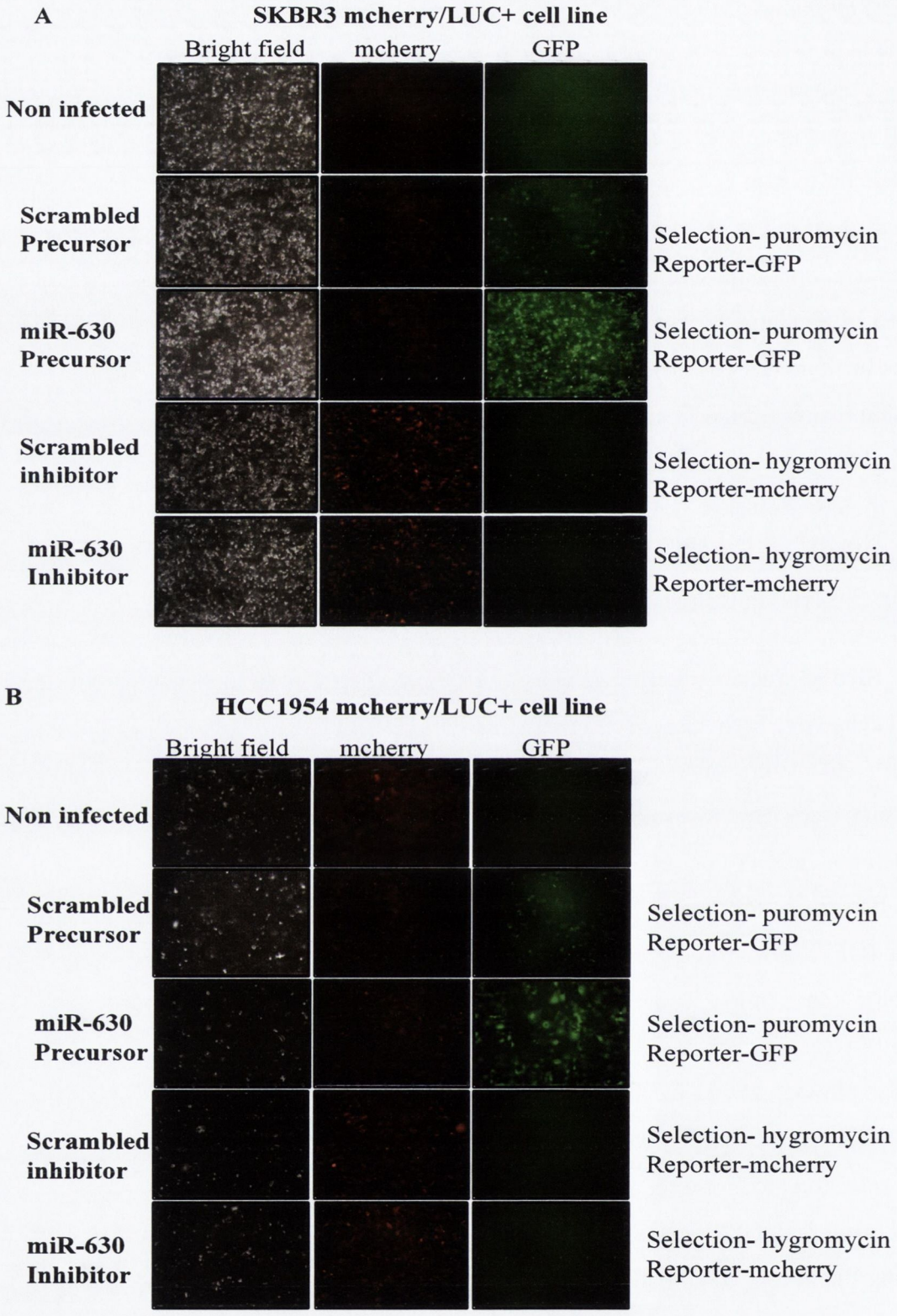

Figure 2.19: Generation of stable miR-630 overexpressing and knockdown cell lines.

Generation of stable miR-630 precursor and inhibitor cells with corresponding scrambled controls using **(A)** SKBR3 mcherry/LUC+ cell (gift from Prof. Polyak) and **(B)** HCC1954 mcherrry/LUC+ cells (generated during course of this thesis).

2.3.13 Characterisation of stable miR-630 overexpressing and knockdown cell lines

Following establishment of the stable miR-630 inhibitor cell lines (now called HCC 630 K/D and SKBR3 630 K/D) and the stable miR-630 precursor cells (now called HCC 630 PRE and SKBR3 630 PRE), we characterised the cells based on miR-630 expression, proliferation, response to chemotherapy and invasion. Here we found that miR-630 was significantly decreased ($p<0.01$) in HCC 630 K/D by 4.2±0.8 fold and SKBR3 630 K/D by 7.3±4.3 fold compared to their respective scrambled controls (HCC SCR K/D and SKBR3 SCR K/D) (Figure 2.20A). Screening the cells for response to various HER-targeted therapies and also docetaxel, demonstrated that while no significant change was observed in response to trastuzumab, miR-630 inhibition increased percentrage cell viability to lapatinib by 8.8±2.9% ($p<0.05$), neratinib by 9.5±0.7% ($p<0.01$), afatinib by 19.5±0.6%($p<0.01$) and docetaxel by 12.4±4.3% ($p=0.053$) in HCC1954 mcherry/LUC+ cells (Figure 2.20B(i)). Similarly, in SKBR3 mcherry/LUC+ cells, miR-630 inhibition increased percentrage cell viability to lapatinib by 13.7±1.2% ($p<0.05$), neratinib by 4.8±1.6% ($p<0.05$), afatinib by 35.3±12.1%($p<0.05$) and docetaxel by 18.5±8.2% ($p=0.077$) (Figure 2.20B(ii)).

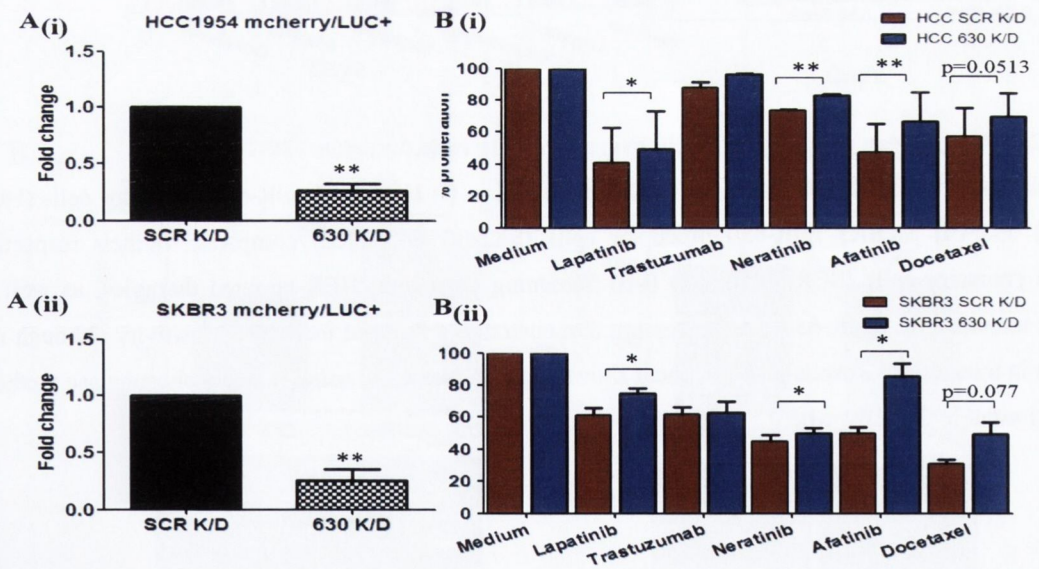

Figure 2.20: Drug screen of stable miR-630 knockdown cells.

(A) The expression of miR-630 was significantly decreased in **(i)** HCC 630 K/D and **(ii)** SKBR3 630 K/D compared to their respective scrambled inhibitor cells (SCR K/D). **(B) (i-ii)** Screening of several HER-targeted therapies as well as docetaxel indicated that miR-630 inhibition can confer resistance to some chemotherapy. Response to treatment shown here was assessed using the acid phosphatase method. Results represent n=3±SEM, where * $p<0.05$ ** $p<0.01$

The expression of miR-630 was significantly increased ($p<0.01$) in HCC 630 PRE by 2.0±0.2 fold and SKBR3 630 PRE by 25.7±3.5 fold compared to their respective scrambled controls (HCC SCR PRE and SKBE3 SCR PRE) (Figure 2.21A). Screening the cells for response to various HER-targeted therapies and also docetaxel, showed that while trends towards increased sensitivity of these drugs were observed, most did not show significant differences in most cases (Figure 2.21B).

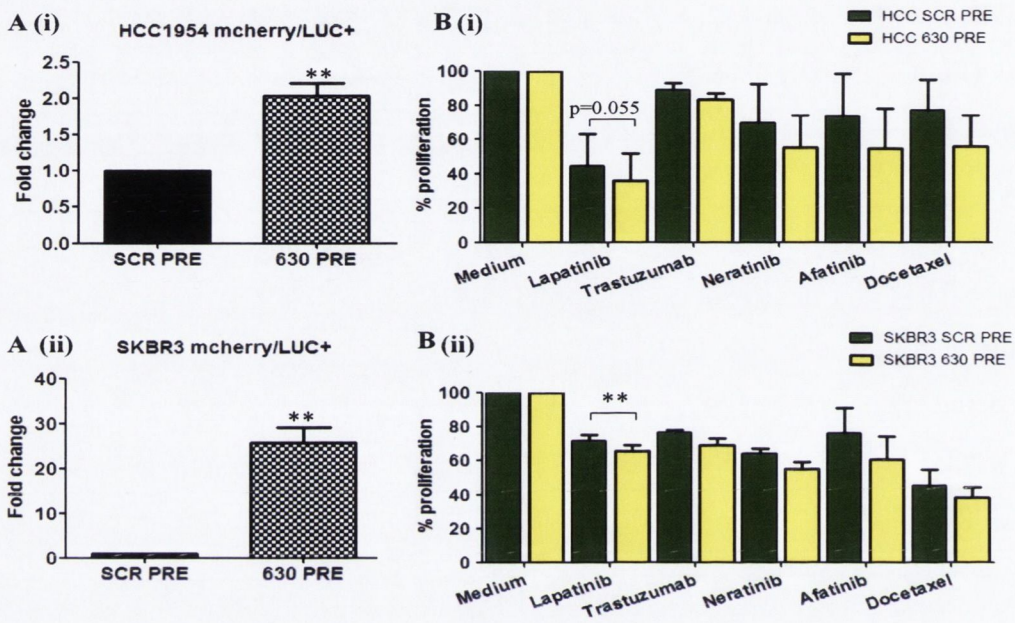

Figure 2.21: Drug screen of stable miR-630 overexpressing cells.

(A) The expression of miR-630 was significantly increased in **(i)** HCC1954 miR-630 precursor cells (HCC 630 PRE) and **(ii)** SKBR3 miR-630 precursor cells (SKBR3 630 PRE) compared to their respective scrambled precursor cells (SCR PRE). **(B) (i-ii)** Screening of several HER-targeted therapies, as well as docetaxel, indicated that miR-630 overexpression demonstrated a trend of increased sensitivity although not significant in most cases. Response to treatment shown here was assessed using the acid phosphatase method. Results represent n=3±SEM, where **$p<0.01$

As HCC1954 cells grow better *in vivo* than SKBR3 cells, our subsequent characterisation focused predominantly on the HCC 630 K/D and HCC 630 PRE cells. Proliferation assays performed over 5 days demonstrated that both stable knockdown and overexpression of miR-630 could significantly alter proliferation by day 5 for both HCC 630 K/D by 1.78±0.1 fold ($p<0.05$) and HCC 630 PRE by 1.6±0.1 ($p<0.01$) compared to their respective scrambled control cells. (Figure 2.22A). Furthermore, invasion assays demonstrated that stable knockdown of miR-630 could significantly ($p<0.05$) increase invasion by 60.4±15.3% compared to scrambled controls, where as stable overexpression of miR-630 could slightly but significantly ($p<0.05$) decrease invasion by 12.0±3.3% (Figure 2.22B).

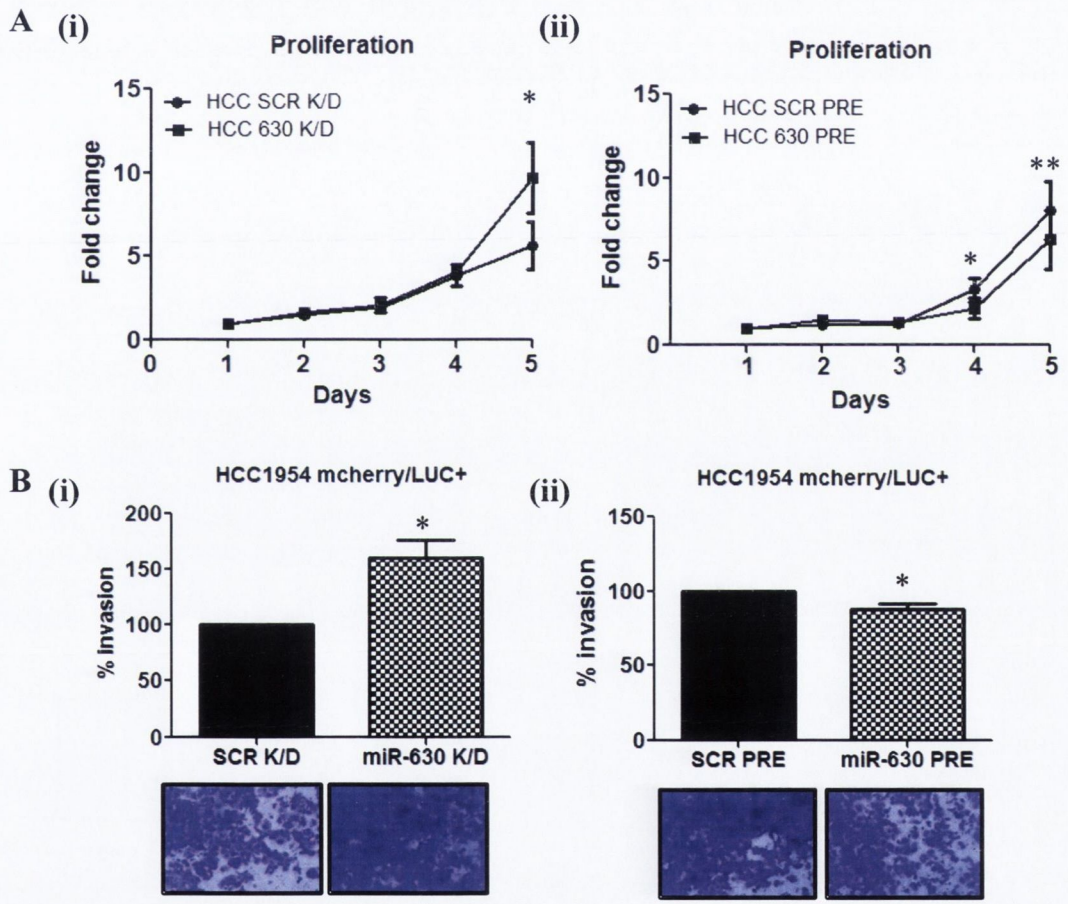

Figure 2.22: Proliferation and invasion of stable miR-630 cells.

(A) Proliferation was significantly increased at day 5 for **(i)** HCC 630 K/D compared to HCC SCR K/D whereas a significant decrease in proliferation was observed for **(ii)** HCC 630 PRE compared to HCC SCR PRE. **(B)** Invasion assays demonstrated a significant increase in **(i)** HCC 630 K/D cells and a slight but significant decrease in **(ii)** HCC 630 PRE compared to their respective control cells. Proliferation shown here was assessed using the acid phosphatase method. Results represent n=3±SEM, where *$p<0.05$ **$p<0.01$

2.3.14 miR-630 may also regulate Neuromedin U

Another predicted target for miR-630, as identified by target prediction software, was Neuromedin U (NmU). NmU is a secreted neuropeptide originally isolated from porcine spinal cord which we identified to be elevated in the cells and CM of acquired-resistant models to HER-targeted agents. This project, discussed in greater detail in Chapter 3, was running in parallel to the miR-630 studies and later we hypothesised that both molecules may be linked in regulating drug-resistance. Stable knockdown of miR-630 was associated with increased NmU protein in HCC1954 mcherry/LUC+ cells by 1.8±0.1 fold ($p<0.01$) and SKBR3 mcherrry/LUC+ cells by 1.6±0.1 fold ($p<0.05$) (Figure 2.23 (i)). No substantial change in NmU expression was observed for miR-630 overexpression (Figure 2.23 (ii)) While results of this observation are somewhat in their infancy, our immunoblots for NmU on the miR-630 stable knockdown cell lines indicate that the expression of miR-630 and NmU maybe inversely correlated (Figure 2.23).

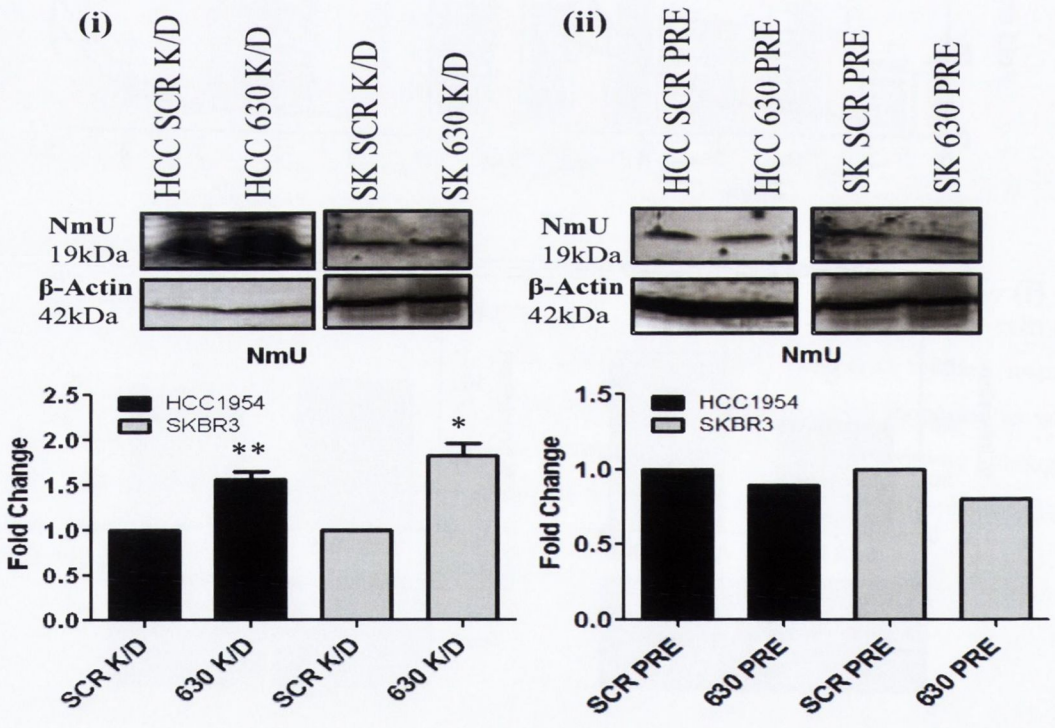

Figure 2.23: miR-630 may regulate Neuromedin U.

Immunoblotting for NmU was performed on cell lines with stable miR-630 overexpression or stable knockdown of miR-630. Here we found that NmU was increased in **(i)** HCC 630 K/D and SKBR3 630 K/D compared to their respective scrambled controls. Conversely, a slight decrease NmU expression was observed for **(ii)** HCC 630 PRE and SKBR3 SCR PRE compared to their respective scrambled controls. Results represent n=3±SEM (for K/D blots) and n=2±SEM (for PRE blots) where *$p<0.05$, **$p<0.01$

2.4 DISCUSSION

The pursuit of extracellular predictive biomarkers offers potential for minimising invasive procedures, such as tissue biopsy procurement in the clinic. Previously, our group reported the existence of RNAs circulating extracellularly in serum/plasma from cancer patients [201]. We have also reported on the detection of circulating miRNAs [206, 249, 270]. In this study we performed global miRNA profiling on the cells and conditioned media (CM) of cell line models for lapatinib and trastuzumab-resistance. Prior to profiling, the success of RNA isolation was determined by assessing yields and quality of RNA in our samples. As expected, yields of cellular samples were high and the 260/280 ratio was within the recommended 1.8-2.0 indicative of pure RNA. For CM samples, yields ranging from 12-27ng/μl (per RNA sample dissolved in 10μl of RNAse free water) were similar to that reported by ourselves and others [201, 271]. While the 260/280 ratio ranged from 1.4-1.6, lower than the recommended 1.8-2.0; this was not surprising because the cellular RNA predominantly consist of ribosomal RNA (rRNA), whereas extracellular RNA does not contain rRNA and is mostly comprised of mRNA and miRNAs that may indicate the low yield observed here [272]. In terms of quality of RNA observed, due to the low yields of RNA present in the CM samples, the 260/280 ratio may not be reliably determined on the Nanodrop spectrophotometer [273].

A substantial number of miRNAs were commonly present in both cells and corresponding CM of all cell lines profiled in this study. The linear regression analysis indicated an R^2 of between 0.32 and 0.4 for the cells and corresponding CM for all cell line variants assessed demonstrating a modest positive correlation between miRNAs detected in cells and corresponding CM. Furthermore, the relative fold changes in miRNA expression of resistant cell lines (SKBR3-TR and SKBR3-LR) compared to sensitive parent cells (SKBR3-Ag) also demonstrated that cells and CM clustered together in hierarchical clustering analysis with a closer similarity of the CM from SKBR3-TR and SKBR3-LR. Taken together these results suggested that CM may carry miRNAs that are reflective of their cells of origin. The suggestion that extracellular miRNAs may reflect their cells of origin have previously been reported [216, 217, 238] although the contrary has also been reported suggesting that miRNAs released may not reflect the abundance of miRNAs within the cell of orign [274, 275]. Whether the observations from our study indicate that the extracellular miRNAs are freely circulating or predominantly vesicle bound remains to

be examined. Future work involving the isolation of vesicle bound RNA (e.g. in exosomes) and comparing to the miRNAs detected in the supernatant following exosome isolation would help to investigate this. We have recently investigated the extracellular miRNA profiles of a panel of prostate cancer cell lines focusing on the miRNAs present in exosomes; this is discussed in further detail in Chapter 5.

Prior to selecting miRNAs for further analysis, venn diagrams were prepared to identify the commonly up- or down-regulated miRNAs in resistant *versus* sensitive cells. In general there was a greater number of miRNAs decreased with drug-resistance. This is not surprising as miRNAs are considered to predominantly act as negative regulators of mRNAs translation [249].

Of the miRNAs chosen for further analysis from global miRNA profiling, miR-630 demonstrated the most consistent and significant results in both the cells and CM from SKBR3-TR and SKBR3-LR compared to age-matched parent controls (SKBR3-Ag). We identified that medium conditioned by both lapatinib- and neratinib-resistant cell line variants of SKBR3 and HCC1954 cells (*i.e.* HCC1954-LR, SKBR3-LR, HCC1954-NR, SKBR3-NR) also demonstrated a significant decrease of miR-630 levels compared to CM from age-matched parent cells (HCC1954-Ag, SKBR3-Ag), correlating with the observation in the corresponding cell lines. This suggests relevance for miR-630 as an extracellular *i.e.* minimally-invasive, predictive biomarker.

To investigate if miR-630 may be altered with innate-resistance as well as acquired-resistance, we initially compared the expression of miR-630 in innately-sensitive SKBR3 cells compared to innately-resistant MDA-MB-453 cells. Having established that miR-630 was decreased in cells and CM of MDA-MB-453 compared to SKBR3, we next elected to use a broader range of HER2-overexpressing cells with varied IC_{50} values for lapatinib. Our findings confirm that decreased expression of miR-630 is associated with increased innate-resistance in the panel of cell lines used in this study.

Limited studies to date have reported on the role of miR-630 in cancer. Specifically, reports using the lung cancer cell line, A549, identified miR-630 as a regulator of cisplatin-induced cell death, with mimicked expression of miR-630 inducing chemo-protective properties [254]. Conversely, the authors of that study also identified that miR-630 failed to protect cells when treated with C_2-CER, $CdCl_2$, etoposide, mitoxantrone, and oxaliplatin

and in some cases induced chemo-sensitivity [254]. In head and neck squamous cell carcinoma, also reporting on cisplatin-induced cell death, Huang *et al.* [255] reported that induced expression of miR-630 with cisplatin treatment of HNSCC cells dramatically decreased cell survival. Induced miR-630 expression decreased levels of anti-apoptotic genes, BCL-2 and BCL2L2, whereas inhibition of miR-630 in HNSCC cells up-regulated these genes and was associated with increased cell survival [255]. The overexpression of miR-630 in the pancreatic cancer cell line PANC-1 has recently been associated with decreased mRNA and protein levels of IGF1R as well as enhanced apoptosis [257]. The motility and invasion of the ANGPTL1 overexpressing lung cancer cell line (CL1-5/ANGPTL1) has been shown to be restored following miR-630 inhibition [256]. To the best of our knowledge, prior to our studies miR-630 has never been associated with any subtype of breast cancer, with response/resistance to HER-targeted drugs and/or breast cancer cell aggression. Here we observed that miR-630 is associated with –and may be causally involved in– regulating resistance to HER-targeting drugs. As mentioned, initially using our cell line models of acquired lapatinib-resistance (HCC1954-LR, SKBR3-LR) and neratinib-resistance (HCC1954-NR, SKBR3-NR) and subsequently in a panel of cell lines with innate-resistance, we observed a decrease in miR-630 expression.

To support our *in vitro* findings, and so indicate the relevance of choosing miR-630 for further functional evaluation, our subsequent analysis was to determine the clinical relevance of miR-630. Evidently, miR-630 was decreased in breast cancer tumours compared to peritumours which was also apparent when assessed in specifically HER2-overexpressing tumours.

Returning to our cell line models, having established that reduced miR-630 expression levels are associated with both innate- and acquired-resistance, we progressed next to establishing if this was specific to lapatinib and neratinib alone or more generally associated with HER-targeting drugs. For this purpose, we also included afatinib in our analyses. For functional assessement of this miRNA, we initially performed transient inhibition and mimicked expression of miR-630. Mimicked expression of miR-630 was confirmed by qPCR and conversely inhibition of miR-630 demonstrated a decrease in miR-630 expression. miRNA inhibitors are designed to specifically bind to and inhibit endogenous miRNA molecules and enable miRNA functional analysis by down-regulation of miRNA activity. However, they are not known to cause degradation of the miRNA, thus

the levels of miR-630 should not necessarily have been changed when assessed by qPCR. Recent studies have suggested that much of the apparent decrease in miRNA expression that may be associated with miRNA inhibitor transfection is attributable to the suppressive effect of antisense inhibitor on the PCR reaction itself [276]. Therefore, other options for reporting the relative functional level of a miRNA have been suggested including the use of a miRNA reporter (such as luciferase or a fluorescent protein under the control of miRNA target sites) [276].

Through inhibition of miR-630 (in sensitive parent cells) or its mimicked expression (in acquired lapatinib-resistant or innately-resistant cells) our studies identified a correlation between miR-630 function and cellular response to all 3 HER-targeting drugs tested *i.e.* lapatinib, neratinib and afatinib.

To more comprehensively evaluate a functional relevance of miR-630 in HER2-overexpressing breast cancer we next investigated whether miR-630 may confer other phenotypic influences. Interestingly we observed that inhibition of miR-630, in sensitive parent SKBR3 and HCC1954 cells, was also associated with increased cell motility, migration, invasion and resistance to *anoikis*. On the contrary, miR-630 mimicked expression in acquired-resistant SKBR3-LR and HCC1954-LR cells resulted in a substantial block on these phenotypic changes. In agreement with our observations, increased cell migration and invasion have widely been reported to be associated with drug-resistance [277-279]. Additionally, we have previously reported that drug-resistance can also be coupled with increased resistance to *anoikis* [237]. Our findings are supported by the recent study by Kou *et al.* [256] demonstrating that lung cancer cells (CL1-5) overexpressing ANGTL1 have reduced motile and invasive capabilities with increased levels of miR-630; whereas increased migration/invasion induced by shANGPTL1 in CL1-0 cells was associated with decreased miR-630 expression [256]. The authors of this study also demonstrated that inhibition of miR-630 in CL1-5/ANGTL1 cells restored invasion and migration [256].

Investigating the mechanism(s) by which miR-630 could be conferring these influences on sensitivity/resistance as well as altered cell aggression, IGF1R (which our bioinformatics analysis initially predicted as a target of miR-630 and more recently was reported by Farhana *et al.* as a target for miR-630 [257]) was found to be a directly

influenced by miR-630 manipulation. Interestingly, elevated IGF1R expression, observed in our acquired lapatinib-resistant cells (SKBR3-LR and HCC1954-LR) compared to their age-matched parent cells was inversely correlated with decreased miR-630 expression in the same resistant cells.

Advancing on this observation, we demonstrate that inhibition of miR-630 -resulting in increased resistance and metastatic phenotype in SKBR3 and HCC1954- was associated with increased IGF1R expression in both cell lines. Mimicked expression of miR-630, which induced an increase in sensitivity to HER-targeting drugs for acquired-resistant SKBR3-LR and HCC1954-LR cells as well as decreased cell aggressiveness, caused a reduction of IGF1R expression. These observations are in keeping with that of several other reports that correlate IGF1R expression with resistance to HER-targeting drugs and other chemotherapy [54-58]. Furthermore, increased IGF1R has also been previously attributed with an increased aggressive phenotype [280-282]. Our studies, however, are the first to determine that the mechanism involved is, at least partly, regulated by aberrant miR-630 expression. This observation is supported by the recent study by Farhana *et al.* [257] who demonstrate that miR-630 pairs to a 7 nucleotide conserved region located in position 2658–2665 of IGF1R 3′-UTR and showed that overexpression of miR-630 reduced the mRNA and protein levels of IGF1R in the pancreatic cancer cell line, PANC-1 [257].

The drugs included in this study target both HER2 and EGFR. For this reason we also investigated whether miR-630 may modulate the expression of these receptors. We initially observed that the acquired lapatinib-resistant cells used for this study (SKBR3-LR and HCC1954-LR) have increased levels of both HER2 and EGFR compared to their age-matched parent controls. This is supported by previous studies reported that increased levels of HER2 or EGFR correlate with resistance to trastuzumab and other chemotherapy [54, 59]. In addition to this, we observed that miR-630 inhibition induced an increase in both HER2 and EGFR, whereas mimicked expression of miR-630 decreased the expression levels of these proteins. Previous studies have indicated that crosstalk between IGF1R and other tyrosine kinases such as HER2 and EGFR can drive cancer progression and drug-resistance [283-285]. This supports our hypothesis that miR-630 directly regulates IGF1R which, subsequently, leads to alterations in HER2 and EGFR potentially

driving the phenotypic affects demonstrated in this study. A model for this proposed mechanism is illustrated in Figure 2.24.

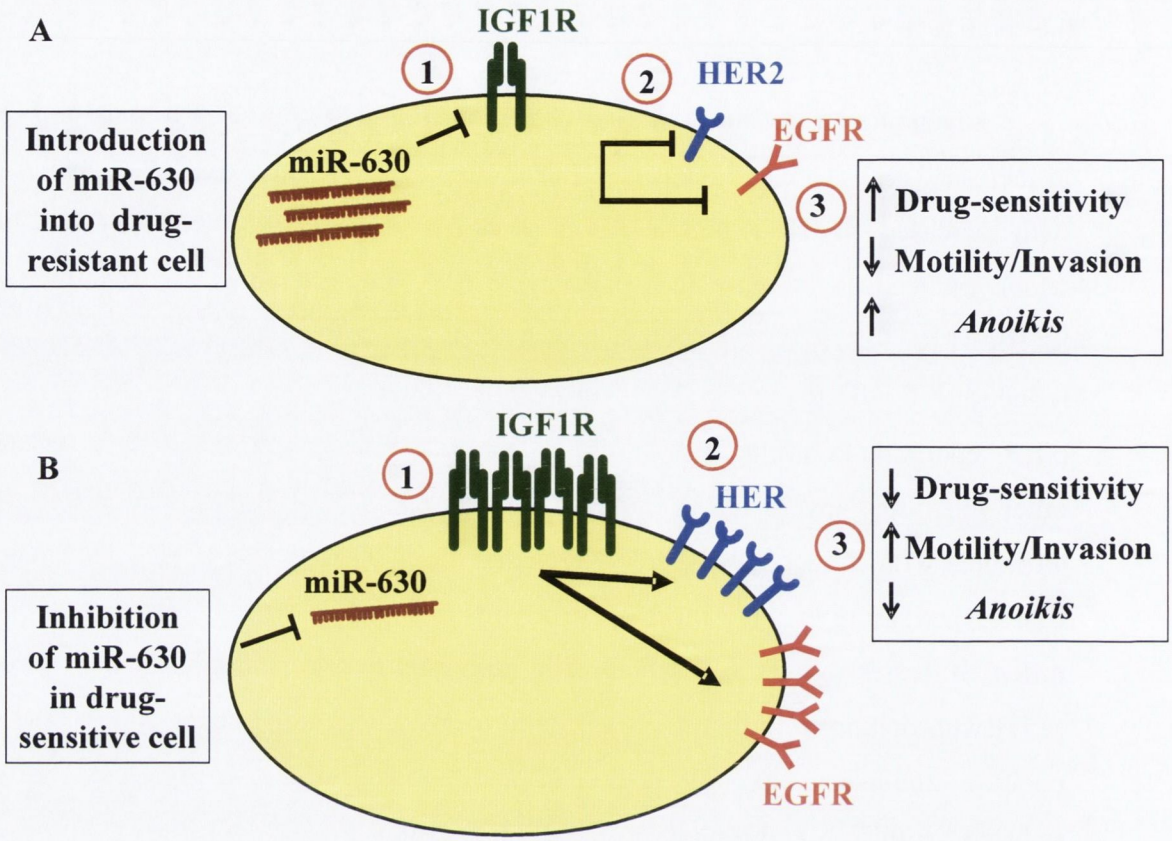

Figure 2.24: Proposed model for outcome from manipulation of miR-630 in breast cancer cells.
Elevated IGF1R, HER2 and EGFR have previously been associated with drug-resistance and cancer cell aggression. Our studies suggest that **(A)** Introducing miR-630 into acquired- or innately-resistant breast cancer cells can (1) directly inhibit the IGF1R mRNA translation. (2) Crosstalk of IGF1R with other receptor tyrosine kinases (HER2 and EGFR) can lead to their subsequent down regulation and so (3) cause cells to become more sensitive to HER-targeting agents as well as decreasing their aggressive phenotype (in terms of motility, invasion and resistance to *anoikis*). **(B)** Conversely, inhibiting the expression of miR-630 in sensitive breast cancer cells can (1) prevent its binding to, and translational suppression of, target mRNA IGF1R. This allows an increase in IGF1R protein expression which in turn can (2) induce elevated HER2 and EGFR expression and, as a result, (3) cells exhibit a more aggressive phenotype.

In order to further investigate the importance of miR-630 in breast cancer, we decided to establish cell lines with stable miR-630 overexpression and knockdown that may potentially be used for future *in vivo* studies. Our drug screen indicated that, in keeping with our transient transfection studies, stable inhibition of miR-630 expression increased resistance to several HER-targeting agents. However drug sensitivity for the stable miR-

630 precursor cells was not significantly altered. Proliferation and invasion were altered with stable knockdown of miR-630, indicating that these stable knockdown cells were to some extent confirming some of the observations from our transient transfection studies.

It may be possible that the lentiviral infection of the precursor however was not efficient enough to elicit the same affects observed when the transient mimic transfected cells were treated with drugs. For example, the expression of miR-630 achieved in the HCC1954 miR-630 precursor stable cell lines was only approximately 2-fold increased whereas the miR-630 mimic transfected cells had several thousand fold increased miR-630 expression.

Sequencing of the commercially-available plasmid constructs was performed to confirm whether the constructs were correct. The miR-630 inhibitor, miR-630 precursor and scrambled controls all showed correct alignment with their expected sequences indicating that the constructs used were correct and so not considered to be a limiting factor in relation to the results achieved with the precursor cells. Repeating the lentiviral infection possibly trying single cell cloning may produce cells with a greater overexpression of miR-630 and so may produce more appropriate models for future miR-630 *in vivo* studies.

Our preliminary analysis of Neuromedin U expression in these stable cell lines may suggest an inverse correlation with miR-630 expression in the stable knockdown cells. Both miR-630 discussed here and Neuromedin U discussed later in Chapter 3 have individually been shown to regulate resistance and cancer cell aggression, the potential link between these two molecules therefore warrants further study.

2.5 CONCLUSIONS

In conclusion, our study indicates that extracellular miRNAs may in fact reflect that of their cells of origin. Furthermore, we have identified for the first time that miR-630 plays an important role in modulating response to HER-targeting drugs, as well as in overall aggressive phenotypic characteristics of HER2-overexpressing breast cancer cells. We have demonstrated that miR-630 may serve as a predictive biomarker for response to treatment in HER2-overexpressing breast cancer; with early indications from our CM studies of its relevance as a minimally-invasive (as well as cell-based) biomarker. Our functional studies provide evidence that introducing exogenous miR-630 in combination with HER-targeted drugs can help to circumvent resistance/insensitivity and reduce cancer

cell aggression in cell lines. Thus, by improving overall response, miR-630 adds value to these HER-targeting drugs.

CHAPTER 3

Neuromedin U: a potential predictive biomarker and a therapeutic target to overcome resistance to HER-tyrosine kinase inhibitors

The contents of this chapter were performed in collaboration with Dr. Sweta Rani, Post-Doctoral Research Fellow, parts of which are included in the following paper submitted currently under peer review:

Neuromedin U: a potential predictive biomarker and a therapeutic target to overcome resistance to HER-tyrosine kinase inhibitors

Sweta Rani, Claire Corcoran*, Serena Germano*, Stephen Madden, Susan Breslin, Martina S McDermott, Brigid C Browne, Norma O'Donovan, John Crown, Lorraine O'Driscoll

3 ABSTRACT

Introduction: Not all HER2-overexpressing breast tumours respond to HER-targeted drugs, and some patients who initially respond, later relapse. There is an urgent need, therefore, to identify predictive biomarkers for improved patient selection and as a means of helping circumvent this resistance.

Methods: Initially studying HER2-overexpressing cell lines, we assessed Neuromedin U (NmU) mRNA and protein levels, in cell lines with acquired- or innate-resistance to trastuzumab, lapatinib or neratinib, and in the conditioned media (CM), and using qPCR and ELISA. Transfection using a plasmid containing NmU cDNA was used to generate cell lines stably overexpressing NmU, whereas siRNAs were used to assess effects of NmU knockdown in cells. Proliferation assays were performed to assess NmU's regulation of response to HER-targeted therapies. Clinical relevance of NmU was assessed in 21 microarray publically-available datasets. Other phenotypic changes associated with cellular aggressiveness were evaluated by motility, invasion and *anoikis* assays.

Results: We found NmU to be present at significantly higher levels in the CM from cells with acquired- or innate-resistance to the HER-targeted drugs, reflecting that of the cells themselves. Short-term exposure of sensitive cells to these HER2-targeted drugs, *i.e.* lapatinib, trastuzumab, neratinib, afatinib, showed a similar trend; suggesting NmU induction is partly an early-response. Analysing 3489 tumours (from the publically-available datasets) showed NmU to be associated with poor outcome for patients, particularly those with HER2-overexpressing tumours; independent of established prognostic indicators. Overexpressing NmU in sensitive cells conferred resistance to all 4 drugs assessed, while knocking it down in both acquired- and innately-unresponsive cells caused drug re-sensitisation. NmU's mechanism-of-action was found to involve complexing with- and induction of- HSP27, its identified partner protein and a known stabiliser of HER2 protein. Conversely, NmU knockdown correlated with reduced HSP27 binding. Further supporting a causative role for NmU, functional NmU receptors on HER2-overexpressing cells were observed, with exogenous NmU increasing HER2 and EGFR expression and inducing a level of drug-resistance. Furthermore, NmU functioned in cellular motility, invasion and *anoikis* resistance. Here we also report on preliminary analysis of cell lines generated for potential *in vivo* studies.

Conclusion: Taken together, these results suggest NmU to be a prognostic and predictive biomarker for HER2-positive cancers and that therapeutic inhibition of NmU could help circumvent resistance and add value to these drugs.

3.1 INTRODUCTION

As previously outlined in Chapters 1 and 2, the use of current HER-targeting agents, trastuzumab and lapatinib, has provided significant clinical benefit in patients with HER2-overexpressing breast cancers. However, innate/primary- and acquired- resistance represent substantial clinical challenges, in addition to the lack of means to predict patients' response. Furthermore, emerging HER-targeting drugs, such as neratinib and afatinib, although demonstrating promising results in clinical trials so far, the possibility of resistance to these drugs may limit their long-term success. Predictive biomarkers for HER-targeting drugs (ideally extracellular, minimally-invasive) are needed for improved patient selection and thus enhanced patient outcome, as are novel therapeutic strategies to circumvent resistance. Our previous studies, including those outlined in Chapter 2, indicate that analysing extracellular RNAs in medium conditioned by cells can be a useful starting point to identifying potential biomarkers, some proving to have functional relevance within the cell [286-290].

Through initial analysis of conditioned media from cell lines with acquired-resistance to lapatinib, we identified Neuromedin U (NmU) as significantly increased with acquired-resistance. This observation was also reflected in the cells themselves. NmU is a secreted neuropeptide originally isolated from porcine spinal cord, along with other neuromedins. Members of the neuromedin peptide family, were classified as such due to their common ability to stimulate smooth muscle contraction [291]. NmU, originally named due to its potent uterine contraction-inducing activity, is synthesised as a 174 amino acid precursor and cleaved to a 25 amino acid biologically-active peptide. NmU is found at high levels in the pituitary and gastrointestinal tissue [292]. Two G-protein coupled receptors (GPCR) for NmU have been identified, NmU-R1 (predominantly in the periphery, especially GI tract) and NmU-R2 (predominantly in central nervous system) [293]. Evidence suggests a role for NmU in pain, stress, immune-mediated inflammatory diseases, and feeding regulation (see reviews [292, 293]). A limited number of studies to date have associated NmU with cancer; with conflicting observations depending on the cancer type. NmU has never previously been independently associated with breast cancer or, indeed, with any HER2-overexpressing cancers.

In this study, we aimed to investigate the relevance of NmU in breast cancer and its potential to regulate response to HER-targeting agents and cancer cell aggression. Our initial analysis of extracellular, as well as intracellular, levels of NmU from our acquired drug-resistant cell lines identified NmU as being significantly increased compared to drug-sensitive age-matched parent cells. Clinical assessment indicated that high expression of NmU is significantly associated with poor outcome, particularly for HER2-positive breast cancer patients. Advancing on these observations, we subsequently performed NmU-overexpression and NmU-knockdown studies to investigate the functional effect of this peptide on cellular response to HER-targeted agents, trastuzumab lapatinib, neratinib and afatinib and the mechanism by which it NmU acts. NmU's effect on cancer cell aggression, assessed by motility, invasion and anoikis assays, was also performed. Here we also report on preliminary findings performed on stable cell lines that may be used for future *in vivo* related studies.

3.2 METHODS

Contribution: As stated at the beginning, the contents of this chapter were performed in collaboration with Dr. Rani. This is indicated throughout and also under the figure legends. Sections solely performed by Dr. Rani are stated as follows: *'These assays were performed by Dr. Sweta Rani'.* In sections that were partly performed by Dr. Rani or others is stated as follows *'These assays were partly performed by ....'* . In terms of 'partly performed' or 'parts of these assays' this indicates that some biological replicates were performed or else experiments were performed on one of the cell lines.

3.2.1 Cell culture and treatments

SKBR3, HCC1954, MDA-MB-361, T47D cells, obtained from ATCC, were cultured in RPMI-1640 (Sigma-Aldrich, R0883) with 10% FCS (PAA Cat. #: A15-151) and 1% L-glutamine (Sigma-Aldrich, Cat. #: G7513). Lapatinib-resistant SKBR3 and lapatinib-resistant HCC1954 cells (SKBR3-LR and HCC1954-LR, respectively- developed by Dr. Sweta Rani, Post-doctoral Research fellow) were established by continuously exposing cells to lapatinib, starting with 5nM and increased stepwise to 250nM over 6 months. Similarly, neratinib-resistant cells (SKBR3-NR, HCC1954-NR-developed by Susan Breslin) were established by continuously exposing cells to neratinib, increasing stepwise to 80nM (for SKBR3-NR) and 250nM (for HCC1954-NR) for over 4 months. SKBR3 trastuzumab-resistant variants (SKBR3-TR) were established through exposure to trastuzumab (SKBR3-TR) over a period of 6 months and were kindly provided by Dr. Norma O'Donovan (Molecular Therapeutics for Cancer Ireland, Dublin City University). Age-matched parent cells (SKBR3-Ag, HCC1954-Ag) were maintained in culture, in parallel, but were not exposed to drug. Working banks of all cell line variants were cryopreserved (freezing media at a final concentration of 5% Dimetyl Sulfoxide (DMSO, Sigma-Aldrich, Cat. #: D2650) and stored in liquid nitrogen. All experiments on acquired-resistant cells and corresponding aged controls were performed within 10 passages in culture and were performed on cells that receieved no drug for a minimum of one week. Passage numbers used were approximately the following: SKBR3-LR/-Ag (p95-105); HCC1954-LR/-Ag (p74-84); SKBR3-NR/-Ag (p99-109); HCC1954-NR/-Ag (p70-80); SKBR3-TR/Ag- (p85-95). Cells were routinely tested for *Mycoplasma* contamination using the PCR Mycoplasma Test Kit 1/RT Variant B (Promocell, Cat. #: PK-CA91-3025B)

and were found to be negative. Lapatinib (Cat. #: SRP01210l), neratinib (Cat. #: SRP06000n) and afatinib (Cat. #: SRP037103a) were obtained from Sequoia Research Chemicals Ltd. (Pangbourne UK). Lapatinib, neratinib and afatinib were prepared in DMSO to a concentration of 10mM and stored in aliquots at -20°C. Working stocks of 10μM were prepared fresh every week as necessary and for each biological replicate of toxicity assays. Trastuzumab was provided by St. James's University Hospital, Dublin; prepared at 21mg/ml in bacteriostatic water for injection and stored at 4°C. Working stocks of 1mg/ml were prepared fresh every week as necessary and for each biological replicate of toxicity assays.

3.2.2 Short-term drug exposure assays

[These assays were performed by Dr. Sweta Rani]

SKBR3 and HCC1954 cells were seeded ($5x10^5$ cells, $25cm^2$ flasks) and allowed to grow to 80% confluency before being exposed, for 48 hours, to lapatinib (1μM), trastuzumab (12.5μg/ml), neratinib (0.5μM), or afatinib (0.5μM). Cell pellets were collected, RNA was isolated (as described in Section 2.2.3) and the expression of NmU was evaluated by qPCR as described in Section 3.2.8.

3.2.3 RNA isolation from conditioned medium

Conditioned medium (CM) was collected, centrifuged and filtered, as previously described [289, 294], prior to NmU mRNA and protein analysis. [Full description of CM collection and subsequent RNA isolation is described in Chapter 2, Section 2.2.2 and 2.2.3]

3.2.4 NmU knockdown and overexpression

[parts of these assays were performed by Dr. Sweta Rani; cloning of the NmU cDNA construct into the pcDNA 3.1(+) vector was performed by Dr. Serena Germano, Post-Doctoral Research fellow]

Two siRNAs, designated NmU-1 and NmU-2 (Ambion, Cat. #: s225456 and s21351), (30nM) were used to target NmU. Scrambled siRNA (Scr) (Ambion, Cat. #:AM4611) was used as a negative control. Transfection was performed using lipofectamine 2000 (Invitrogen, Cat. #: 11668-027) according to the manufacturer's

instructions and described in greater detail in Chapter 2, Section 2.2.7. Transient transfections were harvested 72 hours post-transfection for RNA and protein extraction.

NmU full-length cDNA was sub-cloned by digesting from pOTB7 (clone ID3502168, Open Biosystems) and ligating into pcDNA 3.1(+) zeo-plasmid vector (Invitrogen, Cat. #:V860-20; see vector map information in Appendix I, Section D). The construct was verified by DNA sequencing (see Appendix, Section E, Figures E.1 & E.2). Mock controls used were of pcDNA3.1(+) plasmid lacking NmU cDNA. Cells (SKBR3 and HCC1954) were seeded into $25cm^2$ flasks and allowed to grow to approximately 50-70% confluency and were transfected with 4μg of NmU-containing plasmid or empty plasmid. Lipofectamine 2000 (Invitrogen, Cat. #: 11668-027) was used for transfection following the manufacturer's instructions. Stable transfectants were established by selecting with zeocin (Invitrogen, Cat. #:R250-01) (50μg/ml and 300μg/ml for HCC1954 and SKBR3 transfected cells, respectively; based on Dr. Rani's initial assessment of the toxicity of zeocin on these cells).

3.2.5 Proliferation assays

Cells with acquired-resistance compared to aged-parent cells and NmU cDNA-*versus* mock-transfected cells (HCC1954 variants, $3x10^3$ cells/well; SKBR3 variants, $5x10^3$ cells/well; in 96-well plates) were seeded for 24hrs prior to drug additions. Subsequently, lapatinib (0-1.1μM for SKBR3; 0-6μM for SKBR3-LR; 0-500nM for both SKBR3-mock and SKBR3-NmU; 0-1.1μM for HCC1954; 0-6μM for HCC1954-LR; 0-800nM for HCC1954-mock; 0-15μM for HCC1954-NmU), neratinib (2-40nM for both SKBR3-mock and SKBR3-NmU; 0-750nM for HCC1954-mock; 0nM-1.2μM for HCC1954-NmU), trastuzumab (0-500μg/ml for both HCC1954-mock and HCC1954-NmU) or afatinib (0-32nM for SKBR3-mock; 0-100nM for SKBR3-NmU; 0-50nM for HCC1954-mock; 0-185nM for HCC1954-NmU) was added to the cells. Five days later, acid phosphatase assay was performed as previously detailed in Chapter 2, Section 2.2.9.

3.2.6 *Assessing effects of NmU siRNAs with HER-targeted drugs*

[These assays were performed by Dr. Sweta Rani]

To investigate if knockdown of NmU affected response to HER-targeting, cell lines with acquired lapatinib-resistant (SKBR3-LR, HCC1954-LR) and innately unresponsive (MDA-MB-361, T47D) cells were assessed. Cells were seeded into 24-well plates at a density of $5x10^4$/well (HCC1954-LR, T47D) and $1x10^5$/well (SKBR3-LR, MDA-MB-361). Forty-eight hours following transfection with NmU-1 siRNA, NmU-2 siRNA or Scr sequences, cells were exposed to their approximate IC_{50} concentrations of lapatinib (3μM, SKBR3-LR; 5μM, HCC1954-LR; 1μM, MDA-MB-361; 5μM, T47D), as these IC_{50} values had previously been determined by ourselves and others [263-265]. As in previous studies [265] a fixed concentration of trastuzumab (15μg/ml) was assessed for all 4 cell line variants. Fixed concentrations of neratinib (1μM) and afatinib (0.5μM) were used similar to that of others [295]. These were cultured for 72 hours and subsequently assessed using acid phosphate analysis as previously detailed in Chapter 2, Section 2.2.9.

3.2.7 *NmU peptide treatment and assessing affects with HER-targeted drugs*

[These assays were partly performed by Dr. Sweta Rani]

To assess if functional NmU receptors are expressed on cells, SKBR3 and HCC1954, ($1x10^6$ cells) were seeded in $25cm^2$ flask, allowed to attach overnight and subsequently treated with 1μM of NmU-25 (Bachem, Cat. #: H5538) for 24-48 hrs. Peptide treatments were also performed to assess if endogenous NmU affected response to HER-targeting. Cells were seeded into 24-well plates at a density of $2.5x10^4$/well (HCC1954) and $5x10^4$/well (SKBR3) and allowed to attach overnight. The next day medium was changed and replaced with medium (5ml) containing 1μM of NmU-25 (Bachem, Cat. #: H5538). After 48hrs, medium was changed and cells were treated with lapatinib (1μM), trastuzumab (12.5μg/ml), neratinib (0.5μM), or afatinib (0.5μM) -same as used for pulse-treated assays. These were cultured for 72hrs and subsequently assessed using acid phosphate analysis as previously detailed in Chapter 2, Section 2.2.9.

3.2.8 qPCR

[These assays were partly performed by Dr. Sweta Rani]

Total RNA was isolated from cell lines and CM using TriReagent (Sigma-Aldrich, Cat. #: T9429). In order to remove any potential contaminating genomic DNA, RNA was treated with DNase enzymes and minus reverse transcriptase enzyme controls verified no DNA/pseudogene contamination of starting material (this was performed on overexpressing cell lines) [289]. For DNAse treatment, in brief, RNA samples were treated with 1U of RNase-free DNase (Promega, Cat. #: M6101) per 1µg RNA in a reaction mixture of 10µl including reaction buffer (Promega, Cat. #: M198A). RNA was incubated at 37°C for 30mins in the reaction mixture containing RNase-free DNase (Promega, Cat. #: M6101) as recommended by the manufacturer. To this mixture was added 1µl of RQ1 DNase Stop Solution (Promega, Cat. #: M199A) to terminate the reaction and further incubated at 65°C for 10mins to inactivate the DNase. As a control for qPCR reactions, to ensure no DNA contamination was present, cDNA synthesis (as described below in Section 3.8.2.1) was also performed for samples without reverse transcriptase (-RT). qPCR on H20 was also included as a negative control. Example results of qPCR for Beta Actin with and without RT are shown below (Figure 3.1).

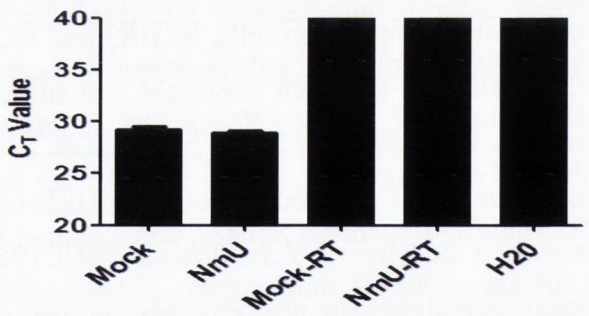

Figure 3.1: Demonstration of qPCR amplification following DNAse treatment.
Sample results are indicated for Beta actin expression where $40C_T$ indicates no expression.

3.2.8.1 cDNA sythesis

cDNA was prepared from 500ng cell-derived and 4µl CM-derived total RNA respectively, [in this case on average approximately 14±1.5ng/µl – some individual examples of quantification and quality of RNA isolated from cells and CM is detailed in

Chapter 2, Section 2.3.1]. RNA, diluted in RNase free water, was incubated with 1µl of 500ng/l oligo dT primers (Eurofins MWG Operon) and 1µl of dNTP (deoxynucleotide triphosphate) (10mM of each dNTP) (Sigma-Aldrich, Cat. #: DNTP100) to a final volume of 10µl. Samples were incubated at 70°C for 10mins. This mixture was then cooled on ice. The following reaction mixture was prepared to make up a final volume of 10µl and added to the contents of each well:

10X buffer (Sigma-Aldrich, Cat. #: B8559)	2µl
RNasin (40U/µl) (Sigma-Aldrich, Cat. #: R2520)	0.5µl
Nuclease-free water (Ambion, Cat. #: AM9916)	6.5µl
MMLV-RT (200U/µl) (Sigma-Aldrich, Cat. #: M1302)	1µl

Table 3.1: Volumes of components used for cDNA synthesis reaction

This mixture was incubated at 37°C for 50mins. The reaction tube was then heated to 80°C for 10mins to denature the MMLV reverse transcriptase. Another RT reaction was set up without MMLV-RT as a negative control.

3.2.8.2 PCR amplification

PCR amplification was performed according to the Applied Biosystems protocol. In brief, each 20µl reaction (per single cDNA sample) consisted of 10µl TaqMan 2X Universal PCR Master Mix, No AmpErase UNG (Applied Biosystems, Cat. #: 4440048), 7µl Nuclease-free water (Ambion, Cat. #: AM9916), 1µl 20X Taqman mRNA Assay, 2µl RT product. NmU (Applied Biosystems, Cat. #:Hs00183624_m1) was quantified using the threshold cycle (C_T) adjusting to the levels of β-actin (Applied Biosystems, Cat. #: 4352933E), established as not differing significantly in expression levels between cell and CM being assessed and so suitable as endogenous control. The PCR reaction was conducted using the ABI 9700 thermal cycler using standard ramp speed, 9600 emulation run mode and the following thermal cycling conditions: hold 95°C 10mins, 40 cycles of 2 steps: 95°C for 15 seconds and 60°C for 60 seconds.

3.2.9 Immunoprecipitation

[Parts of these assays were performed by Dr. Sweta Rani]

HCC1954 and SKBR3 (-mock and -NmU transfected cells) were harvested, washed three times with PBS and lysed using cell extraction buffer (Invitrogen, Cat. #: FNN0011). Protein was quantified and lysate was diluted to 1µg/µl to a final volume of 100µl. Primary antibody was added (2µg/100µl of cell extract), mixed and incubated on a revolving apparatus for 120mins at 4°C. 20µl of 50% protein A agarose beads (Sigma-Aldrich, Cat. #: P7786) was resuspended in the cold lysis buffer (Invitrogen, Cat. #: FNN0011) and then added to the cell extract mix. After mixing, it was incubated with gentle agitation on revolving apparatus for 60mins at 4°C. This mixture was then centrifuged at 5000g for 5mins. The beads were washed 5 times with the cold lysis buffer and centrifuged at 5000g for 2mins. The beads were resuspended in 20µl of Laemmli's sample buffer and boiled (95°C) for 5mins, and centrifuged for 5mins. 18µl of the samples were loaded per lane in a SDS-polyacrylamide gel for electrophoresis.

3.2.10 Immunoblotting and enzyme-linked immunosorbent assay

Cell pellets were lysed and quantified as described in Section 2.2.10. Total cellular proteins [20µg for HSP27 (Enzo life Sciences, Cat. #: ADI-SPA5603); 30µg for EGFR (Cell signalling, Cat. #: D38131), HER2 (Calbiochem, Cat. #: OP15), AKT (Cell Signalling, Cat. #: 9272S), and pAKT (Cell Signalling, Cat. #: S473); and 40µg for NmU-R1 (Sigma-Aldrich, Cat. #: HPA027895) and NmU-R2 (LifeSpan Biosciences, Cat. #: L-B153);] were resolved on PAGEr Gold precast gels for protein electrophoresis (Lonza, Cat. #: 59513(7.5%); Cat. #: 59514(10%); Cat. #: 59515(12%)). The following percentage tris-glycine gels were used: 7.5% for EGFR and HER2; 10% for AKT, pAKT, NmU-R1 and NmU-R2; and 12% for HSP27 and were transferred to PVDF membranes (Bio-Rad laboratories, Cat. #: 162-0177). Blots were incubated in blocking buffer [5% BSA (Sigma-Aldrich, Cat. #A9413) in PBS/0.1% Tween (Sigma-Aldrich, Cat. #: P2287)] at room temperature for 1hr. Primary antibodies were prepared in 5% BSA in PBS/0.1% Tween and diluted as follows: HER2 (1:500 dilution); EGFR (1:1000 dilution); HSP27 (1:1000 dilution); NmU-R1 (1:500 dilution); NmU-R2 (1:500 dilution); β-actin (Sigma-Aldrich, Cat. #: A5316) (1:1000 dilution). Membranes were incubated in primary antibodies over night at 4°C. Membranes were incubated with appropriate horseradish peroxidase-

conjugated secondary antibodies -Anti-mouse (Cell Signalling, Cat. #: 7076); or -Anti-rabbit (Cell Signalling, Cat. #: 7074) for 1hr at room temperature and proteins were visualized by chemiluminescence (Themofisher: Cat. #: 34080). Detection was performed with a Chemidoc exposure system (Bio-Rad Laboratories).

ELISA kit for NmU (Bachem, Cat. #: S1254), HER2 (Calbiochem, Cat. #: QIA10-1E), EGFR (R&D Systems, Cat. #: DYC1854-2), p-EGFR (R&D Systems, Cat. #: DYC1095-2) were used according to the manufacturer's instructions. Concentrations of proteins used for all ELISAs were 20µg/ml.

3.2.11 Wound-healing assay

[These assays were performed by Dr. Sweta Rani]

HCC1954-mock and NmU, HCC1954-LR associated Scr- or siRNA-transfected cell variants ($5x10^5$ cells/well) and SKBR3-mock and NmU variants ($1x10^6$ cells/well) were seeded on 6-well plates and cultured for 48hrs to confluency. Monolayer was scratched with a 200µl pipette tip and the resulting wounded areas were monitored and photographed by phase contrast microscopy using CellA software and measured using NIH Image J software.

3.2.12 Migration/invasion assay

[Parts of these assays were performed by Dr. Sweta Rani]

Migration and invasion assays were performed as detailed in Chapter 2, Section 2.2.12. siRNA- or Scr-transfected cells; and NmU cDNA- versus mock-transfected cells (HCC1954 variants, $1x10^5$/insert; SKBR3 variants, $1x10^6$/insert) were seeded in the upper compartment (non-coated for migration & pre-coated with extracellular matrix (ECM, Sigma-Aldrich, Cat. #: E1270) for invasion) and allowed to migrate/invade for 48hrs for HCC1954 cells and 72hrs for SKBR3 cells.

3.2.13 Anoikis assay

[These assays were performed by Dr. Sweta Rani]

Anoikis assays were performed as detailed in Chapter 2, Section 2.2.13. siRNA- or Scr-transfected cells; and NmU cDNA- versus mock-transfected cells (HCC1954 variants, $1x10^5$ cells/well; SKBR3 variants, $1x10^4$ cells/well) were seeded onto a 24-well plates coated with poly(hydroxyethyl methacrylic) acid (Sigma-Aldrich, Cat. #: P3932) or 95% ethanol and cultured for 24hrs and 48hrs, respectively. Cell viability was determined using alamar blue (Invitrogen Cat. #DAL1100).

3.2.14 Assessing potential clinical relevance of NmU in breast cancer

[This analysis was performed in collaboration with bioinformatician Dr. Stephen Madden]

NmU expression was evaluated in publically-available microarray data from 21 datasets representing 3,489 breast tumours. Gene expression datasets were downloaded from Gene Expression Omnibus (http://www.ncbi.nlm.nih.gov/geo/) or authors' websites in the form of raw data files where possible. Table 1 provides a list of the datasets used. In total 3,489 specimens across 10 different platforms were analysed (30 specimens were removed as they lacked clinical information). Where raw data was unavailable, the normalised data -as published by the original study- was used. In the case of the Affymetrix datasets (.cel files), gene expression values were called using the robust multichip average method [296] and data were quantile normalised using the Bioconductor package, affy (www.bioconductor.org). For the dual-channel platforms, data were loess normalised [297] using the Bioconductor package limma. The R package genefu was used to classify the specimens into the luminal A (n=1,521), luminal B (n=676), HER2 (n=476) and basal (n=454) molecular subtypes using the ssp2003 classifier [298]. 362 specimens did not fall into any of these groups. The Entrez gene ID (10874) corresponding to the array probe targeting NmU was obtained from the Gene database at NCBI (www.ncbi.nlm.nih.gov/gene/). All calculations were carried out in the R statistical environment (http://cran.r-project.org/).

GEO Accession	Availability	Specimen Number	Platform Type	Reference
GSE7849	Processed only	78	Affymetrix Human Genome U95 Version 2 Array	[299]
GSE3143	Raw CEL files	158	Affymetrix Human Genome U95 Version 2 Array	[300]
GSE10510	Raw data available	152	DKFZ Division of Molecular Genome Analysis Human Operon 4.0 oligo Array 35k	[301]
NA	Processed only	295	Agilent	[302]
NA	Processed only	118	Affymetrix U133AAofAv2	[303]
GSE9893	Raw data available	155	MLRG Human 21K V12.0	[304]
GSE7390	Raw CEL files	198	Affymetrix U133A	[305]
GSE16391	Raw CEL files	48	Affymetrix U133 Plus 2.0	[306]
GSE1992	Processed only	99	Agilent	[307]
GSE4922	Raw CEL files	249	Affymetrix U133A/B	[308]
NA	Processed only	69	Agilent 44K oligo array	[309]
GSE9195	Raw CEL files	77	Affymetrix U133 Plus 2.0	[310]
GSE6532	Raw CEL files	414	Affymetrix U133A/B and plus2	[310]
GSE1378, GSE 1379	Processed only	60	Custom 22K oligo array	[311]
GSE3494	Raw CEL files	251	Affymetrix U133A/B	[312]
GSE1456	Raw CEL files	159	Affymetrix U133A/B	[313]
GSE21653	Raw CEL files	266	Affymetrix U133 Plus 2.0	[314]
GSE17907	Raw CEL files	51	Affymetrix U133 Plus 2.0	[314]
GSE11121	Raw CEL files	200	Affymetrix U133A	[315]
GSE2034	Raw CEL files	286	Affymetrix U133A	[316]
GSE12093	Raw CEL files	136	Affymetrix U133A	[317]

Table 3.2: Publically-available data sets used to assess NmU expression.

List of - and references to- gene expression datasets that were downloaded from Gene Expression Omnibus (http://www.ncbi.nlm.nih.gov/geo/) or authors' websites, as used for the assessment of the clinical relevance for NmU in breast cancer.

3.2.15 The generation of stable overexpression and stable knockdown cell lines for future in vivo studies

3.2.15.1 Stable NmU expression in HCC1954-LUC+ cells

To further evaluate the role of NmU, our next step was to generate cell lines that may be used for future *in vivo* analysis. Using HCC1954 cells stably expressing the luciferase gene, (provided as a gift from Dr. Annette Byrne, RCSI) and so appropriate for *in vivo* bioluminescence visualisation, HCC1954-LUC+ cells were transfected with either NmU cDNA containing plasmid or empty plasmid (as described earlier in Section 3.2.4). These newly generated cells were assessed for NmU expression using qPCR, proliferation and response to lapatinib using acid phosphatase and invasion using cell culture inserts, all methods described earlier (Sections 3.2.5, 3.2.5, 3.2.12)

3.2.15.2 Stable NmU knockdown in HCC1954-LR-LUC+ cells

To ensure an unbiased approach to future *in vivo* NmU studies, stable knockdown of NmU using shRNAs was also performed using luciferase expressing lapatinib-resistant cells (HCC1954-LR-LUC+ also provided as a gift from Dr. Annette Byrne, RCSI). Commercially available bacterial glycerol stocks of shRNAs for NmU cloned in the pLKO.1 vector (shRNA #1-#5, Open biosystems, Cat. #: RHS4080_NM-006681) and an empty pLKO.1 vector control (Open Biosystems, Cat. #: RHS4080) were obtained. The vector map information of the pLKO.1 construct is available in the Appendix, Section F, Figure F.1. The bacteria glycerol stocks were streaked onto plates coated with agar (Sigma-Aldrich, Cat. #: L2897) and incubated overnight at 37°C. A single colony from the streaked agar plates was picked and inoculated in starting culture 5ml of LB medium containing the appropriate selective antibiotic (100µg/ml Carbenecillin, Sigma Alidrich, Cat. #: C1613).

2x LB-Lennox Broth 20g/l (Sigma-Aldrich, Cat. #: L7658) medium was prepared in water as follows.

This was incubated for 8hrs at 37°C with vigorous shaking in the Innova 4300 incubator shaker at 300rpm. The starter culture was then diluted 500µl in 100mls selective LB medium with carbenecillin and grown at 37°C for 16hrs with vigorous shaking in the

Innova 4300 incubator shaker at 300rpm. The bacterial cells were harvested at 6000g for 15mins at 4°C. Isolation of the plasmids from bacterial cell pellets was performed using the QIAGEN Endofree Plasmid Maxiprep Purification Kit (Qiagen, Cat. #: 12362) protocol as per manufacturer's instructions. All buffers mentioned in this section were part of the Maxiprep kit. In brief, the bacterial pellets were resuspended in 10mls of Buffer P1. 10mls of Buffer P2 was then added to the suspension and mixed gently but thoroughly by inverting 4-6 times and then was incubated at room temperature for 5mins. 10mls of chilled Buffer P3 was then added to the lysate and mixed immediately but gently by inverting 4-6 times. The lysate was then poured into the barrel of a QiAfilter Cartridge. This was incubated for 10mins at room temperature. The cap of the QiAfilter outlet nozzle was removed and the plunger was inserted gently into the QiAfilter Maxi Cartiridge to filter the cell lysate into a 50ml tube. 2.5ml of Buffer ER was added to the filtered lysate, this was then mixed by inverting the tube 10 times followed by incubation on ice for 30mins. The QIAGEN-tip 500 was equilibrated by applying 10ml Buffer QBT and allowing the column to empty by gravity flow. The filtered lysate was then added to the QIAGEN-tip and allowed to enter the resin by gravity flow. The QIAGEN-tip was washed twice with 30mls of Buffer QC. The DNA was eluted with 15ml Buffer QN. The DNA was then precipitated by adding 10.5mls (0.7 volumes) of room-temperature isopropanol to the eluted DNA, this was mixed and centrifuged immediately at 6,000g for 60mins at 4°C. The supernatant was carefully removed and the DNA pellet was then washed with 5ml endotoxin-free, room temperature 70% ethanol and centrifuged again at 6,000g for 60mins. The supernatant was carefully removed again and the DNA pellet was allowed to air dry for 5-10mins before resuspending in 50µl of endotoxin-free Buffer TE. Quantity and quality of DNA isolated was assessed on the Nanodrop-ND 1000 spectrophotometer.

Once plasmid DNA was isolated, HCC1954-LR LUC+ cells were transfected with 4ug DNA (as described previously in Section 3.2.4). As HCC1954-LR LUC+ cells were already resistant to carbenecillin, selection was performed using puromycin (2µg/ml) 48hrs after transfection (Invitrogen, Cat. #: A11118-03).

3.2.16 Detection of NmU in exosomes

[Exosome isolation was partly performed by Dr. Sweta Rani]

For exosome isolation, all cells were grown in RPMI medium supplemented with 10% of exosomes-depleted fetal calf serum (dFCS) (PAA, Cat. #: A15-151), 1% L-glutamine (Sigma-Aldrich, Cat. #G7513) and 1% penicillin/streptomycin (Invitrogen, Cat. #: 15070-063). Exosomes were isolated from HCC1954-Ag, HCC1954-LR and HCC1954-NR cells using a combination of filtration and ultracentrifugation as described and detailed in full in Chapter 4, Section 4.2.9. All cell line variants were seeded in nine $75cm^2$ flasks at $5x10^5$ cells/flask, medium was changed the following day and exosomes were isolated from the conditioned media after 72hrs. NmU in exosomes was detected using the NmU ELISA kit (Bachem, Cat. #: S1254) using protein concentration of 2µg/ml.

3.2.17 Statistical analysis

Statistical analysis on cell line- and CM-derived data was performed in Excel. P values were generated using Student's T-tests, with $p<0.05$ considered as statistically significant. GraphPad Prism 5.0 (Graph Pad Software Inc, La Jolla, USA) was used for graph generation. Relapse-free survival (RFS) of untreated patients was considered the survival end-point. When RFS information was unavailable, distant metastasis–free survival (DMFS) data was used and, if neither RFS nor DMFS were available, overall survival (OS) was used. Median expression was used to determine high and low expression groups within each of the 21 individual datasets. Once a specimen was assigned to a particular group, the 21 datasets were combined and a global survival analysis was performed. Each dataset was considered separately when determining if a specimen belongs to the high or low expression groups, as the expression of mRNAs (including NmU) varies across the different experiments/platforms. The survival curves were based on Kaplan-Meier estimates and Cox proportional hazards regression was used to estimate proportional hazards for the NmU gene expression and other clinico-pathological variables, in both univariate and multivariate models. R package survival was used to calculate and plot the Kaplan-Meier survival curve.

3.3 RESULTS

3.3.1 Intracellular and extracellular NmU mRNA levels are associated with acquired-resistance to lapatinib.

In our efforts to identify extracellular -as well as intracellular- mRNAs that may be associated with resistance to HER-targeted agents, our initial analysis included HER2 overexpressing cell line models, SKBR3 and HCC1954, that were conditioned with lapatinib over an approx. 6 month time period resulting in cell populations that we termed lapatinib-resistant (LR) compared to their aged-parent populations. Comparing the concentration of lapatinib that inhibits 50% of proliferation (IC_{50}) for SKBR3 that had acquired-resistance (SKBR3-LR) (IC_{50}=3μM) in relation to SKBR3 aged cells (IC_{50}=0.09μM) as controls (and so termed SKBR3-Ag), a 29.8±2.2 fold resistance to lapatinib was observed (Figure 3.2(i)). For HCC1954 cells, a similar trend was observed with a 19.1±2.8 fold resistance to lapatinib in HCC1954-LR (IC_{50}=5μM) compared to its age-matched population, HCC1954-Ag (IC_{50}=0.3μM) (Figure 3.2(ii)).

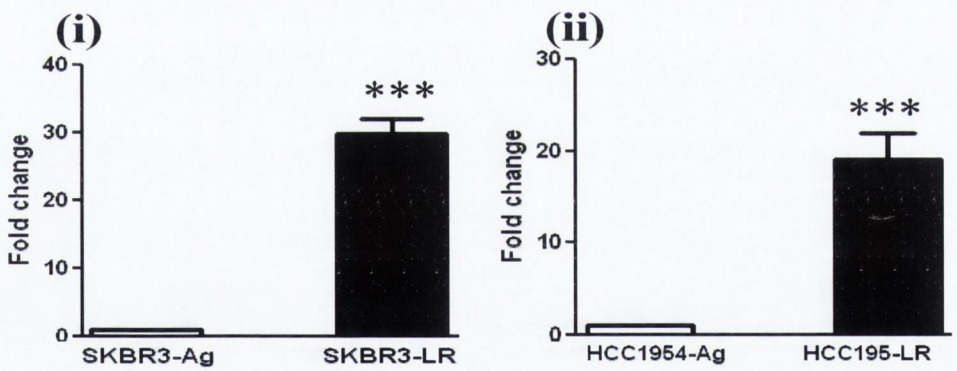

Figure 3.2: Acquired lapatinib-resistance in SKBR3 and HCC1954 cells.

Fold difference in concentration of lapatinib that inhibits proliferation of HER2-overexpressing cells that were conditioned with lapatinib (SKBR3-LR and HCC1954-LR) compared to their aged parent populations (SKBR3-Ag and HCC1954-Ag). Data are presented as fold change assigning control an arbitrary 1. Response to treatment shown here was assessed using the acid phosphatase method. Results represent n=3±SEM, where *** $p < 0.001$. Establishment of lapatinib-resistance was performed by Dr. Sweta Rani.

Evaluating mRNAs, by qPCR, in medium conditioned by SKBR3-LR and HCC1954-LR cells, compared to conditioned medium (CM) from their age-matched control cell lines, indicated significantly higher levels of extracellular NmU in SKBR3-LR by 2.1±0.2 fold ($p<0.01$) and in HC1954-LR by 2.1±0.3 fold ($p<0.05$) (Figure 3.3A (i) & (ii)). The trend of increased NmU mRNA levels observed in CM from the resistant compared to the sensitive cell lines was subsequently found to reflect that in the corresponding cells, whereby NmU was increased in SKBR3-LR by 11.0±0.9 fold ($p<0.001$) and in HCC1954-LR by 4.9±1.2 fold ($p<0.05$) compared to their respective age-matched control cell lines (Figure 3.3B (i) & (ii)).

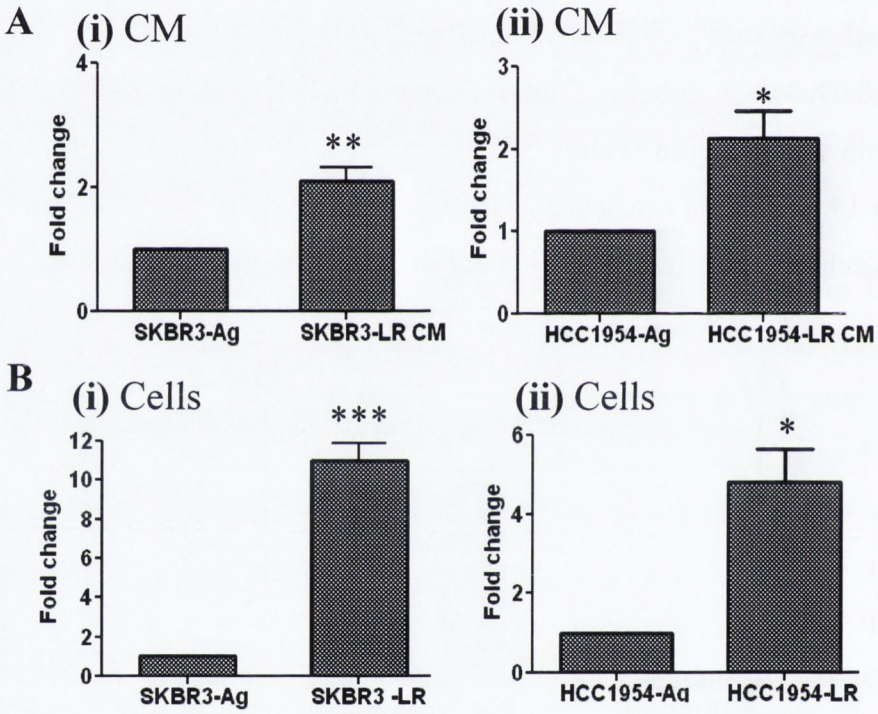

Figure 3.3: NmU is increased with lapatinib-resistance in CM and cells.

(A) qPCR analysis of NmU mRNA in CM from **(i)** SKBR3-LR and **(ii)** HCC1954-LR compared to CM from their aged-parent cells and (B) corresponding NmU mRNA levels within associated cell populations. Data are presented as fold change assigning control an arbitrary 1. Results represent n=3±SEM, where *$p<0.05$, **$p<0.01$, *** $p<0.001$. Assessment of NmU expression here was performed by Dr. Sweta Rani.

3.3.2 Increased expression of NmU may be an early response to drug exposure

Investigating if the induced expression of NmU may be an early response to drug exposure, we treated cells with lapatinib (1μM) for 48hrs and found that the levels of NmU mRNA detectable in CM from the lapatinib-resistant (Figure 3.4A) were significantly higher than in the corresponding untreated control CM for (i) SKBR3-LR by 1.5±0.1 fold ($p<0.001$) and (ii) HCC1954-LR by 1.7±0.2 fold ($p<0.001$) even after this relatively short-term exposure to drug. As expected, a similar trend was found in the corresponding cells with increased NmU expression in SKBR3-LR by 5.4±0.5 fold ($p<0.001$) and in HCC1954-LR by 1.6±0.4 fold ($p<0.01$) (Figure 3.4B).

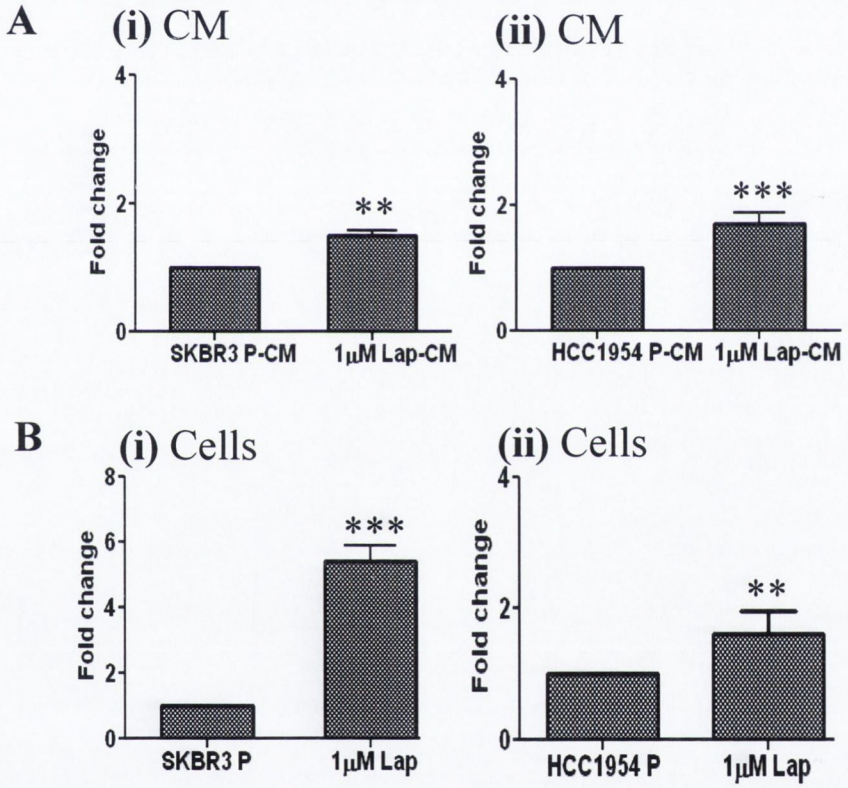

Figure 3.4: Increased NmU with short-term lapatinib treatment.

(A) qPCR analysis of NmU mRNA following short-term (48hrs) exposure of the parent cell populations **(i)** SKBR3 and **(ii)** HCC1954 to lapatinib showing NmU mRNA levels in their respective CM and **(B)** in the corresponding cells. Data are presented as fold change assigning control an arbitrary 1. Results represent n=3±SEM, where **$p<0.01$, *** $p<0.001$. Short term Exposure assays were performed by Dr. Sweta Rani.

Considering a broader range of HER-targeted drugs, treating cells (HCC1954 for example) for 48hrs with trastuzumab (12.5μg/ml) resulted in induced NmU mRNA levels in CM (3.9±1 fold; $p<0.05$) and corresponding cells (3.9±1.15 fold; $p=0.06$) (Figure 3.5A & 3.5B (i)). In relation to neratinib (0.5μM), the resulting induced NmU mRNA was 3.6±1 fold ($p=0.07$) and 3.6±0.54 fold ($p<0.01$) for CM and cells, respectively (Figure 3.5A & 3.5B (ii)); and for afatinib (0.5μM), induced NmU mRNA was 3.3±0.49 fold ($p<0.05$) in CM and 3±0.38 fold ($p<0.01$) in cells (Figure 3.5A & 3.5B (iii)).

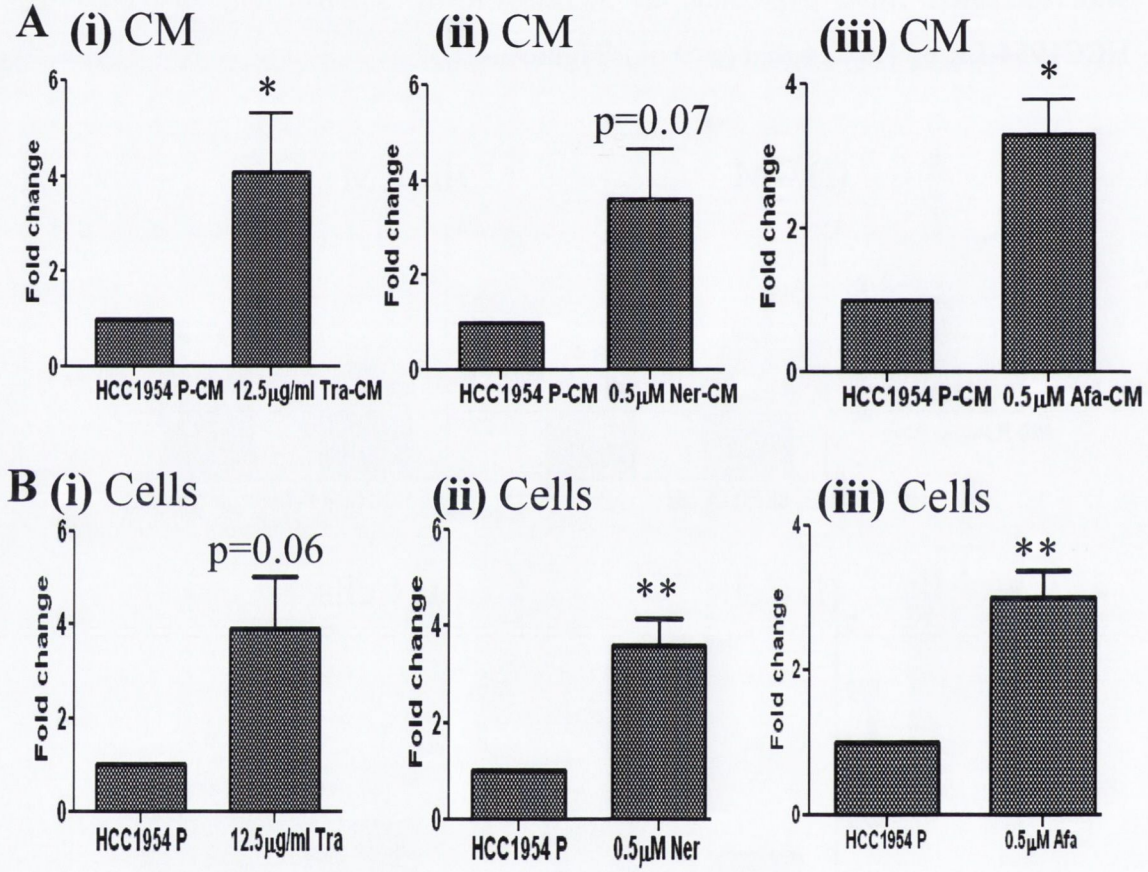

Figure 3.5: Increased NmU with short-term treatment with trastuzumab, neratinib and afatinib.

(A) qPCR analysis of NmU mRNA following short-term exposure of the parent cell populations (HCC1954, as example), to **(i)** trastuzumab, **(ii)** neratinib, and **(iii)** afatinib showing increased NmU mRNA levels in the CM and **(B)** in the corresponding cells. Data are presented as fold change assigning control an arbitrary 1. All results represent biological repeats n=3± SEM, where *=$p<0.05$, **=$p<0.01$. Short-term exposure assays were performed by Dr. Sweta Rani.

3.3.3 *Induced NmU protein expression occurs in cells with acquired-resistance to other HER-targeted agents and is not restricted to lapatinib.*

We questioned if the changes at the mRNA level in acquired-resistant cells translated to NmU protein. In agreement with our mRNA observations, NmU protein levels were significantly increased in lapatinib-conditioned cells, SKBR3-LR by 35.9±9.2% ($p < 0.05$) and HCC1954-LR by 45.6±9.1% ($p<0.01$), compared to their aged-matched control cells (SKBR3-Ag, HCC1954-Ag) (Figure 3.6A (i-ii)). Interestingly, this observation was not limited to lapatinib, but was also found in relation to other HER-targeted drugs where acquired-resistance populations were available. Specifically, a similar trend (*i.e.* significantly increased NmU protein levels) was observed in our trastuzumab-resistant cells (SKBR3-TR or –TR; by 31.±4.5% ($p<0.01$)) and neratinib-resistant (SKBR3-NR or –NR; by 71.8±2.6 % ($p<0.001$)) with their aged-matched control cells (SKBR3-Ag) (Figure 3.6A (i)) and our neratinib-resistant (HCC1954-NR or –NR; by 31.7±10.0% ($p<0.01$)) cells with their control cells (HCC1954-Ag) (Figure 3.6A(ii)).

3.3.4 *Endogenous NmU protein levels may be associated with innate sensitivity/resistance to HER-targeting drugs.*

SKBR3 cells are sensitive to both lapatinib and trastuzumab; HCC1954 cells are sensitive to lapatinib but resistant to trastuzumab; conversely, MDA-MB-361 cells are resistant to lapatinib, but sensitive to trastuzumab [265]. Although T47D cells are described as having normal HER2 expression [318], they are also unresponsive to both these drugs [264, 319] and so we elected to include these in our analysis. As shown in Figure 3.6B, endogenous levels of NmU protein correlate with the innate sensitivity versus resistance profile of these 4 cell lines. Where compared with SKBR3 cells, increased NmU protein expression was observed for HCC1954 by 594.5±403.8%, MDA-MB-361by 801.6±432.4% and T47D by 2521.6±1812.9% (Figure 3.6B).

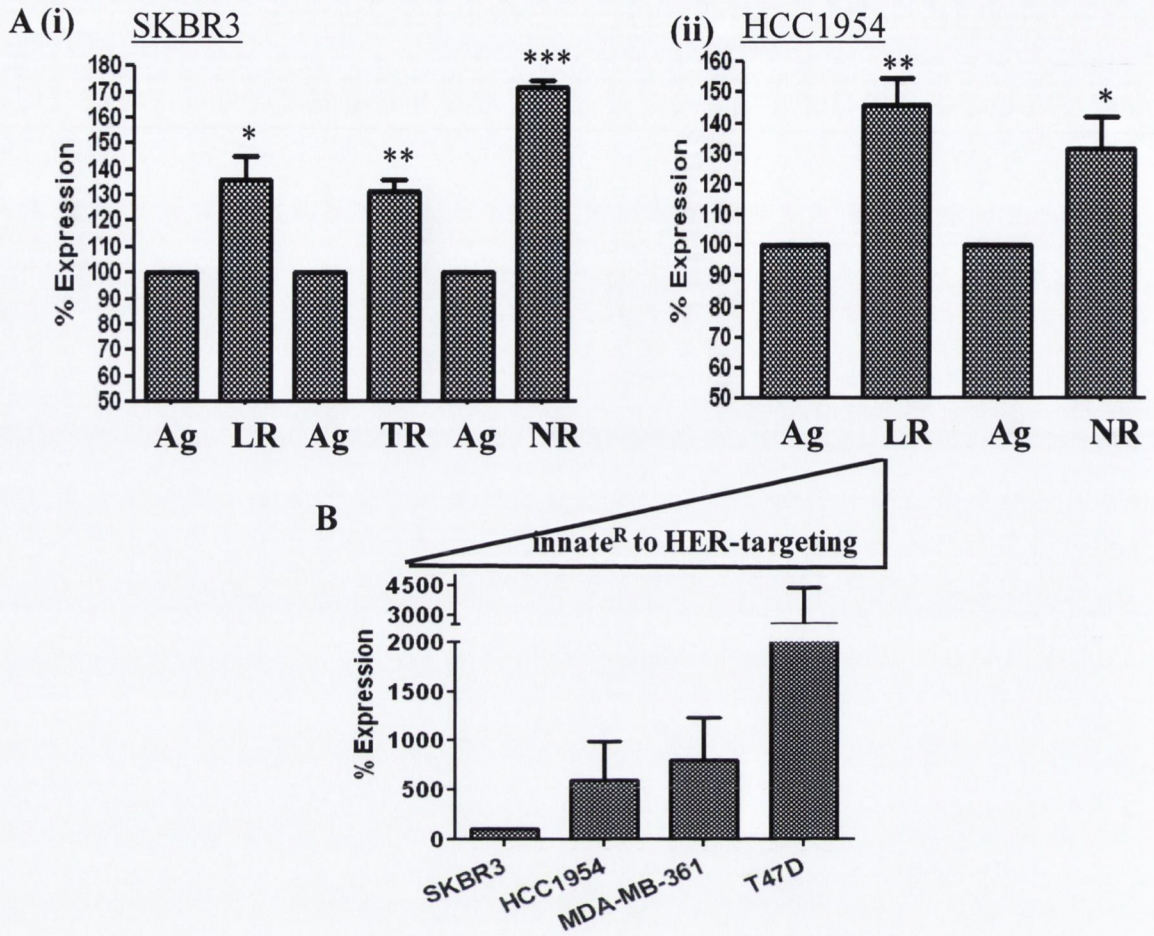

Figure 3.6: NmU protein is increased with acquired- and innate-resistance to HER-targeted drugs. Increased NmU mRNA levels are reflected in significantly increased NmU protein expression in cells with acquired-resistance to other HER-targeted agents, trastuzumab and neratinib, as well as lapatinib and also in innately-resistant versus sensitive cells. **(A)** Higher levels of NmU protein, analysed by ELISA, were also found in **(i)** lapatinib-resistant (SKBR3-LR), trastuzumab-resistant (SKBR3-TR) and neratinib-resistant (SKBR3-NR) SKBR3 cells compared to the corresponding SKBR3-Ag cells. **(ii)** The same trend was found with HCC1954 lapatinib-resistant (HCC1954-LR) and neratinib-resistant (HCC1954-NR) cells compared to their control HCC1954-Ag cells (trastuzumab-resistant HCC1954 cells are not available to evaluate as HCC1954 is innately-resistant to trastuzumab). Data are presented as NmU protein quantity relative to the amount in the control aged (100%) population. **(B)** Increased levels of NmU protein were also associated with innate-resistance to HER-targeted drugs. Results represent n=3±SEM, where *$p<0.05$, **$p<0.01$, ***$p<0.001$. The ELISAs were partly performed by Dr. Sweta Rani.

3.3.5 NmU expression is prognostic for poor outcome for breast cancer patients, particularly those with HER2-positive and luminal A subtypes

To determine if NmU has relevance in human breast cancer rather than being solely a cell line/CM-related observation, we collated and mined microarray data relating to 3,489 breast tumours. Kaplan-Meier estimates of survival (Figure 3.7A) indicated high levels of NmU expression to be associated with poor outcome for breast cancer patients ($p<1e-14$). Considering each of the breast cancer molecular subtypes within this general population of breast tumours, we found NmU expression to be particularly associated with poor outcome for those patients who had HER2-positive tumours (Figure 3.7B; $p<5e-6$) and luminal A tumours (Figure 3.7C; $p<8e-6$). These associations were not significant in patients with luminal B (Figure 3.7D; $p=0.081$) or basal-like (Figure 3.7E; $p=0.456$) tumours.

Although complete clinicopathological information was unavailable for all 3,489 patients, multivariate analysis correcting for tumour size, grade, ER status, lymph node status and age of patient, where this information was available, confirmed NmU as an independent prognostic biomarker rather than it being just a surrogate for an already established parameter (Figure 3.7F). Specifically, considering all tumour types where information on these five parameters was available ($n=966$), high levels of NmU expression was associated with poor outcome ($p=0.007$; hazard ratio=1.4). Considering the HER2-postive subtype, which is particularly relevant to this study, detailed clinical information was available for only ninety-five patients. Following correction, high levels of NmU in HER2 tumours tended towards statistical significance ($p=0.07$; hazard ratio=2.1). As information on tumour grade and lymph node status was available for a substantial number of the HER2-positive tumours ($n=360$ specimens), we evaluated NmU in this cohort and found it to be independently associated with poor outcome for HER2-overexpressing patients ($p=0.004$; hazard ratio=1.8).

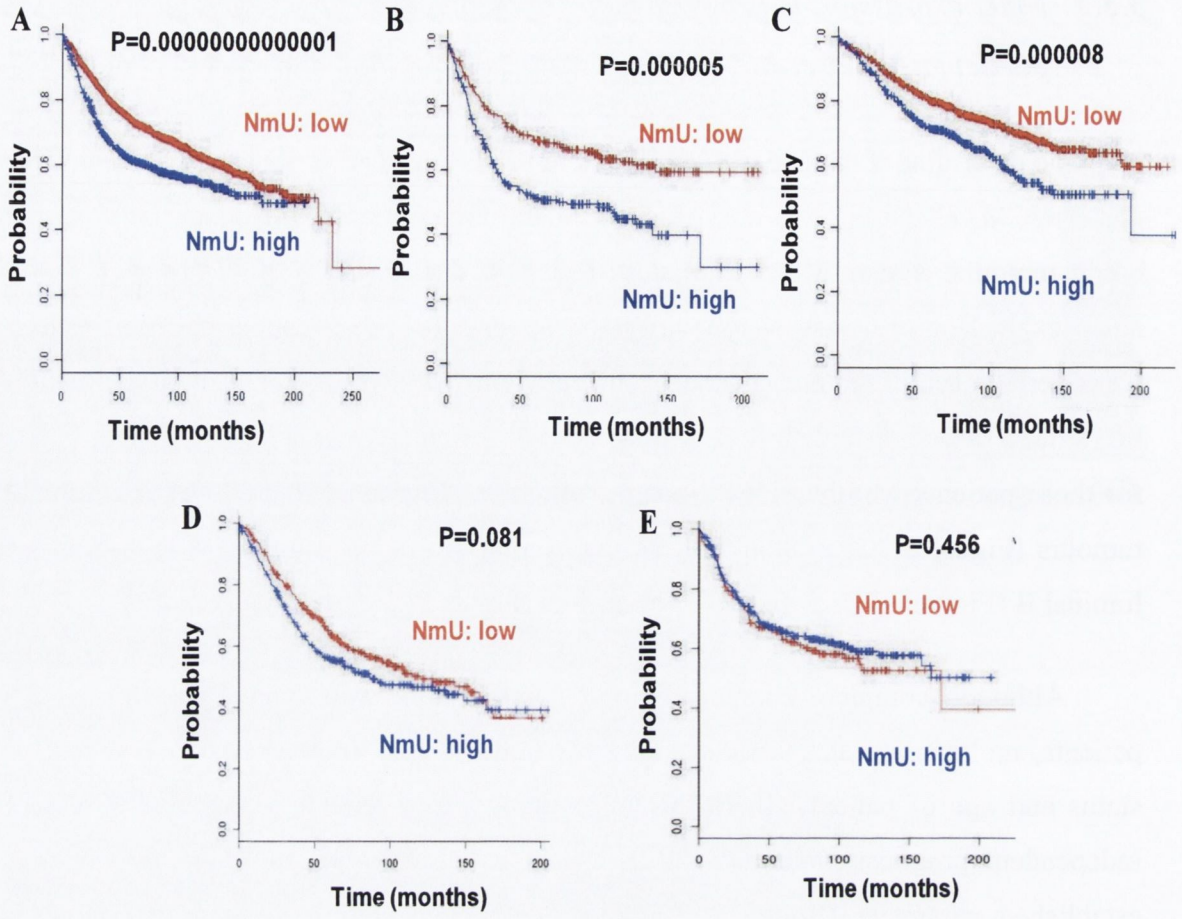

F

Type	Parameters	No. Specimens	P-value	Hazard Ratio
All types	LN, Grade, ER, Size, Age	966	0.007	1.4
HER2$^+$	LN, Grade, ER, Size, Age	95	0.07	2.1
HER2$^+$	LN, Grade	360	0.004	1.8

Figure 3.7: NmU expression is prognostic for poor outcome for breast cancer patients.

(A) Kaplan-Meier estimates indicate that high levels of NmU are associated with poor prognosis in breast cancer (n=3,489). The association of NmU expression with patients outcome in relation to each breast cancer molecular subtype was subsequently investigated and shown to be significant for **(B)** HER2-positive (n=476) and **(C)** luminal A (n=1,521) tumours (but not **(D)** luminal B (n=676) and **(E)** basal-like (n=454)). **(F)** multivariate analysis reporting on NmU following adjustment for a range of established clinicopathological parameters indicated its independence as a poor prognostic biomarker. Clinical analysis was performed in collaboration with Dr. Stephen Madden.

3.3.6 NmU affects sensitivity to lapatinib, trastuzumab, neratinib and afatinib

To assess if NmU might be functionally involved in resistance to HER-targeted drugs, we stably transfected human NmU cDNA into SKBR3 and HCC1954 parent cells. Successful overexpression of NmU in these cells was assessed by qPCR and ELISA. NmU expression in SKBR3-NmU cells was significantly increased by 6058±182.2% (for mRNA, $p<0.001$) and 20.2±6.0% (for protein, $p<0.01$) compared to levels in mock-transfected cells (Figure 3.8A (i)). Similarly, increased NmU expression in HCC1954-NmU cells by 59.9±9.7% (for mRNA, $p<0.01$) and 38.9±11.6% (for protein, $p<0.05$) was also observed (Figure 3.8A (ii)). For all drugs tested, the anti-proliferative effects resulting were significantly compromised in the NmU-transfected cells compared to the mock-transfected cells (Figure 3.8B) *i.e.* lapatinib (by 2.3±0.3 fold ($p<0.01$) for SKBR3-NmU and 39.0±10.7fold ($p<0.05$) for HCC1954-NmU), trastuzumab (by 4.2±2.7 fold ($p<0.001$) for SKBR3-NmU), neratinib (by 1.5±0.1fold ($p<0.001$) for SKBR3-NmU and 10.1±1.7 for HCC1954-NmU ($p<0.05$)) and afatinib (by 6.8±0.8 fold ($p<0.01$) for SKBR3-NmU and 4.6±0.7 fold ($p<0.01$) for HCC1954-NmU). The exception to this being the response of HCC1954-NmU compared to HCC1954-mock cells to trastuzumab (Figure 3.8B(ii)).

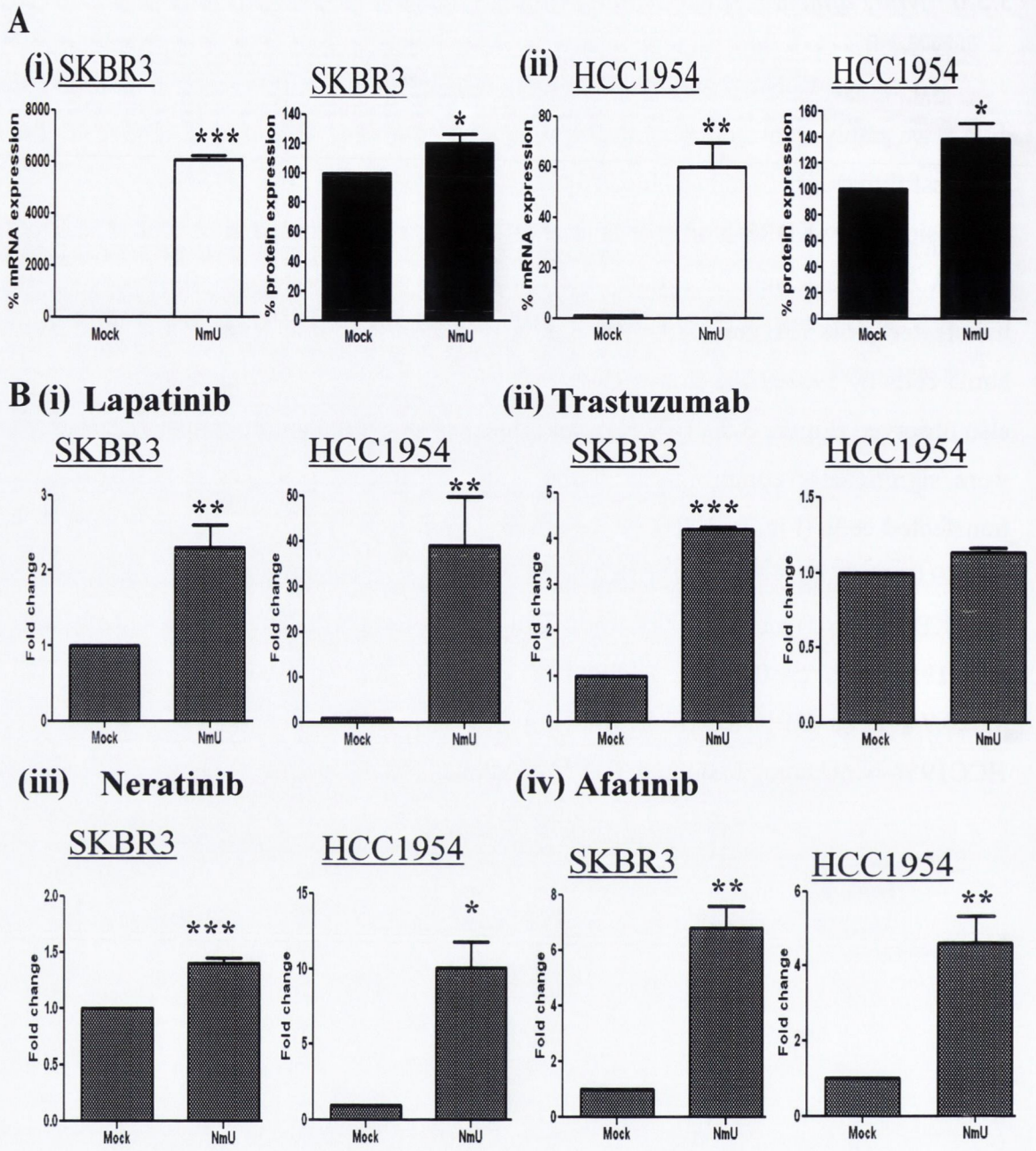

Figure 3.8: NmU overexpression reduces sensitivity to HER-targeted agents.

(A) Following NmU cDNA overexpression, levels of NmU mRNA (qPCR) protein (ELISA) detected in **(i)** SKBR3 and **(ii)** HCC1954 cells compared to mock-transfected populations. **(B)** Magnitude of fold difference in concentration of **(i)** lapatinib, **(ii)** trastuzumab, **(iii)** neratinib and **(iv)** afatinib that inhibits (by 50%) proliferation of SKBR3-NmU and HCC1954-NmU cells compared to the mock-transfected control cells. Response to treatment shown here was assessed using the acid phosphatase method. Results represent n=3±SEM, where *$p<0.05$, **$p<0.01$, ***$p<0.001$. Toxicity assays were partly performed by Susan Breslin.

To further explore a functional role for NmU in resistance to HER-targeted drugs, NmU was subsequently knocked-down in both our acquired-resistant cell lines (SKBR3-LR, HCC1954-LR) and innately-resistant/unresponsive cells (MDA-MB-361, T47D). Again, qPCR and ELISAs established significant knockdown of NmU mRNA as shown in Figure 3.9(i) and protein Figure 3.9(ii), respectively, compared to levels in scrambled (Scr) control cells. Specifically in SKBR3LR, siRNAs (NmU-1 and NmU-2) achieved 62-75% NmU mRNA knockdown and 21-22% NmU protein knockdown. Similarly, siRNA knockdown of NmU in HCC1954-LR (NmU mRNA by 39-64% and NmU protein by 17-21%), in MDA-MB-361 (NmU mRNA by 48-71% and NmU protein by 11-20%) and inT47D (NmU mRNA by 75-78% and NmU protein by 39-41%) was also achieved (Figure 3.9).

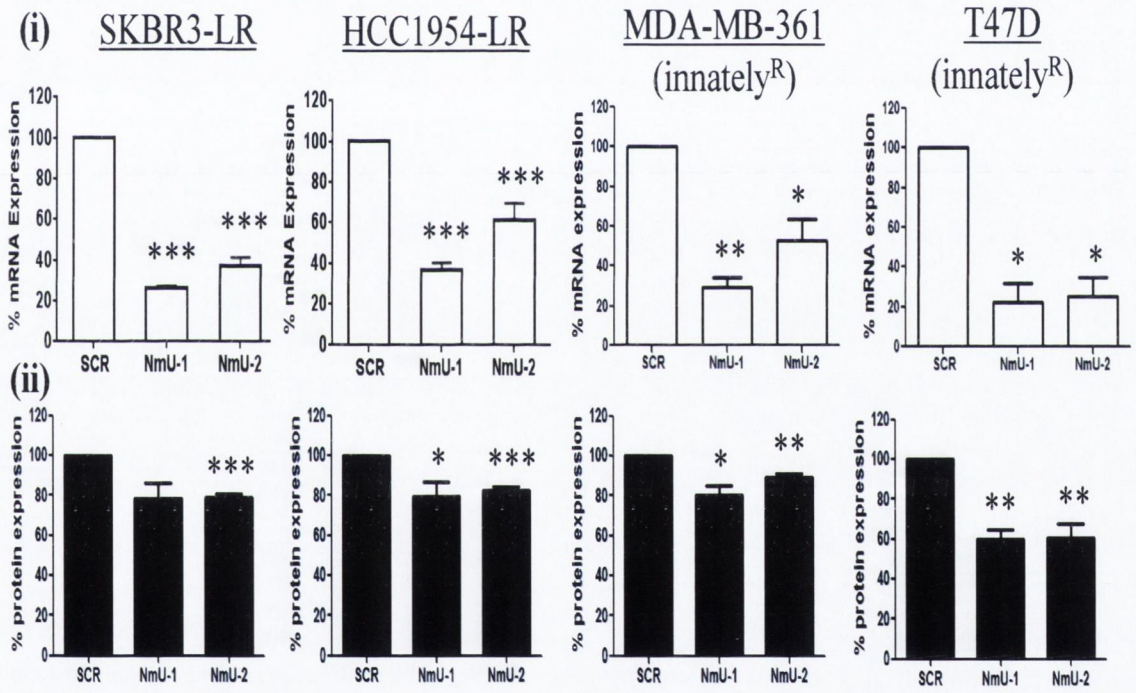

Figure 3.9: NmU mRNA and protein expression following siRNA transfection.

Following transfection with two siRNA targeted to NmU (NmU-1 or NmU-2) or a scrambled sequence (Scr), **(i)**, qPCR analysis of NmU and **(ii)** ELISA analysis of NmU protein showed partial knockdown of NmU expression in both the acquired lapatinib-resistance SKBR3-LR and HCC1954-LR and innately unresponsive T47D and MDA-MB-361 cells. Results represent n=3±SEM, where *p<0.05, **p<0.01, ***p<0.001. siRNA analysis here was partly performed by Dr. Sweta Rani.

In relation to effects on response to drug, while some variation was observed between cell lines and siRNAs, NmU knockdown, by siRNAs (NmU-1 and NmU-2), was found to increase the inhibition of proliferation achieved in response to lapatinib (IC_{50} concentration) by a further 12-49% (Table 3.3). For trastuzumab, NmU knockdown added a further 14-50% inhibition of growth, with corresponding values of 19-58% for neratinib, and 18-47% for afatinib (Table 3.3).

Drug	Drug conc.	Cell Line	Drug + SRC	(+) Anti-proliferative benefit with NmU-1	P-value	(+) Anti-proliferative benefit with NmU-2	P-value
Lapatinib	3 μM	SKBR3-LR	50	20.2	0.006	20.7	0.01
	5 μM	HCC1954-LR	50	49.2	0.006	34.3	0.03
	1 μM	MDA-MB-361	50	43.4	0.00007	13.8	0.002
	5 μM	T47D	50	15.5	0.002	11.8	0.02
Trastuzumab	15 μg/ml	SKBR3-LR	40	41.8	0.0002	20.5	0.009
	15 μg/ml	HCC1954-LR	15	49.6	0.0000004	32.8	0.0001
	15 μg/ml	MDA-MB-361	61	37.3	0.001	17.7	0.02
	15 μg/ml	T47D	46	27.1	0.002	14.1	0.019
Neratinib	1 μM	SKBR3-LR	74	58	0.0004	20	0.04
	1 μM	HCC1954-LR	65	57.3	0.00002	43.9	0.008
	1 μM	MDA-MB-361	75	48.1	0.001	23.7	0.004
	1 μM	T47D	61	36.7	0.002	18.9	0.004
Afatinib	0.5 μM	SKBR3-LR	51	46.5	0.003	25.6	0.029
	0.5 μM	HCC1954-LR	32	39.4	0.0001	27.6	0.000002
	0.5 μM	MDA-MB-361	13	24.9	0.0002	24	0.00004
	0.5 μM	T47D	15	21.5	0.002	18.3	0.004

Table 3.3: NmU knockdown by siRNA can enhance sensitivity to HER-targeted drugs.
NmU knockdown in SKBR3-LR, HCC1954-LR, T47D and MDA-MB-361 cells enhanced the effectiveness of lapatinib, trastuzumab, neratinib and afatinib at decreasing proliferation compared to that observed in corresponding Scr-transfected cells. Response to treatment shown here was assessed using the acid phosphatase method. Results represent n=3±SEM, where *p<0.05, **p<0.01, ***p<0.001. siRNA toxicity assays were performed by Dr. Sweta Rani.

3.3.7 NmU expression is also associated with other phenotypic characteristics including cell motility, invasion and resistance to anoikis

To assess what other functional role(s) NmU may have, NmU-overexpressing and NmU knockdown cells were further evaluated. Events associated with more "aggressive" cancers include the ability of the cells to move (migration assays), digest and migrate through extracellular matrix during intravasation and extravasation (invasion assays) and to survive in suspension, as necessary to survive in the peripheral circulation *en route* to metastasise (*anoikis* assays). NmU cDNA in (i) HCC1954 and (ii) SKBR3 compared to HCC1954-mock and SKBR3-mock, respectively, was associated with increased motility as evaluated by wound-healing (Figure 3.10(i-ii)). Specifically, NmU overexpression demonstrated significant increased wound closure in HCC1954 cells by 49.2±6.0% ($p<0.01$) at 48hrs. Increased wound closure was also observed in SKBR3-NmU cells by 6.6±2.3% ($p<0.05$) at 72hrs (Figure 3.10(i-ii)).

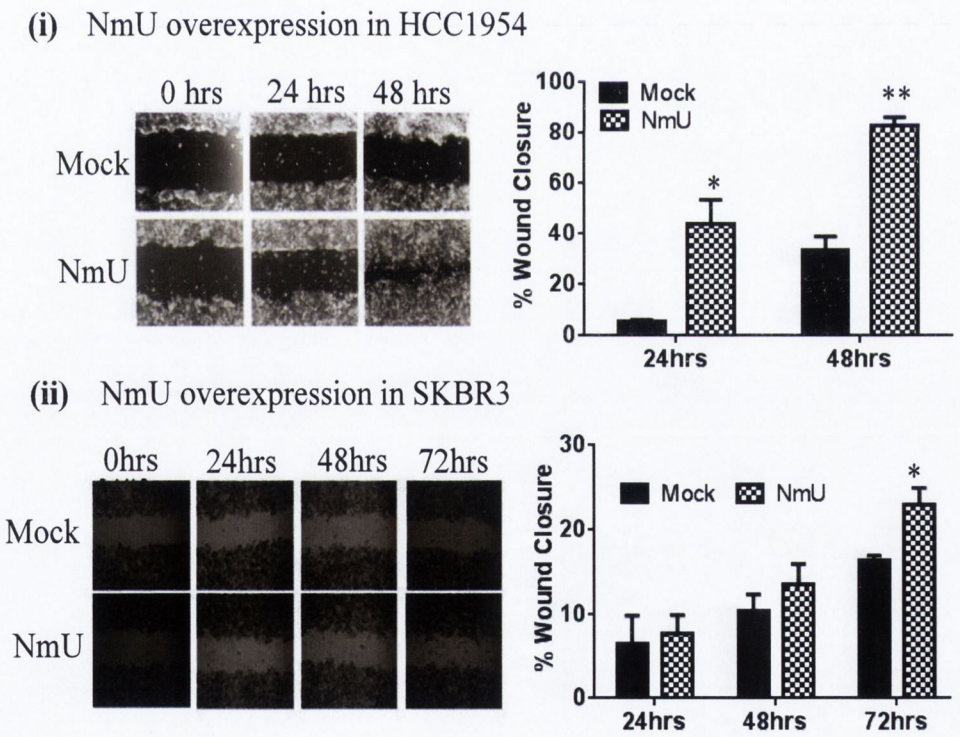

Figure 3.10: Overexpression of NmU increases cell motility.

Overexpression of NmU cDNA in (i) HCC1954 and (ii) SKBR3 cells was associated with increased motility assessed by wound healing compared to mock-transfected cells. Results represent n=3±SEM, where *=$p<0.05$, **= $p<0.01$, ***=$p<0.001$. Motility assays were performed by Dr. Sweta Rani.

Furthermore, increased migration through transwells, increased invasion through ECM-coated transwells and resistance to *anoikis* was also observed in cells overexpressing NmU compared to mock-transfected cells (Figure 3.11). Specifically, significantly increased migration was observed for HCC1954-NmU cells by 221.4±34.9% ($p<0.05$) and SKBR3-NmU cells by 38.8±20.4% ($p<0.01$) (Figure 3.11A). Invasion was also significantly increased in HCC1954-NmU cells by 160.5±4.3% ($p<0.001$) and in SKBR3-NmU cells by 149.8±5.1% ($p<0.01$) (Figure 3.11B). NmU overexpression was associated decreased sensitivity to *anoikis* in HCC1954-NmU cells by 2.2±0.2 fold ($p<0.01$) and in SKBR3 by 3.0±0.7 fold ($p<0.05$) (Figure 3.11C).

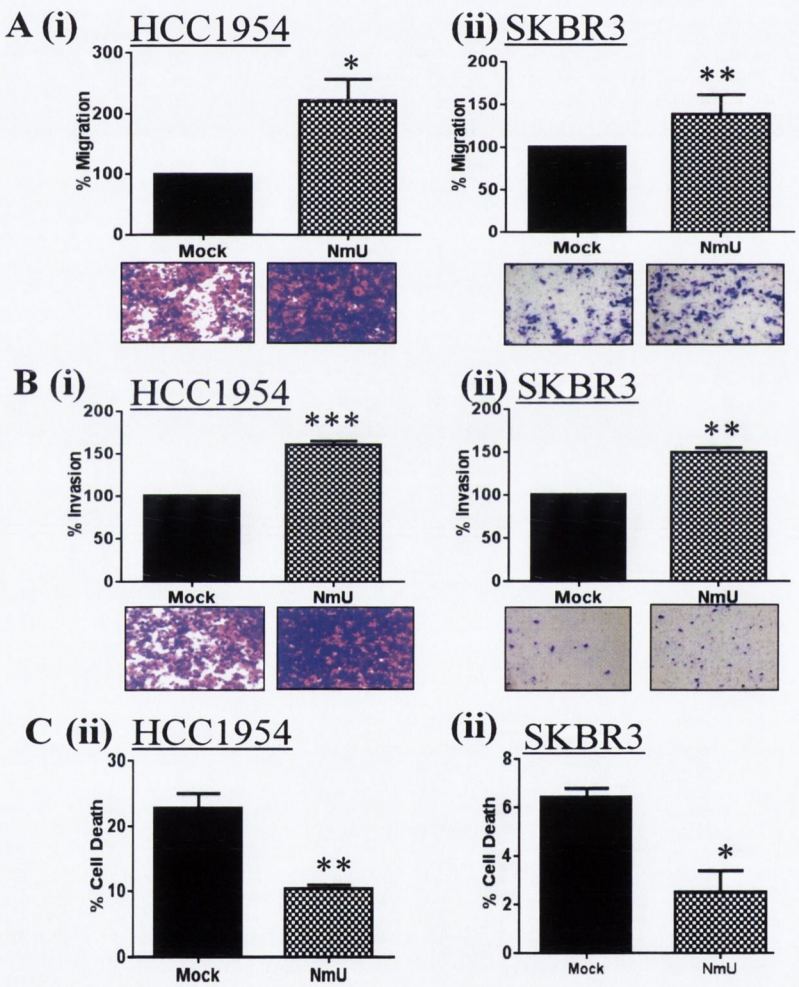

Figure 3.11: Overexpression of NmU increases migration, invasion and resistance to *anoikis*.
Overexpression of NmU cDNA in **(i)** HCC1954 and **(ii)** SKBR3 cells was associated with increased **(A)** migration **(B)** invasion and **(C)** *anoikis* resistance compared to mock-transfected cells. *Anoikis* assays shown here was assessed using alamar blue. Results represent n=3±SEM, where *=$p<0.05$, **= $p<0.01$, ***=$p<0.001$ Migration, invasion and *anoikis* assays were performed by Dr. Sweta Rani.

Conversely, NmU knockdown in HCC1954-LR, was associated with opposite effects *i.e.* decreased cellular motility, decreased migration, decreased invasion and increased sensitivity to cell death by *anoikis* compared to scrambled transfected cells (Figure 3.12). Specifically, knockdown of NmU, by siRNAs (NmU-1 and NmU-2), was associated decreased wound closure by 22-28% ($p<0.05$) at 72hrs (Figure 3.12A). NmU knockdown decreased migration through transwells by 43-52% ($p<0.01$) as well as invasion by 34-40% ($p<0.05$) (Figure 3.12B and 3.12C). Sensitivity to *anoikis* was also increased upon NmU knockdown, by 2-2.1 fold ($p<0.05$) (Figure 3.12D).

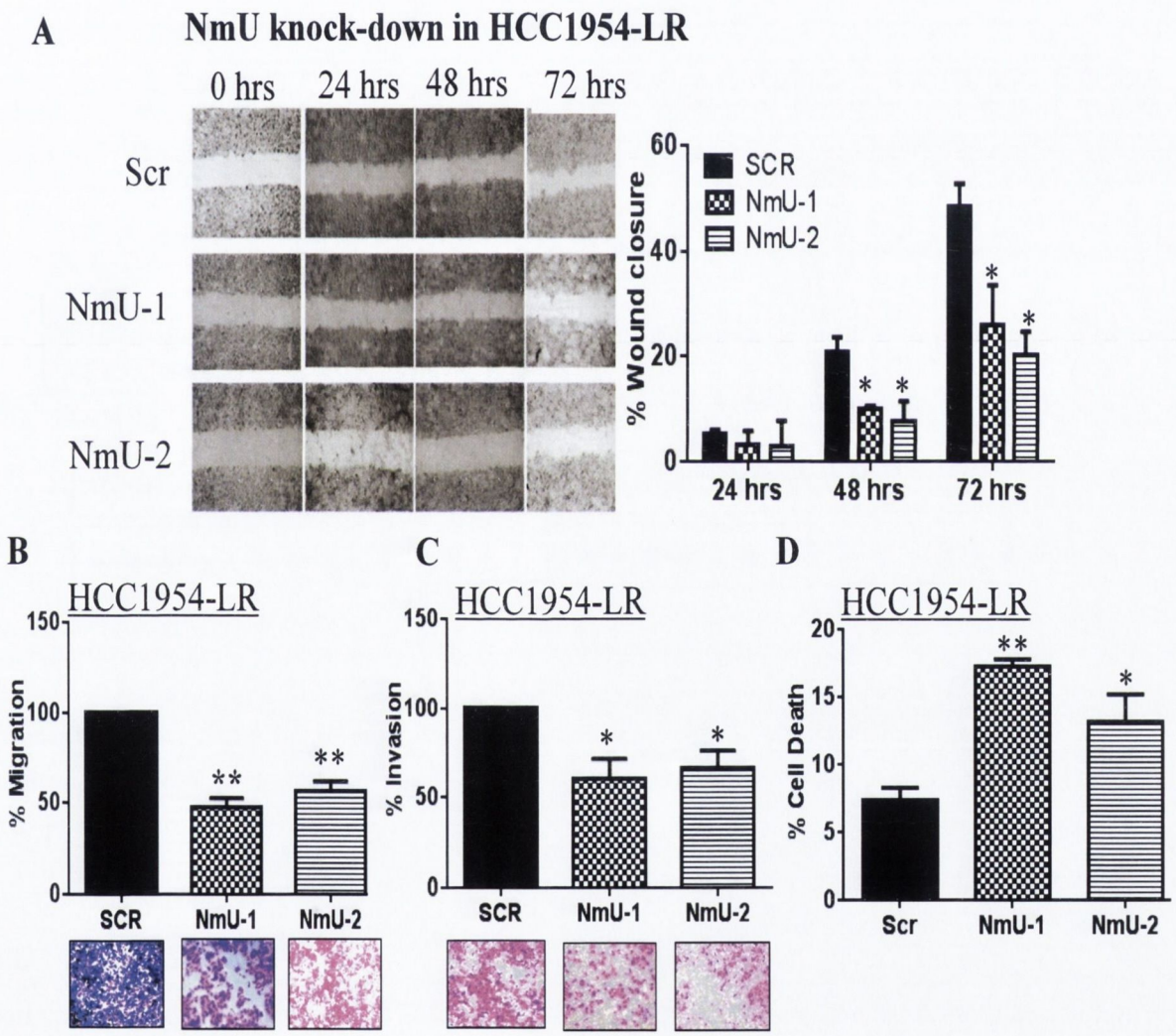

Figure 3.12: NmU knockdown by siRNA decreases motility, migration, invasion and *anoikis* resistance. Knockdown of NmU (by siRNAs NmU-1 and NmU-2) in HCC1954-LR was associated with decreased **(A)** motility by wound healing **(B)** migration through transwells **(C)** invasion and **(D)** increased sensitivity to *anoikis*. *Anoikis* assays shown here was assessed using alamar blue. Results represent n=3±SEM, where *$p<0.05$, **$p<0.01$, ***$p<0.001$. Motility, migration, invasion and *anoikis* assays were performed by Dr. Sweta Rani

3.3.8 Proposed mechanism-of-action for NmU

We next investigated how NmU knockdown may be enhancing the effects of the range of HER-targeted drugs used in this study as well as modulating its effects on cancer cell aggression. As HER2 is a target for all 4 drugs and EGFR is also a target of lapatinib, neratinib and afatinib, we assessed the levels of these specific targets –their total amounts and their phosphorylated forms– using ELISAs and immunoblotting. Of great interest, with both SKBR3-LR and HCC1954-LR cells, NmU knockdown was associated with significantly reduced levels of total HER2 protein (Figure 3.13).

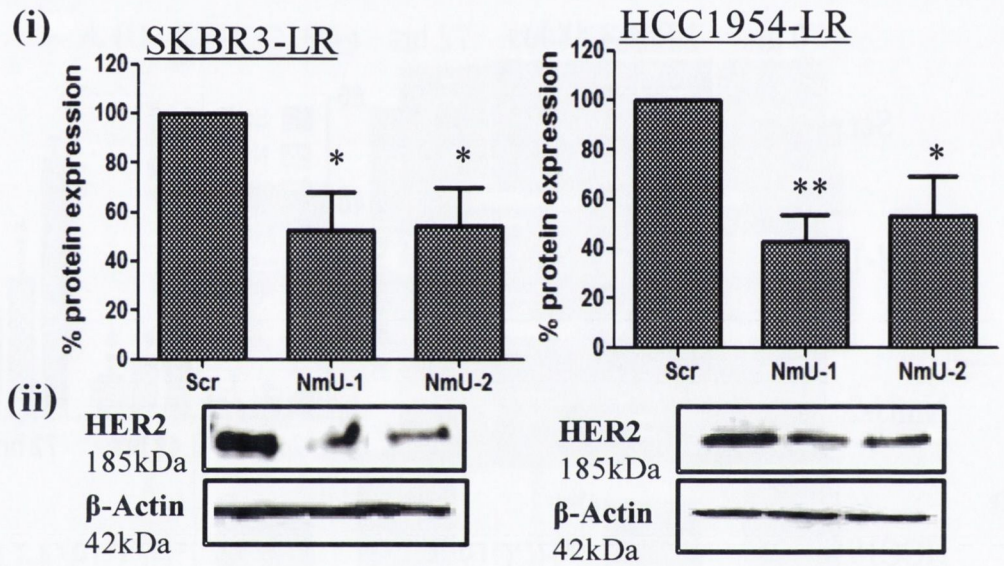

Figure 3.13: NmU knockdown by siRNA decreases HER2 levels.

NmU knockdown with two siRNA (NmU-1 or NmU-2) compared to transfection with a scrambled sequence (Scr) in both SKBR3-LR and HCC1954-LR cells was associated with significantly reduced levels of HER2 protein, as shown by (i) ELISA and (ii) Immunoblotting. Results represent n=3±SEM, where *$p<0.05$, **$p<0.01$.

By mining the literature, we found that HSP27 has previously been reported as highly expressed in HER2-positive breast cancer [320] and, importantly, has been recognized as reducing cellular trastuzumab susceptibility by directly binding to HER2, and thus increasing its stability [71]. In addition, several reports have indicated that HSP27 can regulate cancer cell invasion and metastasis [72-74]. We hypothesised, therefore, that HSP27 may be the linking molecule in this chain of events by which NmU may be contributing to resistance to HER-targeted drugs as well as regulating cancer cell

aggression. To investigate this, NmU was immunoprecipitated and assessed for HSP27 binding. Increased levels of the NmU:HSP27 complex were observed, by immunoblotting, in NmU-overexpressing (HER-drug resistant) cell lines variants compared to their sensitive mock transfected- parent cell lines (Figure 3.14A). Subsequently, knockdown of NmU in lapatinib-resistant SKBR3-LR and HCC1954-LR (Figure 3.14B) demonstrated relative decreased levels of HSP27.

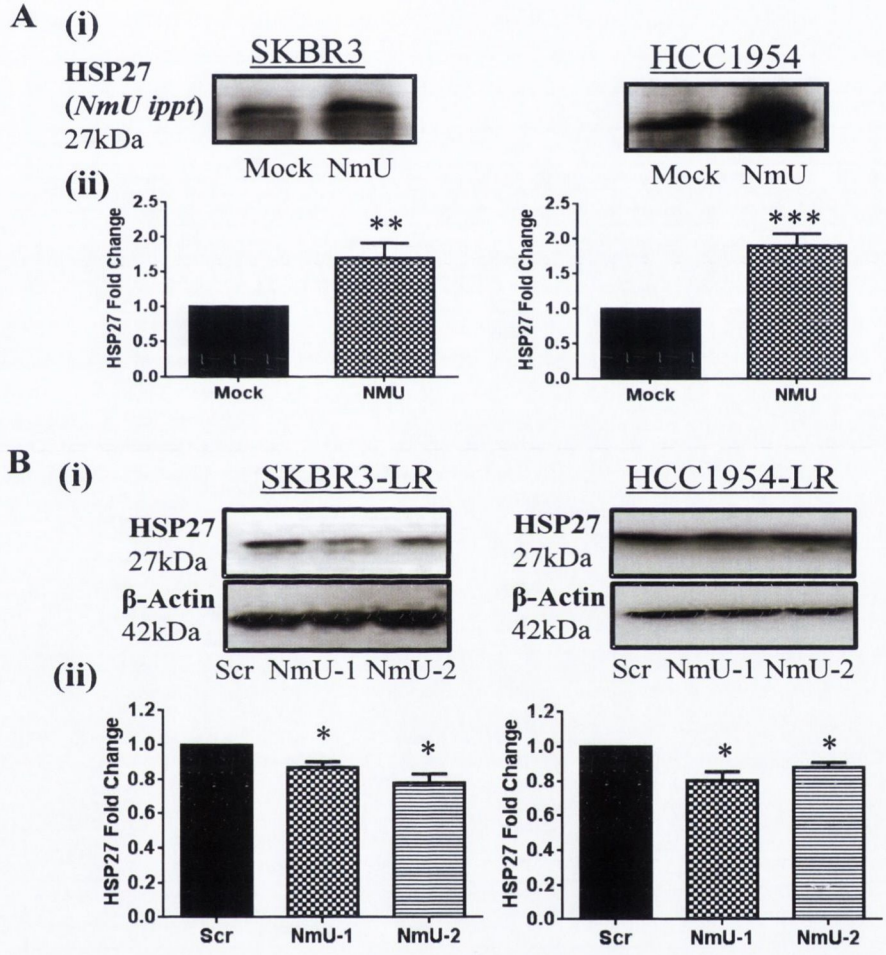

Figure 3.14: NmU partners with HSP27.

(A) Immunoprecipitation of NmU in NmU-overexpressing cells, compared to mock transfected cells, was associated with significantly increased levels of HSP27 as shown by **(i)** immunoblotting and **(ii)** corresponding densitometry. **(B)** NmU knockdown with two siRNA (NmU-1 or NmU-2) compared to transfection with a scrambled sequence (Scr) in both SKBR3-LR and HCC1954-LR cells was associated with significantly reduced levels of HSP27 protein, as shown by **(i)** immunoblotting and **(ii)** corresponding densitometry. Immunoprecipiation was partly performed by Dr. Sweta Rani. Results represent n=3±SEM, where *p<0.05, **p<0.01, ***p<0.001

Upon NmU silencing, the total amounts of EGFR present was not significantly affected in both cell lines (Figure 3.15A), but phosphorylation of the EGFR that was present was significantly reduced (Figure 3.15B). Changes in intracellular signaling through the phosphoinositide-3-kinase/Akt pathway have been associated with resistance to some HER-targeted drugs. For example, phosphorylation of Akt has been associated with low efficacy of lapatinib and/or trastuzumab [20, 265, 321]. Here we observed that in NmU knockdown cells (which correlated with increased sensitivity to all 4 drugs evaluated); there was significantly increased activation/phosphorylation of the remaining Akt (Figure 3.15C).

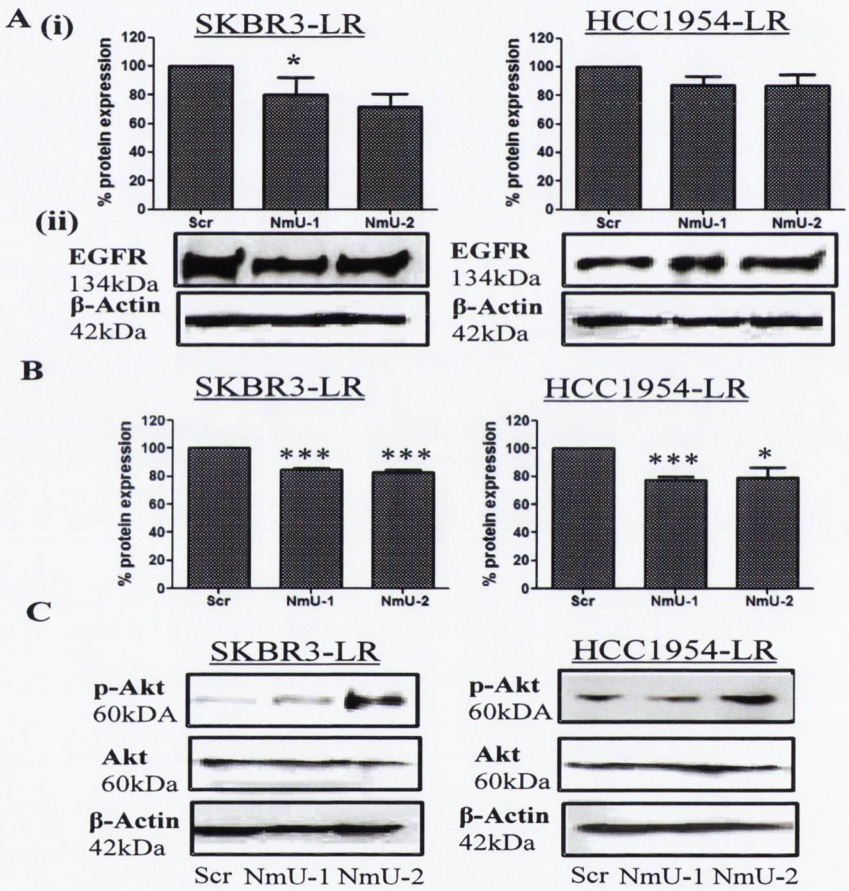

Figure 3.15: NmU also regulates phosphorylated EGFR and AKT.

The mechanism by which NmU affects response to HER-targeted drugs may also involve changes in the phosphorylation of EGFR and AKT. **(A)** Total EGFR (HER1) levels (**(i)** ELISA & **(ii)** immunoblots) was not affected in response to NmU knockdown; however **(B)** phosphorylation (activation) of the EGFR present was significantly reduced as demonstrated by ELISA. **(C)** NmU knockdown, with associated reduced levels of p-EGFR (and HER2) correlated with increased levels of phosphorylated AKT. Results represent n=3±SEM, where *p<0.05, **p<0.01, ***p<0.001.

3.3.9 Exogenous NmU peptide treatment can increase resistance to HER-targeted therapies

To further explore the functional role of NmU, we first treated cells with an exogenous NmU (NmU-25) peptide and assessed the cells expression of NmU receptors (NmU-R1, NmU-R2) which were found to be present for both SKBR3 and HCC1954 cells (Figure 3.16A). We also observed that treating these cells with exogenous NmU (NmU-25) induced expression of both HER2 and EGFR proteins (Figure 3.16A) suggesting that either or both of NmU-R1 and NmU-R2 are functionally active on these cells. As our studies to this point identified a link to HSP27 expression with endogenous NmU, we also assessed whether exogenous NmU may alter the levels of HSP27. Here we found that while no substantial difference was observed in the levels of HSP27 in SKBR3, there was an increase observed in HCC1954 cells following NmU-25 treatment (Figure 3.16B).

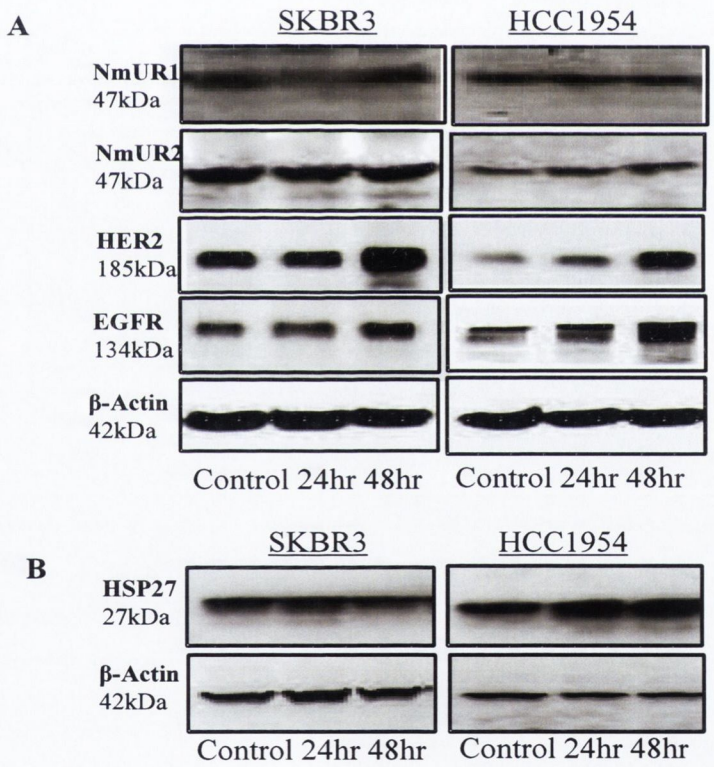

Figure 3.16: Exogenous NmU peptide treatment can also alter protein expression.

(A) NmU-R1 and NmU-R2 receptors were found to be expressed by the parent cells populations using immunoblotting. Treatment with exogenous NmU (24, 48hrs) increased expression of both HER2 and EGFR. **(B)** Treatment with exogenous NmU (24, 48hrs) increased expression of HSP27 in HCC1954 but no substantial change was observed in SKBR3.

Interestingly, this exposure to exogenous NmU also induced a low, but significant, level of resistance to HER-targeted drugs (Figure 3.17). Specifically, resistance to lapatinib in SKBR3 was increased by 31.9±9.9% ($p<0.05$) and in HCC1954 by 13±2.0% ($p<0.001$) compared to cells not exposed to exogenous NmU prior to lapatinib treatment. Similarly, resistance to trastuzumab was increased in SKBR3 by 13.2±3.6 ($p<0.05$) and in HCC1954 by 15.6±1.4% ($p<0.001$). For neratinib, resistance was increased by 10.9±3.5% ($p<0.05$) for SKBR3 and by 6.7±2.6% ($p<0.01$) for HCC1954. Finally, assessment of afatinib demonstrated increased resistance in SKBR3 cells by 24.2±6.5% ($p<0.05$) and in HCC1954 cells by 8.5±2.7% ($p<0.05$).

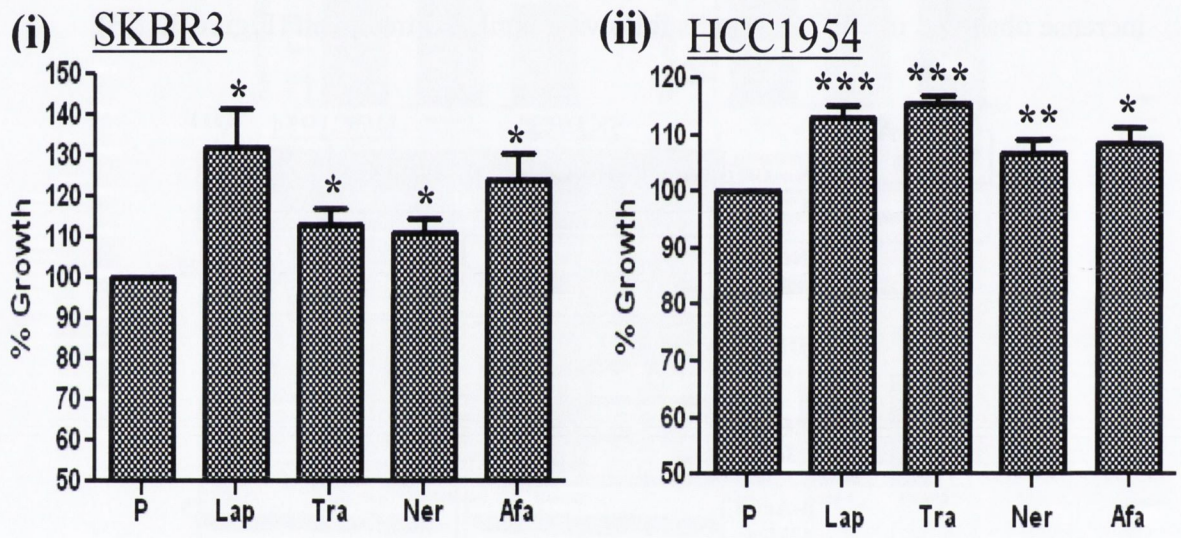

Figure 3.17: Exogenous NmU treatment confers resistance to HER-targeted drugs.

Treatment with exogenous NmU (48hrs) conferred a low, but significant level of resistance to lapatinib (Lap), trastuzumab (Tra), neratinib (Ner) and afatinib (Afa). Effects on untreated cells (the control of this experiment (P)) were set an arbirtrary 100% while growth in the presence of drug treatments was calculated accordingly. Response to treatment shown here was assessed using the acid phosphatase method Results represent n=3±SEM, where *$p<0.05$, **$p<0.01$, ***$p<0.001$.

3.3.10 The generation of stable overexpression and stable knockdown cell lines for future in vivo studies

Our studies to date have indicated that NmU may hold significant relevance to breast cancer progression and resistance to HER-targeted drugs. Our next step to further evaluate the role of NmU was to generate cell lines that may be used for future *in vivo* analysis. Using cells stably expressing the luciferase gene, (provided as a gift from Dr. Annette Byrne, RCSI) and so appropriate for bioluminescence *in vivo* studies, we transfected HCC1954-LUC+ cells with NmU cDNA containing plasmid or empty plasmid. Expression of NmU mRNA, assessed by qPCR, was found to be significantly ($p<0.05$) increased by 10.5±2.5 fold compared to mock transfected cells (Figure 3.18A). While a decreased trend in proliferation was observed for HCC1954-LUC+ NmU compared to mock transfected cells, this was not significant (Figure 3.18B). Assessing the response to lapatinib (Figure 3.18C) demonstrated approximately an 8.0±0.3 fold ($p<0.001$) increase in resistance to lapatinib for HCC1954-LUC+ NmU (IC_{50} approx.: 310nM) compared to mock transfected cells (IC_{50} approx: 2.5μM). Furthermore invasion of HCC1954-LUC+ NmU cells was significantly ($p<0.01$) increased compared to mock transfected cells (Figure 3.18D).

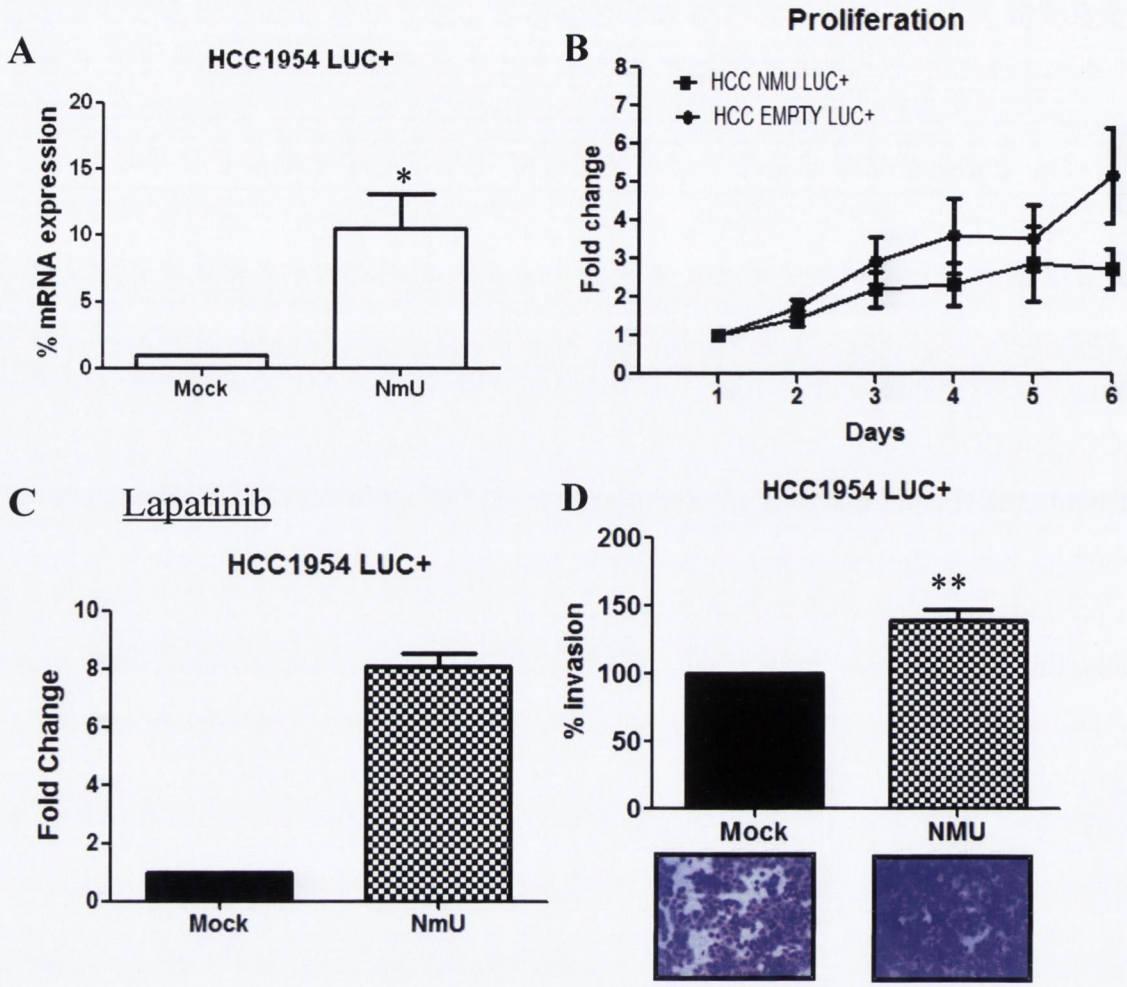

Figure 3.18: Characterisation of HCC1954-LUC+ cells ovexpressing NmU.

(A) Increased NmU expression was confirmed in HCC1954-NmU-LUC+ cells compared to mock transfected cells. **(B)** A trend towards decreased proliferation of HCC1954-NmU-LUC+ cells compared to mock transfected cells. **(C)** HCC1954-NmU-LUC+ cells were 8.0±0.3 fold more resistant to lapatinib than mock transfected cells. **(D)** HCC1954-NmU-LUC+ cells were significantly more invasive than mock transfected cells. Response to treatment and proliferation shown here was assessed using the acid phosphatase method Results represent n=3±SEM, where *$p<0.05$, **$p<0.01$, ***$p<0.001$.

To date the plasmids for NmU shRNAs and empty shRNA have been isolated as described in Section 3.2.15 and the resulting quantifications are displayed in Table 3.4. HCC1954-LR-LUC+ cells were transfected with 4μg of empty shRNA or NmU shRNA #1-#5 and selected in puromycin (2μg/ml). ELISAs to assess NmU expression were performed to determine the level of NmU knockdown by each shRNA (Figure 3.19). Specifically, compared to mock (empty) transfected cells, knockdown of NmU in cells was achieved in all shRNAs at varying amonts: by 89.9±4.9% (shRNA #1); by 82.8±1.6% (for shRNA #2); by 94.3±0.5% (shRNA #5); by 33.7±7.7% (shRNA #4) and by 84.6±5.6% (shRNA #5) (Figure 3.19).These cells are currently growing in culture and will be characterised similar to the characterisation performed for NmU-overexpressing HCC1954 LUC+ cells as shown in Figure 3.18.

Plasmid DNA	Concentration (μg)	260/280
EMPTY shRNA	121.2	1.85
NmU shRNA #1	62.3	1.82
NmU shRNA #2	64.4	1.85
NmU shRNA #3	9.4	1.48
NmU shRNA #4	23.8	1.86
NmU shRNA #5	6.1	1.9

Table 3.4: Plasmid DNA isolated for stable NmU knockdown studies.

Plasmid DNA concentrations (μg) from 50μl samples measured on the NanoDrop ND-1000 spectrophotometer.

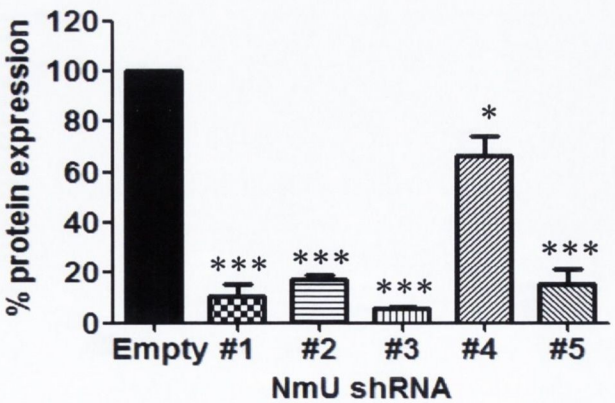

Figure 3.19: NmU protein expression knockdown by shRNAs.

Results represent n=3±SEM, where *p<0.05, ***p<0.001.

3.3.11 NmU is detectable in exosomes

The studies reported in Chapter 2 and 3 to this point have focused on examining the conditioned medium as a means of identifying extracellular biomarkers. During the course of this PhD increasing evidence suggested the RNAs were encapsulated within exosomes. To determing whether NmU was present in exosomes, we therefore performed an ELISA on exosomes derived from HCC1954-Ag, HCC1954-LR and HCC1954-NR cells (Figure 3.20). The NmU levels detected in HCC1954-LR derived exosomes were significantly ($p<0.01$) higher by 61.6±12.1% compared to HCC1954-Ag derived exosomes (Figure 3.20A). Similarly, HCC1954-NR derived exosomes had significantly ($p<0.01$) increased NmU levels, by 63.5±10.8% compared to HCC1954-Ag (Figure 3.20B)

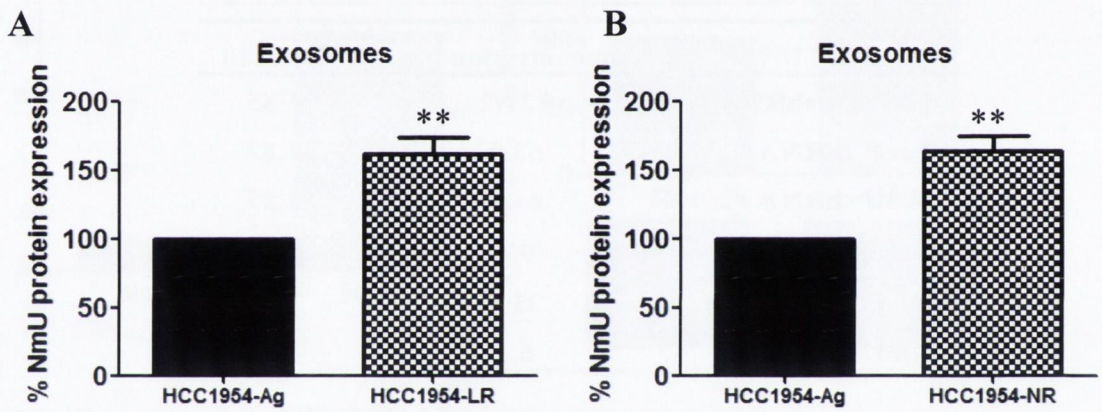

Figure 3.20: Analysis of NmU in exosomes.

NmU protein levels (assessed by ELISA) were significantly increased in **(A)** HCC1954-LR and **(B)** HCC1954-NR derived exosomes compared to HCC1954-Ag derived exosomes. Results represent n=3±SEM, where **$p<0.01$

3.4 DISCUSSION

Neuromedin U (NmU) has previously been associated with cancer, but a specific association between NmU and breast cancer or with HER2-overexpression in any cancer type has not been previously established.

In acute myeloid leukaemia (AML), using the K562 cell line expressing a dominant-negative of c-myb proto-oncogene as model, increased NmU (and NmU-R1) expression was implicated as a growth-promoting autocrine loop [322]. In ovarian cancer, microarray profiling of cell lines derived from ovarian tumour (n=11) and normal (n=2) epithelial cells identified NmU as up-regulated in cancer cells [323]. In pancreatic cancer, immunohistochemistry showed significantly higher levels of NmU and NmU-R2 in ducts from pancreatic tumours (n=6) compared to normal pancreas (n=3) or chronic pancreatitis (n=3). Furthermore, serum NmU levels were significantly lower one week post-major pancreatic resection compared to pre-operative levels [324]. In lung cancer, immunohistochemistry staining of a non-small cell lung cancer (NSCLC) tumour tissue microarray showed NmU expression (n=220 positive; n=106 negative) to be associated (p=0.036) with reduced survival times, and with both increased growth rate and colony formation in lung cancer cell lines [325]. In bladder cancer, NmU overexpression significantly promoted tumour formation of both T24 and T24T cell lines and significantly enhanced T24T lung metastasis [326]. Using RCC10 as renal cancer cell line model, NmU has recently been found to stimulate migration of the cells and to be controlled by von Hippel-Lindau tumour suppressor gene [327]. Conversely, in oesophageal squamous cell carcinoma, reactivation of genes that have been epigenetically silenced in 3 cells lines identified NmU as a potential tumour suppressor gene [328]. In oral cancer, expression profiling of matched tumour and normal specimens (n=5 each) showed NmU as one of 15 mRNAs whose expression levels were reduced in cancer specimens [329].

Here we report that increased NmU mRNA expression is significantly associated with poor outcome in breast cancer; particularly for those patients with HER2 or luminal A tumours. Our data also suggests that NmU expression has independence as a prognostic factor for poor outcome and is not simply a surrogate for an already established prognostic biomarker.

Our initial observation of NmU being associated with resistance to HER-targeting drugs was made through analysis of medium conditioned by cells that had acquired lapatinib-resistance compared to CM from their respective aged-parent populations. The feasibility, quality and yields for CM derived RNA is discussed in Chapter 2. For both cell line variants initially analysed (SKBR3-LR and HCC1954-LR) significantly higher levels of NmU mRNA were present in the CM, reflecting the status in the corresponding cells. This is in keeping with our previous observations from a range of cell lines [286, 287, 289] and, indeed, from pilot study analysis of serum and corresponding tumour tissue from breast cancer patients [288], indicating that full-length mRNAs can be selectively expelled from cells. Similar observations –studying different mRNAs– have been reported by others [330]. To further explore whether or not the response of increased intracellular and extracellular NmU mRNA is an early event, sensitive cells (SKBR3 and HCC1954 parent cells) were exposed to lapatinib short-term (48hrs), showing some increased NmU mRNA transcription and which was released from cells within this time-frame. To establish if the increase in NmU levels (intracellular and extracellular) is specific to lapatinib or if NmU mRNA may have relevance as a biomarker of response to other HER-targeting drugs, our analysis was expanded to also investigate the response to trastuzumab, neratinib and afatinib. In all cases, increased transcription of NmU mRNA resulted. The lower fold changes observed in CM compared to cells may suggest that this is not a dynamic event; that cells limit the amount of mRNAs they select to send out into the extracellular environment; and/or that some of extracellular mRNA was degraded. However, the NmU mRNA levels in CM from resistant cells were always significantly higher than that in CM from sensitive cells and evidence suggests that this effect is partly an early event; *albeit* the levels detected in short-term treated cells were not as enhanced as that in acquired-resistance cells. Studies have suggested that extracellular biomarkers are encapsulated into exosomes [214]. Interestingly, we observed that NmU was detectable at higher levels in exosomes from HCC1954-LR and HCC1953-NR cells compared to parent cells. This observation of NmU as a potential extracellular predictive biomarker and the functional relevance of it presence in exosomes (while not the main focus on this chapter) warrants further investigation.

The main focus of this study after establishing significantly higher levels of NmU mRNA in cells with acquired-resistance to the HER-targeted drug lapatinib, however, turned to further investigate the extent and relevance of this observation. For a more

comprehensive understanding, we also elected to expand these studies to evaluate NmU protein, in addition to mRNA. Considering innately-sensitive and resistant cells, here we found NmU protein levels to correlate with innate-resistance versus sensitivity to HER-targeting drugs *i.e.* with the low levels in SKBR3 (sensitive to trastuzumab and lapatinib) progressively increasing in HCC1954 and MDA-MB-361 (resistant to one or other of these drugs) and at highest levels in T47D (unresponsive to both HER-targeted drugs considered here) cells. While this observation may indicate a correlation with innate response to HER-targeted drugs, it must be considered that other factors such as HER2 expression for example may reflect the results observed. Thus to fully elucidate the potential significance of this finding, a broader panel of cell lines should be assessed with analysis by Spearman's Rank Correlation (as used in similar studies [265, 331]) to investigate the level of NmU expression with response to HER-targeted drugs. In relation to acquired-resistance, NmU proteins levels were always found to be significantly higher in cells with acquired-resistance to lapatinib, trastuzumab and neratinib compared to their aged-control parent populations. This suggests that NmU protein, as well as its mRNA, potentially has broad application as a predictive biomarker for response to HER-targeted drugs.

Progressing to investigating a functional role of NmU in relation to HER-targeting, our overexpression (in sensitive cells) and knockdown (in both acquired-resistant and innately-resistant cells) studies showed NmU levels to inversely correlate with cellular response to all 4 HER-targeting drugs tested *i.e.* lapatinib, trastuzumab, neratinib and afatinib. Specifically, NmU overexpression in SKBR3 and HCC1954 cells generally conferred resistance to the anti-proliferative effects of all drugs tested. (The exception to this was the HCC1954 cells, where NmU overexpression did not affect response to trastuzumab. This is likely to be due to by the fact that HCC1954 cells are innately-resistant to trastuzumab [265]). Our NmU immunoprecipitation and associated investigations to identify the direct mechanism-of-action by which NmU is acting indicated a partnership with HSP27. By directly binding to HER2, HSP27 been shown to increase HER2 stability and thus reduce cellular sensitivity to this drug [71]. This is also in keeping with our observation of knock-on effects of NmU expression increasing HER2 protein levels. The total protein blot for NmU was not performed after immunoprecipitation due to the poor quality of this antibody. A negative IgG control should be performed in future studies to confirm that the protein brought down in the experiment is a result from the specific interaction of the antibody with the antigen protein.

Conversely, considering NmU knockdown, while there were some differences between cell lines and effectiveness of the two NmU siRNAs used, NmU knockdown added substantially (12% to 58%) to the anti-proliferative effects of lapatinib, trastuzumab, neratinib and afatinib in both innately- and acquired- resistant cell lines studied. Interestingly, this knockdown in NmU was directly associated with subsequent reduced expression of its identified partner HSP27, HER2 protein and the phosphorylated/activated form of EGFR, the latter possibly being a consequence of a reduced transactivation by HER2. A proposed mechanism for NmU's action is outlined in Figure 3.21.

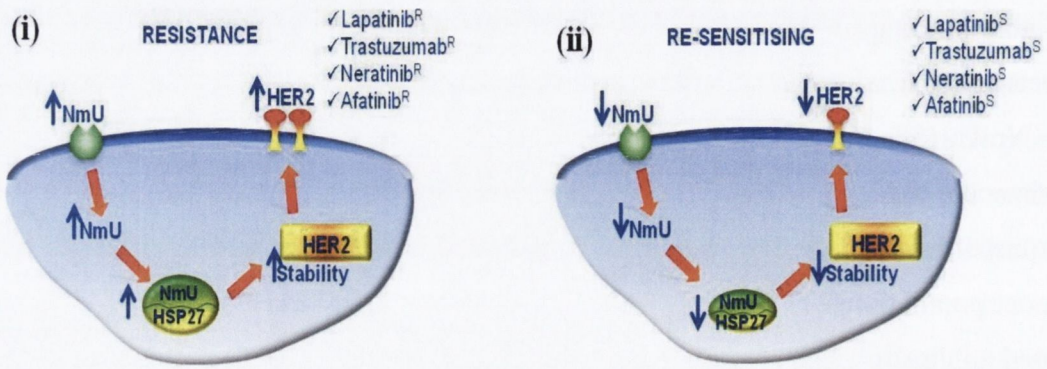

Figure 3.21: Proposed mechanism of action for NmU.

Our proposed mechanism of action by which **(i)** increased NmU (found extracellular, as well as intracellular) results in increased NmU:HSP27 complex, subsequent increased HER2 stability and thus resistance to HER-targeting drugs. **(ii)** In contrast NmU knockdown re-sensitises the resistant cells to these drugs.

The associated increased levels of p-Akt (activation of p-Akt previously shown to be associated with resistance to transtuzumab and/or lapatinib [20, 265, 321]) in response to NmU knockdown suggests the P13/Akt pathway may have become activated by NmU knockdown. As NmU knockdown induced sensitivity to HER-targeted drugs, activation of p-Akt was not necessarily expected, however recent studies have shown that while neratinib can inhibit the phosphorylation of all four HER receptors, reactivation of HER3 and Akt are observed after 24 hours [331]. Interestingly, in the same study, the combination of neratinib and trastuzumab could delay the reactivation of HER3 and Akt compared to neratinib alone [331]. Thus in relation to our findings, use of NmU as a single target may be limited and so better accompanied with the dual targeting of HER receptors.

NmU knockdown also resulted in increased sensitivity of T47D cells to all 4 drugs despite the fact that T47D cells express normal levels of HER2 *i.e.* T47D is not a HER2-

overexpressing cell line [318]. As both targets of these drugs (HER2 for all 4 drugs; also EGFR for lapatinib, neratinib and afatinib) were directly affected by the relatively modest NmU knockdown (up to 40% achieved with siRNA), these suggests that co-targeting NmU, while targeting HER2/EGFR, may help circumvent resistance to these drugs.

In keeping with our hypothesis that NmU is involved in regulating response to HER-targeted drugs, treating sensitive HER2-overexpressing cells (SKBR3 and HCC1954) with exogenous NmU was found to slightly; but significantly, reduce the anti-proliferative effects of lapatinib, trastuzumab, neratinib and afatinib, in association with increased expression of HER2 and EGFR receptors. Furthermore, an increase in HSP27 was observed following exogenous NmU treatment in HCC1954 cells. While no change was observed for SKBR3 cells, it may be possible that the induced changes of HSP27 protein in this cell line may not be evident at the time points used in this study, a longer incubation period with the NmU peptide may necessary thus further investigation into this is warranted.

The potential benefits of targeting/co-targeting NmU in HER2 breast cancer is further supported by our observations that NmU knockdown significantly decreases migration/motility, invasion and resistance to *anoikis*, while its overexpression has the opposite effects. These observations of NmU being associated with more "aggressive" phenotypic characteristics of cancer cells concur with the reports of NmU being associated with oncogenic characteristics in other cancer types including AML, pancreatic, ovarian, lung and bladder cancers [322-324, 327]. Furthermore, HSP27, identified here as a partner protein to NmU, has previously been associated with regulating cancer cell invasion and metastasis [72-74].

To truly establish the role of NmU and its importance in breast cancer, our subsequent studies have progressed to generating cell lines for future *in vivo* studies. At this point the generation of stable NmU knockdown in HCC1954-LR-LUC+ cells has just been established and characterisation is currently on going; however here we present preliminary analysis of newly generated HCC1954-LUC+ cells that overexpress NmU. Our initial assessment on these cells confirm that NmU is regulating lapatinib-resistance and increases invasion compared to mock transfected cells however the effects are not as substantial as those observed from the HCC1954 cells that did not express the luciferase

gene. While NmU was overexpressed in the NmU transfected HCC1954-LUC+ cells (approx.10 fold), the differences in NmU expression compared to mock transfected cells was not as dramatic as that observed for NmU transfected HCC1954 cells (approx. 80 fold) possibly explaining why the phenotypic changes observed were not as substantial. For future studies, it may be necessary to use the previously established NmU-overexpressing HCC1954 cells and transfect those with the Luciferase in the hope that co-transfecting cells in this manner will not affect the efficiency of NmU transfection.

3.5 CONCLUSIONS

In conclusion, here we provide evidence that NmU is associated with poor outcome from breast cancer, particularly being prognostic of unfavourable outcome for patients with HER2-overexpressing tumours; that it has potential as a predictive biomarker of response to a broad range of HER-targeting drugs; and that it is mechanistically involved in conferring this resistance by working in concert with its partner protein HSP27. Our results provide a strong rationale for more extensive analysis of NmU as a companion biomarker for HER-targeted drugs and as a co-target to help circumvent resistance and thus add value to these drugs. Our preliminary studies from Chapter 2 indicate that NmU may be regulated by small RNAs such as miR-630 however the significance of this finding is yet to be fully elucidated.

CHAPTER 4

Docetaxel-resistance in prostate cancer: evaluating associated phenotypic changes and potential for resistance transfer via exosomes

Parts of this chapter are published in the following paper:

Docetaxel-resistance in prostate cancer: evaluating associated phenotypic changes and potential for resistance transfer via exosomes

Claire Corcoran, Sweta Rani, Keith O'Brien, Amanda O'Neill, Maria Prencipe, Rizwan Sheikh, Glen Webb, Ray McDermott, William Watson, John Crown, Lorraine O'Driscoll

PLoS One. 2012;7(12):e50999.

4 ABSTRACT

Background: Castration-resistant prostate cancer remains hindered by inevitable development of resistance to first-line treatment with docetaxel. Recent studies suggest that phenotypic changes associated with cancer may be transferred from cell-to-cell *via* nano-sized extracellular vesicles known as exosomes. Here we aimed to investigate phenotypic changes associated with docetaxel-resistance in order to help determine the complexity of this problem and to assess the relevance of secreted exosomes in prostate cancer.

Methods: Docetaxel-resistant variants of DU145, 22Rv1 and PC3 cell lines were established through continuous exposure of docetaxel for several months. New cell line variants were characterised in terms resistance to docetaxel, cross-resistance to other drugs, morphology, proliferation, motility, invasion, anchorage-independent growth (*anoikis*), colony formation, exosomes secretion and their functional relevance. Preliminary analysis of exosomes from relevant serum specimens was also performed.

Results: Acquired docetaxel-resistance conferred cross-resistance to doxorubicin for all three docetaxel-resistant cell line variants assessed, and induced alterations in motility, invasion, proliferation and *anoikis*. Exosomes expelled from DU145 and 22Rv1 docetaxel-resistant variants (DU145RD and 22Rv1RD) conferred docetaxel-resistance to DU145, 22Rv1 and LNCap cells, which may be partly due to exosomal MDR-1/P-gp transfer. Exosomes from prostate cancer patients' sera induced increased cell proliferation and invasion, compared to exosomes from age-matched controls. Furthermore, exosomes from sera of patients undergoing a course of docetaxel treatment, compared to matched exosomes from the same patients prior to commencing docetaxel treatment, when applied to both DU145 and 22Rv1 cells, showed a correlation between cellular response to docetaxel and patients' response to treatment with docetaxel.

Conclusions: Our studies indicate the complex and multifaceted nature of docetaxel-resistance in prostate cancer and give an indication of aggressive characteristics that may be associated with this resistance. Furthermore, our *in vitro* observations and preliminary clinical studies indicate that exosomes may play an important role in prostate cancer, in cell-to-cell communication, and thus may offer potential as vehicles containing predictive biomarkers and new therapeutic targets.

4.1 INTRODUCTION

While docetaxel offers improvement in overall survival for patients with castration-resistant prostate cancer (CRPC) as evident from two Phase III trials (TAX 327 and SWOG 9916) and subsequent clinical management, unfortunately relapse is almost inevitable. Reasons for failure of docetaxel to increase survival beyond ~2.5 months have yet to be completely elucidated. Drug-resistance is frequently attributed with the overexpression of transporter proteins, including P-glycoprotein (MDR-1/P-gp), associated with the efflux of many anti-cancer (and other) agents [77, 83, 85]. Furthermore, chemo-resistance has also been shown to contribute to alterations in the invasive and motile phenotype of cells [277-279, 332]. Other phenotypic characteristics that may be associated with this problem in prostate cancer have yet to be defined.

Added to this, recent studies suggest that phenotypic changes associated with cancer may be transferred from cell-to-cell *via* microvesicles/exosomes. Exosomes have been described as nano-sized membrane-bound vesicles of endocytic origin [333]. Depending on their cell of origin, these small vesicles have been implicated with several different roles some of which include their association with diseased states such as cancer. Intercellular communication is one such role, through their ability to promote signal transduction [232] and the transfer of membrane receptors, proteins, mRNA, and miRNAs [214, 219] from one cell to another. The relevance of exosomes in terms of their potential to assist in prostate cancer progression and the development of chemo-resistance has yet to be determined.

Due to the complex nature of prostate cancer progression, docetaxel-resistant prostate cell lines were developed and characterised to represent both primary and metastatic tumours as well as androgen-sensitivity and androgen-resistance in prostate cancer. In this study three cell lines were used to develop docetaxel-resistant variants: 22Rv1 (androgen-sensitive; from a primary human tumour), DU145 (androgen-insensitive; from a brain metastasis), PC3 (androgen-insensitive cell lines, derived from a bone metastasis). Cell line variants were assessed for docetaxel-resistance as well as cross-resistance to the other drugs and alterations in motility, migration, invasion, proliferation and anchorage-independent growth. The secretion of exosomes derived from both 22Rv1 and DU145 docetaxel-resistant variants was assessed for their effects on migration,

invasion, proliferation and docetaxel response of secondary cells. Furthermore, exosomes derived from serum from prostate cancer patients was also assessed for affects for phenotypic changes of secondary cells.

4.2 METHODS

4.2.1 Cell culture and treatments

Prostate cancer cell lines, 22Rv1 (androgen-sensitive; from a primary human tumour), DU145 (androgen-insensitive; from a brain metastasis), PC3 (androgen-insensitive cell lines, derived from a bone metastasis), LNCap (androgen-sensitive; from lymph node metastasis) were purchased from the American Type Culture Collection (ATCC). 22Rv1, DU145 and PC3 cells were cultured in RPMI-1640 (Sigma-Aldrich, R0883) with 10% FCS (PAA Cat. #: A15-151) and 1% L-glutamine (Sigma-Aldrich, Cat. #: G7513) at 37°C/5% CO_2. LNCap cells were maintained in advanced RPMI (Invitrogen, Cat. #: 12633) supplemented with 10% fetal calf serum (PAA, Cat. #: A15-151), 1% L-glutamine (Sigma-Aldrich, Cat. #: G7513) and 1% Hepes (Sigma-Aldrich, Cat. #: H3375) and at 37°C/5% CO_2. Docetaxel (Sigma-Aldrich, Cat. #: 01885) was dissolved in DMSO (Sigma-Aldrich, Cat. # D2650) to a concentration of 1mM and stored in aliquots at -20°C. Working stocks of 1μM (stored at 4°C) were prepared fresh every week as necessary and for each biological replicate of toxicity assays. Doxorubicin (Ebewe Pharma); 5-fluorouracil (Moyne Pharma PLC); and carboplatin (Ebewe Pharma) were all provided by St. James's University Hospital, Dublin. Working stocks of 1μM for doxorubicin, 5-fluorouracil and carboplatin were prepared to fresh every week as necessary and for each biological replicate of toxicity assays and were stored at 4°C away from sun-light.

4.2.2 Establishment of docetaxel-resistant cell lines

Docetaxel-resistant cell lines (DU145RD; 22Rv1RD) were developed over a period of 6 months by stepwise increased concentrations of docetaxel. Cells were continuously maintained in docetaxel, with treatments beginning at the initial IC_{50} of the respective parent cell lines. Media containing docetaxel was changed every 2-3 days. As cells displayed resistance to treatments of docetaxel the concentration was subsequently increased with final treatment doses of 100nM. Resistance was judged based on decreased cell death and increased proliferation of cells. Docetaxel-resistant PC3RD cells were a gift from Prof. William Watson's group (University College Dublin) and were generated by initially treating with docetaxel 8nM in 75cm^2 flasks for 48hrs. After treatment, the surviving cells were re-seeded into new flasks and allowed to recover for 2-3 weeks. After 5 treatments at 8nM, the dose of docetaxel was increased to 12nM. The cells underwent a

total of 12 treatment cycles at 12nM. As the passage number of these treated cells (DU145RD, 22Rv1RD and PC3RD) increased over time, a subset of un-treated cells (DU145, 22Rv1 and PC3) were aged alongside these cells as an appropriate control for all experiments. All experiments on acquired-resistant cells and corresponding aged controls were performed within 10 passages in culture and experiments were performed on cells that received no drug for a minimum of one week. Passage numbers used were approximately the following: 22Rv1/22Rv1RD (p40-50); DU145/DU145RD (p46-56); PC3 (p112-122); PC3RD (p108-118). Cells were routinely tested for *Mycoplasma* contamination using the PCR Mycoplasma Test Kit 1/RT Variant B (Promocell, Cat. #: PK-CA91-3025B) and were found to be negative.

4.2.3 Cytotoxicity assays

Cytotoxicity assays for docetaxel, doxorubicin; 5-fluorouracil; and carboplatin were performed on all age-matched parent cells and their docetaxel-resistant variants. In brief, cells were seeded in 96-well plates at a density of $2x10^3$cells/well (DU145 and PC3 variants) and $3x10^3$cells/well (22Rv1 variants). The following day, cells were treated with a range of drug concentrations: docetaxel: 0-11nM (DU145 & 22Rv1); 0-100nM (PC3; PC3RD); 0-550nM (DU145RD, PC3RD); doxorubicin, 5-fluorouracil and carboplatin: 0-8μM (all cell line variants). Five days later, cell viability was evaluated by acid phosphatase method as previously described in Chapter 2, Section 2.2.9.

4.2.4 Cell proliferation assays

All cell lines were seeded $5x10^3$cells/well (in 24-well plates). Cells from 3 wells were trypsinised and separately counted using a haemocytometer at 24hr, 48hr, 72hr, 96hr, and 120hr time-points. Doubling times were calculated using *Doubling Time Software v1.0.10* (http://www.doubling-time.com/compute.php).

4.2.5 Cell motility –assessed using wound healing assays

Cells were seeded at $4x10^5$cells/well (DU145, DU145RD), $6x10^5$cells/well (22Rv1, 22Rv1RD) and $2x10^5$cells/well (PC3, PC3RD) onto 6-well plates and cells were left to grow to 90-100% confluency. Monolayers were scratched with a 200μl pipette tip and cells were gently washed with sterile PBS to remove loose cells following wound generation.

Low serum (0.1%) media was placed on the cells and the resulting wounded areas were monitored, at indicated time-points, by phase contrast microscopy using CellA software and measured using NIH Image J software [334]. Throughout the duration of monitoring wound closure, cells were maintained in low serum (0.1%)-containing medium to reduce any influences due to proliferation. Medium was changed before each time point was photographed.

4.2.6 Cell migration and invasion –assessed using transwell inserts

Migration and invasion assays were performed as detailed in Chapter 2, Section 2.2.12. For the DU145 and PC3 cell line variants, $5x10^4$ cells/well (migration assays) or $1x10^5$cells/well (invasion assays) were seeded in the upper compartment and allowed to migrate for 48hrs. For 22Rv1 variants, $6x10^5$cells/well were seeded and allowed to migrate for 72hrs. Cells were seeded in low serum (0.1%) containing medium in the upper chamber and 10% serum-containing medium in the well below the insert.

4.2.7 Anchorage-independent growth assays

Assays were performed using Cytoselect™ 96-well Cell Transformation kit (Cell Biolabs) according to the manufacturer's instructions. For all variants, $7.5x10^3$cells/well were incubated for 8 days in a semisolid agar media before being lysed and detected with the CyQuant GR Dye in a fluorescence plate reader (FlouStar Optima microplate reader BMG Labtech) using a 485/520 nm filter set. An outline of the protocol as indicated from Cell Biolabs is shown in Figure 4.1.

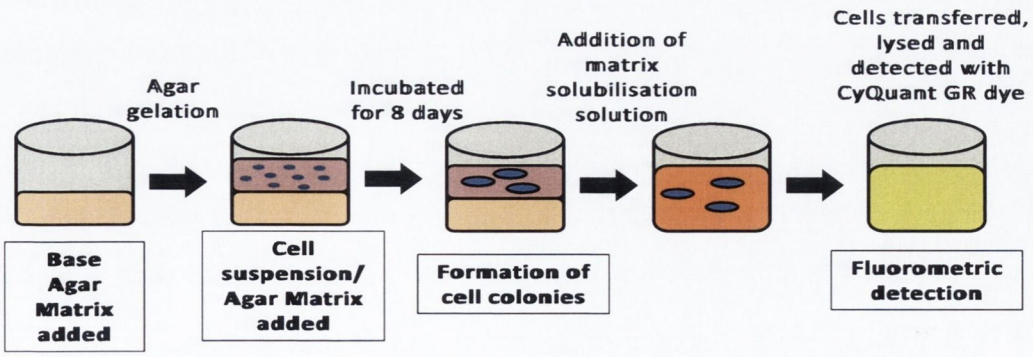

Figure 4.1: Colony formation assay protocol.

Schematic flow diagram (adapted from Cell Biolab's protocol) representing method used to assess anchorage independent growth of cells in soft agar using Cytoselect™ 96-well Cell Transformation kit.

4.2.8 Anoikis assays

Anoikis assays were performed as described in Section 2.2.13. DU145, 22Rv1 and PC3 cell line variants ($1x10^5$cells/well) were plated onto poly-hema- or 95% ethanol-coated plates and were cultured for 24hrs. Alamar blue dye (100µl; Invitrogen Cat. #DAL1100) was then added; incubated for 4hrs and assessed at 570nm. *Anoikis* was calculated as the percentage cell death relative to the adherent controls after 24hrs.

4.2.9 Exosome isolation from conditioned medium

For exosome isolation, all cells were grown in RPMI medium supplemented with 5% of exosomes-depleted fetal calf serum (dFCS) (PAA, Cat. #: A15-151), 1% L-glutamine (Sigma-Aldrich, Cat. #G7513) and 1% penicillin/streptomycin (Invitrogen, Cat. #: 15070-063). FCS was depleted of exosomes by ultracentrifugation at 110,000g for 16hrs [335]. While general cell culture procedures in this thesis did not involve the addition of penicillin/streptomycin, it was necessary for flasks set up for exosome isolation to minimise the potential of contamination occurring (due to the fact that the process of depleting the FCS involved extra handling of the FCS). Each cell line variant was seeded in nine $75cm^2$ flasks at $2x10^5$cells/ flask (for DU145 and PC3 variants) and $5x10^5$cells/flask (for 22Rv1 variants) in regular medium. After allowing cells to attach over-night, medium containing 5% dFCS was replaced and the cells were cultured for 3 (DU145 cell lines) or 5 (22Rv1 cell lines) days in the fresh medium; to reach approximately 80% confluency. Exosomes were subsequently isolated from conditioned medium (CM) using methods that we recently described [335]. In brief, CM from all flasks for each cell line variant was pooled and centrifuged at 2000g for 10mins at 4°C to eliminate dead cells and large debris. The CM was then filtered using 0.45µm pore filters (VWR, Cat. #: 4564) and subsequently ultracentrifuged at 110,000g for 75 min at 4°C on a SW28 swinging bucket rotor. Exosome pellets were washed in phosphate buffered saline (PBS) (Sigma-Aldrich, Cat. #:D8537) and ultracentrifugation was repeated. The resulting exosomes pellets were resuspended in approximately 200µl PBS and stored at -80°C for subsequent quantification (using BioRad protein assay Dye Reagent, as described in Section 2.2.10) and analysis. Schematic flow diagram of exosome isolation is indicated in Figure 4.2.

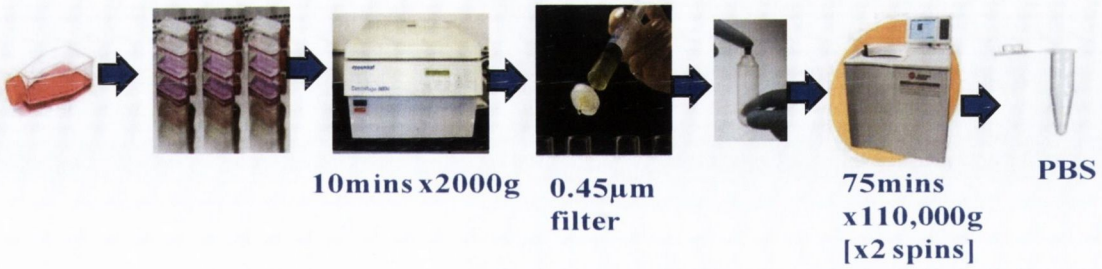

Figure 4.2: Flow diagram summarising the protocol for exosome isolation

4.2.10 Transmission Electron Microscopy

[TEM was performed with the help of Neal Leddy, Chief technical Officer at the Centre for Microscopy and Analysis in Trinity College]

Exosomes were isolated from conditioned media, as described in Section 4.2.10, and were analysed by electron microscopy [272]. Briefly, approximately 10µl of exosomes samples were placed on parafilm (Sigma-Aldrich, Cat. #: P7793) in duplicate. A 300 mesh copper grid was placed on top of the drop and allowed to stand for 45mins. The copper mesh was subsequently washed thrice in fresh 0.05 M phosphate buffer (freshly prepared using dihydrogen potassium phosphate (Merck, Cat. #: 1.04873.0250) and dipotassium hydrogen phosphate (Merck, Cat. #:1.05104.1000)) for five minutes each, fixed in 3% glutaraldehyde (Agar Scientific, Cat. #: 101504)) for 10mins, washed thrice for 5mins each in dH_2O and contrasted in 2% uranyl acetate (BDH, Cat. #: 30550). Grids were then examined by electron microscopy at 100kV using a JEOL JEM-2100 electron microscope.

4.2.11 Exosome isolation from serum specimens

Exosomes from human serum specimens, procured through the All-Ireland Cooperative Oncology Research Group (ICORG) Translational Trial: 08-08, and with consent from the Ethics Committee of Beaumont Hospital, Dublin and the Mater Hospital, Dublin, were isolated using Exoquick (Systems Biosciences, Cat. #: EXOQ5A-1), as per manufacturer's protocol. Serum from 6 prostate cancer patients (denoted by Patient #1-6) and age-matched healthy controls (Control #1-6) were used for invasion and proliferation assays. Exosomes isolated from a further eight prostate cancer patients (denoted by Patient A-H) sera procured both before and during docetaxel treatment were used for "docetaxel-resistance"/cytotoxicity assays. For the purpose of these studies, patients who achieved

decreasing PSA levels with treatment compared to their respective PSA levels pre-treatment were considered as "responders", whereas patients with elevated PSA following treatment were considered as "non-responders".

4.2.12 Immunoblotting

Proteins were extracted from whole cells or exosomes using Cell Extraction Buffer (Invitrogen, Cat. #: FNN0011) as described in Section 2.2.10. Protein quantification of cells and exosomes was performed using BioRad protein assay Dye Reagent (BioRad, Cat. #:500-0006) as described in Section 2.2.10. Protein (50μg for cellular protein samples and 30μg for exosomes from CM samples for the exosome marker TSG101[336, 337] and MDR-1/P-gp; 8μg exosomes for the exosome marker PDC6I/Alix [338] and 30μg for serum-derived exosomes) were resolved on PAGEr Gold precast gels for protein electrophoresis; 7.5% (Lonza, Cat. #: 59513). Immunoblotting involved using the following primary antibodies and dilutions: MDR-1/P-gp (Santa Cruz, Cat. #: SC55510; 1:200), PDC6I/Alix (Abcam, Cat. #:AB76608; 1:1000 dilution) and TSG101 (Abcam, Cat. #4A10; 1:1000 dilution), GAPDH (Cell Signalling, Cat. #2118; 1:1000 dilution), β-actin (Sigma-Aldrich, Cat. #: A5316; 1:1000 dilution). PVDF membranes (Bio-Rad laboratories, Cat. #: 162-0177) were blocked as described in Section 2.2.10 and were incubated in primary antibodies over-night at 4°C. Membranes were incubated with appropriate horseradish peroxidase-conjugated secondary antibodies -Anti-mouse (Cell Signalling, Cat. #: 7074; 1:1000 dilution); or -Anti-rabbit (Cell Signalling, Cat. #: 7076; 1:1000 dilution) for 1hr at room temperature and proteins were visualized by chemiluminescence (Themofisher: Cat. #: 34080). Detection was performed with a Chemidoc exposure system (Bio-Rad Laboratories).

4.2.13 Addition of exosomes to invasion, migration, proliferation and cytotoxicity assays

To assess any influences of exosomes on cell motility, a scaled down version of the wound healing assay described in Section 4.2.5 was used, specifically, $5x10^4$cells/chamber (DU145) were seeded in a 4-chamber slide and 5μg exosomes from DU145 (autologous) or DU145RD (resistant) cells were applied/chamber, as appropriate. After 48hrs, monolayers were scratched and assessed as before in Section 4.2.5.

To evaluate effects on invasion, invasion assays were seeded as detailed above, except that $3x10^5$cells/insert were used for 22Rv1 cell line. DU145 or DU145RD exosomes (15μg) or serum exosomes (25μg) were applied as appropriate to each insert when cells had attached to the inside of the insert (~4hrs after seeding cells). For proliferation and cytotoxicity assays, $4x10^3$cells/well (DU145) and $5x10^3$cells/well (22Rv1 and LNCap) was seeded in a 96-well plate and allowed attach overnight. For LNCap cells, plates were pre-coated with poly-d-lysine (Sigma-Aldrich; Cat. #: P6407) to facilitate adhesion. Cell-derived exosomes (20μg) of (DU145, DU145RD, 22Rv1, 22Rv1RD) or serum exosomes (25μg) were then applied to each well, as appropriate. For cytotoxicity assays, the docetaxel IC_{50} concentration (as determined in Section 4.3.1) was applied to the wells, as set up for proliferation assay, at the same time as exosomes. As a control in proliferation and cytotoxicity assays, the equivalent volume of PBS was substituted where no exosomes were applied. Proliferation and cytotoxicity assays were incubated for 48hrs (for DU145 cells) or 72hrs (for 22Rv1 and LNCap cells) after which effects were assessed using the acid phosphatase method as detailed in Chapter 2, Section 2.2.9.

4.2.14 Statistical Analysis

Statistical analysis was performed on Excel. *P*-values were generated using Student's t-tests, with $p<0.05$ considered as statistically significant. Results are displayed as n=3± standard error of mean (SEM). Except for clinical specimen proliferation and invasion studies which was n=6±SEM (patients versus controls). GraphPad was used for graph generation.

4.3 RESULTS

4.3.1 Determining the extent of resistance to docetaxel and cross resistance to other anti-cancer agents

As detailed in Table 4.1, DU145RD, 22Rv1RD and PC3RD cells were found to be approximately 108-, 71- and 19-fold resistant to docetaxel compared to their respective aged parent cell lines. All resistant cell line variants exhibited cross-resistance (4-8 fold) to doxorubicin (Table 4.1). While no significant differences in sensitivity to 5-fluorouracil or carboplatin were observed for DU145RD or 22Rv1RD in comparison to their respective parent cells, a small but significant ($p<0.05$) increase in resistance to 5-fluorouracil was demonstrated for PC3RD (approximately 3-fold).

Anti Cancer Agent	DU145	DU145RD	Fold Change	22Rv1	22Rv1RD	Fold Change	PC3	PC3RD	Fold Change
Docetaxel(nM)	1.7	183.3	108.7±7.4	4	277	71.3±8.4	2.1	40.7	19.3±2.7
Doxorubicin(nM)	24	97	4.3±1.0	60	500	8.3±2.0	120	500	4.2±1.2
Fluorouracil(nM)	70	77	1.2±0.1	43	70	1.6±0.2	175	517	3.0±0.7
Carboplatin(nM)	700	700	1.0±0.1	950	2000	2.1±0.6	983	1817	1.7±0.4

Table 4.1: Docetaxel-resistance and cross-resistance for prostate cancer cell line variants.
Average IC_{50} values and fold changes of prostate cancer cell lines and docetaxel-resistant variants. Toxicity assays for PC3 cell line variants were partly performed by Anna O'Brien. Toxicity assays were seeded on day 1, treated the following day with a range of drug concentrations and response was assessed 5 days later. Response to treatment shown here was assessed using the acid phosphatase method.

4.3.2 Docetaxel-resistant variants do not differ in morphology but showed different proliferation rates versus parent cell lines

Observation of cell morphology by phase contrast microscopy did not reveal any substantial differences in the morphology of the cells following acquired docetaxel-resistance (Figure 4.3), although in general resistant cells proliferate more slowly (significantly $p<0.05$ for DU145RD and 22Rv1RD but not significant for PC3RD cells) than their docetaxel-sensitive parent populations (Table 4.2).

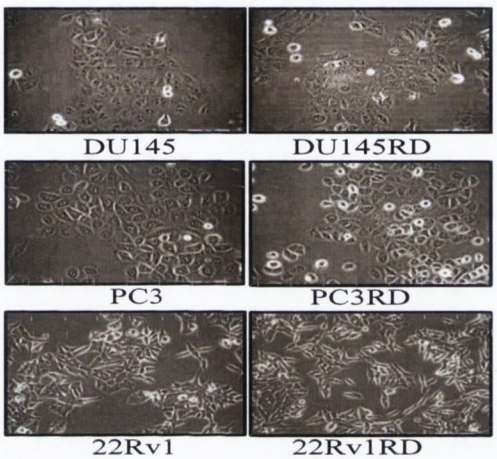

Figure 4.3: Cell morphology of cell line variants

Images of sensitive parent and docetaxel-resistant variants of DU145, PC3 and 22Rv1 cell lines. (Olympus CKX4, 20X magnification).

Cell line variant	Doubling time (hr)
DU145	24.0± 1.4
DU145RD	33.4± 2.4
22Rv1	32.2± 2.3
22Rv1RD	46.0± 4.1
PC3	26.5± 2.8
PC3RD	34.3± 2.8

Table 4.2: Proliferation rates of docetaxel-resistant cell line variants.

Average doubling time for prostate cancer cell lines and respective docetaxel-resistant variants. Proliferation assays for PC3 cell line variants were partly performed by Anna O'Brien. Proliferation assays shown here were manually counted using a haemocytometer and doubling time was calculated using *Doubling Time Software v1.0.10* (http://www.doubling-time.com/compute.php).

4.3.3 Docetaxel-resistant variants have distinct motile and invasive phenotypes versus parent cell lines

Wound-healing assays were used to evaluate the effects of docetaxel-resistance on cell motility (Figure 4.4). After 24hrs, DU145RD cells demonstrated significantly ($p<0.05$) increased wound closure by 8.9±2.7% compared to DU145. In contrast, PC3RD exhibited significantly ($p<0.001$) reduced wound closure by 62.0±2.4% compared to PC3. 22Rv1RD also showed slight, but significantly ($p<0.05$) decreased wound closure by 8.7±1.1% compared to 22Rv1after 48hrs (Figure 4.4). All wound healing assays were performed in low (0.1%) serum to avoid any influences of wound closure due to proliferation.

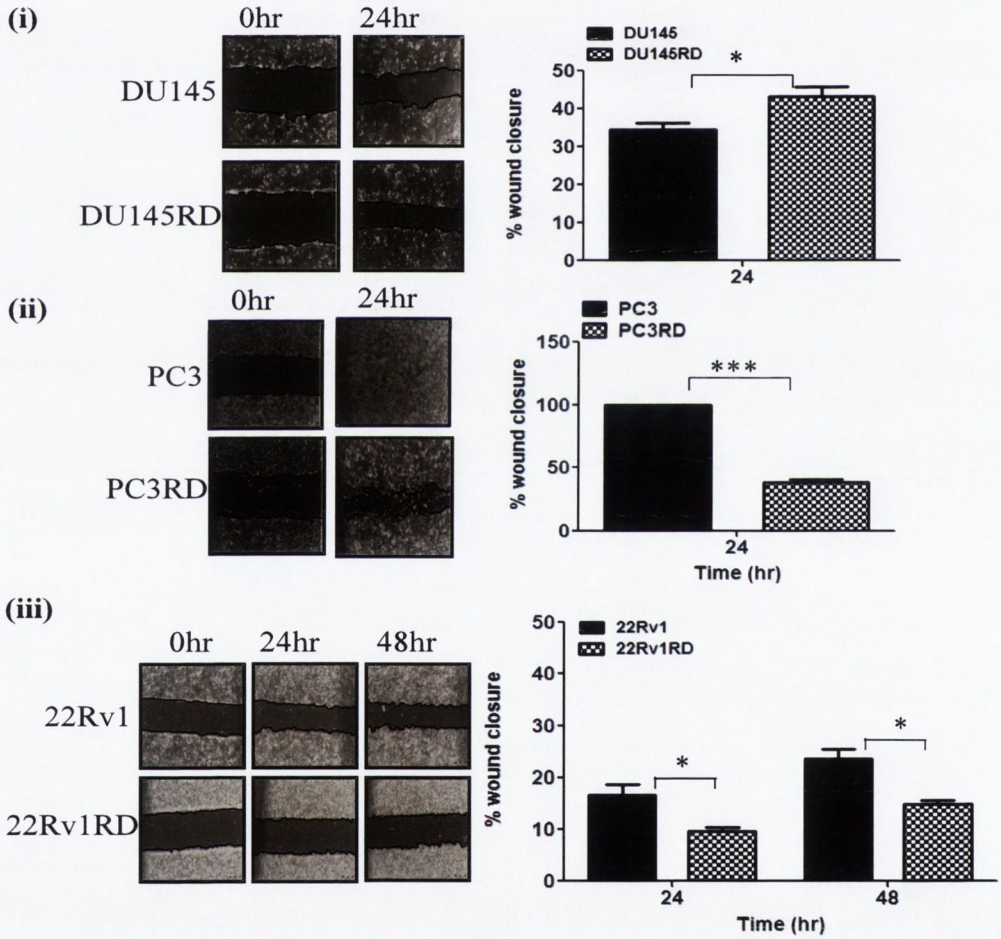

Figure 4.4: Wound healing assays of docetaxel-resistant variants.

(i) DU145RD cells were significantly more motile than DU145 whereas **(ii)** PC3RD and **(ii)** 22Rv1RD were less motile that PC3 and 22Rv1, respectively. Results are displayed as n=3± SEM, where *$p<0.05$, ** $p<0.01$, ***$p<0.001$ (Student's t-test). Wound healing assays for PC3 cell line variants were partly performed by Anna O'Brien.

Possible associations between acquired docetaxel-resistance and cellular migration (Figure 4.5A) and invasion (Figure 4.5B) were also assessed using transwell assays. Again, DU145RD was found to have increased migration by 62.7±9.3% ($p<0.01$) and invasion by 50±13.6% ($p<0.05$) when compared to its aged-parent population DU145. In agreement with motility results from the wound-healing assay, PC3RD demonstrated less migration by 44.1±11.6% ($p<0.05$) and invasion by 46.4±5.4% ($p<0.001$) potential in comparison to PC3. 22Rv1RD compared to 22Rv1 cells also followed the same trend of decreased migration by 29.9±6.2 ($p<0.01$) and invasion by 37.9±6.5 ($p<0.05$). As with wound healing assays in Section 4.3.2, cells were seeded in low serum medium in upper compartment of inserts to avoid proliferation influences.

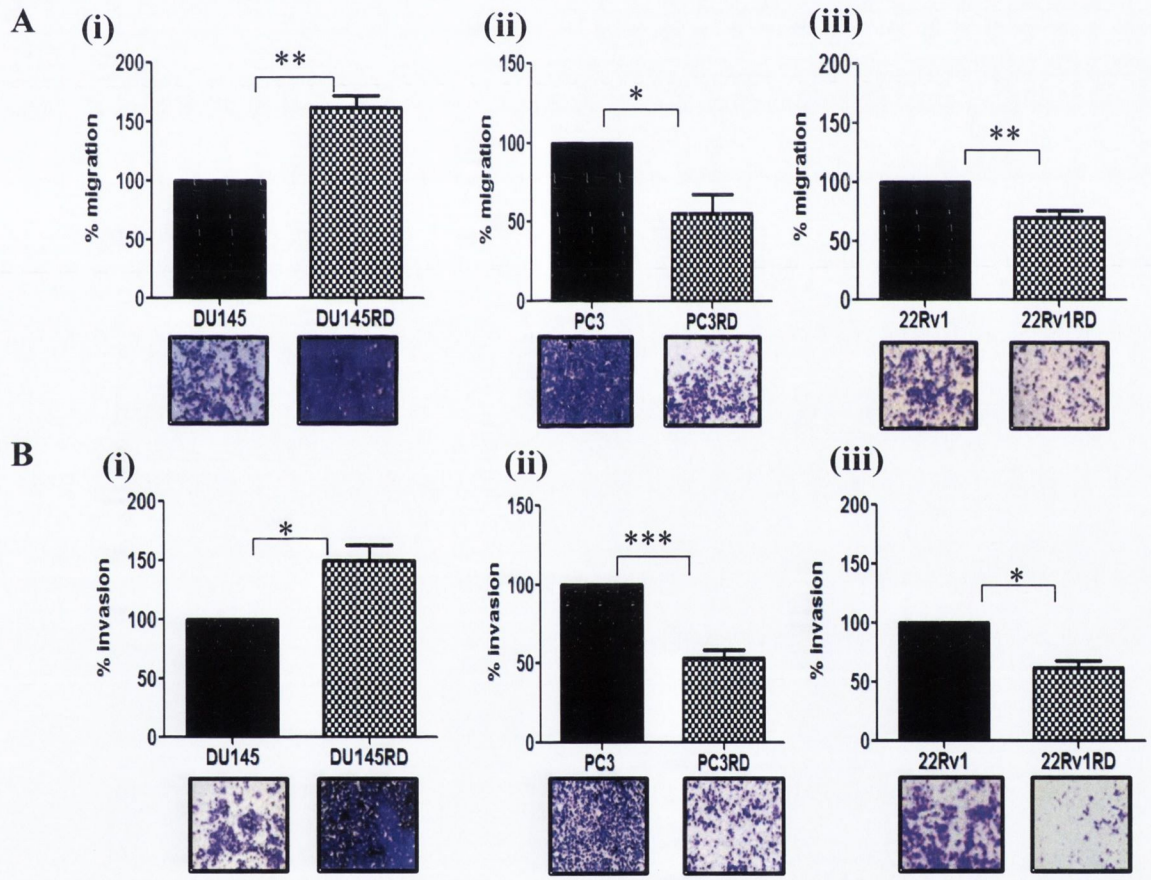

Figure 4.5:Transwell migration and invasion assays of docetaxel-resistant variants.

(A) Migration assays were performed using 8μm pore size 24-well transwell chambers. **(i)** DU145RD cells displayed significantly more migration than DU145 whereas **(ii)** PC3RD and **(ii)** 22Rv1RD was less migratory than PC3 and 22Rv1 respectively. **(B)** The same trends were observed for invasion assays where the inserts were pre-coated with ECM. Results are displayed as n=3± SEM, where *$p<0.05$, ** $p<0.01$, ***$p<0.001$ (Student's t-test).

4.3.4 *Acquired docetaxel-resistance influences anchorage-independent survival and growth*

Investigating if acquired drug-resistance may also confer *anoikis* resistance, we observed drug-resistance to be significantly associated with decreased cell death under *anoikis* conditions for all 3 drug-resistant variants compared to age-matched parent cells. Specifically, decreased cell death was observed for DU145RD by 2.2±0.9 fold ($p<0.05$); 22Rv1RD by 3.6±1.1 fold ($p<0.05$) and PC3RD by 7.5±2.4 fold ($p<0.001$) compared to their respective age-matched control cells (Figure 4.6A). Subsequently evaluating if these viable cells are also able to proliferate in suspension, colony formation in soft agar was found to be significantly increased in DU145RD by 1.3.0±0.4 fold ($p<0.05$) and 22Rv1RD by 7.6±2.2 fold ($p<0.05$) in comparison to their respective parent cells (Figure 4.6B). In contrast, however, PC3RD cells had significantly decreased ability to form colonies by 2.9±0.1 fold compared to PC3 cells ($p<0.001$).

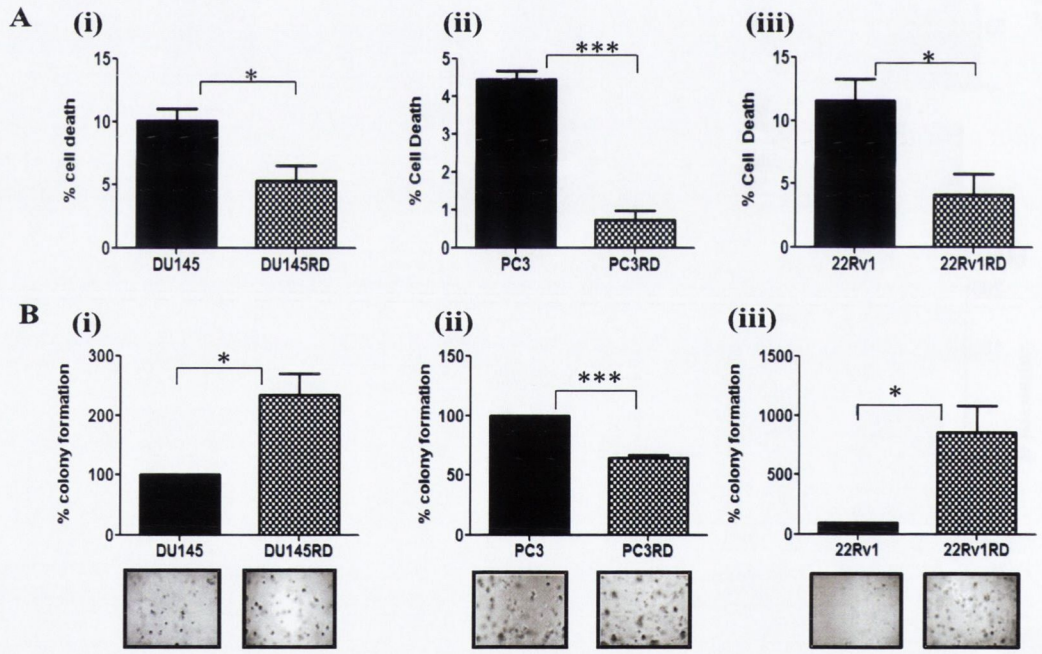

Figure 4.6: Anchorage independent growth of docetaxel-resistant variants.

(A) For *anoikis* assays, cell line variants were plated onto Poly (hydroxyethyl methactylic) acid-coated 24-well plates – or 95% ethanol-coated plates, as controls. **(i-iii)** All docetaxel-resistant cell lines had significant resistance to *anoikis* compared to age-matched control cells. **(B)** Colony formation assays were performed using Cytoselect^{TM} 96-Well Cell Transformation kit. **(i, iii)** Here DU145RD and 22Rv1RD both had significantly increased colony formation compared to age-matched control cells. **(ii)** In contrast, PC3RD cells had decreased colony formation compared to PC3. *Anoikis* assays shown here was assessed using alamar blue. Results are displayed as n=3± SEM, where *$p<0.05$, ***$p<0.001$ (Student's t-test).

4.3.5 Characterisation of exosomes derived from DU145 and 22Rv1 cell line variants

For the purpose of exosome assays in this chapter, DU145 and 22Rv1 cell line variants were used. TEM identified the presence of exosomes isolated from the conditioned medium of DU145 and 22Rv1 cell line variants (Figure 4.7A). Furthermore immunoblotting for both TSG101 and PDC6I/Alix (Figure 4.7B), proteins commonly associated with exosomes formation and thus considered to be important markers of successful isolation of exosomes [335, 339], were detected in isolates from the conditioned medium of DU145 and 22Rv1 cell line variants. No loading control was used for the immunoblot due to the fact that exosomes secreted by cells may vary among experimental conditions and therefore their protein may not be the same. Previous studies have noted this issue when they found inconsistent detection of GAPDH and no detection of Beta Actin (both of which commonly used as loading controls for immunoblots on cell lysates) in their experiments [340]. Amounts of exosomes expelled from the docetaxel-resistant and aged-matched variants did not differ significantly (Figure 4.7C). Examples of the exosomes quantities isolated per $1x10^4$ cells are indicated in Figure 4.7C however further examples of protein and also RNA content for all three cell line variants is indicated in Chapter 5.

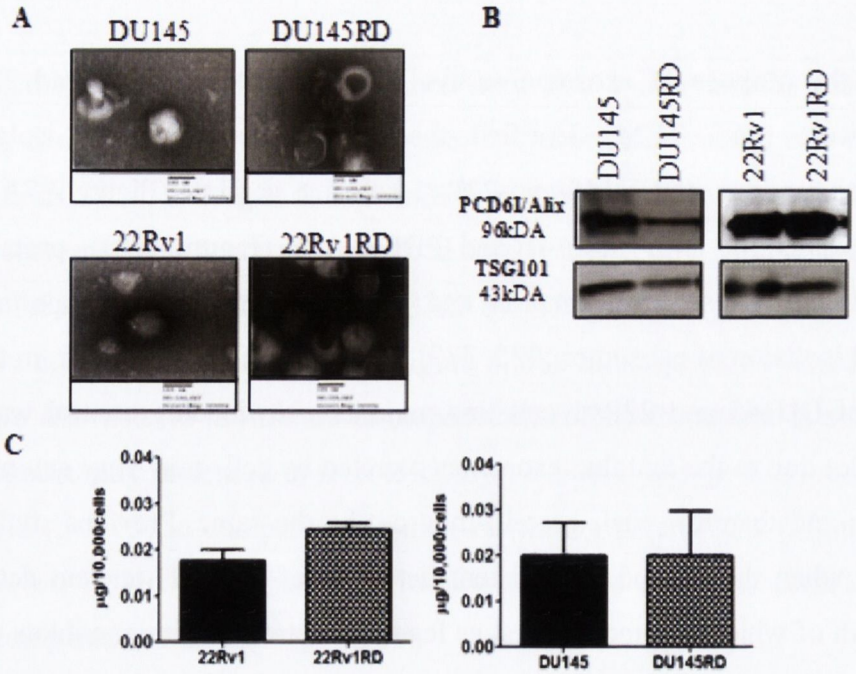

Figure 4.7: Characterisation of cell derived exosomes.

(A) Transmission Electron Microscopy was performed to investigate the approximate size and structure of exosomes. **(B)** Immunoblotting was performed to assess the expression of common exosomes markers in 30µg (TSG101) and 8µg (PDC6I/Alix) exosomes isolated from DU145 and 22Rv1 cell line variants **(C)** Following exosomes isolation, cells were trypsinised from flasks and counted (n=3± SEM) and exosomes were quantified using BioRad protein assay Dye Reagent. Exosomes quantities were calculated per $1x10^4$ cells.

4.3.6 Exosomes secreted from prostate cancer cells can influence response to docetaxel but do not significantly alter proliferation, motility and invasion.

As acquired docetaxel-resistance in the DU145RD cells was associated with increased migration and invasiveness, we next investigated if autologous (DU145 cells) or resistant (DU145RD cells)-derived exosomes could alter motility as assessed by wound-healing capacity (Figure 4.8A) and invasion (Figure 4.8B(i)) of DU145 cells. No significant difference between wound closures of cells in the presence of DU145 or DU145RD exosomes was found. Similarly, when applied to 22Rv1 cells, neither DU145- nor DU145RD-derived exosomes conferred a substantial effect on invasion (Figure.4 8B(ii)).

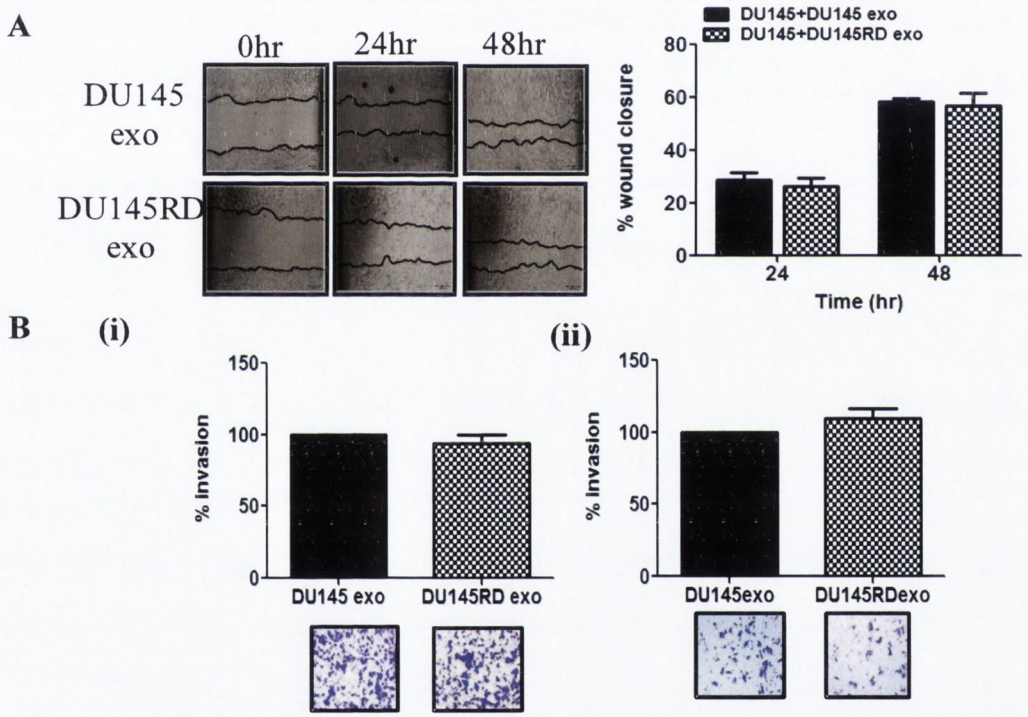

Figure 4.8: Exosomes from DU145 and DU145RD do not alter motility or invasion of secondary cells. **(A)** DU145 wound-healing assays in the presence of exosomes (5μg) from DU145 cell line variants. **(B) (i)** DU145 invasion assays in the presence of exosomes (15μg) from DU145 cell line variants **(ii)** 22Rv1 invasion assays in the presence of exosomes (15μg) from DU145 cell line variants. Results are displayed as n=3± SEM.

A slight increase in proliferation of DU145 cells by 6.8±2.5% in the presence of DU145-derived exosomes was noted. This approached significance ($p=0.053$); however, DU145RD exosomes did not significantly alter the proliferation of DU145 cells (Figure 4.9A(i)); possibly as a consequence of the slower growth rate of the cells from which the latter exosomes were derived. Following treatment with the IC_{50} concentration of docetaxel, a significant level of docetaxel insensitivity (resistance) was induced in DU145 cells the presence of DU145 exosomes by 12.3±2.9% ($p<0.05$) and to a greater extent DU145RD exosomes by 22.2±4.5% ($p<0.01$) (Figure 4.9A (ii))

To more broadly investigate if DU145RD-derived exosomes can induce similar affects when applied to other cell lines, we next investigated the effects of these exosomes on both 22Rv1 and LNCap cells (Figure 4.9B and 4.9C). Neither DU145- nor DU145RD-derived exosomes significantly affected the proliferation of 22Rv1 or LNCap cells (Figure 4.9B (i) and 4.9C(i)). Following treatment with docetaxel, no substantial change in response of 22Rv1 or LNCap cells to docetaxel in the presence of DU145 exosomes was observed when compared to the effect of the drug in the presence of PBS instead of exosomes (Figure 4.9B(ii) and 4.9C(ii)). However, in the presence of DU145RD exosomes, the ability of 22Rv1 and LNCap cells to survive in this concentration of docetaxel was significantly increased by 15.6±1.6% and 11.7±1.3% respectively ($p<0.001$) (Figure 4.9B(ii) and 4.9C(ii)). To determine if this is likely to be specific to exosomes from one cell line variant (DU145RD) or more general to exosomes from docetaxel-resistant cells, exosomes isolated from 22Rv1 and 22Rv1RD variants were subsequently assessed. Here we found the same trend to occur *i.e.* there was no significant increase in proliferation of DU145 or LNCap cells in the presence of either 22Rv1 or 22Rv1RD exosomes (Figure 4.9D(i) and Figure 4.9E(i)). There was no significant change in response to docetaxel, by either DU145 or LNCap cells, in the presence of aged-parent 22Rv1-derived exosomes. However, in the presence of exosomes from the resistant-variant 22Rv1RD, both DU145 and LnCap cells demonstrated a significant increase in resistance to docetaxel by 12.3±1.5% ($p<0.01$) (Figure 4.9D(ii)) and and by 17.1±3.5% ($p<0.01$) (Figure 4.9E(ii)) respectively.

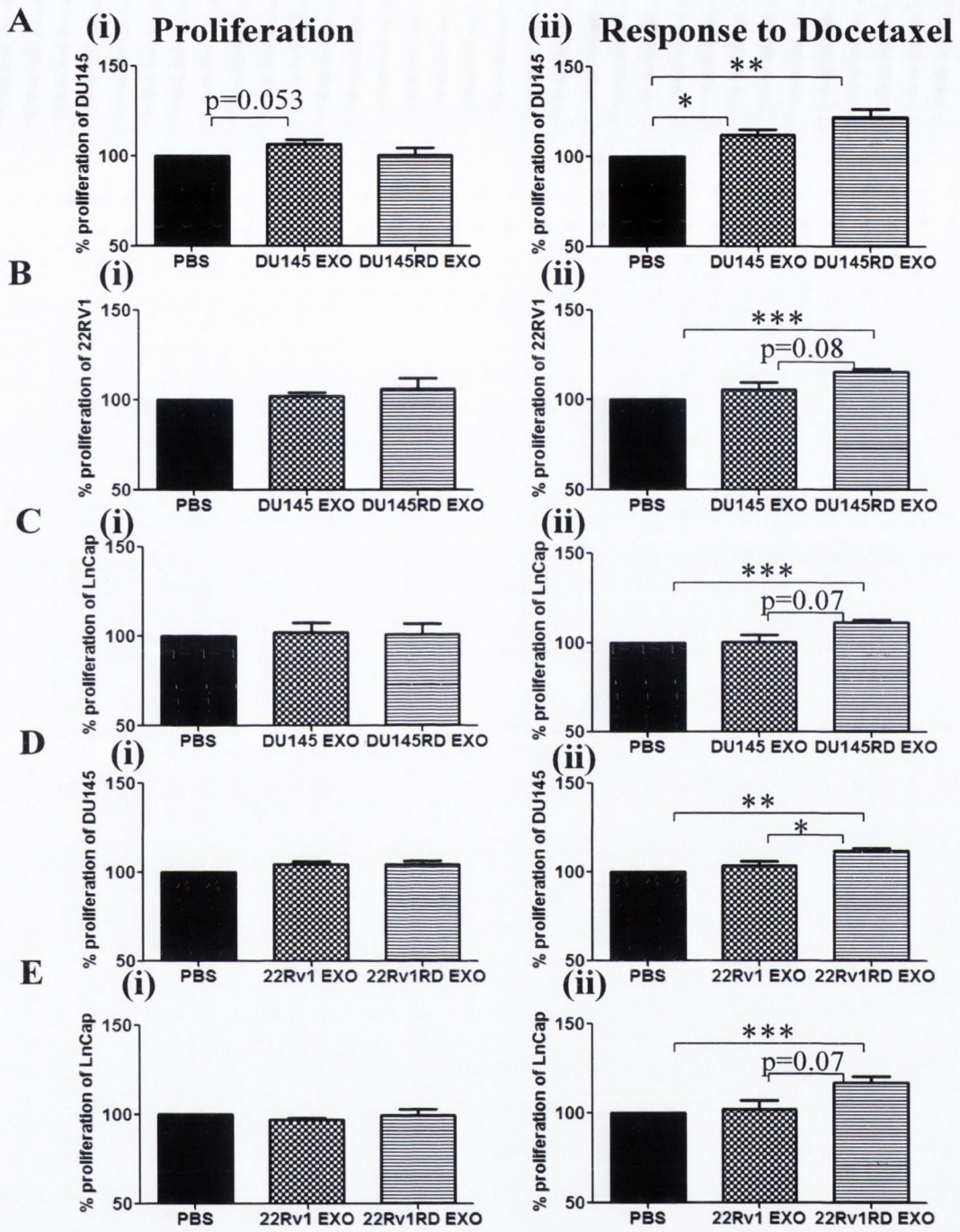

Figure 4.9: Proliferation and toxicity assays in the presence of exosomes.

(A-C) (i) DU145, 22Rv1 and LNCap proliferation in the presence of exosomes (20μg) from DU145 cell line variants; **(A-C) (ii)** Response of DU145, 22Rv1 and LNCap cells to docetaxel in the presence of exosomes (20μg) from DU145 cell line variants; **(D-E) (i)** DU145 and LNCap proliferation in the presence of exosomes (20μg) from 22Rv1 cell line variants; **D-E (ii)** Response of DU145 and LNCap cells to docetaxel in the presence of exosomes (20μg) from 22Rv1 cell line variants. Response to treatment shown here was assessed using the acid phosphatase method Results are displayed as n=3± SEM, where *$p<0.05$, **$p<0.01$, ***$p<0.001$ (Student's t-test).

We have previously reported that both DU145RD -and 22Rv1RD to a greater extent- expressed MDR-1/P-gp, whereas MDR-1/P-gp was undetected in the age-matched control cells, DU145 and 22Rv1 as well as PC3 cell line variants [90] (Figure 4.10A). To investigate whether MDR-1/P-gp is possibly carried *via* exosomes from DU145RD or 22Rv1RD cells, we investigated the presence of this efflux pump in exosomes isolated from these resistant variants. Here we report that MDR-1/P-gp is, in fact, present in the corresponding exosomal extractions (Figure 4.10B).

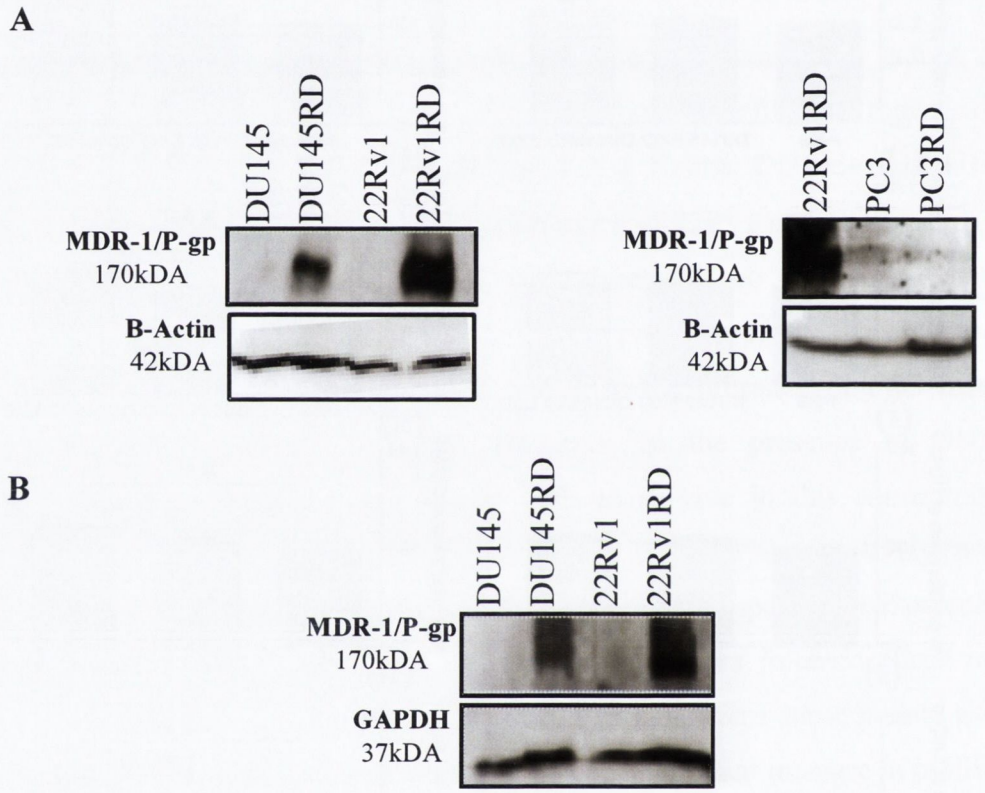

Figure 4.10: MDR-1/P-gp expression in cells and exosomes.

(A) Immunoblotting was performed to assess the expression of MDR-1/P-gp in total cellular protein (50µg) of DU145, 22Rv1 and PC3 cell line variants **(B)** corresponding exosomes (30µg) of DU145 and 22Rv1 cell line variants.

4.3.7 Exosomes are detected in serum from prostate cancer patients and can influence cellular proliferation, invasion and response to docetaxel

Immunoblotting for both exosomes markers TSG101 and PDC6I/Alix (Figure 4.11A) demonstrated the successful isolation of exosomes from sera of prostate cancer patients and healthy controls. Amounts of exosomes detected in the sera of prostate cancer patients and aged-matched controls did not differ significantly (Figure 4.11B). When added to DU145 cells, exosomes from docetaxel-naïve prostate cancer patients (n=6) demonstrated a significant ($p<0.001$) increase in invasion by 25.3±6.4% when compared to exosomes from age-matched healthy controls (Figure 4.11C). Furthermore, when applied to 22Rv1 cells, there was a significant increase in proliferation by 11.6±4.5% in the presence of prostate cancer exosomes in comparison to those from healthy controls ($p<0.01$) (Figure 4.11D).

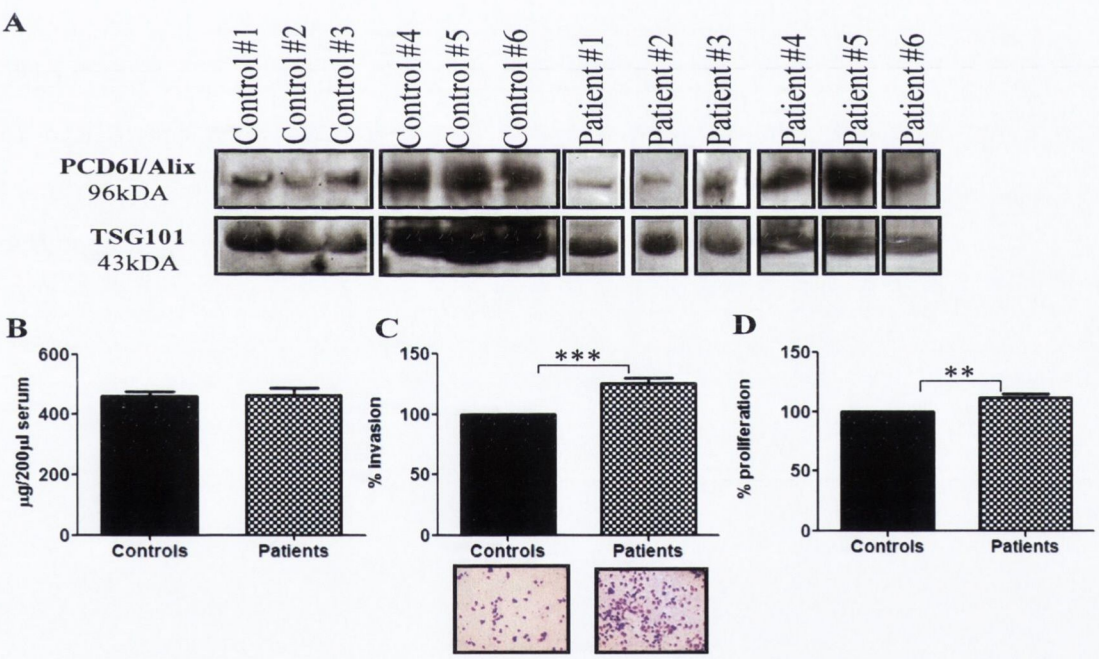

Figure 4.11: Isolation of exosomes from serum and assessment of effects on cells.

(A) Immunoblotting was performed to assess the expression of common exosome markers in 30µg exosomes isolated from sera of docetaxel-naïve patients (patient #1-6) and age-matched healthy controls (control #1-6). **(B)** Exosome quantification per 200µl of serum from treatment naïve patients and age-matched healthy controls **(C)** DU145 invasion in the presence of exosomes from docetaxel-naïve patients and aged-matched healthy controls (25µg), with representative invasion image displayed. **(D)** 22Rv1 proliferation in the presence of exosomes from treatment-naïve patients and age-matched healthy controls (25µg). Results are displayed as n=6± SEM, where **p<0.01, ***p<0.001

For the purpose of assessing potential relevance of circulating exosomes with regards to how they may help predict or, indeed, affect patients' response to docetaxel treatment, the influences of exosomes isolated from patients pre-docetaxel treatment (n=8) compared to matched exosomes isolated from the same patients during the course of their 10 cycles of docetaxel treatment were assessed. Based on the availability of patient specimens, the selection of patients was based on those patients who had a blood samples and PSA information taken prior to any treatment and then the furthest cycle that they had received for which PSA information was available. For consistency, patients were selected mainly from cycle 7 or 8 which the exception of one patient who was at an earlier stage in their treatment regime and so at cycle 3. For the purpose of this pilot study, patients (n=6) who achieved decreasing PSA levels with treatment compared to their pre-treatment PSA levels were considered as "responders", while those (n=2) whose PSA levels increased during the course of treatment were considered as "non-responders". As indicated in Table 4.3, 22Rv1 and DU145 cells were exposed to their approximate IC_{50} concentrations of docetaxel and the resulting cell viability was subsequently assigned an arbitrary value of 1. The exosomes isolated during the course of treatment from patients with increasing PSA levels (Patients A & B; "non-responders") were found to protect both 22Rv1 and DU145 cells from the effects of docetaxel. In contrast, for the 6 docetaxel "responders", the exosomes isolated during their course of treatment seemed to enhance the inhibitory effects of docetaxel on both the 22Rv1 and DU145 cells.

Patient	Pre-tx. PSA (ng/ml)	PSA during the course of tx. [pre-cycle x]	With Pre-tx. exosomes: + Docetaxel [IC_{50}]	With exosomes procured during the course of tx. + Docetaxel [IC_{50}]	With exosomes procured during the course of tx. + Docetaxel [IC_{50}]
			22Rv1, DU145: viable cells = arbitrary 1	**22Rv1**: viable cells relative to arbitrary 1	**DU145**: viable cells relative to arbitrary 1
A	18.8	35.7 [pre-cycle 7]	1	1.28	1.40
B	11.0	42.8 [pre-cycle 7]	1	1.17	1.33
C	2803.0	1843 [pre-cycle 8]	1	0.65	0.91
D	128.7	69.5 [pre-cycle 7]	1	0.57	0.87
E	23.8	1.5 [pre-cycle 8]	1	0.82	0.87
F	15.7	0.2 [pre-cycle 7]	1	0.86	0.89
G	1152.4	28.6 [pre-cycle 7]	1	0.86	0.83
H	812.1	98.2 [pre-cycle 3]	1	0.74	0.86

Table 4.3: Assessment of serum derived exosomes in relation to docetaxel response.

Response, to docetaxel, of 22Rv1 and DU145 cells in the presence of serum-derived exosomes from patients with elevated PSA levels (n=2; Patients A & B) and in the presence of exosomes from the patients with decreased PSA levels (n=6; Patients C-H). Response to treatment shown here was assessed using the acid phosphatase method.

4.4 DISCUSSION

While docetaxel remains as the current gold standard for CRPC treatment, it only increases overall survival by on average of 2.5 months and those patients who initially respond eventually develop resistance to this drug. In this study, we demonstrate the complex nature of docetaxel-resistance through the use of *in vitro* human prostate cancer cell line models. All docetaxel-resistant cell line variants in this study demonstrated cross-resistance to doxorubicin, which is consistent with previous studies of docetaxel-resistant pancreatic cancer cells [84] and breast cancer cells [341]. In addition, paclitaxel, from which docetaxel is synthetically-derived, has been associated with cross-resistance to doxorubicin in paclitaxel-resistant prostate cancer cell lines [83]. Interestingly, unlike DU145RD and 22Rv1RD, PC3RD also displayed some cross resistance to 5-fluorouracil. The fact that 5-fluorouracil is not a substrate for MDR-1/P-gp [342, 343], which we found was expressed in DU145RD and 22Rv1RD but not PC3RD, may account for the slight variation in cross-resistance phenotype of these cells.

In this study we found that while DU145RD cells had increased migration and invasion compared to DU145, the other two resistant cell lines, PC3RD and 22Rv1RD demonstrated decreased trends compared to their respective parent cell lines, PC3 and 22Rv1. Increased invasion and migration have previously been linked with chemo-resistance [277-279], however it has been demonstrated that while the knockdown of beta catenin in osetocarcinoma cells increased resistance to doxorubicin, cellular invasion was suppressed [332]. Furthermore, multi-drug resistant cell lines derived from the Dunning R3327 model of rat prostatic carcinoma have previously been shown to lose metastatic potential in host animals in comparison to their parent cells [344]. A recent study, using docetaxel-resistant prostate cancer cells derived from DU145 and PC3, revealed a contradictory overlap of differentially expressed genes in both cell line variants associated with several cellular mechanisms including cell growth, apoptosis and the ECM [345]. Specifically, LAMC2 was found to be significantly down regulated in the two docetaxel-resistant PC3 cell line variants, while expression of this gene was up-regulated in the DU145 resistant variant [345]. An overexpression of LAMC2 has previously been associated with increased cell migration in prostate cancer [346]. It is feasible to suggest that the opposing invasion and motile effects found in the cell line variants of our study

may be partially due to differential deregulation of genes associated with motility, such as LAMC2, as chemoresistance develops.

Previous studies using colorectal cancer cells (HT29), breast cancer (T47D) cells and colon cancer (H630) cells, in accordance with our own, have found that acquired chemo-resistance can reduce the rate cell proliferation [347, 348]. Reduced cell proliferation due to the presence of chromosomal instability, which is associated with multi-drug-resistance, has recently been demonstrated in colorectal cancer cells [349]. Thus the increased ability of docetaxel-resistant variants to resist cell death under *anoikis* conditions cannot be attributed to the rate of proliferation. The association between increased clonogenic survival and chemo-resistance, observed in both DU145RD and 22Rv1RD, is consistent with several other studies [347, 350, 351]. The disparate colony formation of PC3RD cells further indicates the complex nature of docetaxel-resistance, suggesting that the pathway of docetaxel-resistance in this cell line may not be associated with, or rely upon, altering colony formation.

Several characteristics, including cross-resistance to doxorubicin, proliferation and *anoikis* that were assessed with the three docetaxel-resistant cell lines were common to all. However it must be considered that some characteristics (such as migration, invasion and colony formation) differed. As this cannot be associated with already known difference between cell lines (primary vs. metastasis and androgen-resistant vs. –sensitive), it further emphasizes the need for such studies and the inclusion of larger panels of cell line models, which may better reflect other patient-to-patient diversities and so increase our understanding of the complexity of docetaxel-resistance in prostate cancer.

The emerging evidence that cells may communicate with neighbouring "or secondary cells" through the secretion of micro- or nano-sized vesicles (known as exosomes) carrying cellular information has recently highlighted the importance of these entities [352]. We, therefore, investigated the potential of exosomes to be expelled and transfer phenotypic changes, associated with docetaxel-resistance, to secondary cells. For the exosome studies in this Chapter, we chose to use DU145 and 22Rv1 cell line variants as the yields of exosomes from these cell lines were generally higher and more consistent between isolations than the PC3 cell line variant (See Chapter 5 Section 5.3.2). The quantities of exosomes chosen for assays were based on several conditions, including the

yields of exosomes from our isolations, any optimised procedures deemed successful in out laboratory and previous reports from other studies. For example, 15μg per insert from cell derived exosomes was used for invasion assays, a similar study within our lab group using this same quantity from triple negative breast cancer cells was found to increase invasion of secondary cells [218]. Wound healing assays have previously been shown to be altered in the presence of 1μg of cell-derived exosomes [242], while this quantity did not demonstrate any substantial differences on an initial trial, 5μg was therefore used, although this did not demonstrate any differences either. For proliferation and toxicity assays, 20μg per well from cell-derived exosomes were used which is in keeping with that used by Ciravolo *et al*, for their studies involving trastuzumab [240]. For serum-derived exosomes, the yield of exosomes was more concentrated using exoquick and so it was possible to use a higher amount of exosomes for assays. In all cases however, equal quantities of exosomes between test and control conditions was used for assays (i.e. exosomes derived from parent *versus* –resistant cell line variants; or exosoms derived from sera of controls *versus* patients; or sera from pre-treated patients *versus* post-treated patients).

No substantial differences in the motility, invasion or proliferation of DU145 and 22Rv1 cells were observed in the presence of DU145- or DU145RD-derived exosomes. Limited studies, to date, have demonstrated that exosomes expressing amphiregulin [243] and HSP90α [242] can increase cancer cell motility and migration. However, this does not appear to be the case with the prostate cancer cell-derived exosomes assessed here.

Interestingly we found induced docetaxel-resistance with DU145 cells in the presence of DU145RD exosomes (approx. 22%), compared to when these cells were exposed to their own exosomes. This suggests that DU145RD exosomes are, in fact, transferring resistance to docetaxel. Furthermore, a similar pattern was found when DU145- and DU145RD-derived exosomes were added to 22Rv1 and LNCap cells. Specifically, a significant increase in docetaxel-resistance (approx. 15% for 22Rv1; 16% for LNCap), independent of proliferation influences, resulted. This, for the first time suggests that exosomes may be a means of communicating docetaxel-resistance between cells. To confirm that the observed effects of DU145RD-derived exosomes are not limited to this cell line variant, we performed a similar investigation with 22Rv1 and 22Rv1RD exosomes. In keeping with the findings from our initial DU145RD exosomes assays, we

observed a similar trend of conferred docetaxel-resistance (*i.e.* an increase of approx. 11-12%) to both DU145 and LNCap cells in the presence of 22Rv1RD exosomes.

MDR-1/P-gp is expressed by both our DU145RD and 22Rv1RD cells but is undetectable in the parent cells, implicating it as involved in the acquired docetaxel-resistance (this observation is somewhat in keeping with the clinical situation where the majority of prostate cancers are MDR-1/P-gp-positive [353]). Importantly, we found that the expression pattern in the corresponding exosomes reflected that of the cells from which they were derived, further supporting the potential of resistance transfer and our suggestion that MDR1/P-gp could potentially be, at least partially, involved in the newly-acquired-resistance conferred by the exosomes. However, the difference in MDR-1/P-gp levels between exosomes from docetaxel-resistant variants compared to their parental cells does not necessarily imply a causal role for MDR1-/P-gp in the drug-resistance observed.

To further investigate the potential of exosomes in a clinical setting, as a pilot study we isolated exosomes from docetaxel-naïve prostate cancer patients and age-matched healthy controls. We investigated effects of these exosomes on cancer cell invasion and proliferation. The increased proliferation and invasion of cells in the presence of exosomes from cancer patients suggests a causative role for these exosomes. While this is a small pilot study, taken together with our cell line-derived exosome studies, it further supports the hypothesis that exosomes may have a role in prostate cancer cell communication.

In the context of docetaxel-resistance, we subsequently investigated the relevance of exosomes derived from relevant patients. Specifically this pilot study (n=8 patients) included matched serum exosomes obtained before and during the course of docetaxel treatment. Here we assessed the response of DU145 and 22Rv1 cells to their IC_{50} concentrations of docetaxel (as shown in Table 4.1 *i.e.* 1.7nM for DU145 cells; 4nM for 22Rv1 cells) in the presence of these exosomes populations. The observed docetaxel-resistance conferred to both cell lines by exosomes isolated from pre-cycle 7 sera (n=2 patients) correlated with the patients' increase in PSA levels. The exosomes from the remaining 6 patients seemed to confer increased sensitivity to both DU145 and 22Rv1 cells, correlating with the patients (n=6) decreased levels of PSA over their course of treatment.

A possible explanation for the manner whereby exosomes are affecting the phenotype of the "target" cells is that they are transferring mRNAs, miRNAs and/or proteins from the acquired-resistance cells that are causal molecules in changing the cellular phenotype of the recipient secondary cells. This is in keeping with accumulating evidence that exosomes play an important role in cell-to-cell communication. For example, in 2007 Valadi et al. demonstrated that mRNAs carried via exosomes from mast cells are translated into protein on their transfer to target cells [214]. The successful uptake of exosomes by secondary cells was also demonstrated by Skog et al. [219] when fluorescently-labelled glioblastoma exosomes were incubated with endothelial cells. Many more recent examples of these observations have been reported and a recent opinion by Mittelbrunn and Sanchez-Madrid [354] further describes how this transfer of genetic information may occur, with the effects of exosomes on secondary cells potentially contributing to carcinogenesis and tumour growth; moulding the tumour microenvironment; promoting angiogenesis; and modulating immune response [355, 356]. Specifically in relation to modulating response to anti-cancer therapy, HER2-overexpressing exosomes from donor cells have been shown to decrease sensitivity of recipient cells to trastuzumab [240]. So while we cannot speculate, at this point, as to the particular molecules that may be carried *via* exosomes from our resistant cells to induce phenotypic changes in target cells (other than to suggest that the transfer of MDR-1/P-gp protein may, in part, be a contributing factor), it is reasonable to suggest that it may be a single -or combination of- mRNAs, miRNAs and/or proteins that have a causal role in docetaxel-resistance. Thus, now that functional relevance has been associated with these exosomes in conferring a level of docetaxel-resistance, profiling the content of these exosomes is warranted to better understand the precise molecule(s) and mechanism(s) involved. Chapter 5 discusses subsequent miRNA profiling performed on the docetaxel-resistant cell line variants used in this chapter and their corresponding exosomes

4.5 CONCLUSIONS

In conclusion, this study corroborates that docetaxel-resistance in prostate cancer is highly-complex and may be associated with varied cellular effects in terms of resistance to other chemotherapeutic drugs, motility, invasion, and anchorage-independent growth. It is clear, however, that given the multi-faceted nature of docetaxel-resistance that not one, but several factors are likely to mediate their effects in prostate cancer. Here we show, for the first time, that cellular communication *via* exosomes may, in part, result in conferred docetaxel-resistance to secondary cells. Future studies on larger cohorts of serum specimens, from both docetaxel-naïve patients and also from patients following docetaxel treatment, are warranted –assessing both the effects of and the molecular contents of the exosomes– to expand our understanding of exosomes and their relevance to cell communication and docetaxel-resistance in prostate cancer.

CHAPTER 5

miR-34a is an intracellular and exosomal predictive biomarker for response to docetaxel with clinical relevance to prostate cancer progression

5 ABSTRACT

Background: Despite initial success of docetaxel in the treatment of castration-resistant prostate cancer, most patients unfortunately relapse due to the emergence of docetaxel-resistance. miRNAs have potential as diagnostic, prognostic and predictive biomarkers, as well as replacement therapies. Here we investigated the intracellular and exosomal miRNA levels in a panel of cell line models of docetaxel-resistance (described in Chapter 4), as a means of identifying extracellular miRNAs regulating docetaxel-resistance, which are representative of their cells of origin.

Methods: We performed global miRNA profiling using Taqman low density arrays on the cells and corresponding exosomes from three cell line models of docetaxel-resistance (i.e. DU145/DU145RD, 22Rv1/22Rv1RD and PC3/PC3RD). We analysed the data to identify miRNAs that were commonly de-regulated in both the cells and exosomes. To evaluate the clinical relevance of our selected miRNAs, we assessed the expression of these miRNAs in 4 clinical cohorts representing tissues and urine from prostate cancer *versus* benign patients, as well as prostate tissues from patients with biochemical recurrence *versus* non-recurrence and also from patients presenting with metastatic disease *versus* primary disease and benign tissue. Immunoblotting was used to assess miR-34a's target proteins. Transfection of miR-34a mimics and inhibitors was used to manipulate the expression of miR-34a in docetaxel-resistant or –sensitive cells to enable its direct effect on response to docetaxel to be determined.

Results: Our findings demonstrate a correlation between miRNAs detected in the exosomes and their corresponding cells of origin. Of the miRNAs chosen for further validation and clinical assessment (miR-598, miR-34a, miR-146a and miR-148a), decreased miR-34a expression showed substantial clinical relevance and so was chosen for further functional assessment. Our knockdown and overexpression studies confirmed that miR-34a directly regulates BCL-2. Introducing miR-34a into docetaxel-resistant cells also indicated that this miRNA can, in part, increase cellular sensitivity to docetaxel.

Conclusion: This study confirms that exosomes derived from the media conditioned by a panel of docetaxel-sensitive and –resistant prostate cancer cell lines do represent the

cells of origin. Furthermore, our functional assessment of miR-34a supports its role as a predictive biomarker for docetaxel-resistance in prostate cancer.

5.1 INTRODUCTION

As detailed in Chapter 1, Section 1.1.2, increased release of PSA into circulation has been associated with the onset of prostate cancer. Thus PSA's detection levels in serum has become a universal tool in screening for the disease; particularly in combination with digital rectal examination (DRE) [12]. Despite this finding, the use of PSA as a prostate cancer biomarker has faced some limitations [13]. This highlights the need to identify more biomarkers, particularly those that could be asessed in a minimally-invasive manner. This could perhaps support PSA diagnostics and ultimately aid in earlier detection of prostate cancer together with monitoring disease progression and potentially predict treatment response.

Castration-resistant prostate cancer (CRPC) refers to prostate cancer that has progressed despite castrate serum levels of testosterone [36] and is associated with significant morbidity and mortality [37]. While docetaxel, which is currently the first-line treatment for patients with CRPC, offers some improvement in overall survival in comparison to other anti-cancer agents; unfortunately relapse is almost inevitable, leaving patients with a poor prognosis. As described in Chapter 1, Section 1.3.3, the failure of taxanes to increase survival beyond the median of 2.5 months may be caused, at least in part, by multidrug-resistance (MDR) mechanisms protecting cancer cells against cytotoxic drugs. MDR is frequently attributed with the overexpression of one or several transporter proteins, located on the cell membrane, that act as drug efflux pumps [76]. We have previously shown, in Chapter 4, that MDR-1/P-gp is over-expressed in some docetaxel-resistant prostate cancer cell lines [90, 237] although we have also reported mechanisms independent of MDR-1/P-gp expression to also contribute to docetaxel-resistance [90].

Growing evidence supports the role of microRNAs (miRNAs) as potential biomarkers for a range of diseases including cancer. Their post-translational regulation of mRNA transcription has implicated these short non-coding RNAs (approximately 18–25 nucleotides long) in a range of essential biological activities [249]. Reports on the stability of miRNAs in biological fluids have suggested their latent use as minimally-invasive biomarkers [203, 249]. These miRNAs may be encapsulated into nano-sized vesicles (known as exosomes) and secreted from cells into circulation [214]. Recently studies have suggested that exosomal miRNA profiles can reflect their cells of origin [216, 238].

Using acquired-resistant cell line models developed during the course of his project (see Chapter 4, Section 4.2.2), representing the clinical problem of docetaxel-resistance in prostate cancer, we aimed to investigate the intracellular and extracellular (cell-derived exosomes) miRNA profile as a means of identifying potential clinically relevant biomarkers for docetaxel response in prostate cancer. Our study reports a direct correlation between the detected miRNAs in the cells and corresponding exosomes for all cell lines assessed. We demonstrate that reduced miR-34a expression has substantial clinical relevance. Furthermore, our functional studies indicate that miR-34a can directly regulate BCL-2 and may, in part, increase the sensitivity of cells to docetaxel.

5.2 METHODS

5.1.1 Cell lines and cell culture

Prostate cancer cell lines, 22Rv1 (androgen-sensitive; from a primary human tumour), DU145 (androgen-insensitive; from a brain metastasis) and PC3 (androgen-sensitive; from bone metastasis) were purchased from the American Type Culture Collection (ATCC). All cells were maintained in RPMI-1640 (Sigma-Aldrich, R0883) with 10% FCS (PAA Cat. #: A15-151) and 1% L-glutamine (Sigma-Aldrich, Cat. #: G7513). at 37°C/5% CO_2. Docetaxel-resistant cell line variants, 22Rv1RD, DU145RD, and PC3RD were generated as previously described [90, 237] and in further detail in Chapter 4, Section 4.2.2. Age-matched parent cells (22Rv1, DU145 and PC3) were maintained in culture, unexposed to docetaxel, as controls for all experiments. All experiments on acquired-resistant cells and corresponding aged controls were performed within 10 passages in culture and experiments were performed on cells that received no drug for a minimum of one week. Passage numbers used were approximately the following: 22Rv1/22Rv1RD (p40-50); DU145/DU145RD (p46-56); PC3 (p112-122); PC3RD (p108-118). Cells were routinely tested for mycoplasma contamination using the PCR Mycoplasma Test Kit 1/RT Variant B (Promocell, Cat. #: PK-CA91-3025B) and were found to be negative.

5.1.2 Exosome isolation from conditioned medium

For exosomes isolation, all cells were grown in RPMI medium supplemented with 5% of exosomes-depleted fetal calf serum (dFCS) (PAA, Cat. #: A15-151), 1% L-glutamine (Sigma-Aldrich, Cat. #G7513) and 1% penicillin/streptomycin (Invitrogen, Cat. #: 15070-063). FCS was depleted of exosomes by ultracentrifugation for 16hrs. Cells were seeded at a density of $1x10^5$ cells/ flask (for DU145 and PC3 variants) and $5x10^5$cells/flask (for 22Rv1 variants). After allowing cells to attach over-night, medium was replaced and the cells were cultured for 3 (DU145 cell lines) or 5 (22Rv1, PC3 cell lines) days in the fresh dFCS medium; to approximately 80% confluency. Exosomes were subsequently isolated from conditioned medium (CM) using methods that are detailed in Chapter 4, Section 4.2.9. The resulting exosomes pellets were resuspended in approximately 200µl PBS (Sigma-Aldrich, Cat. #:D8537) and stored at -80°C for subsequent quantification (using BioRad protein assay Dye Reagent, Cat. #:500-0006, as described in Section 2.2.10)

and for RNA analysis. The corresponding cells from which the exosomes were isolated were harvested for subsequent RNA analysis. Cells were washed twice with PBS and pelleted for RNA analysis.

5.1.3 Transmission Electron Microscopy

Exosomes were isolated from conditioned media as described above, and analysed by electron microscopy as detailed in Chapter 4, Section 4.2.10 and similar to a protocol previously described [272].

5.1.4 Immunoblotting

Total cellular proteins were extracted from whole cells and exosomes using cell extraction buffer (Invitrogen Cat. #: FNN0011) as described in Section 2.2.10. Protein quantification of cells and exosomes was performed using BioRad protein assay Dye Reagent (BioRad, Cat. #:500-0006) as described in Section 2.2.10. Protein (50μg for cellular protein samples and 20μg for exosomes from CM samples) were resolved on PAGEr Gold precast gels for protein electrophoresis; 7.5% (Lonza, Cat. #: 59513) for exosome markers (TSG101[336, 337] and PDC6I/Alix [338]) and 12% (Lonza, Cat. #: 59515) for BCL-2. Immunoblotting involved using the following primary antibodies and dilutions: PDC6I/Alix (Abcam, Cat. #: Ab76608; 1:1000 dilution) and TSG101 Abcam, Cat. #:4A10; 1:1000 dilution), BCL-2 (Calbiochem, Cat. #: OP60; 1:500 dilution), β-actin (Sigma-Aldrich, Cat. #: A5316; 1:1000 dilution). Membranes were then incubated in primary antibodies over night at 4°C. Membranes were incubated with appropriate horseradish peroxidase-conjugated secondary antibodies -Anti-mouse (Cell Signalling, Cat. #: 7074; dilution); or -Anti-rabbit (Cell Signalling, Cat. #: 7076; 1:1000 dilution) for 1hr at room temperature and proteins were visualized by chemiluminescence (Themofisher: Cat. #: 34080). Detection was performed with a Chemidoc exposure system (Bio-Rad Laboratories).

5.1.5 RNA isolation of cells and exosomes

Total RNA was isolated from cells and corresponding exosomes of all three docetaxel-resistant cell line variants and respective aged-parent controls using the miRNeasy mini kit (Qiagen, Cat. #: 217004) according to manufacturer's instructions.

Isolation from exosome suspensions was based on a slightly optimised Exiqon protocol for RNA isolation from biological fluids using the miRNeasy kit, specifically concerning the volume of QIAzol and chloroform used and the addition of an extra wash step with RPE buffer. In brief, cell pellets and exosomes (in 200µl PBS) were disrupted using QIAzol (700µl for cells; 750µl for exosomes) followed by vortexing for 1min. To facilitate homogenisation of cells, cell/QIAzol suspensions were passed through a needle and syringe several times. Homogenates were incubated at room temperature for 5mins, followed by the addition of chloroform (Sigma-Aldrich, Cat. #: C2432) (140µl for cell samples; 200µl for exosome samples). Tubes were shaken vigorously for 15 seconds and then allowed to stand at room temperature for 2-3mins. Samples were then centrifuged at 12,000g at 4°C for 15mins. The upper aqueous phase was transferred into a new collection tube followed by the addition of 1.5 volumes of 100% ethanol (Sigma-Aldrich, Cat. #: E7418) which was mixed thoroughly by pipetting up and down several times. 700µl of the mixture was transferred into an RNeasy spin column and centrifuged at 13,000g at room temperature for 30 seconds. This step was repeated with the remainder of the sample. 700µl of buffer RWT (provided in kit) was added to the spin column and centrifuged at 13,000g for 1min. 500µl of buffer RPE (provided in kit) was then added to the spin column and centrifuged at 13,000g for 1min; this step was repeated 3 times. After each centrifugation step to this point, the flow- through was discarded. The spin column was transferred to a new collection tube and centrifuged at 13,000g for 2mins. The columns were left open for 1min and then placed into a new RNAse-free 1.5ml Eppendorf tube (Sigma-Aldrich, Cat. #:Z606340). DNase/RNase free water (Ambion, Cat. #: AM9916) was added to the spin columns (50µl for cell samples and 20µl exosome samples), incubated for 1min at room temperature and the centrifuged at 13,000g for 1min. Yield and quality of RNA was assessed on the Nanodrop ND-1000 spectrophotometer.

5.1.6 Global miRNA profiling of cells and exosomes

The method for global profiling of miRNAs using the ABI Taqman miRNA Low density arrays (TLDA, Applied Biosystems) is previously detailed in Chapter 2, Section 2.2.4, however some changes to the method are outlined in this section. TLDA (Version 3.0, Cat. #: 4444913) panels A and B for the assessment of a total of 754 miRNA assays were used for the miRNA profiling. cDNA was prepared from 3µl of cellular and exosomal RNA following TLDA RT protocol as described in Chapter 2, Section 2.2.4. RNA for the

RT step was diluted to a constant amount for the cells and exosomes from all cell line variants – (85ng for 22Rv1 and DU145 cell line variants, and 50ng for PC3 cell line variants - due to lower RNA yields from the exosomes of the latter). cDNA (2.5µl) was pre-amplified and then quantified using Applied Biosystems ViiA7 Real-Time PCR system. Global miRNA profiling data was normalised to the mean of three miRNAs (miR-618, miR-659 and miR-454) that were found not to be significantly altered between our resistant cell line variants and their respective parent controls for cells and exosomes and so deemed suitable as an endogenous control. A similar strategy of normalising TLDA data to several stable miRNAs has been recently reported [357]. Normalisation is outlined below:

$\Delta C_T = C_T$ cell line variant – mean C_T of miR-618, miR-659 and miR-454

$\Delta\Delta C_T = C_T$ Resistant variant – C_T Sensitive parent

Where, C_T = Cycle threshold at which the miRNA was detected

Fold change = $2^{(-\Delta\Delta CT)}$

5.1.7 Validation of selected miRNAs by qPCR

miRNAs selected for further validation were based on the following criteria: miRNAs significantly ($p<0.05$) altered by ≥ 1.5 fold in both the cells and exosomes of at least two docetaxel-resistant cell line variants compared to their aged-matched drug-sensitive parent cell lines. In Chapter 2, a cut-off of 1.2 fold change was selected for the miRNAs chosen for validation, however, due to the low number of miRNAs that validated successfully, for this study a 1.5 fold change cut-off was selected to improve validation of selected miRNAs. cDNA was prepared from 10ng cell-derived and exosome-derived total RNA, as we described previously [358] and further detailed in Chapter 2, Section 2.2.5. Taqman miRNA assays (Applied Biosystems, Cat. #: 4427975) used for miRNA validation: miR-598 (Assay ID #: 001988), miR-148a (Assay ID #: 000470), miR-34a (Assay ID #: 000426) and miR-146a (Assay ID #: 000468) were quantified using the cycle threshold (C_T) adjusting to the levels of miR-618 (Assay ID #: 001593) as an endogenous control as it showed no significant changes among cells and exosomes of parent and resistant cell line variants and so deemed a suitable for data normalisation.

5.1.8 Assessment of miRNA expression in clinical specimens

As a means of selecting the most appropriate miRNA to further evaluate for functional relevance, we assessed the clinical impact of the four validated miRNAs using publically available datasets on the gene expression omnibus.

Of the datasets available, the expression of these miRNAs were initially assessed in localised prostate cancer tissue (n=21) *versus* matched benign tissue (n=21) (GSE36802; http://www.ncbi.nlm.nih.gov/geo/query/acc.cgi?acc=GSE36802). To assess the extracellular relevance of these miRNAs, their expression was assessed in urine samples from prostate cancer patients (n=9) *versus* patients with benign prostatic hyperplasia (n=8) (GSE39314; http://www.ncbi.nlm.nih.gov/geo/query/acc.cgi?acc=GSE39314).

To establish the relevance of miRNAs with more aggressive disease, where information was available, tissues from patients with known biochemical recurrence following radical prostatectomy (n=30) was compared to those with non-recurrence (n=53) (GSE26247; http://www.ncbi.nlm.nih.gov/geo/query/acc.cgi?acc=GSE26247). Furthermore, the association of our selected miRNAs was assessed in a cohort of patients with known metastases (n=14) compared to either primary disease (n=99) or normal adjacent tissue (n=28) (GSE21036; http://www.ncbi.nlm.nih.gov/geo/query/acc.cgi?acc=GSE21036). An online software tool, MIRUMIR [359] http://www.bioprofiling.de/GEO/MIRUMIR/mirumir.html was used to predict the association between miR-34a and overall survival from prostate cancer on the GSE21036 dataset.

5.1.9 miRNA inhibition/mimic manipulation in cells

As miR-34a was not significantly altered with docetaxel-resistance in the DU145 cell line variant, PC3 and 22Rv1 cell line variants were therefore used for subsequent studies. PC3 and 22Rv1 cells were transfected with miR-34a inhibitor (Applied Biosystems, Cat. #: 4464084, ID: MH11030) or miRNA inhibitor negative control (Applied Biosystems, Cat. #: 4464076). Similarly, PC3RD and 22Rv1RD cells were transfected with miR-34a mimic (Applied Biosystems, Cat. #: 4464066, ID MC11030) or miRNA mimic negative control (Applied Biosystems, Cat. #: 4464058). Transfections were performed using a final concentration of 30nM (inhibitor/mimic) and transfected using lipofectamine 2000 (Invitrogen, Cat. #: 11668-027) following manufacturer's instructions and further detailed

in Chapter 2, Section 2.2.7. Cells were seeded at a density of 2.5 $x10^4$cells/well (PC3 variants) and $5x10^4$cells/well (22Rv1 variants) in 24-well plates. For assessment of protein changes, transfected cell pellets were collected after 48hrs for subsequent immunoblotting (as detailed in Section 5.2.4).

5.1.10 Assessing effects of miR-34a – regulated cellular response to Docetaxel

Following transfection with the miR-34a inhibitor, miR-34a mimic or their relevant negative controls for 6hrs, 22Rv1 and 22Rv1RD cells were exposed to their approximate IC_{50} concentrations of docetaxel (Sigma-Aldrich, Cat. #: 01885) as previously determined [237] and indicated in Chapter 4, Section 4.3.1. Following 48hrs incubation with docetaxel, cell viability was assessed using acid phosphate analysis as described in Chapter 2, Section 2.2.9.

5.1.11 Statistical Analysis

Statistical analysis was performed on Excel. *P*-values were generated using Student's t-tests, with $p<0.05$ considered as statistically significant. Results are displayed as n=3± standard error of mean. GraphPad was used for graph generation. Linear regression analysis and the calculation of R^2 were performed on GraphPad and p-values were calculated based on deviation from zero. Hierarchical clustering was performed using DChip online software and based on advice from bioinformatician Dr. Jai Prakesh Metha. For clinical data obtained from publically available datasets on Gene Expression Omnibus (GEO) (http://www.ncbi.nlm.nih.gov/geo/) [262], miRNA expression levels and p-values between groups were determined using the GEO2R analysis function. For survival analysis of miR-34a, the MIRUMIR online software [359] uses the R statistical package to perform survival analyses and to draw Kaplan Meier plots. TargetScan 6.2 and Diana miRPath online softwares were used to assess the predicted targets for miR-34a.

5.3 RESULTS

5.1.12 Characterisation of isolated exosomes

Exosomes, isolated from the conditioned medium of all cell line variants, were assessed by transmission electron microscopy to identify the presence of vesicles of approximately 100nm in diameter, indicative of exosomes (Figure 5.1A). TSG101 and PDC6I/Alix proteins commonly associated with the formation of exosomes and thus considered to be important markers of successful isolation of exosomes were detected [335, 339] by immunoblotting of isolates from the conditioned medium of all cell line variants (Figure 5.1B).

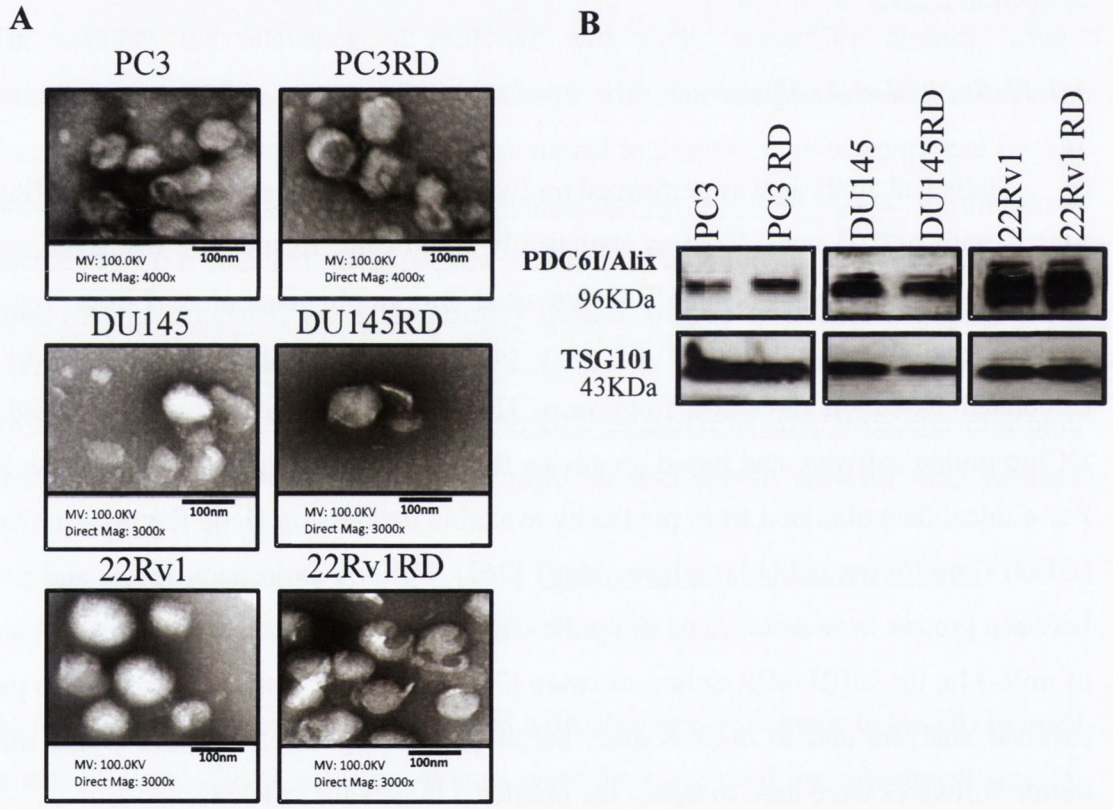

Figure 5.1: Confirmation of exosomes isolation from conditioned media isolates.

(A) Transmission Electron Microscopy was performed to investigate size and structure of exosomes;

(B) Immunoblotting was performed to assess the expression of common exosomes markers (TSG101 and PDC6I/Alix) in exosomes isolated from PC3, DU145 and 22Rv1 cell line variants.

5.1.13 Yield and quality of cellular and exosomal RNA

Following isolation and prior to performing miRNA profiling, the yield of exosomes was determined by quantifying the protein content of the exosomes using the BioRad protein assay as described in Chapter 2, Section 2.2.10. RNA was subsequently isolated from the exosomes and pellets of the corresponding cells of origin using the miRNeasy kit. The yield of exosomes isolated (represented by protein quantity), the RNA yield and RNA quality (measured by 260/280 reading on the Nanodrop ND-1000 spectrophotometer) from exosomes and corresponding cells are indicated in Tables 5.1-5.3.

Cell Samples	RNA (µg)	260/280	Exosome Samples	Quantity of exosomes [protein (µg)]	RNA (ng/µl)	260/280
PC3 R1	47.0	2.06	PC3 R1	37.5	0.25	1.74
PC3 R2	62.2	2.05	PC3 R2	101.1	0.46	1.95
PC3 R3	37.3	2.07	PC3 R3	84.8	0.41	1.92
PC3RD R1	32.4	2.01	PC3RD R1	27.8	0.21	1.75
PC3RD R2	58.9	2.06	PC3RD R2	62.1	0.31	1.73
PC3RD R3	40.2	2.07	PC3RD R3	77.6	0.18	1.72

Table 5.1: Exosomes quantities, RNA yields and quality as assessed by for cells and corresponding exosomes of the PC3 cell line variants.

Biological replicates are indicated by R1, R2 and R2. Yields of exosomes isolated, measured by protein is also indicated.

Cell Samples	RNA (µg)	260/280	Exosome Samples	Quantity of exosomes [protein (µg)]	RNA (ng/µl)	260/280
DU145 R1	57.8	2.08	DU145 R1	49.8	0.61	2.06
DU145 R2	52.9	2.08	DU145 R2	54.9	0.60	1.99
DU145 R3	119.0	1.8	DU145 R3	68.1	0.54	2.07
DU145RD R1	66.5	2.06	DU145RD R1	86.5	0.29	1.84
DU145RD R2	64.3	2.07	DU145RD R2	59.4	0.45	1.9
DU145RD R3	89.7	2.02	DU145RD R3	41.9	0.69	1.97

Table 5.2: Exosome quantitites, RNA yields and quality as assessed for cells and corresponding exosomes of the DU145 cell line variants.

Biological replicates are indicated by R1, R2 and R2. Yields of exosomes isolated, measured by protein is also indicated.

Cell Samples	RNA (µg)	260/280	Exosome Samples	Quantity of exosomes [protein (µg)]	RNA (ng/µl)	260/280
22Rv1 R1	124.0	1.87	22Rv1 R1	107.9	2.20	2.05
22Rv1 R2	121.1	1.84	22Rv1 R2	139.8	2.30	2.02
22Rv1 R3	66.7	2.07	22Rv1 R3	139.4	2.12	2.06
22Rv1RD R1	115.6	1.83	22Rv1RD R1	103.6	2.24	2.06
22Rv1RD R2	97.1	2	22Rv1RD R2	167.6	3.60	2.02
22Rv1RD R3	109.2	1.89	22Rv1RD R3	131.7	1.39	2

Table 5.3: RNA yields and quality as assessed for cells and corresponding exosomes of the 22Rv1 cell line variants.

Biological replicates are indicated by R1, R2 and R2. Yields of exosomes isolated, measured by protein is also indicated.

5.1.14 miRNA profiling of docetaxel-resistant cells and corresponding exosomes

Global miRNA profiling of cells and exosomes of all the docetaxel-resistant cell line variants (PC3RD, DU145RD and 22Rv1RD) and their respective age-matched parent controls (PC3, DU145 and 22Rv1) was performed for 754 miRNAs (see Section 5.2.6). All sets of samples were run in biological triplicate. Taking a cut-off point of 35-cycles threshold (C_T), miRNAs detected <35C_T were considered as 'present' where as those with values >35C_T were considered as 'undetected'. The mean distribution of miRNAs detected for all cell line variants is shown in Figure 5.2.

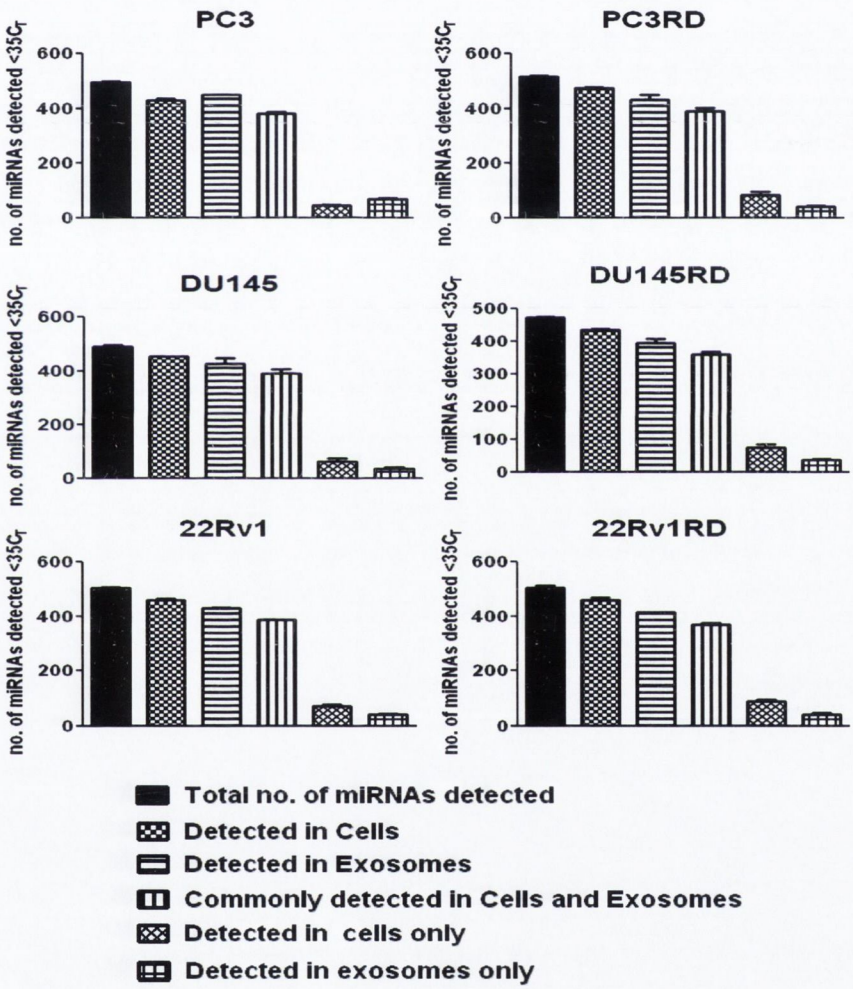

Figure 5.2: Distribution of miRNA expression for cells and exosomes from all cell line variants.
The presence of a miRNA was taken at a set cut-off of 35C_T, thus miRNAs detected below 35C_T were considered as 'present' where as miRNAs detected beyond 35C_T were classified as 'undetected'. The relevant mean distribution of miRNAs detected in cells and exosomes for each cell line variant is displayed. Results represent n=3±SEM.

Setting the combined number of all miRNAs detected in cells and exosomes as an arbitrary one hundred per cent, the corresponding percentages of miRNAs detected in each population of cells and exosomes are shown in Table 5.4. The average percentage of miRNAs detected in cells from all cell line variants (with the exception of PC3) was significantly greater ($p<0.01$) compared to their corresponding exosomes (Table 5.4). Interestingly, on average almost 77% of miRNAs detected in any cell line variant was found in the corresponding exosomes. Furthermore, the average percentage of miRNAs solely detected in cells was significantly ($p<0.01$) greater than that of exosomes only (Table 5.4).

Cell line	Detected in Cells	Detected in Exosomes	Detected in Cells & Exosomes	Detected in Cells only	Detected in Exo only
PC3	86.2±1.1	90.9±0.5	77.0±1.0	9.12±0.5	13.8±1.1
PC3RD	91.9±0.7	83.9±2.6	75.8±2.0	16.1±2.6	8.1±0.7
DU145	92.6±1.2	85.4±2.9	79.8±1.7	12.8±2.9	7.4±1.2
DU145RD	92.8±0.8	85.9±1.9	76.1±1.3	16.1±1.9	7.8±0.8
22Rv1	91.4±0.6	85.5±1.0	76.9±0.5	14.5±1.0	8.6±0.6
22Rv1RD	91.3±0.9	82.3±1.4	73.6±1.9	17.7±1.4	8.7±0.9
Average	**90.2**	**86.4**	**76.5**	**13.6**	**9.8**

Table 5.4: Percentage and distribution of microRNAs detected <35C_T in all cell line variants.
Taking a cut-off point of 35-cycle thresholds (C_T), miRNAs detected <35C_T were considered as 'present' where as those with values >35C_T were considered as 'undetected'. Setting the total number of miRNAs detected as an arbitrary one hundred per cent, the corresponding percentages of miRNAs detected in cells and exosomes are shown. Results represent mean percentages for n=3 biological repeats.

Linear regression analysis on miRNAs detected <35C_T in cells and exosomes indicated a significant ($p<0.0001$) strong correlation for all cell line variants between cells and corresponding exosomes (Figure 5.3). Specifically, PC3 ($R^2=0.8316$), PC3RD ($R^2=0.8144$), DU145 ($R^2=0.8140$), DU145RD ($R^2=0.7793$), 22Rv1 ($R^2=0.7325$), 22Rv1RD ($R^2=0.6897$). This suggests that exosomes strongly represent their cells of origin.

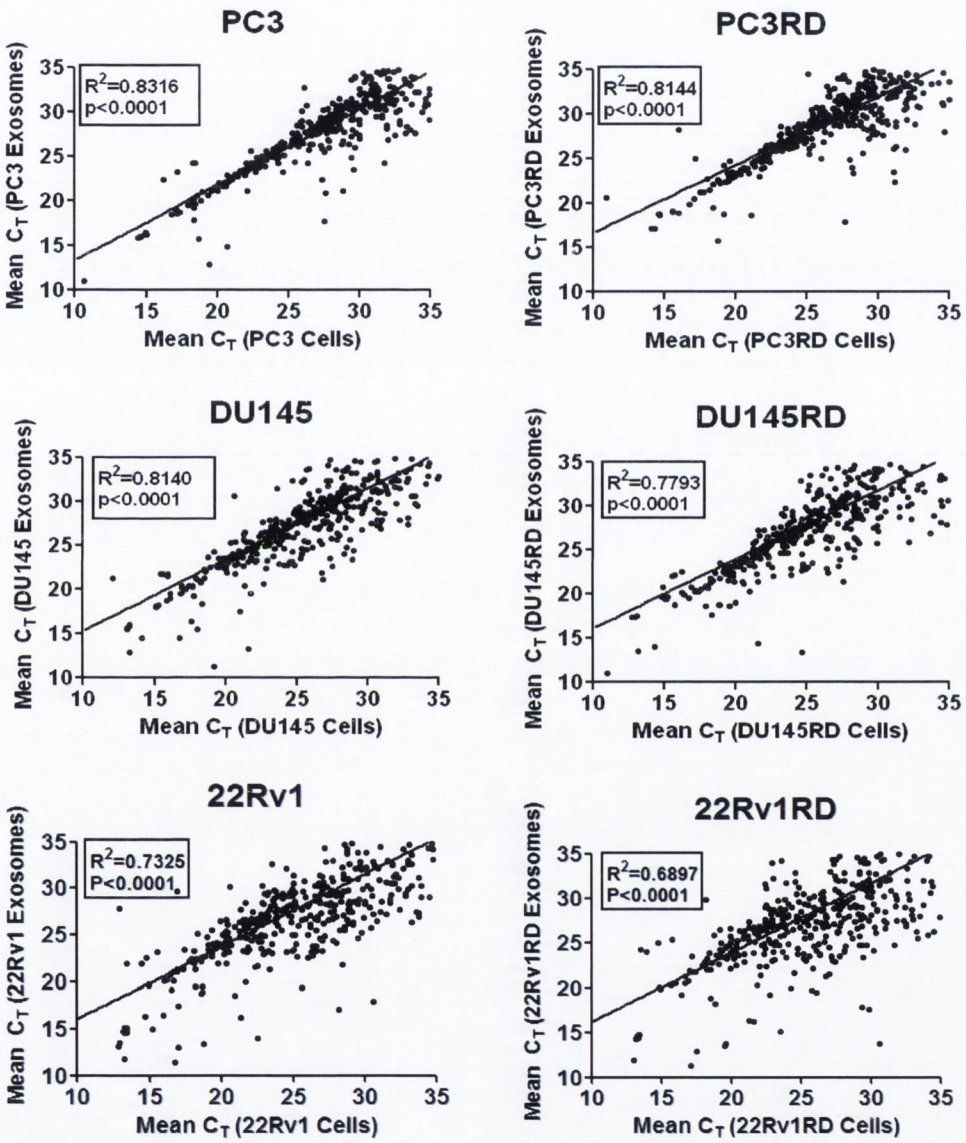

Figure 5.3: Linear regression analysis.

Linear regression analysis was performed to demonstrate the correlation between the mean C_T values of miRNAs detected for cells and corresponding exosomes for each cell line variant. Results represent mean C_T values from n=3 biological repeats.

Hierarchical clustering using normalised fold changes (using $2^{(-\Delta\Delta CT)}$) method as described in Section 5.2.6) for all biological replicates (denoted by R1, R2, R3) of the 3 resistant cell line variants compared to respective parent cell lines (PC3RD, 22Rv1RD, DU145RD) was performed. Clustering of miRNA fold changes for each cell line with its corresponding exosomes was observed for all three resistant variants (PC3RD, 22Rv1RD, DU145RD) (Figure 5.4).

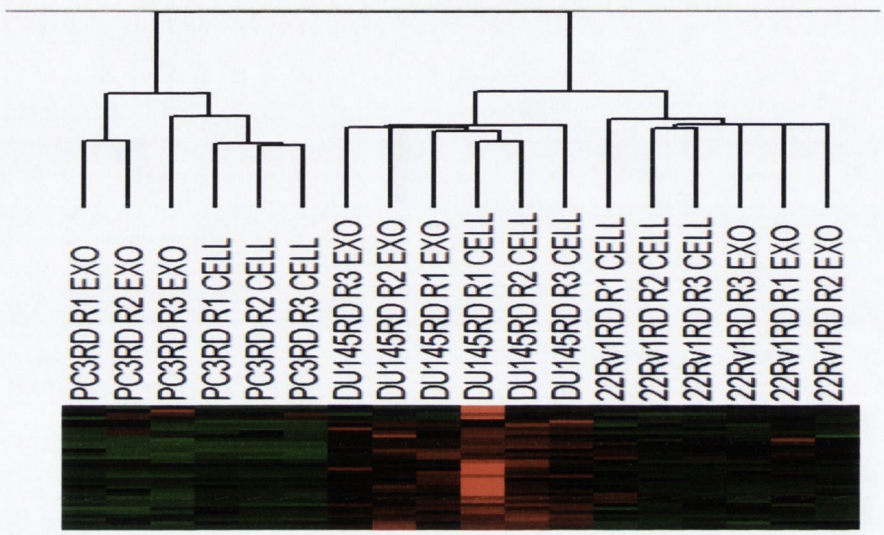

Figure 5.4: Hierachical cluster analysis

Hierarchical clustering of miRNA expression fold changes for docetaxel-resistant cell lines (PC3RD, DU145RD and 22Rv1RD) compared to their respective age-parent controls (R1, R2 and R3 denotes each biological replicate performed for cells and exosomes (EXO))

5.1.15 Selection of miRNAs for validation

Following normalisation of the global miRNA profiling data, analysis of deregulated miRNAs between cell line variants – within cells and exosomes -were performed using Venn diagrams to identify key miRNAs that may play an important role in docetaxel-resistance. Taking a cut-off point of 1.5 fold up- or down-regulated expression in resistant cell line variants compared to their parent cell lines, the common miRNAs (from the 3 biological replicates) that were identified in cells and exosomes were selected for further assessment. Furthermore, we identified miRNAs common in cells and exosomes as well as between all cell lines. Compared to their respective age-parent control cells and exosomes, 44 miRNAs were determined to have commonly reduced levels in cells and exosomes in PC3RD. Similarly, 12 miRNAs for DU145RD and 12 miRNAs for 22Rv1RD were also reduced (Figure 5.5).

Overall, one miRNA was commonly decreased in cells and exosomes of all three cell line variants and 6 other miRNAs were identified as decreased in at least two of the three docetaxel-resistant cell line variants compared to age-parent control cells and exosomes (Figure 5.5).

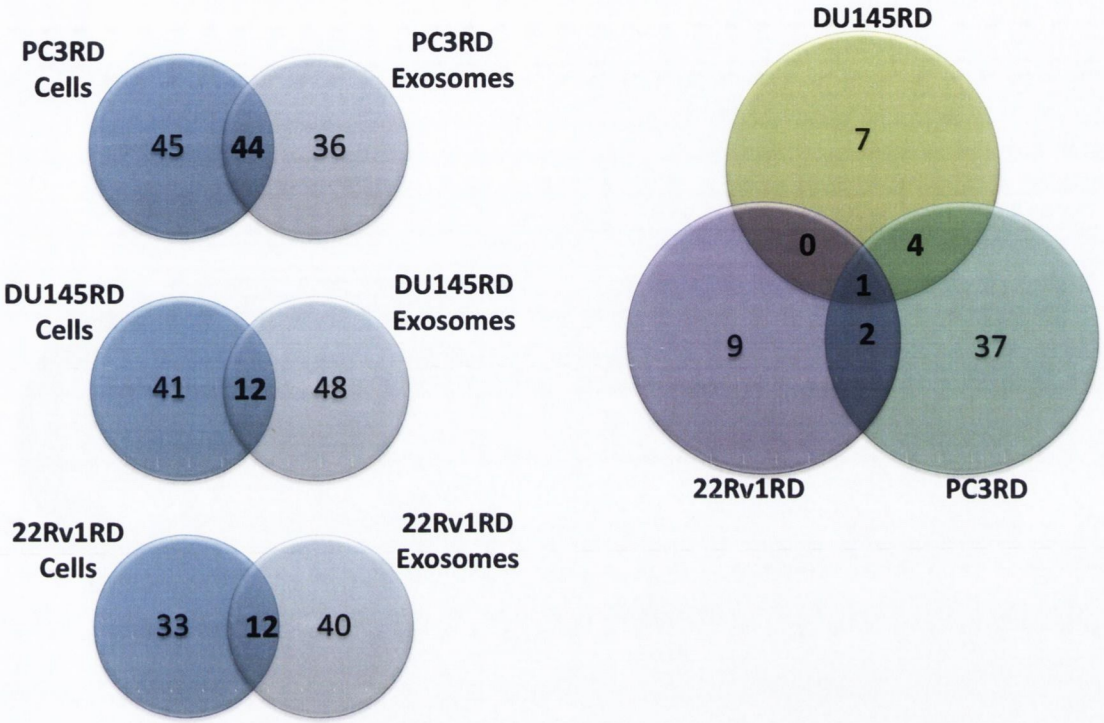

Figure 5.5: Identification of miRNAs decreased with docetaxel-resistance.

Venn diagrams were used to assess the miRNAs that had decreased levels greater than 1.5 fold in the cells and corresponding exosomes of docetaxel-resistant cell lines (PC3RD, DU145RD and 22Rv1RD) compared to their respective age-matched parent controls. Results represent mean of n=3 biological repeats.

While a total of 84, 18 and 5 miRNAs were commonly increased in cells and exosomes of PC3RD, DU145RD and 22Rv1RD, respectively, there were no miRNAs identified as commonly increased among the three cell line variants compared to their age-parent control cells and exosomes (Figure 5.6).

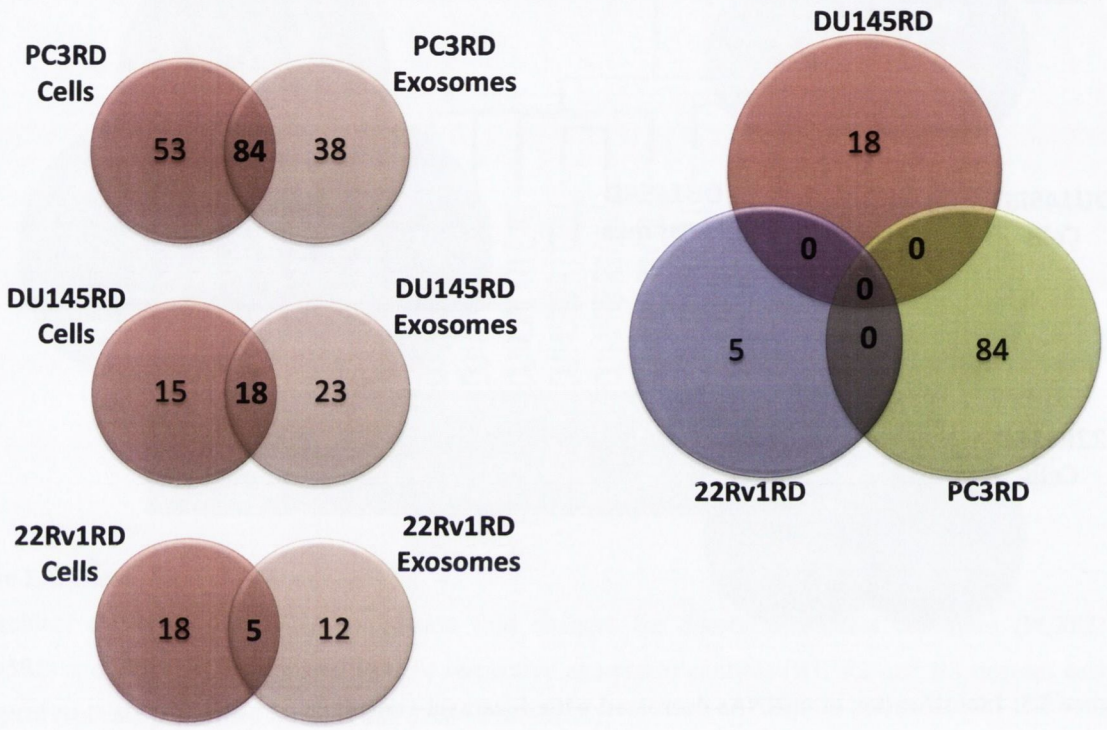

Figure 5.6: Identification of miRNAs increased with docetaxel-resistance.

Venn diagrams were used to assess the miRNAs that had increased levels greater than 1.5 fold in the cells and corresponding exosomes of docetaxel-resistant cell lines (PC3RD, DU145RD and 22Rv1RD) compared to their respective age-matched parent controls. Results represent mean of n=3 biological repeats.

The expression of the 7 most substantially decreased miRNAs in docetaxel-resistant cell line variants comparted to their sensitive-parent cell lines, as identified from the global profiling, is shown in Figure 5.7.

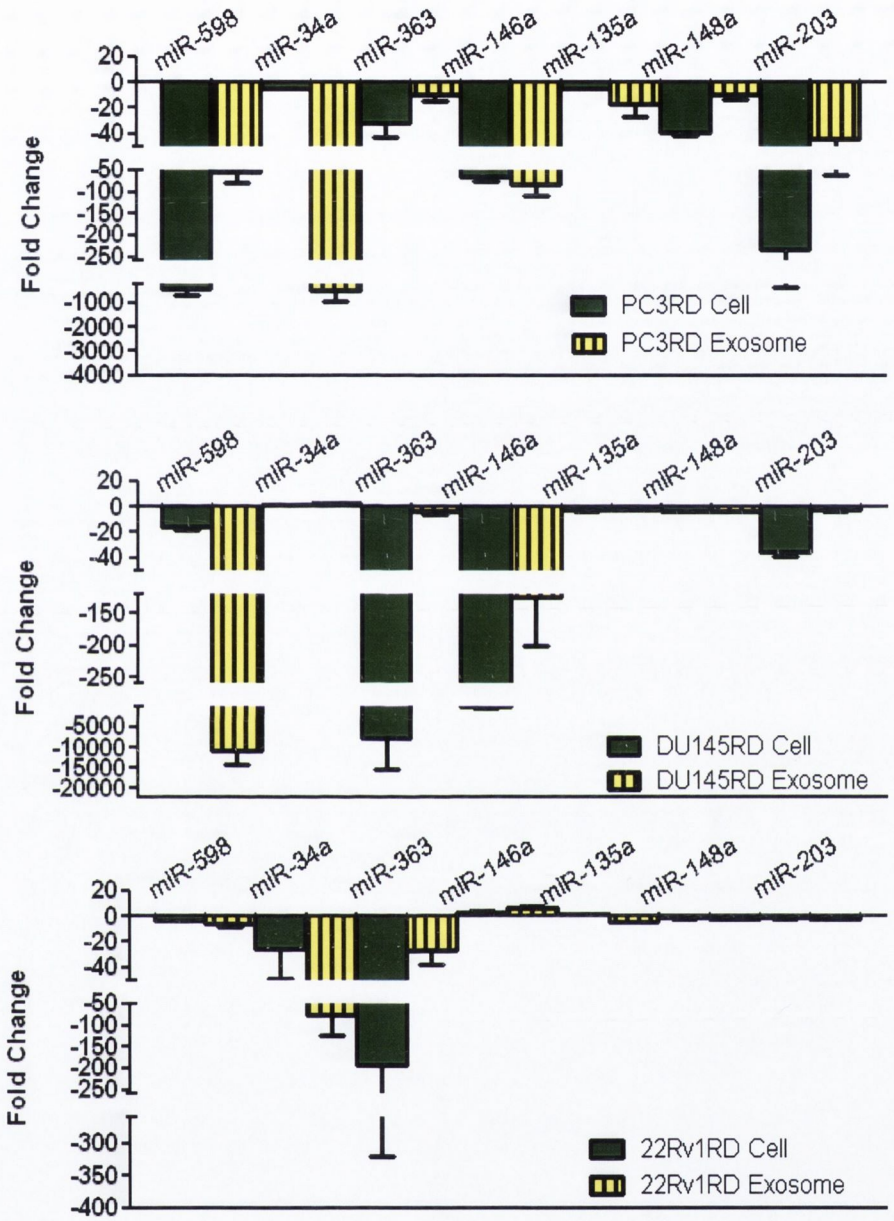

Figure 5.7: Top miRNAs decreased with docetaxel-resistance.

The expression of the 7 most substantially down-regulated miRNAs, as identified from the global miRNA profiling, are shown. Results represent n=3±SEM.

Volcano plots were used to demonstrate the spatial expression of all miRNAs assessed (Figure 5.8).

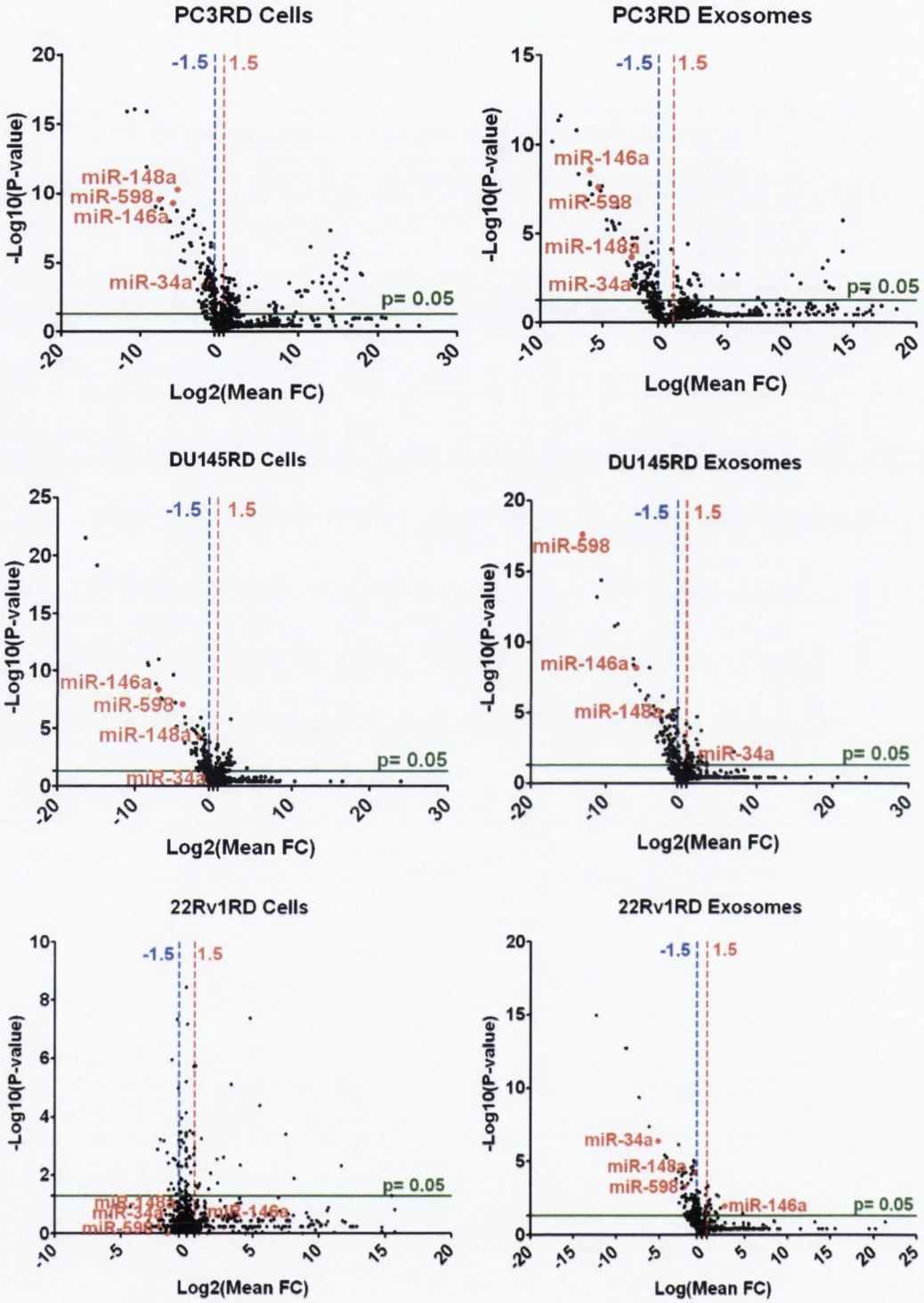

Figure 5.8: Volcano plots were used to demonstrate the spatial expression of all miRNAs assessed. Four miRNAs were selected for independent validation by qPCR as indicated on the volcano plots. Results represent mean fold changes of n=3±SEM

Fold changes of these miRNAs that were individually validated by qPCR are shown in Table 5.5.

miR-598	Cells Fold Change (Mean±SEM)	P-Value	Exosomes Fold Change (Mean±SEM)	P-Value
22Rv1RD	-2.08±0.21	0.0001	-2.01±0.42	0.0021
DU145RD	-15.65±4.9	0.0301	-15.62±3.14	0.0061
PC3RD	-95.5±19.87	0.0086	-16.93±6.42	0.0492
miR-148a	**Cells Fold Change (Mean±SEM)**	**P-Value**	**Exosomes Fold Change (Mean±SEM)**	**P-Value**
22Rv1RD	-1.27±0.5	0.0000	-2.39±0.2	0.0001
DU145RD	-8.37±2.38	0.0172	-3.95±1.06	0.0095
PC3RD	-48.64±3.97	0.0002	-9.93±4.27	0.0626
miR-34a	**Cells Fold Change (Mean±SEM)**	**P-Value**	**Exosomes Fold Change (Mean±SEM)**	**P-Value**
22Rv1RD	-7.80±0.61	0.0001	-11.13±0.85	0.0001
DU145RD	-1.08±1.12	0.1378	1.33±0.3	0.3331
PC3RD	-4.68±1.71	0.0294	-5.69±1.98	0.0278
miR-146a	**Cells Fold Change (Mean±SEM)**	**P-Value**	**Exosomes Fold Change (Mean±SEM)**	**P-Value**
22Rv1RD	2.14±0.05	0.0000	3.06±0.95	0.0953
DU145RD	-54.42±16.41	0.0279	-81.16±13.42	0.0036
PC3RD	-120.41±96.5	0.2758	-72.65±7.87	0.0007

Table 5.5: miRNAs selected for validation for qPCR.

Validation of miR-598, miR-148a, miR-34a and miR-146a expression in cells and corresponding exosomes by qPCR. Fold changes in expression were calculated for all docetaxel-resistant cell line variants (22Rv1RD, DU145RD and PC3RD) compared to age-matched parent controls (22Rv1, DU145 and PC3). Results represent n=3±SEM.

5.1.16 The clinical relevance of selected miRNAs

In order to determine whether any of the selected miRNAs from the global profiling were worthy of pursuing for further functional assessment, we next assessed if these miRNAs had significant association in a clinical setting. Using publically-available datasets on the gene expression omnibus and analysing using the GEO2R function, we assessed the expression of miR-34a, miR-598, miR-148a and miR-146a in a number of

patient cohorts (Figure 5.9 and Figure 5.10). miR-34a was found to be significantly decreased ($p<0.05$) in prostate cancer tissue compared to matched benign tissue from the same individuals (Figure 5.9A (i)), while a significant increase ($p<0.01$) of miR-148a was observed (Figure 5.10B (i)). No significant difference in miR-598 or miR-146a was observed (Figure 5.10A (i) and 5.10C (i)). To investigate the potential of our selected miRNAs to be used as circulating and thus minimally-invasive biomarkers, we examined their expression in urine samples from patients with benign prostatic hyperplasia (BPH) compared with patients with prostate cancer. A trend towards decreased miR-34a expression was observed in urine from prostate cancer patients (Figure 5.9A (ii)). miR-148a also showed significantly decreased ($p<0.05$) expression in urine from prostate cancer patients compared to those with BPH whereas the expression of miR-598 or miR-146a was not significantly altered (Figure 5.10A-C (ii)). Biochemical recurrence, defined as a rise in serum prostate specific antigen (PSA) levels following radical prostatectomy and/or radiation therapy, is considered an indicator of more aggressive disease and predictive of early treatment failure [360]. Here we identified a significant decrease of miR-34a expression ($p<0.05$) in the tissues from a cohort of prostate cancer patients experiencing biochemical recurrence compared to patients that had no recurrence (Figure 5.9A (iii)). Assessment of miR-598, miR-148a and miR-146a did not demonstrate any significant discrimination between biochemical recurrence and non-recurrence (Figure 5.10A-C (iii)). As a final assessment of miRNA expression and aggressive disease, we next examined tissue specimens from patients with evidence of metastasis compared to patients with primary localised prostate cancer and also normal adjacent tissues. miR-34a was significantly decreased in both primary ($p<0.01$) and metastatic ($p<0.01$) disease compared to non-malignant tissue (Figure 5.9A (iv)). Furthermore, there was a significant ($p<0.05$) further decrease in miR-34a expression in metastatic compared to primary disease. The other selected miRNAs (miR-598, miR-148a and miR-146a) displayed some significant alterations in expression, although no consistent trend was observed (Figure 5.10A-C (iv)). Using an online tool (MIRUMIR) [359] to examine miRNA association with cancer survival, we identified that low expression of miR-34a, while not statistically significant ($p=0.075$), tended towards an association with poor survival in prostate cancer (Figure 5.9B).

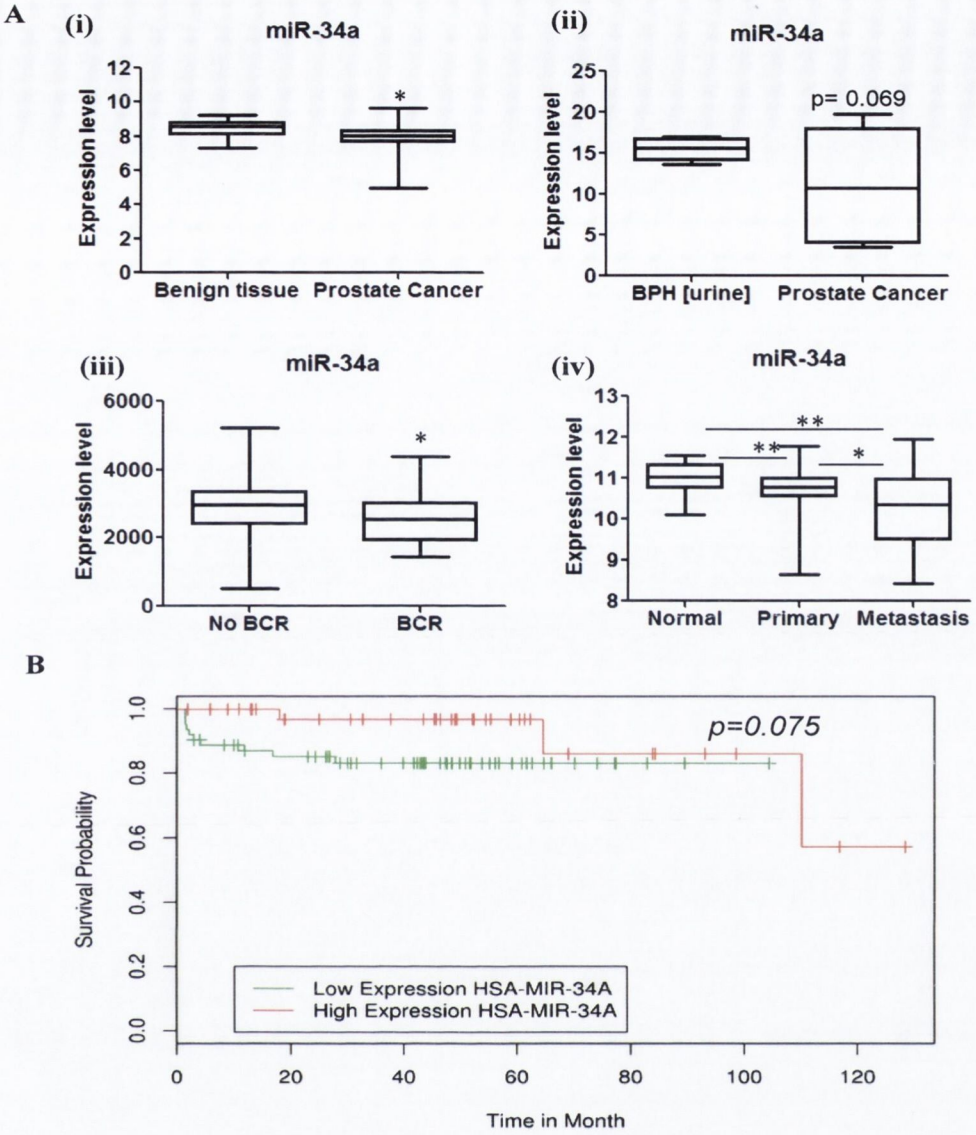

Figure 5.9: Clinical assessment of miR-34a.

Using publically available datasets on the gene expression omnibus and analysing using the GEO2R function, we assessed the expression of miR-34a in a number of patient cohorts **(A) (i)** miR-34a was found to be significantly decreased ($p<0.05$) in prostate cancer tissue (n=21) compared to matched benign tissue (n=21). **(ii)** A trend towards decreased miR-34a expression was observed in urine from prostate cancer patients (n=9) compared to patients with benign prostatic hyperplasia (BPH) (n=8). **(iii)** Here a significant decrease of miR-34a expression ($p<0.05$) in the tissues from a cohort of prostate cancer patients experiencing biochemical recurrence (BCR) (n=30) compared to patients that had no recurrence (no BCR) (n=53) was observed. **(iv)** miR-34a was significantly decreased in both primary (n=99) ($p<0.01$) and metastatic (n=14) ($p<0.01$) disease compared to non-malignant tissue (n=28). Furthermore, there was a significant ($p<0.05$) further decrease in miR-34a in metastatic compared to primary disease. **(B)** Using an online tool (MIRUMIR) to predict miRNA association with cancer survival, we identified that low expression of miR-34a, while not statistically significant ($p=0.075$), tended towards an association with poor survival in prostate cancer. *$p<0.05$ **$p<0.01$

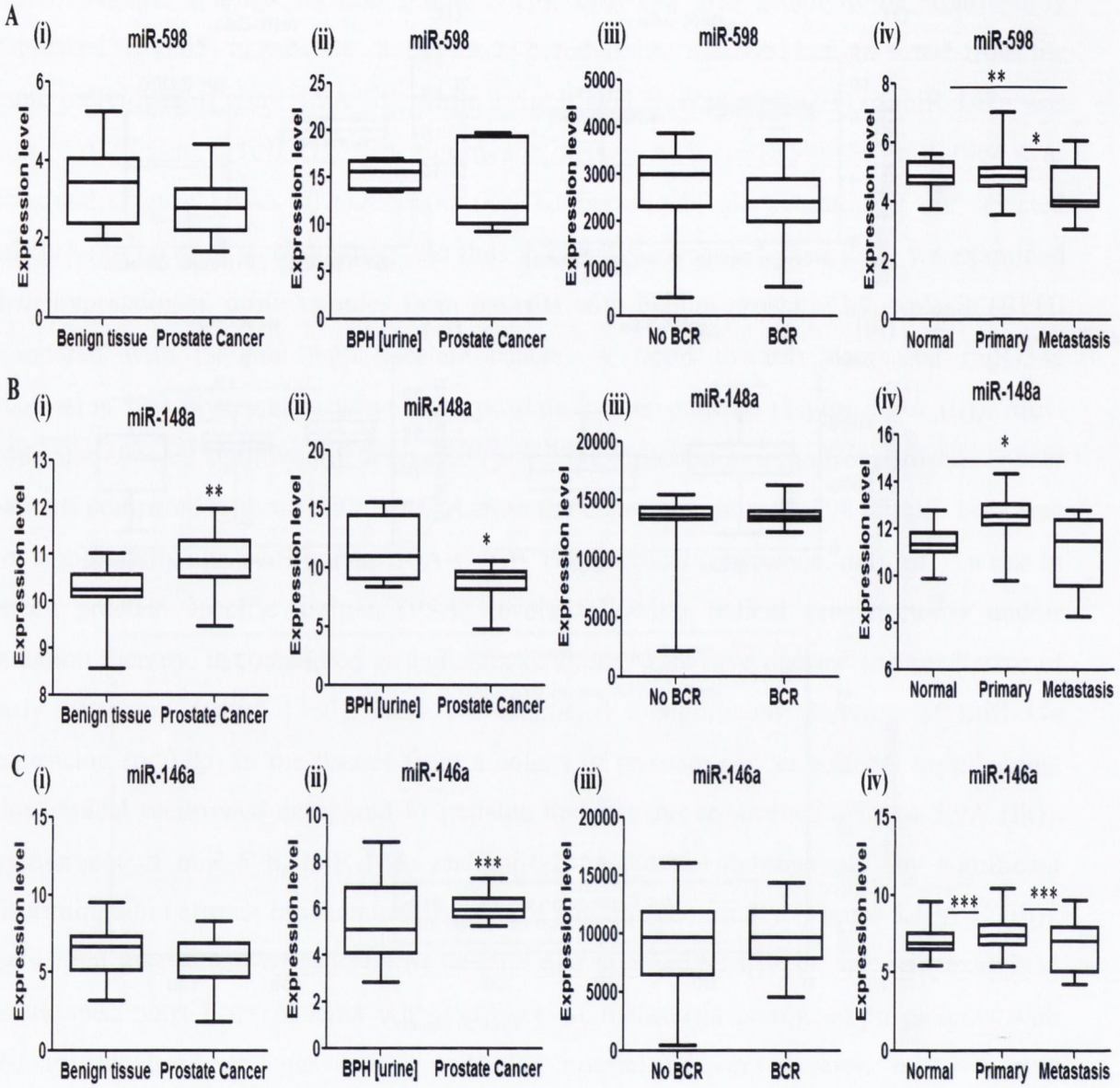

Figure 5.10: Clinical assessment of miR-598, miR-148a and miR-146a.

Using publically-available datasets on the gene expression omnibus and analysing using the GEO2R function, we assessed the expression of miR-598, miR-148a and miR-146a in a number of patient cohorts. **(A-C) (i)** No significant difference in miR-598 or miR-146a was observed in prostate cancer tissue (n=21) compared to matched benign tissue (n=21), conversely a significant increase ($p<0.01$) of miR-148a was observed. **(ii)** miR-148a also showed significantly decreased ($p<0.05$) levels in urine from prostate cancer patients (n=9) compared to those with Benign Prostatic hyperplasia (BPH) (n=8), whereas the expression of miR-598 or miR-146a was not significantly altered. **(iii)** miR-598, miR-148a and miR-146a did not demonstrate any significant discrimination between biochemical recurrence (BCR) (n=30) and non-recurrence (No BCR) (n=53). **(iv)** Assessment of miR-598, miR-148a and miR-146a displayed some significant alterations in expression in primary (n=99) or metastatic (n=14) disease compared to normal adjacent tissue (n=28) although no consistent trend was observed.*$p<0.05$ **$p<0.01$, ***$p<0.001$

5.1.17 Mechanism of action and functional relevance of miR-34a

Since miR-34a showed the most consistent clinical relevance in the 4 cohorts of patient specimens assessed, our subsequent analysis was to further assess the function of miR-34a in our prostate cancer cell lines. Using target prediction software and literature survey, we identified B-cell Lymphoma 2 (BCL-2) as a potential target of miR-34a. Initial assessment of basal BCL-2 expression did not show a significant difference in PC3RD compared to age-matched parent cells; however, a significant increase in BCL-2 expression was observed in 22Rv1RD by 2.1±0.2 fold compared to 22Rv1 ($p<0.01$) (Figure 5.11A). Inhibition of miR-34a in parent cells (PC3 and 22Rv1) caused a significant, increase in BCL-2 protein expression by 1.5±0.1 fold (for PC3RD; $p<0.01$) and 1.8±0.2 fold (for 22Rv1RD; $p<0.05$), compared to BCL-2 levels in corresponding negative control inhibitor transfected cells (Figure 5.11B). Conversely, mimicked expression of miR-34a in PC3RD and 22Rv1RD cells caused a significant reduction in BCL-2 expression by 2.4±0.1 fold (for PC3RD; $p<0.001$) and by 2.0±0.3 fold (for 22Rv1RD; $p<0.01$) compared to negative control mimic transfected cells (Figure 5.11C).

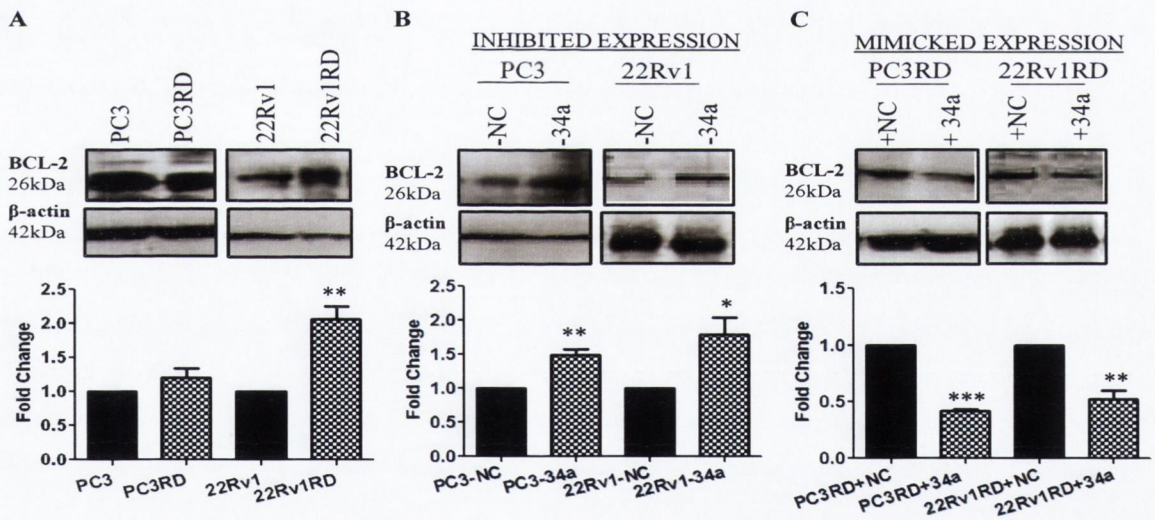

Figure 5.11: miR-34a mechanism of action.

(A) Initial assessment of basal BCL-2 expression did not show a significant difference in PC3RD compared to PC3; however, a significant increase ($p<0.01$) in BCL-2 expression was observed in 22Rv1RD compared to 22Rv1. **(B)** Inhibition of miR-34a in parent cells (PC3 and 22Rv1) resulted in a significant ($p<0.01$, $p<0.05$) increase in BCL-2 protein expression, compared to BCL-2 levels in negative control (NC) inhibitor transfected cells. **(C)** Conversely, mimicked expression of miR-34a in PC3RD and 22Rv1RD cells caused a significant reduction in BCL-2 expression ($p<0.001$, $p<0.01$) compared to NC mimic transfected cells. Results represent n=3±SEM, where *$p<0.05$, **$p<0.01$, ***$p<0.001$.

As the innate expression of BCL-2 was significantly increased in 22Rv1RD cells compared to 22Rv1 (whereas no significant difference was observed in PC3 compared to PC3RD) we elected to use these cell line variants to assess whether altering miR-34a expression could have an effect on proliferation and response to docetaxel (Figure 5.12). No significant difference was observed on either the proliferation or response off 22Rv1 to docetaxel in the presence of miR-34a inhibitor compared to NC inhibitor (Figure 5.12A). While, again, no significant difference was observed on the proliferation of 22Rv1RD after miR-34a introduction, there was however a significant ($p<0.01$) decrease by 9.7±0.3% in resistance to docetaxel in the presence of miR-34a mimic compared to NC mimic (Figure 5.12B).

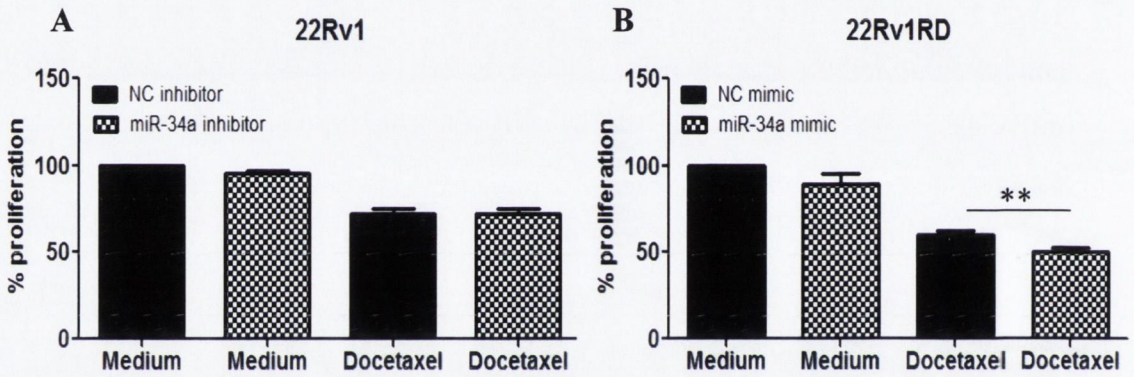

Figure 5.12: Effect of miR-34a on proliferation and response to docetaxel in 22Rv1 and 22Rv1RD cells. Proliferation of cells in the absence (medium only) or presence of docetaxel following miR-34a manipulated expression. **(i)** No significant difference was observed on either the proliferation or response of 22Rv1 to docetaxel in the presence of miR-34a inhibitor compared to NC inhibitor. **(ii)** While no significant difference was observed on the proliferation of 22Rv1RD, there was however a significant ($p<0.01$) decrease in resistance to docetaxel in the presence of miR-34a mimic compared to NC mimic. Proliferation and response to treatment shown here was assessed using the acid phosphatase method. Results represent n=3±SEM, where **$p<0.01$.

5.4 DISCUSSION

While the first line-treatment for castration-resistant prostate cancer (CRPC), docetaxel, has demonstrated initial success in improving overall survival, evidence of acquired-resistance among patients is continuing to be an immense problem in attempts to circumvent the disease. Substantial findings to date have suggested that aberrant miRNA expression is implicated in cancer initiation and progression [95, 361] and more recently the relevance of miRNAs regulating drug-resistance has also been reported [362]. Thus the detection of miRNAs for use as diagnostic, prognostic and predictive biomarkers for treatment response is now warranted to advance this field. The detection of these miRNAs in an extracellular environment, offers the prospect of a minimally-invasive and easily attainable biomarker for the clinic. Expanding research in the quest to identify circulating (extracellular) biomarkers has indicated that molecules such as miRNAs may be actively secreted within nano-sized vesicles, known as exosomes, with the potential of being taken up into secondary cells [215, 217-219]. We have previously reported in Chapter 4 that exosomes derived from the conditioned media of docetaxel-resistant cell lines can be up taken into secondary cells and induce docetaxel-resistance; at least in part, it seems, by the transfer of proteins like the multidrug-resistance protein 1 (MDR-1/P-gp) [237]. To further explore the role of exosomes in prostate cancer progression and docetaxel-resistance, we elected to perform global miRNA profiling of the cells and corresponding exosomes from a panel of cell lines with acquired-resistance to docetaxel and their age-matched sensitive parent cells. Before miRNA profiling was performed, the exosomes isolated from the conditioned media of all cell line variants were assessed by TEM for size and shape and by immunoblotting for the expression of exosomal proteins. The general size of the isolated vesicles for all cell line variants was of approximately 100nm and taken together with the expression of exosome markers TSG101 and PDC6I/Alix we confirmed the presence of exosomes.

Prior to performing miRNA profiling, the RNA yield and quality isolated from the cells and corresponding exosomes was assessed using the Nanodrop ND-1000 spectrophotometer. Initial observations indicated that the 22Rv1 cell line variants had the largest yield of exosomal RNA while PC3 cell line variants had the lowest. The quantity of RNA isolated, however, was generally indicative of the initial yield of exosomes (measured in protein) that was isolated from the conditioned media for each cell line

variant, thus the 22Rv1 cell line variants in this case also generated the highest yield of exosomes. One suggestion for the varied production of exosomes between cell lines is the difficulty associated with achieving high density cell cultures using adherent cells as opposed to suspension cells for example [363]. Due to the nature of 22Rv1 cell line variants in terms of morphology (See Chapter 4, Figure 4.1) and growth patterns it was possible to seed these cells at a higher numbers than PC3 or DU145 cell line variants – which were visually larger in size, grew faster and so would reach the desired confluency in a shorter period of time. The 22Rv1 cell line variants could have a higher number of cells per flask without the cells becoming too confluent. Similar to the miRNA profiling study discussed in Chapter 2, the quality of RNA (measured by 260/280 ratio on the Nanodrop) used in this study was also assessed. The 260/280 ratio for all cellular RNA was again within the expected range of 1.8-2.0. Interestingly however, the exosomal RNA had a higher 260/280 ratio (1.7-2.0) than that reported for the conditioned media RNA in Chapter 2. There are some possible reasons for this: Firstly, exosomes have been known to protect RNAs from RNAse activity [364]; it may be likely therefore that any freely circulating RNA from the conditioned media (that was not solely encapsulated in exosomes) used in Chapter 2 may be subject to partial degradation due to RNases. Secondly, the RNA isolated in Chapter 2 was from just 250µl CM as opposed to the exosome samples (which were resuspended in 200µl PBS) that were isolated from 90mls of CM, representing nine 75cm^2 flasks. Thus the yields of RNA from the exosomes which were derived from a larger volume of media had in general larger amounts of RNA ultimately leading to better reads on the 260/280 ratio. Thirdly, different methods of RNA isolation were used in Chapter 2 (TriReagent) and Chapter 5 (miRNeasy mini kit). As the risk of phenol contamination may be more likely to occur with TriReagent than with the miRNeasy kit this may be another reason for lower 260/280 ratios observed. Finally, the RNA isolations used for the miRNA profiling in Chapter 2 were performed at an earlier stage of this Phd compared to the RNA isolated for the miRNA profiling in Chapter 5, thus a great degree of experience with RNA may have correlated with the quality and yields of RNA isolated.

Initial assessment of our miRNA profiling data identified that of the total miRNAs detected in cells and exosomes, approximately 77% were commonly detected in both cells and exosomes of all cell line variants. Linear regression analysis indicated a positive strong correlation of the miRNA detection of all cell lines when compared to their corresponding

exosomes. Furthermore, hierarchical clustering using relative fold changes (*i.e.* the fold change of miRNA expression of each docetaxel-resistant cell line variant compared to its respective age-matched parent control) for all three docetaxel-resistant cell lines clustered together with their corresponding exosomes. This observation is in keeping with that of several others studying other cancer types [216, 217, 238]. In a panel of 8 miRNAs assessed, Taylor and Gercel-Taylor observed a correlation between miRNA expression in tumours from patients with ovarian cancer compared to the miRNA expression derived from the serum of the same patients [217]. Furthermore, a strong correlation between the expression of 12 miRNAs in non-small cell lung cancer tumours and the levels of peripheral blood–derived exosomal miRNAs has also been observed [216]. More recently, Xiao et al. [238] performed global mRNA and miRNA profiling on the cells and corresponding exosomes derived from melanoma cells (A375) and human epidermal melanocyte cells (HEMa-LP) and demonstrated a correlation between the mRNA and miRNA content of each cell line and their corresponding exosomes [238]. Taken together our data suggests that exosomal miRNA presence does, in fact, strongly reflect that of their cells of origin and so supports the potential use of exosomes derived from biological fluids as a source of biomarkers that may be easily attained with minimal invasion and also likely to be representative of the clinical situation. Some studies have suggested that exosomal miRNAs are selectively secreted or retained by cells and that their miRNA expression does not directly reflect the cells of origin [274, 275]; while this is not the primary observation of this study, we cannot solely exclude the fact that some miRNAs may be detected at higher levels in the cells compared to exosomes and *vice versa*. As shown in Figure 5.2, some miRNAs were detected in the exosomes only suggesting that these may have been selectively secreted from the cells. The objective of this study, however, was to focus on miRNAs that had similar detection intracellularly and extracellularly in association with the development of docetaxel-resistance, as a means of identifying potential biomarkers representative of the cellular phenotype.

After profiling 754 miRNAs in cells and exosomes, we selected four miRNAs for further evaluation. Specifically, we selected miR-598 for validation by qPCR and assessment in clinical data sets as it was decreased in all three docetaxel-resistant cells and exosomes compared to their respective age-matched controls and has never previously been associated with prostate cancer or drug-resistance indicating that miRNA may be novel to docetaxel-resistance in prostate cancer. We also selected miRNAs that had

previous associations with either prostate cancer and/or drug-resistance. miR-146a and miR-148a, both of which were decreased in the cells and exosomes in at least 2 of the cell lines assessed, have been associated with prostate cancer [172, 365-368]. miR-148a has also been associated with regulating response to paclitaxel in prostate cancer [367], cisplatin in breast cancer [369], 5-fluorouracil and cisplatin in oesophageal cancer cells [370]. miR-146a has been demonstrated to regulate resistance to interferon α in hepatocellular carcinoma [371] . Our fourth miRNA selected for validation was miR-34a; its association with prostate cancer has been reported [162, 372, 373] and here we found it to be decreased in cells and exosomes of two (i.e. 22Rv1RD and PC3RD) out of three docetaxel-resistant cell lines. Studies have also shown this miRNA to regulate resistance to camptothecin and paclitaxel in prostate cancer [187, 188], docetaxel-resistance in breast cancer [184] and cisplatin resistance in bladder cancer [374]. Subsequent data mining from clinical specimens indicated that of these four miRNAs, miR-34a was the most consistently deregulated miRNA in all clinical cohorts assessed *i.e.* it was significantly decreased in cancer *versus* normal tissues; in biochemical recurrence *versus* non-recurrence tissue; in metastatic *versus* primary disease prostate tissue; and it also held relevance as an extracellular marker in terms of demonstrating a decreased trend in urine from prostate cancer patients compared to those with benign prostatic hyperplasia. None of the other three miRNAs showed such consistent and/or significant trends in all four of the clinical cohorts assessed. For this reason, we focused our subsequent further functional analysis on miR-34a.

TargetScan 6.2 and Diana miRPath softwares identified B-Cell Lymphoma 2 (BCL-2) to be a target of miR-34a. Studies using other cell lines or in other cancer types have also suggested the association of miR-34a with BCL-2 regulation, thus we elected to assess its relevance in our study [184, 188, 375]. BCL-2 was confirmed as a target of miR-34a, by manipulating miR-34a expression in our parent and docetaxel-resistant cell lines and subsequently assessing BCL-2 levels. Specifically, upon inhibition of miR-34a in sensitive parent cells (PC3 and 22Rv1) an increase in BCL-2 expression was observed, whereas mimicking miR-34a expression in docetaxel-resistant cells (PC3RD and 22Rv1RD) resulted in decreased BCL-2 expression. Several reports have indicated an association between increased BCL-2 expression and drug-resistance [91-93, 375]. In fact, miR-34a regulation of BCL-2 has previously been reported to attenuate paclitaxel resistance in acquired paclitaxel-resistant prostate cancer cells [188]. More recently, miR-34a has been

demonstrated to induce sensitivity to sorafenib in hepatocellular carcinoma cell lines by inhibiting BCL-2 expression [375] while *in vitro* and *in vivo* models of multiple myeloma indicate that the use of synthetic miR-34a mimics can down regulate BCL-2 expression [376]. The association between miR-34a targeting BCL-2 and regulating docetaxel-resistance in breast cancer has also been reported, although the authors in this study found that miR-34a was elevated with docetaxel-resistance [184]. Although this observation in breast cancer conflicts with the findings of our study, there is a greater number of studies that support miR-34a as being decreased with drug-resistance and/or to negatively regulate BCL-2 [188, 374-379]. Here we found that, while inhibition of miR-34a in 22Rv1 cells did not alter response to docetaxel, introducing miR-34a into docetaxel-resistant 22Rv1RD cells enhanced the cytotoxic effects of docetaxel.

5.5 CONCLUSIONS

In conclusion, we have identified a panel of miRNAs that are commonly decreased in the cells and exosomes of acquired docetaxel-resistant cell lines. To the best of our knowledge this is the first study to perform global miRNA profiling of both cells and corresponding exosomes in the setting of docetaxel-resistance in prostate cancer and to identify a correlation of miRNA expression in the cells and exosomes of all cell lines used in this study. Furthermore, the clinical evaluation of our chosen miRNAs supports the relevance of miR-34a in particular with prostate cancer incidence and progression. The observed decreased expression of miR-34a in tissues from patients with biochemical recurrence also suggests its relevance as an indicator of potential early treatment failure while its detection and corresponding decrease in urine from prostate cancer patients compared to patients with benign prostatic hyperplasia further supports its potential as a minimally-invasive biomarker. Finally our functional analysis indicates that miR-34a may have a role in influencing cell response to docetaxel, at least partly by its regulation of anti-apoptotic protein BCL-2. The association of miR-34a with docetaxel-resistance in prostate cancer observed here has not be previously reported but is supported by several studies in other cancers and/or with resistance to other treatments. To the best of our knowledge this is the first study to identify the novelty of miR-34a to also be utilised a minimally-invasive biomarker predictive of response to docetaxel in prostate cancer. Despite the growth of research in exosomes in recent years, few studies have focused on profiling of both cells and their corresponding exosomes. In order to determine if exosomes do in fact represent

their cell of origin, and so could be utilised as potential circulating biomarkers to be used in the clinic, a study like this reported here is a necessary starting point for determining predictive biomarkers that could be obtained in a mimially-invasive manner.

CHAPTER 6

6 Discussion & Conclusion

6.1 Discussion & Conclusion

The aim of this PhD was to determine the mechanisms behind resistance to treatments for the leading causes of cancer among the male population (prostate cancer) and female populations (breast cancer). As discussed in Chapter 1, the diagnostic and prognostic tools for these cancers are inadequate and there are limited means of predicting response to treatments. Thus the second aim of this PhD was to identify biomarkers predictive of response to treatments for both cancer types, ideally with potential to be obtained in a minimally-invasive manner. Part of the research undertaken for this thesis, therefore, had an emphasis on biomarkers identified in an extracellular environment.

The miRNA profiling performed in Chapter 2 indicated that there was a modest positive correlation between miRNAs detected in cells and corresponding conditioned medium (CM). This initial observation indicates that the miRNAs detected in the extracellular environment may be representative of their cells of origin. Studies within our laboratory focused initially on biomarkers that could be detected in biological fluids such as CM and serum for example [201, 206, 289]. Over the course of this PhD however, increasing evidence emerged that many of the biomarkers detected in biological fluids may be encapsulated into nano-sized vesicles such as exosomes. Thus, research in this PhD then evolved to focus on exosomal content of biological fluids. In Chapter 5, miRNA profiling was performed in a similar manner to Chapter 2, but this time focusing on docetaxel-resistance in prostate cancer cell lines and using exosomes derived from CM. Here we found that detection of miRNAs in the exosomes in fact demonstrated a strong correlation with the detection of miRNAs in the corresponding cells of origin. The stronger correlation observed between cells and exosomes compared to the cells and CM may be a result of several possibilities.

Firstly, CM contains both freely circulating and vesicle (exosome) contained miRNAs, thus the lower R^2 value, observed for in the linear regression analysis of in Chapter 2, may be due to the mixed populations of extracellular miRNAs (i.e. freely circulating and vesicle bound) examined. As the prostate cancer study focused solely on concentrated exosomal miRNAs rather than all circulating miRNAs, exosome isolation prior to profiling may have increased the sensitivity of miRNA detection and so resulting in a better correlation with the corresponding cells of origin. A recent study by Gallo *et al.* [380], supports this

hypothesis whereby the authors concluded that the majority of miRNAs detected in serum and saliva are concentrated in exosomes. In that study, on comparison of both exosome depleted supernatants compared to exosomes fractions, the authors demonstrated the miRNA content was higher in exosomes [380]. Furthermore, on comparison of unfractionated serum compared to exosomes from the same serum specimens, the detection of miRNAs was increased in the exosomes. While these suggestions are possible, direct comparisons between both miRNA profiling studies (CM *versus* exosomes) in this thesis is not possible as different cell lines were assessed. The differences observed here may be a cell line and/or cancer specific phenomenon. Nevertheless, one of the common observations that was found in both studies is that a substantial number of miRNAs (~75%) were detectable in both cells and their corresponding extracellular environments further supporting the relevance of examining circulating miRNAs as potential minimally-invasive biomarkers in breast and prostate cancer.

To truly assess whether the miRNAs or mRNAs of interest are predominantly enriched in exosomes or freely circulating would involve examining the exosome fraction and the corresponding supernatants simultaneously. While a study of this description is important for future studies, the main focus of this PhD however was twofold, firstly to detect biomarkers that may be associated with drug-resistance in breast and prostate cancer and secondly to determine if these biomarkers demonstrated a similar trend in the extracellular environment. Identifying the exact format of how these biomarkers exist in circulation (be it freely circulating, within exosomes or both) was not the initial focus of this PhD. The latter chapters of this thesis had a greater focus on the role of exosomes in drug-resistance as it was becoming clear that exosomes may have an important role to play in cancer biology.

In this thesis, miR-630 is demonstrated to be significantly down-regulated with resistance to HER-targeted RTKIs – lapatinib, neratinib and trastuzumab. To the best of our knowledge this is the first association of miR-630 with resistance to HER-targeted treatments and also to breast cancer. Our observations are supported by studies that have shown miR-630 to regulate cisplatin response in head and neck carcinoma cells [255]. In addition to drug-resistance, this thesis also shows that miR-630 may regulate other phenotypic affects including motility, invasion and *anoikis* some of which were also observed in recent studies in lung cancer [256]. From our subsequent functional studies,

our proposed mechanism of action involves IGF1R, an RTK that has previously been associated with both drug-resistance and cancer cell aggression [54-58, 280-282]. Furthermore, recently the link between miR-630 and IGF1R has been demonstrated in pancreatic cancer [257] .

While the miR-630 project was ongoing, a second study (discussed in Chapter 3) investigating NmU was underway in our laboratory. Here we demonstrate that NmU could also be associated with resistance to RTKIs and, similarly to miR-630, could also regulate other phenotypic changes such as motility, invasion and *anoikis*. These studies also demonstrated the relevance of NmU as an extracellular biomarker, detectable in CM but also in exosome derived from CM. This finding, in addition to that from the miR-630 studies, further supports the relevance of assessing the extracellular environment for biomarker discovery. We found that the mechanism of NmU's action involved its chaperoning with HSP27. HSP27 has previously been associated with both drug-resistance and cancer cell aggression [71-74]. Interestingly, assessment of the predicted targets for miR-630 also indicated that NmU may be regulated by miR-630. While our preliminary results support this possibility, further studies are necessary to confirm the significance of their relationship.

Clinical assessment of miR-630 and NmU in publically-available datasets indicated that these biomarkers may hold relevance in not only HER2-overexpressing breast cancers but in other subtypes also. While the scope of this PhD focused on HER2-overexpressing breast cancer, future studies are necessary to fully elucidate the full spectrum of NmU and miR-630's activity. Furthermore, considering that miR-630, for example, has previously been associated with cisplatin resistance [255] suggests that it may have relevance in other therapies. Assessment of miR-630 in a publically available data from patients with high risk ER+ breast cancer receiving adjuvant tomoxifen therapy indicated that low miR-630 expression was associated with overall poor outcome [see Appendix I, Section G]. Our initial drug screen of stable miR-630 knockdown cells (as shown in Chapter 2, Section 2.3.12) indicated that inhibition of miR-630 increased resistance to docetaxel which approached significance. Future studies examining the relationship of miR-630 with docetaxel and/or other classical chemotherapy would be useful to determine its relevance in other treatment strategies.

In Chapter 4 the multifaceted and complex nature of docetaxel-resistance in prostate cancer is demonstrated. While all three docetaxel-resistance cell lines studied shared some common characteristics such as cross-resistance to doxorubicin, decreased proliferation and resistance to *anoikis* there were, however, other phenotypic differences observed between the drug-resistant cell line variants such as motility, invasion and colony formation. This study further emphasises the importance of using several cell lines when performing *in vitro* experiments to better predict the likely patient diversities that may present in a clinical situation. Two of the three docetaxel-resistant cell lines expressed the drug-efflux pump, MDR-1/P-gp which was also observed to be present in the exosomes derived from these cells. Incidentally, exosomes derived from these cell line variants induced an increase in docetaxel-resistance when applied to secondary cells, further supported by a pilot study using exosomes derived from clinical specimens. These observations strongly support the significant functional role of exosomes in prostate cancer. As mentioned earlier in this Chapter, to further elucidate the mechanisms behind docetaxel-resistance and the content of the cell-derived exosomes, we performed global miRNA profiling (as described in Chapter 5). The limited number of miRNAs detected to be commonly decreased in the cells and exosomes of all three cell line variants further highlights the complex nature of docetaxel-resistance in prostate cancer. Considering the number of variables included in this profiling study may also be a reason for the low numbers of common miRNAs identified (i.e. 3 sensitive cell lines, 3 resistant variants and corresponding exosomes for all cell lines). Nevertheless, we identified miR-34a as one of the miRNAs that may regulate docetaxel-resistance and may also be an exosomal biomarker. Supported by mining of several publically-available clinical datasets, previous associations with drug-resistance [188, 374-379] and an identified mechanism through the targeting of BCL-2, these studies suggest that miR-34a may be an important regulator of docetaxel-resistance in prostate cancer. The clinical data sets support an association with prostate cancer but to truly assess the clinical relevance of miR-34a with docetaxel response, a cohort of patients that have received docetaxel treatment should be assessed. We are currently collaborating with Prof. Colm Morrissey at University of Washington to address this issue by assessing the levels of miR-34a in a cohort of tissues from patients who either responded or failed to respond to docetaxel treatment.

In conclusion, here presented is research investigating the limiting factor of drug-resistance that currently is associated with HER-targeted therapies and docetaxel for the

treatment of breast cancer and prostate cancer, respectively. This PhD highlights the multidimensional nature of drug-resistance in both cancer types and emphasises the critical role that miRNAs can play in cancer biology. Furthermore, this PhD confirms the importance of many types of protein families in the regulation of drug-resistance and cancer cell aggression including receptor tyrosine kinases, heat shock proteins, drug-efflux pumps and apoptosis-regulating proteins. Finally the novel observations demonstrating the relevance of biomarkers in an extracellular environment, particularly those encapsulated in exosomes highlights the importance of assessing biological fluids for biomarker discovery. There are several questions that remain to be answered from the research within this PhD and although it was not possible to address all elements in this field, some suggested future directions are outlined in Section 6.2.

6.2 Future Directions

- *Assessment of miR-630 in the CM from a broad panel of cell lines*

  In Chapter 2, Figure 2.9, an association of miR-630 expression with innate sensitivity/resistance in a broad panel of HER2-overexpressing cell lines was observed. To investigate if the findings from these cells are similar to that of the extracellular environment, the CM (and/or specifically exosomes) from these cell lines should also be assessed for the levels of miR-630 also.

- *Is miR-630 concentrated in exosomes?*

  Our studies on miR-630 so far has demonstrated decreased expression in cells and CM of acquired-resistant cells to HER-targeted drugs. Deciphering whether miR-630 is present in exosomes or freely circulating may further increase our knowledge of its function relevance.

- *Can NmU in exosomes be transferred to secondary cells?*

  In studies, not detailed in this thesis, our group has demonstrated that exosomes derived from lapatinib- and neratinib-resistant cell lines can increase lapatinib-resistance in secondary cells. Whether this is due to transfer of NmU within exosomes remains to be interpreted. In this thesis, NmU was demonstrated to be present in exosomes, with higher levels in exosomes derived from lapatinib- and neratinib-resistant cell lines compared to parent cell lines. Assessing NmU

expression of secondary cells following incubation of exosomes expressing NmU may indicate if NmU is uptaken into secondary cells.

- *Assessment of miR-630 in vivo*

  In order to fully elucidate the significance of miR-630, *in vivo* studies involving the effects of stable knockdown and overexpression of miR-630 are necessary. As described in Chapter 2, stable cell lines were established however the miR-630 precursor cells did not demonstrate strong overexpression of miR-630 and so there were little or no changes observed in the phenotype of these cells. Thus before proceeding further, attempts at generating these cells again (this time perhaps using single cell cloning) should be performed.

- *Assessment of NmU in vivo*

  As described in Chapter 3, NmU appears to play a significant role in HER2 overexpressing breast cancer and is associated with overall poor prognosis. To further examine the functional role of NmU in breast cancer, we have generated cell lines that have stable overexpression and knockdown of NmU for *in vivo* analysis. Ethics approval is currently being sought for this study.

- *Further analysis of miR-630 and NmU relationship.*

  In Chapter 2, a preliminary study on miR-630's regulation of NmU was performed. Here we observed that stable knockdown of miR-630 caused an increase in NmU protein levels. This potential relationship should be further examined, by checking if, for example, overexpression of miR-630 can decrease NmU. While immunoblots for the stable miR-630 precursor cells were performed, these cells did not achieve substantial overexpression of miR-630 and so significant differences in NmU was not observed. The direct interaction of miR-630 with NmU could be demonstrated using a 3'UTR luciferase assay.

- *Assessment of miR-630 and NmU in serum*

  The significance of both extracellular miR-630 and NmU was demonstrated in the conditioned media from our acquired-resistant cell lines. In order to investigate if this applies to the clinical situation, serum is currently being collected from patients

undergoing treatment for HER2 overexpressing breast cancer. This study is part of the All Ireland Cooperative Oncology Research Group (ICORG 10-15) trial.

- *Does miR-630/NmU have a significant functional role in other breast cancer subtypes and treatments?*

  Assessment of miR-630 and NmU in the publically-available data sets indicated that both miR-630 and NmU may hold relevance in other breast cancer subtypes. As indicated in the Appendix I, Section G, low expression of miR-630 may is associated with poor survival of ER+ patients treated with tomoxifen. Thus it is possible that miR-630 may regulate response to other treatments in addition to HER-targeting drugs. It is important for future studies to investigate this further as a wider application of miR-630/NmU would be attractive for pharmaceutical companies.

- *Does miR-630/NmU hold relevance in other cancers?*

  Some studies have indicated the role of miR-630 in pancreatic cancer, lung cancer and head and neck cancer. Similarly, increased NmU has been previously associated with acute myeloid leukemia, ovarian, pancreatic cancer and bladder cancer. Further broadening our studies to assess treatment response in these cancer types and other cancer types may support their significance as universal predictive biomarkers.

- *Does miR-34a correlate with response to docetaxel?*

  While much of the publically available data sets demonstrate that decreased miR-34a is associated with prostate cancer and metastatic disease, an obvious question that remains to be answered is its clinical relevance in association with docetaxel treatment. We are currently collaborating with Prof. Colm Morrissey in the University of Washington with the aim of obtaining tissue specimens from patients who responded to or failed docetaxel treatment. Furthermore, the ICORG 08-08 trial, from which the serum specimens in Chapter 4, Table 4.3 were obtained is currently still recruiting and once a substantial cohort of 'responders' and 'non-responders' have been collected, miR-34a expression will also be assessed in these specimens.

- *Do exosomes derived from docetaxel-resistant cells increase the levels of MDR-1/P-gp or BCL-2 in secondary cells?*

  In Chapter 4, we demonstrated that exosomes derived from cells expressing MDR-1/P-gp also have detectable levels of this protein and that application of exosomes from these cells can induce docetaxel-resistance. To further assess whether this is due to transfer of MDR-1/P-gp, its expression level should be assessed in the recipient cells following incubation with these exosomes. Similarly, we proposed that BCL-2 was regulated by miR-34a and may also regulated docetaxel-resistance. Assessment of this protein in exosomes and in secondary cells following incubation with exosomes may also be an important study to perform.

- *miR-34a in vivo*

  Similar to the proposed *in vivo* studies for miR-630, generation of cell lines with miR-34a knockdown and overexpression would be necessary to support the importance of the molecule in prostate cancer and in regulating response to docetaxel.

- *Can MRX034 reverse docetaxel-resistance?*

  MiRNA Therapeutics have recently developed a miR-34 mimic (MRX034) that has currently started Phase I clinical trials for the treatment of patients with primary liver cancer or those with liver metastasis from other cancers. A potential collaboration with this company to obtain a sample of their therapeutic may be worthwhile to see if it may reverse or reduce docetaxel-resistance in our cell lines.

The future directions listed above are some examples of where the research presented in this thesis could be taken to next, the results of which may open new ideas to exploring other cancer types and drugs-treatments where relevant.

7 REFERENCES

1. American Cancer Society A: **Global Cancer Facts and Figures, 2nd Edition.** 2011.

2. Ireland NCR: **Cancer in Ireland 2013: Annual report of the National Cancer Registry.** 2013.

3. Ireland NCR: **Cancer projections 2005-2035.** 2008.

4. Siegel R, Naishadham D, Jemal A: **Cancer statistics, 2013.** *CA Cancer J Clin* 2013, **63:**11-30.

5. Paranjape T, Slack F, Weidhaas J: **MicroRNAs: tools for cancer diagnostics.** *Gut* 2009, **58:**1546-1554.

6. Germano S, O'Driscoll L: **Breast cancer: understanding sensitivity and resistance to chemotherapy and targeted therapies to aid in personalised medicine.** *Curr Cancer Drug Targets* 2009, **9:**398-418.

7. Heneghan H, Miller N, Lowery A, Sweeney K, Kerin M: **MicroRNAs as Novel Biomarkers for Breast Cancer.** *J Oncol* 2009, **2009:**950201.

8. Elmore J, Miglioretti D, Reisch L, Barton M, Kreuter W, Christiansen C, Fletcher S: **Screening mammograms by community radiologists: variability in false-positive rates.** *J Natl Cancer Inst* 2002, **94:**1373-1380.

9. Thompson A, Brennan K, Cox A, Gee J, Harcourt D, Harris A, Harvie M, Holen I, Howell A, Nicholson R, et al: **Evaluation of the current knowledge limitations in breast cancer research: a gap analysis.** *Breast Cancer Res* 2008, **10:**R26.

10. Viale G, Ghioni M, Mastropasqua MG: **Traditional molecular markers and response to adjuvant endocrine or trastuzumab-based therapies.** *Curr Opin Oncol* 2010, **22:**541-546.

11. Paik S, Kim C, Wolmark N: **HER2 status and benefit from adjuvant trastuzumab in breast cancer.** *N Engl J Med* 2008, **358:**1409-1411.

12. Catalona WJ, Smith DS, Ratliff TL, Dodds KM, Coplen DE, Yuan JJ, Petros JA, Andriole GL: **Measurement of prostate-specific antigen in serum as a screening test for prostate cancer.** *N Engl J Med* 1991, **324:**1156-1161.

13. Gjertson CK, Albertsen PC: **Use and assessment of PSA in prostate cancer.** *Med Clin North Am* 2011, **95:**191-200.

14. MacFarlane RJ, Gelmon KA: **Lapatinib for breast cancer: a review of the current literature.** *Expert Opin Drug Saf* 2011, **10:**109-121.

15. Slamon DJ, Clark GM, Wong SG, Levin WJ, Ullrich A, McGuire WL: **Human breast cancer: correlation of relapse and survival with amplification of the HER-2/neu oncogene.** *Science* 1987, **235:**177-182.

16. Slamon DJ, Godolphin W, Jones LA, Holt JA, Wong SG, Keith DE, Levin WJ, Stuart SG, Udove J, Ullrich A, et al.: **Studies of the HER-2/neu proto-oncogene in human breast and ovarian cancer.** *Science* 1989, **244:**707-712.

17. Nahta R, Esteva FJ: **HER2 therapy: molecular mechanisms of trastuzumab resistance.** *Breast Cancer Res* 2006, **8:**215.

18. Xia W, Mullin RJ, Keith BR, Liu LH, Ma H, Rusnak DW, Owens G, Alligood KJ, Spector NL: **Anti-tumor activity of GW572016: a dual tyrosine kinase inhibitor blocks EGF activation of EGFR/erbB2 and downstream Erk1/2 and AKT pathways.** *Oncogene* 2002, **21:**6255-6263.

19. Rusnak DW, Lackey K, Affleck K, Wood ER, Alligood KJ, Rhodes N, Keith BR, Murray DM, Knight WB, Mullin RJ, Gilmer TM: **The effects of the novel, reversible epidermal growth factor receptor/ErbB-2 tyrosine kinase inhibitor, GW2016, on the growth of human normal and tumor-derived cell lines in vitro and in vivo.** *Mol Cancer Ther* 2001, **1:**85-94.

20. Wang L, Zhang Q, Zhang J, Sun S, Guo H, Jia Z, Wang B, Shao Z, Wang Z, Hu X: **PI3K pathway activation results in low efficacy of both trastuzumab and lapatinib.** *BMC Cancer* 2011, **11:**248.

21. Liu L, Greger J, Shi H, Liu Y, Greshock J, Annan R, Halsey W, Sathe GM, Martin AM, Gilmer TM: **Novel mechanism of lapatinib resistance in HER2-positive breast tumor cells: activation of AXL.** *Cancer Res* 2009, **69:**6871-6878.

22. Wang Q, Quan H, Zhao J, Xie C, Wang L, Lou L: **RON confers lapatinib resistance in HER2-positive breast cancer cells.** *Cancer Lett* 2013, **340:**43-50.

23. Franklin MC, Carey KD, Vajdos FF, Leahy DJ, de Vos AM, Sliwkowski MX: **Insights into ErbB signaling from the structure of the ErbB2-pertuzumab complex.** *Cancer Cell* 2004, **5:**317-328.

24. Gianni L, Pienkowski T, Im YH, Roman L, Tseng LM, Liu MC, Lluch A, Staroslawska E, de la Haba-Rodriguez J, Im SA, et al: **Efficacy and safety of neoadjuvant pertuzumab and trastuzumab in women with locally advanced, inflammatory, or early HER2-positive breast cancer (NeoSphere): a randomised multicentre, open-label, phase 2 trial.** *Lancet Oncol* 2012, **13:**25-32.

25. Zardavas D, Cameron D, Krop I, Piccart M: **Beyond trastuzumab and lapatinib.** *Am Soc Clin Oncol Educ Book* 2013, **2013:**2-11.

26. Rabindran SK, Discafani CM, Rosfjord EC, Baxter M, Floyd MB, Golas J, Hallett WA, Johnson BD, Nilakantan R, Overbeek E, et al: **Antitumor activity of HKI-272, an orally active, irreversible inhibitor of the HER-2 tyrosine kinase.** In *Cancer Res. Volume* 64. United States2004: 3958-3965

27. Burstein HJ, Sun Y, Dirix LY, Jiang Z, Paridaens R, Tan AR, Awada A, Ranade A, Jiao S, Schwartz G, et al: **Neratinib, an irreversible ErbB receptor tyrosine kinase inhibitor, in patients with advanced ErbB2-positive breast cancer.** In *J Clin Oncol. Volume* 28. United States2010: 1301-1307

28. Lin NU, Winer EP, Wheatley D, Carey LA, Houston S, Mendelson D, Munster P, Frakes L, Kelly S, Garcia AA, et al: **A phase II study of afatinib (BIBW 2992), an irreversible ErbB family blocker, in patients with HER2-positive metastatic breast cancer progressing after trastuzumab.** *Breast Cancer Res Treat* 2012, **133:**1057-1065.

29. Adair JR, Howard PW, Hartley JA, Williams DG, Chester KA: **Antibody-drug conjugates - a perfect synergy.** *Expert Opin Biol Ther* 2012, **12:**1191-1206.

30. LoRusso PM, Weiss D, Guardino E, Girish S, Sliwkowski MX: **Trastuzumab emtansine: a unique antibody-drug conjugate in development for human epidermal growth factor receptor 2-positive cancer.** *Clin Cancer Res* 2011, **17:**6437-6447.

31. Verma S, Miles D, Gianni L, Krop IE, Welslau M, Baselga J, Pegram M, Oh DY, Diéras V, Guardino E, et al: **Trastuzumab emtansine for HER2-positive advanced breast cancer.** *N Engl J Med* 2012, **367:**1783-1791.

32. Singh J, Trabulsi EJ, Gomella LG: **Is there an optimal management for localized prostate cancer?** *Clin Interv Aging* 2010, **5:**187-197.

33. Damber JE, Aus G: **Prostate cancer.** *Lancet* 2008, **371:**1710-1721.

34. Chowdhury S, Burbridge S, Harper PG: **Chemotherapy for the treatment of hormone-refractory prostate cancer.** *Int J Clin Pract* 2007, **61:**2064-2070.

35. Koochekpour S: **Androgen receptor signaling and mutations in prostate cancer.** *Asian J Androl* 2010, **12:**639-657.

36. Galsky MD, Vogelzang NJ: **Docetaxel-based combination therapy for castration-resistant prostate cancer.** *Ann Oncol* 2010, **21:**2135-2144.

37. Berthold DR, Sternberg CN, Tannock IF: **Management of advanced prostate cancer after first-line chemotherapy.** *J Clin Oncol* 2005, **23:**8247-8252.

38. Scher HI, Halabi S, Tannock I, Morris M, Sternberg CN, Carducci MA, Eisenberger MA, Higano C, Bubley GJ, Dreicer R, et al: **Design and end points of clinical trials for patients with progressive prostate cancer and castrate levels of testosterone: recommendations of the Prostate Cancer Clinical Trials Working Group.** *J Clin Oncol* 2008, **26:**1148-1159.

39. Sinibaldi VJ: **Docetaxel treatment in the elderly patient with hormone refractory prostate cancer.** *Clin Interv Aging* 2007, **2:**555-560.

40. Stein CA: **Mechanisms of action of taxanes in prostate cancer.** *Semin Oncol* 1999, **26:**3-7.

41. Oudard S: **TROPIC: Phase III trial of cabazitaxel for the treatment of metastatic castration-resistant prostate cancer.** *Future Oncol* 2011, **7:**497-506.

42. Fizazi K: **Nonhormone therapy for metastatic castration-resistant prostate cancer.** *Am Soc Clin Oncol Educ Book* 2013, **2013:**161-165.

43. Harshman LC, Taplin ME: **Abiraterone acetate: targeting persistent androgen dependence in castration-resistant prostate cancer.** *Adv Ther* 2013, **30:**727-747.

44. Ryan CJ, Cheng ML: **Abiraterone acetate for the treatment of prostate cancer.** *Expert Opin Pharmacother* 2013, **14:**91-96.

45. Ryan CJ, Smith MR, de Bono JS, Molina A, Logothetis CJ, de Souza P, Fizazi K, Mainwaring P, Piulats JM, Ng S, et al: **Abiraterone in metastatic prostate cancer without previous chemotherapy.** *N Engl J Med* 2013, **368:**138-148.

46. Semenas J, Dizeyi N, Persson JL: **Enzalutamide as a second generation antiandrogen for treatment of advanced prostate cancer.** *Drug Des Devel Ther* 2013, **7:**875-881.

47. Nelson WG, Yegnasubramanian S: **Resistance emerges to second-generation antiandrogens in prostate cancer.** *Cancer Discov* 2013, **3:**971-974.

48. Vlahovic G, Crawford J: **Activation of tyrosine kinases in cancer.** *Oncologist* 2003, **8:**531-538.

49. Lemmon MA, Schlessinger J: **Cell signaling by receptor tyrosine kinases.** *Cell* 2010, **141:**1117-1134.

50. Zwick E, Bange J, Ullrich A: **Receptor tyrosine kinase signalling as a target for cancer intervention strategies.** *Endocr Relat Cancer* 2001, **8:**161-173.

51. Baselga J: **Treatment of HER2-overexpressing breast cancer.** *Ann Oncol* 2010, **21 Suppl 7:**vii36-40.

52. Rosenzweig SA: **Acquired resistance to drugs targeting receptor tyrosine kinases.** *Biochem Pharmacol* 2012, **83:**1041-1048.

53. Sierra JR, Cepero V, Giordano S: **Molecular mechanisms of acquired resistance to tyrosine kinase targeted therapy.** *Mol Cancer* 2010, **9:**75.

54. Gallardo A, Lerma E, Escuin D, Tibau A, Muñoz J, Ojeda B, Barnadas A, Adrover E, Sánchez-Tejada L, Giner D, et al: **Increased signalling of EGFR and IGF1R, and deregulation of PTEN/PI3K/Akt pathway are related with trastuzumab resistance in HER2 breast carcinomas.** *Br J Cancer* 2012, **106:**1367-1373.

55. Browne BC, Crown J, Venkatesan N, Duffy MJ, Clynes M, Slamon D, O'Donovan N: **Inhibition of IGF1R activity enhances response to trastuzumab in HER-2-positive breast cancer cells.** *Ann Oncol* 2011, **22:**68-73.

56. Wang YH, Xiong J, Wang SF, Yu Y, Wang B, Chen YX, Shi HF, Qiu Y: **Lentivirus-mediated shRNA targeting insulin-like growth factor-1 receptor (IGF-1R) enhances chemosensitivity of osteosarcoma cells in vitro and in vivo.** *Mol Cell Biochem* 2010, **341:**225-233.

57. Luk F, Yu Y, Walsh WR, Yang JL: **IGF1R-targeted therapy and its enhancement of doxorubicin chemosensitivity in human osteosarcoma cell lines.** *Cancer Invest* 2011, **29:**521-532.

58. Lu Y, Zi X, Zhao Y, Mascarenhas D, Pollak M: **Insulin-like growth factor-I receptor signaling and resistance to trastuzumab (Herceptin).** *J Natl Cancer Inst* 2001, **93:**1852-1857.

59. Knuefermann C, Lu Y, Liu B, Jin W, Liang K, Wu L, Schmidt M, Mills GB, Mendelsohn J, Fan Z: **HER2/PI-3K/Akt activation leads to a multidrug resistance in human breast adenocarcinoma cells.** *Oncogene* 2003, **22:**3205-3212.

60. Chell V, Balmanno K, Little AS, Wilson M, Andrews S, Blockley L, Hampson M, Gavine PR, Cook SJ: **Tumour cell responses to new fibroblast growth factor receptor tyrosine kinase inhibitors and identification of a gatekeeper mutation in FGFR3 as a mechanism of acquired resistance.** *Oncogene* 2012.

61. Ware KE, Hinz TK, Kleczko E, Singleton KR, Marek LA, Helfrich BA, Cummings CT, Graham DK, Astling D, Tan AC, Heasley LE: **A mechanism of resistance to gefitinib mediated by cellular reprogramming and the acquisition of an FGF2-FGFR1 autocrine growth loop.** *Oncogenesis* 2013, **2:**e39.

62. Zucali PA, Ruiz MG, Giovannetti E, Destro A, Varella-Garcia M, Floor K, Ceresoli GL, Rodriguez JA, Garassino I, Comoglio P, et al: **Role of cMET expression in non-small-cell lung cancer patients treated with EGFR tyrosine kinase inhibitors.** *Ann Oncol* 2008, **19:**1605-1612.

63. Archer SL, Weir EK, Wilkins MR: **Basic science of pulmonary arterial hypertension for clinicians: new concepts and experimental therapies.** *Circulation* 2010, **121:**2045-2066.

64. Feder ME, Hofmann GE: **Heat-shock proteins, molecular chaperones, and the stress response: evolutionary and ecological physiology.** *Annu Rev Physiol* 1999, **61:**243-282.

65. Ciocca DR, Arrigo AP, Calderwood SK: **Heat shock proteins and heat shock factor 1 in carcinogenesis and tumor development: an update.** *Arch Toxicol* 2013, **87:**19-48.

66. O'Connell K, Prencipe M, O'Neill A, Corcoran C, Rani S, Henry M, Dowling P, Meleady P, O'Driscoll L, Watson W, O'Connor R: **The use of LC-MS to identify differentially expressed proteins in docetaxel-resistant prostate cancer cell lines.** *Proteomics* 2012, **12:**2115-2126.

67. Gabai VL, Budagova KR, Sherman MY: **Increased expression of the major heat shock protein Hsp72 in human prostate carcinoma cells is dispensable for their viability but confers resistance to a variety of anticancer agents.** *Oncogene* 2005, **24:**3328-3338.

68. Ren A, Yan G, You B, Sun J: **Down-regulation of mammalian sterile 20-like kinase 1 by heat shock protein 70 mediates cisplatin resistance in prostate cancer cells.** *Cancer Res* 2008, **68:**2266-2274.

69. Whitesell L, Lindquist SL: **HSP90 and the chaperoning of cancer.** *Nat Rev Cancer* 2005, **5:**761-772.

70. Neckers L: **Hsp90 inhibitors as novel cancer chemotherapeutic agents.** *Trends Mol Med* 2002, **8:**S55-61.

71. Kang SH, Kang KW, Kim KH, Kwon B, Kim SK, Lee HY, Kong SY, Lee ES, Jang SG, Yoo BC: **Upregulated HSP27 in human breast cancer cells reduces Herceptin susceptibility by increasing Her2 protein stability.** *BMC Cancer* 2008, **8:**286.

72. Pavan S, Musiani D, Torchiaro E, Migliardi G, Gai M, Cunto FD, Erriquez J, Olivero M, Renzo MF: **HSP27 is required for invasion and metastasis triggered by hepatocyte growth factor.** *Int J Cancer* 2013.

73. Shiota M, Bishop JL, Nip KM, Zardan A, Takeuchi A, Cordonnier T, Beraldi E, Bazov J, Fazli L, Chi K, et al: **Hsp27 regulates epithelial mesenchymal transition, metastasis, and circulating tumor cells in prostate cancer.** *Cancer Res* 2013, **73:**3109-3119.

74. Zhu Z, Xu X, Yu Y, Graham M, Prince ME, Carey TE, Sun D: **Silencing heat shock protein 27 decreases metastatic behavior of human head and neck squamous cell cancer cells in vitro.** *Mol Pharm* 2010, **7:**1283-1290.

75. Xia Y, Rocchi P, Iovanna JL, Peng L: **Targeting heat shock response pathways to treat pancreatic cancer.** *Drug Discov Today* 2012, **17:**35-43.

76. Munoz M, Henderson M, Haber M, Norris M: **Role of the MRP1/ABCC1 multidrug transporter protein in cancer.** *IUBMB Life* 2007, **59:**752-757.

77. David-Beabes GL, Overman MJ, Petrofski JA, Campbell PA, de Marzo AM, Nelson WG: **Doxorubicin-resistant variants of human prostate cancer cell lines DU 145, PC-3, PPC-1, and TSU-PR1: characterization of biochemical determinants of antineoplastic drug sensitivity.** *Int J Oncol* 2000, **17:**1077-1086.

78. Zalcberg J, Hu XF, Slater A, Parisot J, El-Osta S, Kantharidis P, Chou ST, Parkin JD: **MRP1 not MDR1 gene expression is the predominant mechanism of acquired multidrug resistance in two prostate carcinoma cell lines.** *Prostate Cancer Prostatic Dis* 2000, **3:**66-75.

79. Lee JT, Steelman LS, McCubrey JA: **Phosphatidylinositol 3'-kinase activation leads to multidrug resistance protein-1 expression and subsequent chemoresistance in advanced prostate cancer cells.** *Cancer Res* 2004, **64:**8397-8404.

80. Schummer B, Siegsmund M, Steidler A, Toktomambetova L, Köhrmann KU, Alken P: **Expression of the gene for the multidrug resistance-associated protein in human prostate tissue.** *Urol Res* 1999, **27:**164-168.

81. Theyer G, Schirmböck M, Thalhammer T, Sherwood ER, Baumgartner G, Hamilton G: **Role of the MDR-1-encoded multiple drug resistance phenotype in prostate cancer cell lines.** *J Urol* 1993, **150:**1544-1547.

82. Ranganathan S, Benetatos CA, Colarusso PJ, Dexter DW, Hudes GR: **Altered beta-tubulin isotype expression in paclitaxel-resistant human prostate carcinoma cells.** *Br J Cancer* 1998, **77:**562-566.

83. Takeda M, Mizokami A, Mamiya K, Li YQ, Zhang J, Keller ET, Namiki M: **The establishment of two paclitaxel-resistant prostate cancer cell lines and the mechanisms of paclitaxel resistance with two cell lines.** *Prostate* 2007, **67:**955-967.

84. Liu B, Staren ED, Iwamura T, Appert HE, Howard JM: **Mechanisms of taxotere-related drug resistance in pancreatic carcinoma.** *J Surg Res* 2001, **99:**179-186.

85. Yu D, Liu B, Jing T, Sun D, Price JE, Singletary SE, Ibrahim N, Hortobagyi GN, Hung MC: **Overexpression of both p185c-erbB2 and p170mdr-1 renders breast cancer cells highly resistant to taxol.** *Oncogene* 1998, **16:**2087-2094.

86. Qiao L, Wong BC: **Targeting apoptosis as an approach for gastrointestinal cancer therapy.** *Drug Resist Updat* 2009, **12:**55-64.

87. Soengas MS, Lowe SW: **Apoptosis and melanoma chemoresistance.** *Oncogene* 2003, **22:**3138-3151.

88. Fiandalo MV, Kyprianou N: **Caspase control: protagonists of cancer cell apoptosis.** *Exp Oncol* 2012, **34:**165-175.

89. Devarajan E, Sahin AA, Chen JS, Krishnamurthy RR, Aggarwal N, Brun AM, Sapino A, Zhang F, Sharma D, Yang XH, et al: **Down-regulation of caspase 3 in breast cancer: a possible mechanism for chemoresistance.** *Oncogene* 2002, **21:**8843-8851.

90. O'Neill AJ, Prencipe M, Dowling C, Fan Y, Mulrane L, Gallagher WM, O'Connor D, O'Connor R, Devery A, Corcoran C, et al: **Characterisation and manipulation of docetaxel resistant prostate cancer cell lines.** *Mol Cancer* 2011, **10:**126.

91. Haarman EG, Kaspers GJ, Pieters R, van Zantwijk CH, Broekema GJ, Hählen K, Veerman AJ: **BCL-2 expression in childhood leukemia versus spontaneous apoptosis, drug induced apoptosis, and in vitro drug resistance.** *Adv Exp Med Biol* 1999, **457:**325-333.

92. Borgovan T, Bellistri JP, Slack KN, Kopelovich L, Desai M, Joe AK: **Inhibition of BCL2 expression and activity increases H460 sensitivity to the growth inhibitory effects of polyphenon E.** *J Exp Ther Oncol* 2009, **8:**129-144.

93. Volm M, Mattern J: **Increased expression of bcl-2 in drug-resistant squamous-cell lung carcinomas.** *Int J Oncol* 1995, **7:**1333-1338.

94. Vila M, Przedborski S: **Targeting programmed cell death in neurodegenerative diseases.** *Nat Rev Neurosci* 2003, **4:**365-375.

95. Lu J, Getz G, Miska EA, Alvarez-Saavedra E, Lamb J, Peck D, Sweet-Cordero A, Ebert BL, Mak RH, Ferrando AA, et al: **MicroRNA expression profiles classify human cancers.** *Nature* 2005, **435:**834-838.

96. Rosenfeld N, Aharonov R, Meiri E, Rosenwald S, Spector Y, Zepeniuk M, Benjamin H, Shabes N, Tabak S, Levy A, et al: **MicroRNAs accurately identify cancer tissue origin.** *Nat Biotechnol* 2008, **26:**462-469.

97. Metias S, Lianidou E, Yousef G: **MicroRNAs in clinical oncology: at the crossroads between promises and problems.** *J Clin Pathol* 2009, **62:**771-776.

98. Hennessy E, O'Driscoll L: **Molecular medicine of microRNAs: structure, function and implications for diabetes.** *Expert Rev Mol Med* 2008, **10:**e24.

99. Borchert G, Lanier W, Davidson B: **RNA polymerase III transcribes human microRNAs.** *Nat Struct Mol Biol* 2006, **13:**1097-1101.

100. Gregory R, Yan K, Amuthan G, Chendrimada T, Doratotaj B, Cooch N, Shiekhattar R: **The Microprocessor complex mediates the genesis of microRNAs.** *Nature* 2004, **432:**235-240.

101. Han J, Lee Y, Yeom K, Kim Y, Jin H, Kim V: **The Drosha-DGCR8 complex in primary microRNA processing.** *Genes Dev* 2004, **18:**3016-3027.

102. Lee Y, Ahn C, Han J, Choi H, Kim J, Yim J, Lee J, Provost P, Rådmark O, Kim S, Kim V: **The nuclear RNase III Drosha initiates microRNA processing.** *Nature* 2003, **425:**415-419.

103. Lee R, Feinbaum R, Ambros V: **The C. elegans heterochronic gene lin-4 encodes small RNAs with antisense complementarity to lin-14.** *Cell* 1993, **75:**843-854.

104. Friedman R, Farh K, Burge C, Bartel D: **Most mammalian mRNAs are conserved targets of microRNAs.** *Genome Res* 2009, **19:**92-105.

105. Hayashita Y, Osada H, Tatematsu Y, Yamada H, Yanagisawa K, Tomida S, Yatabe Y, Kawahara K, Sekido Y, Takahashi T: **A polycistronic microRNA cluster, miR-17-92, is overexpressed in human lung cancers and enhances cell proliferation.** *Cancer Res* 2005, **65:**9628-9632.

106. Zhang B, Pan X, Anderson T: **MicroRNA: a new player in stem cells.** *J Cell Physiol* 2006, **209:**266-269.

107. Jovanovic M, Hengartner M: **miRNAs and apoptosis: RNAs to die for.** *Oncogene* 2006, **25:**6176-6187.

108. Calin G, Dumitru C, Shimizu M, Bichi R, Zupo S, Noch E, Aldler H, Rattan S, Keating M, Rai K, et al: **Frequent deletions and down-regulation of micro- RNA genes miR15 and miR16 at 13q14 in chronic lymphocytic leukemia.** *Proc Natl Acad Sci U S A* 2002, **99:**15524-15529.

109. Iorio M, Ferracin M, Liu C, Veronese A, Spizzo R, Sabbioni S, Magri E, Pedriali M, Fabbri M, Campiglio M, et al: **MicroRNA gene expression deregulation in human breast cancer.** *Cancer Res* 2005, **65:**7065-7070.

110. Coppola V, De Maria R, Bonci D: **MicroRNAs and prostate cancer.** *Endocr Relat Cancer* 2010, **17:**F1-17.

111. Takamizawa J, Konishi H, Yanagisawa K, Tomida S, Osada H, Endoh H, Harano T, Yatabe Y, Nagino M, Nimura Y, et al: **Reduced expression of the let-7 microRNAs in human lung cancers in association with shortened postoperative survival.** *Cancer Res* 2004, **64:**3753-3756.

112. Yanaihara N, Caplen N, Bowman E, Seike M, Kumamoto K, Yi M, Stephens R, Okamoto A, Yokota J, Tanaka T, et al: **Unique microRNA molecular profiles in lung cancer diagnosis and prognosis.** *Cancer Cell* 2006, **9:**189-198.

113. Michael M, O' Connor S, van Holst Pellekaan N, Young G, James R: **Reduced accumulation of specific microRNAs in colorectal neoplasia.** *Mol Cancer Res* 2003, **1:**882-891.

114. Zhang B, Pan X, Cobb G, Anderson T: **microRNAs as oncogenes and tumor suppressors.** *Dev Biol* 2007, **302:**1-12.

115. Manikandan J, Aarthi J, Kumar S, Pushparaj P: **Oncomirs: The potential role of non-coding microRNAs in understanding cancer.** *Bioinformation* 2008, **2:**330-334.

116. Selcuklu SD, Donoghue MT, Spillane C: **miR-21 as a key regulator of oncogenic processes.** *Biochem Soc Trans* 2009, **37:**918-925.

117. Spandidos D, Anderson M: **Oncogenes and onco-suppressor genes: their involvement in cancer.** *J Pathol* 1989, **157:**1-10.

118. Lu Z, Liu M, Stribinskis V, Klinge C, Ramos K, Colburn N, Li Y: **MicroRNA-21 promotes cell transformation by targeting the programmed cell death 4 gene.** *Oncogene* 2008, **27:**4373-4379.

119. Frankel L, Christoffersen N, Jacobsen A, Lindow M, Krogh A, Lund A: **Programmed cell death 4 (PDCD4) is an important functional target of the microRNA miR-21 in breast cancer cells.** *J Biol Chem* 2008, **283:**1026-1033.

120. Coppola V, Musumeci M, Patrizii M, Cannistraci A, Addario A, Maugeri-Saccà M, Biffoni M, Francescangeli F, Cordenonsi M, Piccolo S, et al: **BTG2 loss and miR-21 upregulation contribute to prostate cell transformation by inducing luminal markers expression and epithelial-mesenchymal transition.** *Oncogene* 2013, **32:**1843-1853.

121. Yan LX, Wu QN, Zhang Y, Li YY, Liao DZ, Hou JH, Fu J, Zeng MS, Yun JP, Wu QL, et al: **Knockdown of miR-21 in human breast cancer cell lines inhibits proliferation, in vitro migration and in vivo tumor growth.** *Breast Cancer Res* 2011, **13:**R2.

122. Reis ST, Pontes-Junior J, Antunes AA, Dall'Oglio MF, Dip N, Passerotti CC, Rossini GA, Morais DR, Nesrallah AJ, Piantino C, et al: **miR-21 may acts as an oncomir by targeting RECK, a matrix metalloproteinase regulator, in prostate cancer.** *BMC Urol* 2012, **12:**14.

123. Si M, Zhu S, Wu H, Lu Z, Wu F, Mo Y: **miR-21-mediated tumor growth.** *Oncogene* 2007, **26:**2799-2803.

124. Li T, Li D, Sha J, Sun P, Huang Y: **MicroRNA-21 directly targets MARCKS and promotes apoptosis resistance and invasion in prostate cancer cells.** *Biochem Biophys Res Commun* 2009, **383:**280-285.

125. Zhu S, Si M, Wu H, Mo Y: **MicroRNA-21 targets the tumor suppressor gene tropomyosin 1 (TPM1).** *J Biol Chem* 2007, **282:**14328-14336.

126. Song B, Wang C, Liu J, Wang X, Lv L, Wei L, Xie L, Zheng Y, Song X: **MicroRNA-21 regulates breast cancer invasion partly by targeting tissue inhibitor of metalloproteinase 3 expression.** *J Exp Clin Cancer Res* 2010, **29:**29.

127. Mertens-Talcott S, Chintharlapalli S, Li X, Safe S: **The oncogenic microRNA-27a targets genes that regulate specificity protein transcription factors and the G2-M checkpoint in MDA-MB-231 breast cancer cells.** *Cancer Res* 2007, **67:**11001-11011.

128. Fletcher CE, Dart DA, Sita-Lumsden A, Cheng H, Rennie PS, Bevan CL: **Androgen-regulated processing of the oncomir miR-27a, which targets Prohibitin in prostate cancer.** *Hum Mol Genet* 2012, **21:**3112-3127.

129. Scott G, Mattie M, Berger C, Benz S, Benz C: **Rapid alteration of microRNA levels by histone deacetylase inhibition.** *Cancer Res* 2006, **66:**1277-1281.

130. Guttilla I, White B: **Coordinate regulation of FOXO1 by miR-27a, miR-96, and miR-182 in breast cancer cells.** *J Biol Chem* 2009, **284:**23204-23216.

131. Mo W, Zhang J, Li X, Meng D, Gao Y, Yang S, Wan X, Zhou C, Guo F, Huang Y, et al: **Identification of novel AR-targeted microRNAs mediating androgen signalling through critical pathways to regulate cell viability in prostate cancer.** *PLoS One* 2013, **8:**e56592.

132. Nassirpour R, Mehta PP, Baxi SM, Yin MJ: **miR-221 promotes tumorigenesis in human triple negative breast cancer cells.** *PLoS One* 2013, **8:**e62170.

133. Galardi S, Mercatelli N, Giorda E, Massalini S, Frajese GV, Ciafrè SA, Farace MG: **miR-221 and miR-222 expression affects the proliferation potential of human prostate carcinoma cell lines by targeting p27Kip1.** *J Biol Chem* 2007, **282:**23716-23724.

134. Guttilla IK, Phoenix KN, Hong X, Tirnauer JS, Claffey KP, White BA: **Prolonged mammosphere culture of MCF-7 cells induces an EMT and repression of the estrogen receptor by microRNAs.** *Breast Cancer Res Treat* 2012, **132:**75-85.

135. Mercatelli N, Coppola V, Bonci D, Miele F, Costantini A, Guadagnoli M, Bonanno E, Muto G, Frajese GV, De Maria R, et al: **The inhibition of the highly expressed miR-221 and miR-222 impairs the growth of prostate carcinoma xenografts in mice.** *PLoS One* 2008, **3:**e4029.

136. Zou C, Xu Q, Mao F, Li D, Bian C, Liu LZ, Jiang Y, Chen X, Qi Y, Zhang X, et al: **MiR-145 inhibits tumor angiogenesis and growth by N-RAS and VEGF.** *Cell Cycle* 2012, **11:**2137-2145.

137. Hart M, Wach S, Nolte E, Szczyrba J, Menon R, Taubert H, Hartmann A, Stoehr R, Wieland W, Grässer FA, Wullich B: **The proto-oncogene ERG is a target of microRNA miR-145 in prostate cancer.** *FEBS J* 2013, **280:**2105-2116.

138. Spizzo R, Nicoloso M, Lupini L, Lu Y, Fogarty J, Rossi S, Zagatti B, Fabbri M, Veronese A, Liu X, et al: **miR-145 participates with TP53 in a death-promoting regulatory loop and targets estrogen receptor-alpha in human breast cancer cells.** *Cell Death Differ* 2010, **17:**246-254.

139. Huang S, Guo W, Tang Y, Ren D, Zou X, Peng X: **miR-143 and miR-145 inhibit stem cell characteristics of PC-3 prostate cancer cells.** *Oncol Rep* 2012, **28:**1831-1837.

140. Wang S, Bian C, Yang Z, Bo Y, Li J, Zeng L, Zhou H, Zhao R: **miR-145 inhibits breast cancer cell growth through RTKN.** *Int J Oncol* 2009, **34:**1461-1466.

141. Avgeris M, Stravodimos K, Fragoulis EG, Scorilas A: **The loss of the tumour-suppressor miR-145 results in the shorter disease-free survival of prostate cancer patients.** *Br J Cancer* 2013, **108:**2573-2581.

142. Iorio M, Casalini P, Piovan C, Di Leva G, Merlo A, Triulzi T, Ménard S, Croce C, Tagliabue E: **microRNA-205 regulates HER3 in human breast cancer.** *Cancer Res* 2009, **69:**2195-2200.

143. Verdoodt B, Neid M, Vogt M, Kuhn V, Liffers ST, Palisaar RJ, Noldus J, Tannapfel A, Mirmohammadsadegh A: **MicroRNA-205, a novel regulator of the anti-apoptotic protein Bcl2, is downregulated in prostate cancer.** *Int J Oncol* 2013, **43:**307-314.

144. Wu H, Zhu S, Mo Y: **Suppression of cell growth and invasion by miR-205 in breast cancer.** *Cell Res* 2009, **19:**439-448.

145. Liu J, Mao Q, Liu Y, Hao X, Zhang S, Zhang J: **Analysis of miR-205 and miR-155 expression in the blood of breast cancer patients.** *Chin J Cancer Res* 2013, **25:**46-54.

146. Gandellini P, Profumo V, Casamichele A, Fenderico N, Borrelli S, Petrovich G, Santilli G, Callari M, Colecchia M, Pozzi S, et al: **miR-205 regulates basement membrane deposition in human prostate: implications for cancer development.** *Cell Death Differ* 2012, **19:**1750-1760.

147. Piovan C, Palmieri D, Di Leva G, Braccioli L, Casalini P, Nuovo G, Tortoreto M, Sasso M, Plantamura I, Triulzi T, et al: **Oncosuppressive role of p53-induced miR-205 in triple negative breast cancer.** *Mol Oncol* 2012, **6:**458-472.

148. Majid S, Dar AA, Saini S, Yamamura S, Hirata H, Tanaka Y, Deng G, Dahiya R: **MicroRNA-205-directed transcriptional activation of tumor suppressor genes in prostate cancer.** *Cancer* 2010, **116:**5637-5649.

149. Hossain A, Kuo M, Saunders G: **Mir-17-5p regulates breast cancer cell proliferation by inhibiting translation of AIB1 mRNA.** *Mol Cell Biol* 2006, **26:**8191-8201.

150. Xu Y, Fang F, Zhang J, Josson S, St Clair WH, St Clair DK: **miR-17* suppresses tumorigenicity of prostate cancer by inhibiting mitochondrial antioxidant enzymes.** *PLoS One* 2010, **5:**e14356.

151. Shen J, Ambrosone CB, Zhao H: **Novel genetic variants in microRNA genes and familial breast cancer.** *Int J Cancer* 2009, **124:**1178-1182.

152. Zhang X, Ladd A, Dragoescu E, Budd WT, Ware JL, Zehner ZE: **MicroRNA-17-3p is a prostate tumor suppressor in vitro and in vivo, and is decreased in high grade prostate tumors analyzed by laser capture microdissection.** *Clin Exp Metastasis* 2009, **26:**965-979.

153. Gong AY, Eischeid AN, Xiao J, Zhao J, Chen D, Wang ZY, Young CY, Chen XM: **miR-17-5p targets the p300/CBP-associated factor and modulates androgen receptor transcriptional activity in cultured prostate cancer cells.** *BMC Cancer* 2012, **12:**492.

154. Huang Q, Gumireddy K, Schrier M, le Sage C, Nagel R, Nair S, Egan D, Li A, Huang G, Klein-Szanto A, et al: **The microRNAs miR-373 and miR-520c promote tumour invasion and metastasis.** *Nat Cell Biol* 2008, **10:**202-210.

155. Yang K, Handorean AM, Iczkowski KA: **MicroRNAs 373 and 520c are downregulated in prostate cancer, suppress CD44 translation and enhance invasion of prostate cancer cells in vitro.** *Int J Clin Exp Pathol* 2009, **2:**361-369.

156. Han M, Liu M, Wang Y, Mo Z, Bi X, Liu Z, Fan Y, Chen X, Wu C: **Re-expression of miR-21 contributes to migration and invasion by inducing epithelial-mesenchymal transition consistent with cancer stem cell characteristics in MCF-7 cells.** *Mol Cell Biochem* 2012, **363:**427-436.

157. Connolly EC, Van Doorslaer K, Rogler LE, Rogler CE: **Overexpression of miR-21 promotes an in vitro metastatic phenotype by targeting the tumor suppressor RHOB.** *Mol Cancer Res* 2010, **8:**691-700.

158. Huang T, Wu F, Loeb G, Hsu R, Heidersbach A, Brincat A, Horiuchi D, Lebbink R, Mo Y, Goga A, McManus M: **Up-regulation of miR-21 by HER2/neu signaling promotes cell invasion.** *J Biol Chem* 2009, **284:**18515-18524.

159. Li L, Xie X, Luo J, Liu M, Xi S, Guo J, Kong Y, Wu M, Gao J, Xie Z, et al: **Targeted expression of miR-34a using the T-VISA system suppresses breast cancer cell growth and invasion.** *Mol Ther* 2012, **20:**2326-2334.

160. Li L, Yuan L, Luo J, Gao J, Guo J, Xie X: **MiR-34a inhibits proliferation and migration of breast cancer through down-regulation of Bcl-2 and SIRT1.** *Clin Exp Med* 2013, **13:**109-117.

161. Yang S, Li Y, Gao J, Zhang T, Li S, Luo A, Chen H, Ding F, Wang X, Liu Z: **MicroRNA-34 suppresses breast cancer invasion and metastasis by directly targeting Fra-1.** *Oncogene* 2013, **32:**4294-4303.

162. Liu C, Kelnar K, Liu B, Chen X, Calhoun-Davis T, Li H, Patrawala L, Yan H, Jeter C, Honorio S, et al: **The microRNA miR-34a inhibits prostate cancer stem cells and metastasis by directly repressing CD44.** *Nat Med* 2011, **17:**211-215.

163. Kashat M, Azzouz L, Sarkar SH, Kong D, Li Y, Sarkar FH: **Inactivation of AR and Notch-1 signaling by miR-34a attenuates prostate cancer aggressiveness.** *Am J Transl Res* 2012, **4:**432-442.

164. Wang R, Wang HB, Hao CJ, Cui Y, Han XC, Hu Y, Li FF, Xia HF, Ma X: **MiR-101 is involved in human breast carcinogenesis by targeting Stathmin1.** *PLoS One* 2012, **7:**e46173.

165. Varambally S, Cao Q, Mani RS, Shankar S, Wang X, Ateeq B, Laxman B, Cao X, Jing X, Ramnarayanan K, et al: **Genomic loss of microRNA-101 leads to overexpression of histone methyltransferase EZH2 in cancer.** *Science* 2008, **322:**1695-1699.

166. Ren G, Baritaki S, Marathe H, Feng J, Park S, Beach S, Bazeley PS, Beshir AB, Fenteany G, Mehra R, et al: **Polycomb protein EZH2 regulates tumor invasion via the transcriptional repression of the metastasis suppressor RKIP in breast and prostate cancer.** *Cancer Res* 2012, **72:**3091-3104.

167. Valastyan S, Reinhardt F, Benaich N, Calogrias D, Szász A, Wang Z, Brock J, Richardson A, Weinberg R: **A pleiotropically acting microRNA, miR-31, inhibits breast cancer metastasis.** *Cell* 2009, **137:**1032-1046.

168. Fuse M, Kojima S, Enokida H, Chiyomaru T, Yoshino H, Nohata N, Kinoshita T, Sakamoto S, Naya Y, Nakagawa M, et al: **Tumor suppressive microRNAs (miR-222 and**

miR-31) regulate molecular pathways based on microRNA expression signature in prostate cancer. *J Hum Genet* 2012, **57:**691-699.

169. Lin PC, Chiu YL, Banerjee S, Park K, Mosquera JM, Giannopoulou E, Alves P, Tewari AK, Gerstein MB, Beltran H, et al: **Epigenetic repression of miR-31 disrupts androgen receptor homeostasis and contributes to prostate cancer progression.** *Cancer Res* 2013, **73:**1232-1244.

170. Hurst DR, Edmonds MD, Scott GK, Benz CC, Vaidya KS, Welch DR: **Breast cancer metastasis suppressor 1 up-regulates miR-146, which suppresses breast cancer metastasis.** *Cancer Res* 2009, **69:**1279-1283.

171. Wang D, Liu D, Gao J, Liu M, Liu S, Jiang M, Liu Y, Zheng D: **TRAIL-induced miR-146a expression suppresses CXCR4-mediated human breast cancer migration.** *FEBS J* 2013, **280:**3340-3353.

172. Xu B, Wang N, Wang X, Tong N, Shao N, Tao J, Li P, Niu X, Feng N, Zhang L, et al: **MiR-146a suppresses tumor growth and progression by targeting EGFR pathway and in a p-ERK-dependent manner in castration-resistant prostate cancer.** *Prostate* 2012, **72:**1171-1178.

173. Lin SL, Chiang A, Chang D, Ying SY: **Loss of mir-146a function in hormone-refractory prostate cancer.** *RNA* 2008, **14:**417-424.

174. Zhang Y, Yang P, Sun T, Li D, Xu X, Rui Y, Li C, Chong M, Ibrahim T, Mercatali L, et al: **miR-126 and miR-126* repress recruitment of mesenchymal stem cells and inflammatory monocytes to inhibit breast cancer metastasis.** *Nat Cell Biol* 2013, **15:**284-294.

175. Musiyenko A, Bitko V, Barik S: **Ectopic expression of miR-126*, an intronic product of the vascular endothelial EGF-like 7 gene, regulates prostein translation and invasiveness of prostate cancer LNCaP cells.** *J Mol Med (Berl)* 2008, **86:**313-322.

176. Bu Y, Lu C, Bian C, Wang J, Li J, Zhang B, Li Z, Brewer G, Zhao RC: **Knockdown of Dicer in MCF-7 human breast carcinoma cells results in G1 arrest and increased sensitivity to cisplatin.** *Oncol Rep* 2009, **21:**13-17.

177. Bourguignon LY, Spevak CC, Wong G, Xia W, Gilad E: **Hyaluronan-CD44 interaction with protein kinase C(epsilon) promotes oncogenic signaling by the stem cell marker Nanog and the Production of microRNA-21, leading to down-regulation of the tumor suppressor protein PDCD4, anti-apoptosis, and chemotherapy resistance in breast tumor cells.** *J Biol Chem* 2009, **284:**26533-26546.

178. Mei M, Ren Y, Zhou X, Yuan XB, Han L, Wang GX, Jia Z, Pu PY, Kang CS, Yao Z: **Downregulation of miR-21 enhances chemotherapeutic effect of taxol in breast carcinoma cells.** *Technol Cancer Res Treat* 2010, **9:**77-86.

179. Gong C, Yao Y, Wang Y, Liu B, Wu W, Chen J, Su F, Yao H, Song E: **Up-regulation of miR-21 mediates resistance to trastuzumab therapy for breast cancer.** *J Biol Chem* 2011, **286:**19127-19137.

180. Wang ZX, Lu BB, Wang H, Cheng ZX, Yin YM: **MicroRNA-21 modulates chemosensitivity of breast cancer cells to doxorubicin by targeting PTEN.** *Arch Med Res* 2011, **42:**281-290.

181. Anastasov N, Höfig I, Vasconcellos IG, Rappl K, Braselmann H, Ludyga N, Auer G, Aubele M, Atkinson MJ: **Radiation resistance due to high expression of miR-21 and G2/M checkpoint arrest in breast cancer cells.** *Radiat Oncol* 2012, **7:**206.

182. Ribas J, Ni X, Haffner M, Wentzel EA, Salmasi AH, Chowdhury WH, Kudrolli TA, Yegnasubramanian S, Luo J, Rodriguez R, et al: **miR-21: an androgen receptor-regulated microRNA that promotes hormone-dependent and hormone-independent prostate cancer growth.** *Cancer Res* 2009, **69:**7165-7169.

183. Shi GH, Ye DW, Yao XD, Zhang SL, Dai B, Zhang HL, Shen YJ, Zhu Y, Zhu YP, Xiao WJ, Ma CG: **Involvement of microRNA-21 in mediating chemo-resistance to docetaxel in androgen-independent prostate cancer PC3 cells.** *Acta Pharmacol Sin* 2010, **31:**867-873.

184. Kastl L, Brown I, Schofield AC: **miRNA-34a is associated with docetaxel resistance in human breast cancer cells.** *Breast Cancer Res Treat* 2012, **131:**445-454.

185. Li XJ, Ji MH, Zhong SL, Zha QB, Xu JJ, Zhao JH, Tang JH: **MicroRNA-34a modulates chemosensitivity of breast cancer cells to adriamycin by targeting Notch1.** *Arch Med Res* 2012, **43:**514-521.

186. Hui C, Yujie F, Lijia Y, Long Y, Hongxia X, Yong Z, Jundong Z, Qianyong Z, Mantian M: **MicroRNA-34a and microRNA-21 play roles in the chemopreventive effects of 3,6-dihydroxyflavone on 1-methyl-1-nitrosourea-induced breast carcinogenesis.** *Breast Cancer Res* 2012, **14:**R80.

187. Fujita Y, Kojima K, Hamada N, Ohhashi R, Akao Y, Nozawa Y, Deguchi T, Ito M: **Effects of miR-34a on cell growth and chemoresistance in prostate cancer PC3 cells.** *Biochem Biophys Res Commun* 2008, **377:**114-119.

188. Kojima K, Fujita Y, Nozawa Y, Deguchi T, Ito M: **MiR-34a attenuates paclitaxel-resistance of hormone-refractory prostate cancer PC3 cells through direct and indirect mechanisms.** *Prostate* 2010, **70:**1501-1512.

189. Cochrane DR, Spoelstra NS, Howe EN, Nordeen SK, Richer JK: **MicroRNA-200c mitigates invasiveness and restores sensitivity to microtubule-targeting chemotherapeutic agents.** *Mol Cancer Ther* 2009, **8:**1055-1066.

190. Chen J, Tian W, Cai H, He H, Deng Y: **Down-regulation of microRNA-200c is associated with drug resistance in human breast cancer.** *Med Oncol* 2012, **29:**2527-2534.

191. Lin J, Liu C, Gao F, Mitchel RE, Zhao L, Yang Y, Lei J, Cai J: **miR-200c enhances radiosensitivity of human breast cancer cells.** *J Cell Biochem* 2013, **114:**606-615.

192. Kopp F, Oak PS, Wagner E, Roidl A: **miR-200c sensitizes breast cancer cells to doxorubicin treatment by decreasing TrkB and Bmi1 expression.** *PLoS One* 2012, **7:**e50469.

193. Manavalan TT, Teng Y, Litchfield LM, Muluhngwi P, Al-Rayyan N, Klinge CM: **Reduced expression of miR-200 family members contributes to antiestrogen resistance in LY2 human breast cancer cells.** *PLoS One* 2013, **8:**e62334.

194. Puhr M, Hoefer J, Schäfer G, Erb HH, Oh SJ, Klocker H, Heidegger I, Neuwirt H, Culig Z: **Epithelial-to-mesenchymal transition leads to docetaxel resistance in prostate cancer and is mediated by reduced expression of miR-200c and miR-205.** *Am J Pathol* 2012, **181:**2188-2201.

195. Watahiki A, Macfarlane RJ, Gleave ME, Crea F, Wang Y, Helgason CD, Chi KN: **Plasma miRNAs as Biomarkers to Identify Patients with Castration-Resistant Metastatic Prostate Cancer.** *Int J Mol Sci* 2013, **14:**7757-7770.

196. Bhatnagar N, Li X, Padi SK, Zhang Q, Tang MS, Guo B: **Downregulation of miR-205 and miR-31 confers resistance to chemotherapy-induced apoptosis in prostate cancer cells.** *Cell Death Dis* 2010, **1:**e105.

197. Körner C, Keklikoglou I, Bender C, Wörner A, Münstermann E, Wiemann S: **MicroRNA-31 sensitizes human breast cells to apoptosis by direct targeting of protein kinase C epsilon (PKCepsilon).** *J Biol Chem* 2013, **288:**8750-8761.

198. Jung EJ, Santarpia L, Kim J, Esteva FJ, Moretti E, Buzdar AU, Di Leo A, Le XF, Bast RC, Park ST, et al: **Plasma microRNA 210 levels correlate with sensitivity to trastuzumab and tumor presence in breast cancer patients.** *Cancer* 2012, **118:**2603-2614.

199. Cheng HH, Mitchell PS, Kroh EM, Dowell AE, Chéry L, Siddiqui J, Nelson PS, Vessella RL, Knudsen BS, Chinnaiyan AM, et al: **Circulating microRNA profiling identifies a subset of metastatic prostate cancer patients with evidence of cancer-associated hypoxia.** *PLoS One* 2013, **8:**e69239.

200. Uehara M, Kinoshita T, Hojo T, Akashi-Tanaka S, Iwamoto E, Fukutomi T: **Long-term prognostic study of carcinoembryonic antigen (CEA) and carbohydrate antigen 15-3 (CA 15-3) in breast cancer.** *Int J Clin Oncol* 2008, **13:**447-451.

201. O'Driscoll L, Kenny E, Mehta J, Doolan P, Joyce H, Gammell P, Hill A, O'Daly B, O'Gorman D, Clynes M: **Feasibility and relevance of global expression profiling of gene transcripts in serum from breast cancer patients using whole genome microarrays and quantitative RT-PCR.** *Cancer Genomics Proteomics* 2008, **5:**94-104.

202. Tsang J, Lo Y: **Circulating nucleic acids in plasma/serum.** *Pathology* 2007, **39:**197-207.

203. Gilad S, Meiri E, Yogev Y, Benjamin S, Lebanony D, Yerushalmi N, Benjamin H, Kushnir M, Cholakh H, Melamed N, et al: **Serum microRNAs are promising novel biomarkers.** *PLoS One* 2008, **3:**e3148.

204. Mitchell P, Parkin R, Kroh E, Fritz B, Wyman S, Pogosova-Agadjanyan E, Peterson A, Noteboom J, O'Briant K, Allen A, et al: **Circulating microRNAs as stable blood-based markers for cancer detection.** *Proc Natl Acad Sci U S A* 2008, **105:**10513-10518.

205. Chen X, Ba Y, Ma L, Cai X, Yin Y, Wang K, Guo J, Zhang Y, Chen J, Guo X, et al: **Characterization of microRNAs in serum: a novel class of biomarkers for diagnosis of cancer and other diseases.** *Cell Res* 2008, **18:**997-1006.

206. Rani S, Gately K, Crown J, O'Byrne K, O'Driscoll L: **Global analysis of serum microRNAs as potential biomarkers for lung adenocarcinoma.** *Cancer Biol Ther* 2013, **14**.

207. Xi Y, Nakajima G, Gavin E, Morris C, Kudo K, Hayashi K, Ju J: **Systematic analysis of microRNA expression of RNA extracted from fresh frozen and formalin-fixed paraffin-embedded samples.** *RNA* 2007, **13:**1668-1674.

208. Lawrie C, Gal S, Dunlop H, Pushkaran B, Liggins A, Pulford K, Banham A, Pezzella F, Boultwood J, Wainscoat J, et al: **Detection of elevated levels of tumour-associated microRNAs in serum of patients with diffuse large B-cell lymphoma.** *Br J Haematol* 2008, **141:**672-675.

209. Wang J, Chen J, Chang P, LeBlanc A, Li D, Abbruzzesse J, Frazier M, Killary A, Sen S: **MicroRNAs in plasma of pancreatic ductal adenocarcinoma patients as novel blood-based biomarkers of disease.** *Cancer Prev Res (Phila Pa)* 2009, **2:**807-813.

210. Huang Z, Huang D, Ni S, Peng Z, Sheng W, Du X: **Plasma microRNAs are promising novel biomarkers for early detection of colorectal cancer.** *Int J Cancer* 2009 Oct 28, **[Epub ahead of print]**.

211. Ng E, Chong W, Jin H, Lam E, Shin V, Yu J, Poon T, Ng S, Sung J: **Differential expression of microRNAs in plasma of patients with colorectal cancer: a potential marker for colorectal cancer screening.** *Gut* 2009, **58:**1375-1381.

212. Zhu W, Qin W, Atasoy U, Sauter E: **Circulating microRNAs in breast cancer and healthy subjects.** *BMC Res Notes* 2009, **2:**89.

213. Heneghan H, Miller N, Lowery A, Sweeney K, Newell J, Kerin M: **Circulating microRNAs as novel minimally invasive biomarkers for breast cancer.** *Ann Surg* 2010, **251:**499-505.

214. Valadi H, Ekström K, Bossios A, Sjöstrand M, Lee JJ, Lötvall JO: **Exosome-mediated transfer of mRNAs and microRNAs is a novel mechanism of genetic exchange between cells.** *Nat Cell Biol* 2007, **9:**654-659.

215. Hunter M, Ismail N, Zhang X, Aguda B, Lee E, Yu L, Xiao T, Schafer J, Lee M, Schmittgen T, et al: **Detection of microRNA expression in human peripheral blood microvesicles.** *PLoS One* 2008, **3:**e3694.

216. Rabinowits G, Gerçel-Taylor C, Day J, Taylor D, Kloecker G: **Exosomal microRNA: a diagnostic marker for lung cancer.** *Clin Lung Cancer* 2009, **10:**42-46.

217. Taylor D, Gercel-Taylor C: **MicroRNA signatures of tumor-derived exosomes as diagnostic biomarkers of ovarian cancer.** *Gynecol Oncol* 2008, **110:**13-21.

218. O'Brien K, Rani S, Corcoran C, Wallace R, Hughes L, Friel AM, McDonnell S, Crown J, Radomski MW, O'Driscoll L: **Exosomes from triple-negative breast cancer cells can transfer phenotypic traits representing their cells of origin to secondary cells.** *Eur J Cancer* 2013, **49:**1845-1859.

219. Skog J, Würdinger T, van Rijn S, Meijer D, Gainche L, Sena-Esteves M, Curry WJ, Carter B, Krichevsky A, Breakefield X: **Glioblastoma microvesicles transport RNA and**

proteins that promote tumour growth and provide diagnostic biomarkers. *Nat Cell Biol* 2008, **10:**1470-1476.

220. Wang F, Zheng Z, Guo J, Ding X: **Correlation and quantitation of microRNA aberrant expression in tissues and sera from patients with breast tumor.** *Gynecol Oncol* 2010, **119:**586-593.

221. Yaman Agaoglu F, Kovancilar M, Dizdar Y, Darendeliler E, Holdenrieder S, Dalay N, Gezer U: **Investigation of miR-21, miR-141, and miR-221 in blood circulation of patients with prostate cancer.** *Tumour Biol* 2011, **32:**583-588.

222. Asaga S, Kuo C, Nguyen T, Terpenning M, Giuliano AE, Hoon DS: **Direct serum assay for microRNA-21 concentrations in early and advanced breast cancer.** *Clin Chem* 2011, **57:**84-91.

223. Zhang HL, Yang LF, Zhu Y, Yao XD, Zhang SL, Dai B, Zhu YP, Shen YJ, Shi GH, Ye DW: **Serum miRNA-21: elevated levels in patients with metastatic hormone-refractory prostate cancer and potential predictive factor for the efficacy of docetaxel-based chemotherapy.** *Prostate* 2011, **71:**326-331.

224. Si H, Sun X, Chen Y, Cao Y, Chen S, Wang H, Hu C: **Circulating microRNA-92a and microRNA-21 as novel minimally invasive biomarkers for primary breast cancer.** *J Cancer Res Clin Oncol* 2013, **139:**223-229.

225. Madhavan D, Zucknick M, Wallwiener M, Cuk K, Modugno C, Scharpff M, Schott S, Heil J, Turchinovich A, Yang R, et al: **Circulating miRNAs as surrogate markers for circulating tumor cells and prognostic markers in metastatic breast cancer.** *Clin Cancer Res* 2012, **18:**5972-5982.

226. Bryant RJ, Pawlowski T, Catto JW, Marsden G, Vessella RL, Rhees B, Kuslich C, Visakorpi T, Hamdy FC: **Changes in circulating microRNA levels associated with prostate cancer.** *Br J Cancer* 2012, **106:**768-774.

227. Guo LJ, Zhang QY: **Decreased serum miR-181a is a potential new tool for breast cancer screening.** *Int J Mol Med* 2012, **30:**680-686.

228. Duijvesz D, Luider T, Bangma CH, Jenster G: **Exosomes as Biomarker Treasure Chests for Prostate Cancer.** *Eur Urol* 2010.

229. Simpson RJ, Jensen SS, Lim JW: **Proteomic profiling of exosomes: current perspectives.** *Proteomics* 2008, **8:**4083-4099.

230. Théry C, Zitvogel L, Amigorena S: **Exosomes: composition, biogenesis and function.** *Nat Rev Immunol* 2002, **2:**569-579.

231. Keller S, Sanderson MP, Stoeck A, Altevogt P: **Exosomes: from biogenesis and secretion to biological function.** *Immunol Lett* 2006, **107:**102-108.

232. Calzolari A, Raggi C, Deaglio S, Sposi NM, Stafsnes M, Fecchi K, Parolini I, Malavasi F, Peschle C, Sargiacomo M, Testa U: **TfR2 localizes in lipid raft domains and is released in exosomes to activate signal transduction along the MAPK pathway.** *J Cell Sci* 2006, **119:**4486-4498.

233. Safaei R, Larson BJ, Cheng TC, Gibson MA, Otani S, Naerdemann W, Howell SB: **Abnormal lysosomal trafficking and enhanced exosomal export of cisplatin in drug-resistant human ovarian carcinoma cells.** *Mol Cancer Ther* 2005, **4:**1595-1604.

234. Liu C, Yu S, Zinn K, Wang J, Zhang L, Jia Y, Kappes JC, Barnes S, Kimberly RP, Grizzle WE, Zhang HG: **Murine mammary carcinoma exosomes promote tumor growth by suppression of NK cell function.** *J Immunol* 2006, **176:**1375-1385.

235. Ginestra A, La Placa MD, Saladino F, Cassarà D, Nagase H, Vittorelli ML: **The amount and proteolytic content of vesicles shed by human cancer cell lines correlates with their in vitro invasiveness.** *Anticancer Res* 1998, **18:**3433-3437.

236. Clayton A, Mitchell JP, Court J, Mason MD, Tabi Z: **Human tumor-derived exosomes selectively impair lymphocyte responses to interleukin-2.** *Cancer Res* 2007, **67:**7458-7466.

237. Corcoran C, Rani S, O'Brien K, O'Neill A, Prencipe M, Sheikh R, Webb G, McDermott R, Watson W, Crown J, O'Driscoll L: **Docetaxel-Resistance in Prostate Cancer: Evaluating Associated Phenotypic Changes and Potential for Resistance Transfer via Exosomes.** *PLoS One* 2012, **7:**e50999.

238. Xiao D, Ohlendorf J, Chen Y, Taylor DD, Rai SN, Waigel S, Zacharias W, Hao H, McMasters KM: **Identifying mRNA, microRNA and protein profiles of melanoma exosomes.** *PLoS One* 2012, **7:**e46874.

239. Ochieng J, Pratap S, Khatua AK, Sakwe AM: **Anchorage-independent growth of breast carcinoma cells is mediated by serum exosomes.** *Exp Cell Res* 2009, **315:**1875-1888.

240. Ciravolo V, Huber V, Ghedini GC, Venturelli E, Bianchi F, Campiglio M, Morelli D, Villa A, Della Mina P, Menard S, et al: **Potential role of HER2-overexpressing exosomes in countering trastuzumab-based therapy.** *J Cell Physiol* 2012, **227:**658-667.

241. Cai Z, Yang F, Yu L, Yu Z, Jiang L, Wang Q, Yang Y, Wang L, Cao X, Wang J: **Activated T cell exosomes promote tumor invasion via Fas signaling pathway.** *J Immunol* 2012, **188:**5954-5961.

242. McCready J, Sims JD, Chan D, Jay DG: **Secretion of extracellular hsp90alpha via exosomes increases cancer cell motility: a role for plasminogen activation.** *BMC Cancer* 2010, **10:**294.

243. Higginbotham JN, Demory Beckler M, Gephart JD, Franklin JL, Bogatcheva G, Kremers GJ, Piston DW, Ayers GD, McConnell RE, Tyska MJ, Coffey RJ: **Amphiregulin exosomes increase cancer cell invasion.** *Curr Biol* 2011, **21:**779-786.

244. Makeyev E, Maniatis T: **Multilevel regulation of gene expression by microRNAs.** *Science* 2008, **319:**1789-1790.

245. Davis S, Lollo B, Freier S, Esau C: **Improved targeting of miRNA with antisense oligonucleotides.** *Nucleic Acids Res* 2006, **34:**2294-2304.

246. Liu Z, Sall A, Yang D: **MicroRNA: an Emerging Therapeutic Target and Intervention Tool.** *Int J Mol Sci* 2008, **9:**978-999.

247. Meng F, Henson R, Wehbe-Janek H, Ghoshal K, Jacob S, Patel T: **MicroRNA-21 regulates expression of the PTEN tumor suppressor gene in human hepatocellular cancer.** *Gastroenterology* 2007, **133:**647-658.

248. Crowder R, Lombardi D, Ellis M: **Successful targeting of ErbB2 receptors-is PTEN the key?** *Cancer Cell* 2004, **6:**103-104.

249. Corcoran C, Friel AM, Duffy MJ, Crown J, O'Driscoll L: **Intracellular and extracellular microRNAs in breast cancer.** *Clin Chem* 2011, **57:**18-32.

250. Arteaga CL, Sliwkowski MX, Osborne CK, Perez EA, Puglisi F, Gianni L: **Treatment of HER2-positive breast cancer: current status and future perspectives.** *Nat Rev Clin Oncol* 2012, **9:**16-32.

251. Cobleigh MA, Vogel CL, Tripathy D, Robert NJ, Scholl S, Fehrenbacher L, Wolter JM, Paton V, Shak S, Lieberman G, Slamon DJ: **Multinational study of the efficacy and safety of humanized anti-HER2 monoclonal antibody in women who have HER2-overexpressing metastatic breast cancer that has progressed after chemotherapy for metastatic disease.** *J Clin Oncol* 1999, **17:**2639-2648.

252. Browne BC, O'Brien N, Duffy MJ, Crown J, O'Donovan N: **HER-2 signaling and inhibition in breast cancer.** *Curr Cancer Drug Targets* 2009, **9:**419-438.

253. Nahta R, Esteva FJ: **Trastuzumab: triumphs and tribulations.** *Oncogene* 2007, **26:**3637-3643.

254. Galluzzi L, Morselli E, Vitale I, Kepp O, Senovilla L, Criollo A, Servant N, Paccard C, Hupé P, Robert T, et al: **miR-181a and miR-630 regulate cisplatin-induced cancer cell death.** *Cancer Res* 2010, **70:**1793-1803.

255. Huang Y, Chuang A, Hao H, Talbot C, Sen T, Trink B, Sidransky D, Ratovitski E: **Phospho-ΔNp63α is a key regulator of the cisplatin-induced microRNAome in cancer cells.** *Cell Death Differ* 2011, **18:**1220-1230.

256. Kuo TC, Tan CT, Chang YW, Hong CC, Lee WJ, Chen MW, Jeng YM, Chiou J, Yu P, Chen PS, et al: **Angiopoietin-like protein 1 suppresses SLUG to inhibit cancer cell motility.** *J Clin Invest* 2013, **123:**1082-1095.

257. Farhana L, Dawson MI, Murshed F, Das JK, Rishi AK, Fontana JA: **Upregulation of miR-150* and miR-630 induces apoptosis in pancreatic cancer cells by targeting IGF-1R.** *PLoS One* 2013, **8:**e61015.

258. Mestdagh P, Van Vlierberghe P, De Weer A, Muth D, Westermann F, Speleman F, Vandesompele J: **A novel and universal method for microRNA RT-qPCR data normalization.** *Genome Biol* 2009, **10:**R64.

259. Sepramaniam S, Tan JR, Tan KS, Desilva DA, Tavintharan S, Woon FP, Wang CW, Yong FL, Karolina DS, Kaur P, et al: **Circulating MicroRNAs as Biomarkers of Acute Stroke.** *Int J Mol Sci* 2014, **15:**1418-1432.

260. Hunsberger JG, Fessler EB, Chibane FL, Leng Y, Maric D, Elkahloun AG, Chuang DM: **Mood stabilizer-regulated miRNAs in neuropsychiatric and neurodegenerative diseases: identifying associations and functions.** *Am J Transl Res* 2013, **5:**450-464.

261. An IS, An S, Park S, Lee SN, Bae S: **Involvement of microRNAs in epigallocatechin gallate-mediated UVB protection in human dermal fibroblasts.** *Oncol Rep* 2013, **29:**253-259.

262. Biagioni F, Bossel Ben-Moshe N, Fontemaggi G, Canu V, Mori F, Antoniani B, Di Benedetto A, Santoro R, Germoni S, De Angelis F, et al: **miR-10b*, a master inhibitor of the cell cycle, is down-regulated in human breast tumours.** *EMBO Mol Med* 2012, **4:**1214-1229.

263. Konecny GE, Pegram MD, Venkatesan N, Finn R, Yang G, Rahmeh M, Untch M, Rusnak DW, Spehar G, Mullin RJ, et al: **Activity of the dual kinase inhibitor lapatinib (GW572016) against HER-2-overexpressing and trastuzumab-treated breast cancer cells.** *Cancer Res* 2006, **66:**1630-1639.

264. Hegde PS, Rusnak D, Bertiaux M, Alligood K, Strum J, Gagnon R, Gilmer TM: **Delineation of molecular mechanisms of sensitivity to lapatinib in breast cancer cell lines using global gene expression profiles.** *Mol Cancer Ther* 2007, **6:**1629-1640.

265. O'Brien NA, Browne BC, Chow L, Wang Y, Ginther C, Arboleda J, Duffy MJ, Crown J, O'Donovan N, Slamon DJ: **Activated phosphoinositide 3-kinase/AKT signaling confers resistance to trastuzumab but not lapatinib.** In *Mol Cancer Ther. Volume* 9. United States2010: 1489-1502

266. O'Neill F, Madden SF, Aherne ST, Clynes M, Crown J, Doolan P, O'Connor R: **Gene expression changes as markers of early lapatinib response in a panel of breast cancer cell lines.** *Mol Cancer* 2012, **11:**41.

267. McMillin DW, Delmore J, Negri JM, Vanneman M, Koyama S, Schlossman RL, Munshi NC, Laubach J, Richardson PG, Dranoff G, et al: **Compartment-Specific Bioluminescence Imaging platform for the high-throughput evaluation of antitumor immune function.** *Blood* 2012, **119:**e131-138.

268. McMillin DW, Jacobs HM, Delmore JE, Buon L, Hunter ZR, Monrose V, Yu J, Smith PG, Richardson PG, Anderson KC, et al: **Molecular and cellular effects of NEDD8-activating enzyme inhibition in myeloma.** *Mol Cancer Ther* 2012, **11:**942-951.

269. McMillin DW, Delmore J, Weisberg E, Negri JM, Geer DC, Klippel S, Mitsiades N, Schlossman RL, Munshi NC, Kung AL, et al: **Tumor cell-specific bioluminescence platform to identify stroma-induced changes to anticancer drug activity.** *Nat Med* 2010, **16:**483-489.

270. Friel A, Corcoran C, Crown J, O'Driscoll L: **Relevance of circulating tumor cells, extracellular nucleic acids, and exosomes in breast cancer.** *Breast Cancer Res Treat* 2010, **123:**613-625.

271. Sisco KL: **Is RNA in serum bound to nucleoprotein complexes?** *Clin Chem* 2001, **47:**1744-1745.

272. Lässer C, Eldh M, Lötvall J: **Isolation and characterization of RNA-containing exosomes.** *J Vis Exp* 2012:e3037.

273. Achilles J, Stahl F, Harms H, Müller S: **Isolation of intact RNA from cytometrically sorted Saccharomyces cerevisiae for the analysis of intrapopulation diversity of gene expression.** *Nat Protoc* 2007, **2:**2203-2211.

274. Pigati L, Yaddanapudi SC, Iyengar R, Kim DJ, Hearn SA, Danforth D, Hastings ML, Duelli DM: **Selective release of microRNA species from normal and malignant mammary epithelial cells.** *PLoS One* 2010, **5:**e13515.

275. Mittelbrunn M, Gutiérrez-Vázquez C, Villarroya-Beltri C, González S, Sánchez-Cabo F, González M, Bernad A, Sánchez-Madrid F: **Unidirectional transfer of microRNA-loaded exosomes from T cells to antigen-presenting cells.** *Nat Commun* 2011, **2:**282.

276. Thomson DW, Bracken CP, Szubert JM, Goodall GJ: **On measuring miRNAs after transient transfection of mimics or antisense inhibitors.** *PLoS One* 2013, **8:**e55214.

277. Shah AN, Summy JM, Zhang J, Park SI, Parikh NU, Gallick GE: **Development and characterization of gemcitabine-resistant pancreatic tumor cells.** *Ann Surg Oncol* 2007, **14:**3629-3637.

278. Cheng GZ, Chan J, Wang Q, Zhang W, Sun CD, Wang LH: **Twist transcriptionally up-regulates AKT2 in breast cancer cells leading to increased migration, invasion, and resistance to paclitaxel.** *Cancer Res* 2007, **67:**1979-1987.

279. Yang AD, Fan F, Camp ER, van Buren G, Liu W, Somcio R, Gray MJ, Cheng H, Hoff PM, Ellis LM: **Chronic oxaliplatin resistance induces epithelial-to-mesenchymal transition in colorectal cancer cell lines.** *Clin Cancer Res* 2006, **12:**4147-4153.

280. Dunn SE, Ehrlich M, Sharp NJ, Reiss K, Solomon G, Hawkins R, Baserga R, Barrett JC: **A dominant negative mutant of the insulin-like growth factor-I receptor inhibits the adhesion, invasion, and metastasis of breast cancer.** *Cancer Res* 1998, **58:**3353-3361.

281. Long L, Rubin R, Brodt P: **Enhanced invasion and liver colonization by lung carcinoma cells overexpressing the type 1 insulin-like growth factor receptor.** *Exp Cell Res* 1998, **238:**116-121.

282. Xie Y, Skytting B, Nilsson G, Brodin B, Larsson O: **Expression of insulin-like growth factor-1 receptor in synovial sarcoma: association with an aggressive phenotype.** *Cancer Res* 1999, **59:**3588-3591.

283. Nahta R, Yuan LX, Zhang B, Kobayashi R, Esteva FJ: **Insulin-like growth factor-I receptor/human epidermal growth factor receptor 2 heterodimerization contributes to trastuzumab resistance of breast cancer cells.** *Cancer Res* 2005, **65:**11118-11128.

284. Ueda S, Hatsuse K, Tsuda H, Ogata S, Kawarabayashi N, Takigawa T, Einama T, Morita D, Fukatsu K, Sugiura Y, et al: **Potential crosstalk between insulin-like growth factor receptor type 1 and epidermal growth factor receptor in progression and metastasis of pancreatic cancer.** *Mod Pathol* 2006, **19:**788-796.

285. Morgillo F, Kim WY, Kim ES, Ciardiello F, Hong WK, Lee HY: **Implication of the insulin-like growth factor-IR pathway in the resistance of non-small cell lung cancer cells to treatment with gefitinib.** *Clin Cancer Res* 2007, **13:**2795-2803.

286. O'DRISCOLL L, KENNY E, DE VILLARREAL MP, CLYNES M: **Detection of Specific mRNAs in Culture Medium Conditioned by Human Tumour Cells: Potential for New Class of Cancer Biomarkers in Serum.** *Cancer Genomics - Proteomics* 2005, **2:**43-52.

287. Friel AM, Corcoran C, Crown J, O'Driscoll L: **Relevance of circulating tumor cells, extracellular nucleic acids, and exosomes in breast cancer.** *Breast Cancer Res Treat* 2010, **123:**613-625.

288. O'Driscoll L, Kenny E, Mehta JP, Doolan P, Joyce H, Gammell P, Hill A, O'Daly B, O'Gorman D, Clynes M: **Feasibility and relevance of global expression profiling of gene transcripts in serum from breast cancer patients using whole genome microarrays and quantitative RT-PCR.** *Cancer Genomics Proteomics* 2008, **5:**94-104.

289. Rani S, Clynes M, O'Driscoll L: **Detection of amplifiable mRNA extracellular to insulin-producing cells: potential for predicting beta cell mass and function.** *Clin Chem* 2007, **53:**1936-1944.

290. Rani S, O'Driscoll L: **Reverse-transcriptase polymerase chain reaction to detect extracellular mRNAs.** *Methods Mol Biol* 2011, **784:**15-25.

291. Minamino N, Kangawa K, Matsuo H: **Neuromedin U-8 and U-25: novel uterus stimulating and hypertensive peptides identified in porcine spinal cord.** In *Biochem Biophys Res Commun. Volume* 130. United States1985: 1078-1085

292. Budhiraja S, Chugh A: **Neuromedin U: physiology, pharmacology and therapeutic potential.** *Fundam Clin Pharmacol* 2009, **23:**149-157.

293. Mitchell JD, Maguire JJ, Davenport AP: **Emerging pharmacology and physiology of neuromedin U and the structurally related peptide neuromedin S.** *Br J Pharmacol* 2009, **158:**87-103.

294. O'Driscoll L, Gammell P, McKiernan E, Ryan E, Jeppesen PB, Rani S, Clynes M: **Phenotypic and global gene expression profile changes between low passage and high passage MIN-6 cells.** In *J Endocrinol. Volume* 191. England2006: 665-676

295. McGowan PM, Mullooly M, Caiazza F, Sukor S, Madden SF, Maguire AA, Pierce A, McDermott EW, Crown J, O'Donovan N, Duffy MJ: **ADAM-17: a novel therapeutic target for triple negative breast cancer.** *Ann Oncol* 2013, **24:**362-369.

296. Irizarry RA, Hobbs B, Collin F, Beazer-Barclay YD, Antonellis KJ, Scherf U, Speed TP: **Exploration, normalization, and summaries of high density oligonucleotide array probe level data.** In *Biostatistics. Volume* 4. England2003: 249-264

297. Yang YH, Dudoit S, Luu P, Lin DM, Peng V, Ngai J, Speed TP: **Normalization for cDNA microarray data: a robust composite method addressing single and multiple slide systematic variation.** *Nucleic Acids Res* 2002, **30:**e15.

298. Sorlie T, Tibshirani R, Parker J, Hastie T, Marron JS, Nobel A, Deng S, Johnsen H, Pesich R, Geisler S, et al: **Repeated observation of breast tumor subtypes in independent gene expression data sets.** In *Proc Natl Acad Sci U S A. Volume* 100. United States2003: 8418-8423

299. Anders CK, Acharya CR, Hsu DS, Broadwater G, Garman K, Foekens JA, Zhang Y, Wang Y, Marcom K, Marks JR, et al: **Age-specific differences in oncogenic pathway deregulation seen in human breast tumors.** *PLoS One* 2008, **3:**e1373.

300. Bild AH, Yao G, Chang JT, Wang Q, Potti A, Chasse D, Joshi MB, Harpole D, Lancaster JM, Berchuck A, et al: **Oncogenic pathway signatures in human cancers as a guide to targeted therapies.** In *Nature. Volume* 439. England2006: 353-357

301. Calabro A, Beissbarth T, Kuner R, Stojanov M, Benner A, Asslaber M, Ploner F, Zatloukal K, Samonigg H, Poustka A, Sultmann H: **Effects of infiltrating lymphocytes and estrogen receptor on gene expression and prognosis in breast cancer.** *Breast Cancer Res Treat* 2009, **116:**69-77.

302. Chang HY, Nuyten DS, Sneddon JB, Hastie T, Tibshirani R, Sorlie T, Dai H, He YD, van't Veer LJ, Bartelink H, et al: **Robustness, scalability, and integration of a wound-response gene expression signature in predicting breast cancer survival.** In *Proc Natl Acad Sci U S A. Volume* 102. United States2005: 3738-3743

303. Chin K, DeVries S, Fridlyand J, Spellman PT, Roydasgupta R, Kuo WL, Lapuk A, Neve RM, Qian Z, Ryder T, et al: **Genomic and transcriptional aberrations linked to breast cancer pathophysiologies.** In *Cancer Cell. Volume* 10. United States2006: 529-541

304. Chanrion M, Negre V, Fontaine H, Salvetat N, Bibeau F, Mac Grogan G, Mauriac L, Katsaros D, Molina F, Theillet C, Darbon JM: **A gene expression signature that can predict the recurrence of tamoxifen-treated primary breast cancer.** In *Clin Cancer Res. Volume* 14. United States2008: 1744-1752

305. Desmedt C, Piette F, Loi S, Wang Y, Lallemand F, Haibe-Kains B, Viale G, Delorenzi M, Zhang Y, d'Assignies MS, et al: **Strong time dependence of the 76-gene prognostic signature for node-negative breast cancer patients in the TRANSBIG multicenter independent validation series.** In *Clin Cancer Res. Volume* 13. United States2007: 3207-3214

306. Desmedt C, Giobbie-Hurder A, Neven P, Paridaens R, Christiaens MR, Smeets A, Lallemand F, Haibe-Kains B, Viale G, Gelber RD, et al: **The Gene expression Grade Index: a potential predictor of relapse for endocrine-treated breast cancer patients in the BIG 1-98 trial.** In *BMC Med Genomics. Volume* 2. England2009: 40

307. Hu Z, Fan C, Oh DS, Marron JS, He X, Qaqish BF, Livasy C, Carey LA, Reynolds E, Dressler L, et al: **The molecular portraits of breast tumors are conserved across microarray platforms.** In *BMC Genomics. Volume* 7. England2006: 96

308. Ivshina AV, George J, Senko O, Mow B, Putti TC, Smeds J, Lindahl T, Pawitan Y, Hall P, Nordgren H, et al: **Genetic reclassification of histologic grade delineates new clinical subtypes of breast cancer.** In *Cancer Res. Volume* 66. United States2006: 10292-10301

309. Kok M, Linn SC, Van Laar RK, Jansen MP, van den Berg TM, Delahaye LJ, Glas AM, Peterse JL, Hauptmann M, Foekens JA, et al: **Comparison of gene expression profiles predicting progression in breast cancer patients treated with tamoxifen.** *Breast Cancer Res Treat* 2009, **113:**275-283.

310. Loi S, Haibe-Kains B, Desmedt C, Wirapati P, Lallemand F, Tutt AM, Gillet C, Ellis P, Ryder K, Reid JF, et al: **Predicting prognosis using molecular profiling in estrogen**

receptor-positive breast cancer treated with tamoxifen. In *BMC Genomics. Volume* 9. England2008: 239

311. Ma XJ, Wang Z, Ryan PD, Isakoff SJ, Barmettler A, Fuller A, Muir B, Mohapatra G, Salunga R, Tuggle JT, et al: **A two-gene expression ratio predicts clinical outcome in breast cancer patients treated with tamoxifen.** In *Cancer Cell. Volume* 5. United States2004: 607-616

312. Miller LD, Smeds J, George J, Vega VB, Vergara L, Ploner A, Pawitan Y, Hall P, Klaar S, Liu ET, Bergh J: **An expression signature for p53 status in human breast cancer predicts mutation status, transcriptional effects, and patient survival.** In *Proc Natl Acad Sci U S A. Volume* 102. United States2005: 13550-13555

313. Pawitan Y, Bjohle J, Amler L, Borg AL, Egyhazi S, Hall P, Han X, Holmberg L, Huang F, Klaar S, et al: **Gene expression profiling spares early breast cancer patients from adjuvant therapy: derived and validated in two population-based cohorts.** In *Breast Cancer Res. Volume* 7. England2005: R953-964

314. Sabatier R, Finetti P, Cervera N, Lambaudie E, Esterni B, Mamessier E, Tallet A, Chabannon C, Extra JM, Jacquemier J, et al: **A gene expression signature identifies two prognostic subgroups of basal breast cancer.** *Breast Cancer Res Treat* 2011, **126:**407-420.

315. Schmidt M, Bohm D, von Torne C, Steiner E, Puhl A, Pilch H, Lehr HA, Hengstler JG, Kolbl H, Gehrmann M: **The humoral immune system has a key prognostic impact in node-negative breast cancer.** In *Cancer Res. Volume* 68. United States2008: 5405-5413

316. Wang Y, Klijn JG, Zhang Y, Sieuwerts AM, Look MP, Yang F, Talantov D, Timmermans M, Meijer-van Gelder ME, Yu J, et al: **Gene-expression profiles to predict distant metastasis of lymph-node-negative primary breast cancer.** In *Lancet. Volume* 365. England2005: 671-679

317. Zhang Y, Sieuwerts AM, McGreevy M, Casey G, Cufer T, Paradiso A, Harbeck N, Span PN, Hicks DG, Crowe J, et al: **The 76-gene signature defines high-risk patients that benefit from adjuvant tamoxifen therapy.** *Breast Cancer Res Treat* 2009, **116:**303-309.

318. Seoane S, Montero JC, Ocana A, Pandiella A: **Effect of multikinase inhibitors on caspase-independent cell death and DNA damage in HER2-overexpressing breast cancer cells.** *J Natl Cancer Inst* 2010, **102:**1432-1446.

319. Narayan M, Wilken JA, Harris LN, Baron AT, Kimbler KD, Maihle NJ: **Trastuzumab-induced HER reprogramming in "resistant" breast carcinoma cells.** *Cancer Res* 2009, **69:**2191-2194.

320. Zhang D, Tai LK, Wong LL, Chiu LL, Sethi SK, Koay ES: **Proteomic study reveals that proteins involved in metabolic and detoxification pathways are highly expressed in HER-2/neu-positive breast cancer.** *Mol Cell Proteomics* 2005, **4:**1686-1696.

321. Gayle SS, Arnold SL, O'Regan RM, Nahta R: **Pharmacologic inhibition of mTOR improves lapatinib sensitivity in HER2-overexpressing breast cancer cells with primary trastuzumab resistance.** *Anticancer Agents Med Chem* 2012, **12:**151-162.

322. Shetzline SE, Rallapalli R, Dowd KJ, Zou S, Nakata Y, Swider CR, Kalota A, Choi JK, Gewirtz AM: **Neuromedin U: a Myb-regulated autocrine growth factor for human myeloid leukemias.** *Blood* 2004, **104:**1833-1840.

323. Euer NI, Kaul S, Deissler H, Mobus VJ, Zeillinger R, Weidle UH: **Identification of L1CAM, Jagged2 and Neuromedin U as ovarian cancer-associated antigens.** *Oncol Rep* 2005, **13:**375-387.

324. Ketterer K, Kong B, Frank D, Giese NA, Bauer A, Hoheisel J, Korc M, Kleeff J, Michalski CW, Friess H: **Neuromedin U is overexpressed in pancreatic cancer and increases invasiveness via the hepatocyte growth factor c-Met pathway.** In *Cancer Lett. Volume* 277. Ireland2009: 72-81

325. Takahashi K, Furukawa C, Takano A, Ishikawa N, Kato T, Hayama S, Suzuki C, Yasui W, Inai K, Sone S, et al: **The neuromedin U-growth hormone secretagogue receptor 1b/neurotensin receptor 1 oncogenic signaling pathway as a therapeutic target for lung cancer.** *Cancer Res* 2006, **66:**9408-9419.

326. Wu Y, McRoberts K, Berr SS, Frierson HF, Jr., Conaway M, Theodorescu D: **Neuromedin U is regulated by the metastasis suppressor RhoGDI2 and is a novel promoter of tumor formation, lung metastasis and cancer cachexia.** *Oncogene* 2007, **26:**765-773.

327. Harten SK, Esteban MA, Shukla D, Ashcroft M, Maxwell PH: **Inactivation of the von Hippel-Lindau tumour suppressor gene induces Neuromedin U expression in renal cancer cells.** In *Mol Cancer. Volume* 10. England2011: 89

328. Yamashita K, Upadhyay S, Osada M, Hoque MO, Xiao Y, Mori M, Sato F, Meltzer SJ, Sidransky D: **Pharmacologic unmasking of epigenetically silenced tumor suppressor genes in esophageal squamous cell carcinoma.** *Cancer Cell* 2002, **2:**485-495.

329. Alevizos I, Mahadevappa M, Zhang X, Ohyama H, Kohno Y, Posner M, Gallagher GT, Varvares M, Cohen D, Kim D, et al: **Oral cancer in vivo gene expression profiling assisted by laser capture microdissection and microarray analysis.** *Oncogene* 2001, **20:**6196-6204.

330. Silva J, Garcia V, Garcia JM, Pena C, Dominguez G, Diaz R, Lorenzo Y, Hurtado A, Sanchez A, Bonilla F: **Circulating Bmi-1 mRNA as a possible prognostic factor for advanced breast cancer patients.** In *Breast Cancer Res. Volume* 9. England2007: R55

331. Canonici A, Gijsen M, Mullooly M, Bennett R, Bouguern N, Pedersen K, O'Brien NA, Roxanis I, Li JL, Bridge E, et al: **Neratinib overcomes trastuzumab resistance in HER2 amplified breast cancer.** *Oncotarget* 2013, **4:**1592-1605.

332. Zhang F, Chen A, Chen J, Yu T, Guo F: **SiRNA-mediated Silencing of beta-catenin Suppresses Invasion and Chemosensitivity to Doxorubicin in MG-63 Osteosarcoma Cells.** *Asian Pac J Cancer Prev* 2011, **12:**239-245.

333. Andre F, Escudier B, Angevin E, Tursz T, Zitvogel L: **Exosomes for cancer immunotherapy.** *Ann Oncol* 2004, **15 Suppl 4:**iv141-144.

334. Germano S, Kennedy S, Rani S, Gleeson G, Clynes M, Doolan P, McDonnell S, Hughes L, Crown J, O'Driscoll L: **MAGE-D4B is a novel marker of poor prognosis and potential therapeutic target involved in breast cancer tumorigenesis.** *Int J Cancer* 2011.

335. Rani S, O'Brien K, Kelleher FC, Corcoran C, Germano S, Radomski MW, Crown J, O'Driscoll L: **Isolation of Exosomes for Subsequent mRNA, MicroRNA, and Protein Profiling.** *Methods Mol Biol* 2011, **784:**181-195.

336. Fernández-Llama P, Khositseth S, Gonzales PA, Star RA, Pisitkun T, Knepper MA: **Tamm-Horsfall protein and urinary exosome isolation.** *Kidney Int* 2010, **77:**736-742.

337. Guescini M, Genedani S, Stocchi V, Agnati LF: **Astrocytes and Glioblastoma cells release exosomes carrying mtDNA.** *J Neural Transm* 2010, **117:**1-4.

338. Shtanko O, Watanabe S, Jasenosky LD, Watanabe T, Kawaoka Y: **ALIX/AIP1 is required for NP incorporation into Mopeia virus Z-induced virus-like particles.** *J Virol* 2011, **85:**3631-3641.

339. Théry C, Ostrowski M, Segura E: **Membrane vesicles as conveyors of immune responses.** *Nat Rev Immunol* 2009, **9:**581-593.

340. Malik ZA, Kott KS, Poe AJ, Kuo T, Chen L, Ferrara KW, Knowlton AA: **Cardiac myocyte exosomes: stability, HSP60, and proteomics.** *Am J Physiol Heart Circ Physiol* 2013, **304:**H954-965.

341. Guo B, Villeneuve DJ, Hembruff SL, Kirwan AF, Blais DE, Bonin M, Parissenti AM: **Cross-resistance studies of isogenic drug-resistant breast tumor cell lines support recent clinical evidence suggesting that sensitivity to paclitaxel may be strongly compromised by prior doxorubicin exposure.** *Breast Cancer Res Treat* 2004, **85:**31-51.

342. Li D, Jang SH, Kim J, Wientjes MG, Au JL: **Enhanced drug-induced apoptosis associated with P-glycoprotein overexpression is specific to antimicrotubule agents.** *Pharm Res* 2003, **20:**45-50.

343. Kondratov RV, Komarov PG, Becker Y, Ewenson A, Gudkov AV: **Small molecules that dramatically alter multidrug resistance phenotype by modulating the substrate specificity of P-glycoprotein.** *Proc Natl Acad Sci U S A* 2001, **98:**14078-14083.

344. Bashir I, Sikora K, Abel P, Foster CS: **Establishment and in vivo characterization of multidrug-resistant dunning R3327 rat prostate-carcinoma cell-lines.** *Int J Cancer* 1994, **57:**719-726.

345. Desarnaud F, Geck P, Parkin C, Carpinito G, Makarovskiy AN: **Gene expression profiling of the androgen independent prostate cancer cells demonstrates complex mechanisms mediating resistance to docetaxel.** *Cancer Biol Ther* 2011, **11:**204-212.

346. Drake JM, Barnes JM, Madsen JM, Domann FE, Stipp CS, Henry MD: **ZEB1 coordinately regulates laminin-332 and {beta}4 integrin expression altering the invasive phenotype of prostate cancer cells.** *J Biol Chem* 2010, **285:**33940-33948.

347. Dallas NA, Xia L, Fan F, Gray MJ, Gaur P, van Buren G, Samuel S, Kim MP, Lim SJ, Ellis LM: **Chemoresistant colorectal cancer cells, the cancer stem cell phenotype, and**

increased sensitivity to insulin-like growth factor-I receptor inhibition. *Cancer Res* 2009, **69:**1951-1957.

348. Guo X, Goessl E, Jin G, Collie-Duguid ES, Cassidy J, Wang W, O'Brien V: **Cell cycle perturbation and acquired 5-fluorouracil chemoresistance.** *Anticancer Res* 2008, **28:**9-14.

349. Lee AJ, Endesfelder D, Rowan AJ, Walther A, Birkbak NJ, Futreal PA, Downward J, Szallasi Z, Tomlinson IP, Howell M, et al: **Chromosomal instability confers intrinsic multidrug resistance.** *Cancer Res* 2011, **71:**1858-1870.

350. Gabai VL, Budagova KR, Sherman MY: **Increased expression of the major heat shock protein Hsp72 in human prostate carcinoma cells is dispensable for their viability but confers resistance to a variety of anticancer agents.** *Oncogene* 2005, **24:**3328-3338.

351. Shibata T, Kokubu A, Miyamoto M, Hosoda F, Gotoh M, Tsuta K, Asamura H, Matsuno Y, Kondo T, Imoto I, et al: **DEK oncoprotein regulates transcriptional modifiers and sustains tumor initiation activity in high-grade neuroendocrine carcinoma of the lung.** *Oncogene* 2010, **29:**4671-4681.

352. Lee TH, D'Asti E, Magnus N, Al-Nedawi K, Meehan B, Rak J: **Microvesicles as mediators of intercellular communication in cancer-the emerging science of cellular 'debris'.** *Semin Immunopathol* 2011.

353. Bhangal G, Halford S, Wang J, Roylance R, Shah R, Waxman J: **Expression of the multidrug resistance gene in human prostate cancer.** *Urol Oncol* 2000, **5:**118-121.

354. Mittelbrunn M, Sánchez-Madrid F: **Intercellular communication: diverse structures for exchange of genetic information.** *Nat Rev Mol Cell Biol* 2012, **13:**328-335.

355. Alvarez-Erviti L, Seow Y, Yin H, Betts C, Lakhal S, Wood MJ: **Delivery of siRNA to the mouse brain by systemic injection of targeted exosomes.** *Nat Biotechnol* 2011, **29:**341-345.

356. Kharaziha P, Ceder S, Li Q, Panaretakis T: **Tumor cell-derived exosomes: A message in a bottle.** *Biochim Biophys Acta* 2012, **1826:**103-111.

357. Ortega JF, Fernández-Elías VE, Hamouti N, Mora-Rodriguez R: **Increased blood cholesterol after a high saturated fat diet is prevented by aerobic exercise training.** *Appl Physiol Nutr Metab* 2013, **38:**42-48.

358. Hennessy E, O'Driscoll L: **MicroRNA expression analysis: techniques suitable for studies of intercellular and extracellular microRNAs.** *Methods Mol Biol* 2011, **784:**99-107.

359. Antonov AV, Knight RA, Melino G, Barlev NA, Tsvetkov PO: **MIRUMIR: an online tool to test microRNAs as biomarkers to predict survival in cancer using multiple clinical data sets.** *Cell Death Differ* 2013, **20:**367.

360. Bruce JY, Lang JM, McNeel DG, Liu G: **Current controversies in the management of biochemical failure in prostate cancer.** *Clin Adv Hematol Oncol* 2012, **10:**716-722.

361. Calin GA, Croce CM: **MicroRNA signatures in human cancers.** *Nat Rev Cancer* 2006, **6:**857-866.

362. Ma J, Dong C, Ji C: **MicroRNA and drug resistance.** *Cancer Gene Ther* 2010, **17:**523-531.

363. Mitchell JP, Court J, Mason MD, Tabi Z, Clayton A: **Increased exosome production from tumour cell cultures using the Integra CELLine Culture System.** *J Immunol Methods* 2008, **335:**98-105.

364. Boon RA, Vickers KC: **Intercellular transport of microRNAs.** *Arterioscler Thromb Vasc Biol* 2013, **33:**186-192.

365. Lin SL, Chiang A, Chang D, Ying SY: **Loss of mir-146a function in hormone-refractory prostate cancer.** *RNA* 2008, **14:**417-424.

366. Xu B, Feng NH, Li PC, Tao J, Wu D, Zhang ZD, Tong N, Wang JF, Song NH, Zhang W, et al: **A functional polymorphism in Pre-miR-146a gene is associated with prostate cancer risk and mature miR-146a expression in vivo.** *Prostate* 2010, **70:**467-472.

367. Fujita Y, Kojima K, Ohhashi R, Hamada N, Nozawa Y, Kitamoto A, Sato A, Kondo S, Kojima T, Deguchi T, Ito M: **MiR-148a attenuates paclitaxel resistance of hormone-refractory, drug-resistant prostate cancer PC3 cells by regulating MSK1 expression.** *J Biol Chem* 2010, **285:**19076-19084.

368. Murata T, Takayama K, Katayama S, Urano T, Horie-Inoue K, Ikeda K, Takahashi S, Kawazu C, Hasegawa A, Ouchi Y, et al: **miR-148a is an androgen-responsive microRNA that promotes LNCaP prostate cell growth by repressing its target CAND1 expression.** *Prostate Cancer Prostatic Dis* 2010, **13:**356-361.

369. Pogribny IP, Filkowski JN, Tryndyak VP, Golubov A, Shpyleva SI, Kovalchuk O: **Alterations of microRNAs and their targets are associated with acquired resistance of MCF-7 breast cancer cells to cisplatin.** *Int J Cancer* 2010, **127:**1785-1794.

370. Hummel R, Watson DI, Smith C, Kist J, Michael MZ, Haier J, Hussey DJ: **Mir-148a improves response to chemotherapy in sensitive and resistant oesophageal adenocarcinoma and squamous cell carcinoma cells.** *J Gastrointest Surg* 2011, **15:**429-438.

371. Tomokuni A, Eguchi H, Tomimaru Y, Wada H, Kawamoto K, Kobayashi S, Marubashi S, Tanemura M, Nagano H, Mori M, Doki Y: **miR-146a suppresses the sensitivity to interferon-α in hepatocellular carcinoma cells.** *Biochem Biophys Res Commun* 2011, **414:**675-680.

372. Yamamura S, Saini S, Majid S, Hirata H, Ueno K, Deng G, Dahiya R: **MicroRNA-34a modulates c-Myc transcriptional complexes to suppress malignancy in human prostate cancer cells.** *PLoS One* 2012, **7:**e29722.

373. Kong D, Heath E, Chen W, Cher M, Powell I, Heilbrun L, Li Y, Ali S, Sethi S, Hassan O, et al: **Epigenetic silencing of miR-34a in human prostate cancer cells and tumor tissue specimens can be reversed by BR-DIM treatment.** *Am J Transl Res* 2012, **4:**14-23.

374. Vinall RL, Ripoll AZ, Wang S, Pan CX, deVere White RW: **MiR-34a chemosensitizes bladder cancer cells to cisplatin treatment regardless of p53-Rb pathway status.** *Int J Cancer* 2012, **130:**2526-2538.

375. Yang F, Li QJ, Gong ZB, Zhou L, You N, Wang S, Li XL, Li JJ, An JZ, Wang DS, et al: **MicroRNA-34a Targets Bcl-2 and Sensitizes Human Hepatocellular Carcinoma Cells to Sorafenib Treatment.** *Technol Cancer Res Treat* 2013.

376. Di Martino MT, Leone E, Amodio N, Foresta U, Lionetti M, Pitari MR, Cantafio ME, Gullà A, Conforti F, Morelli E, et al: **Synthetic miR-34a mimics as a novel therapeutic agent for multiple myeloma: in vitro and in vivo evidence.** *Clin Cancer Res* 2012, **18:**6260-6270.

377. Fujita Y, Kojima K, Hamada N, Ohhashi R, Akao Y, Nozawa Y, Deguchi T, Ito M: **Effects of miR-34a on cell growth and chemoresistance in prostate cancer PC3 cells.** *Biochem Biophys Res Commun* 2008, **377:**114-119.

378. Nakatani F, Ferracin M, Manara MC, Ventura S, Del Monaco V, Ferrari S, Alberghini M, Grilli A, Knuutila S, Schaefer KL, et al: **miR-34a predicts survival of Ewing's sarcoma patients and directly influences cell chemo-sensitivity and malignancy.** *J Pathol* 2012, **226:**796-805.

379. Weeraratne SD, Amani V, Neiss A, Teider N, Scott DK, Pomeroy SL, Cho YJ: **miR-34a confers chemosensitivity through modulation of MAGE-A and p53 in medulloblastoma.** *Neuro Oncol* 2011, **13:**165-175.

380. Gallo A, Tandon M, Alevizos I, Illei GG: **The majority of microRNAs detectable in serum and saliva is concentrated in exosomes.** *PLoS One* 2012, **7:**e30679.

APPENDIX I

A. Packaging and envelope plasmids for lentivirus production

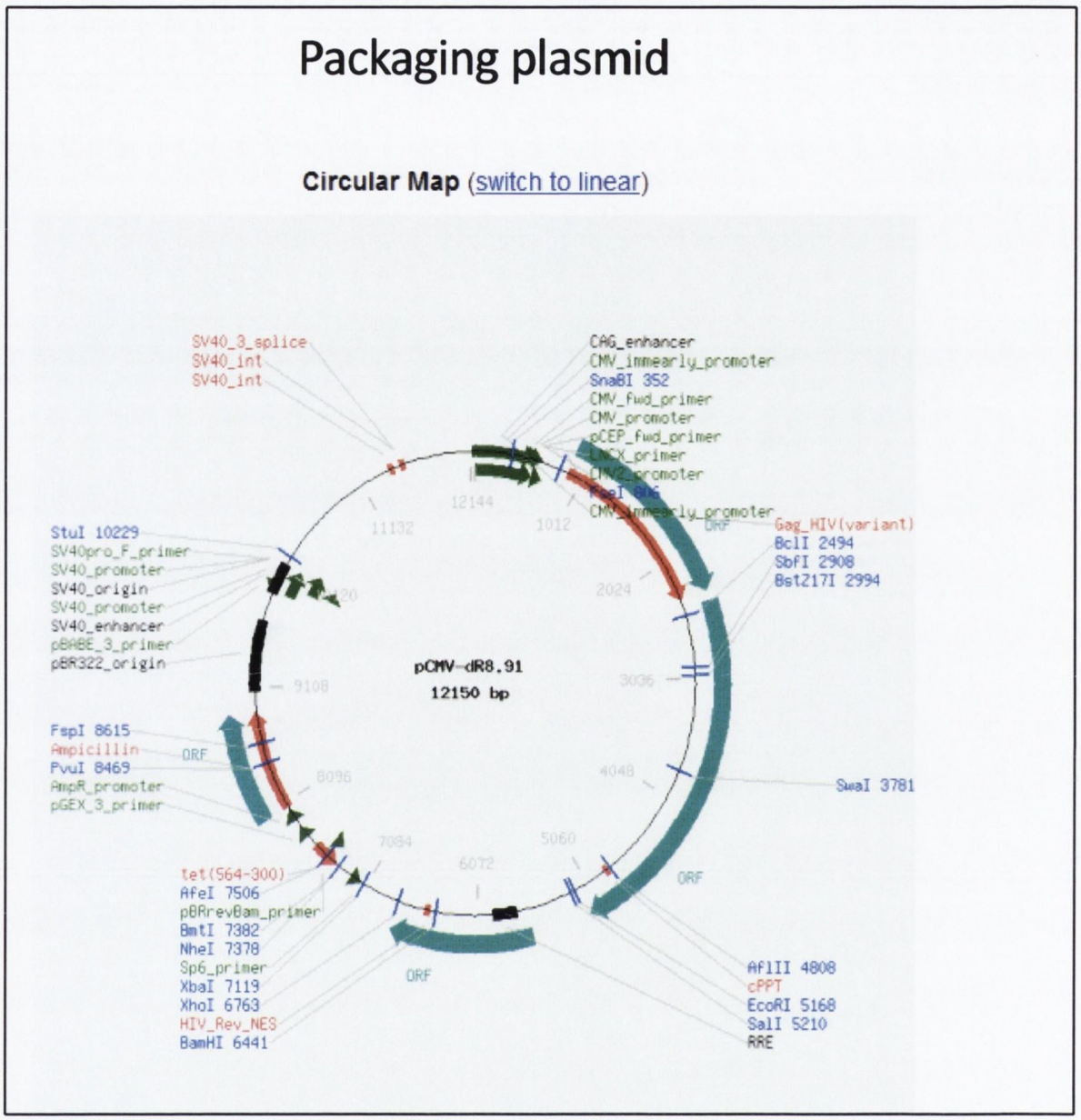

Figure A.1: Vector map of packaging plasmid.
The packaging plasmid was used for the generation of lentiviruses; this vector information was obtained from: http://www.addgene.org/vector-database/2221/

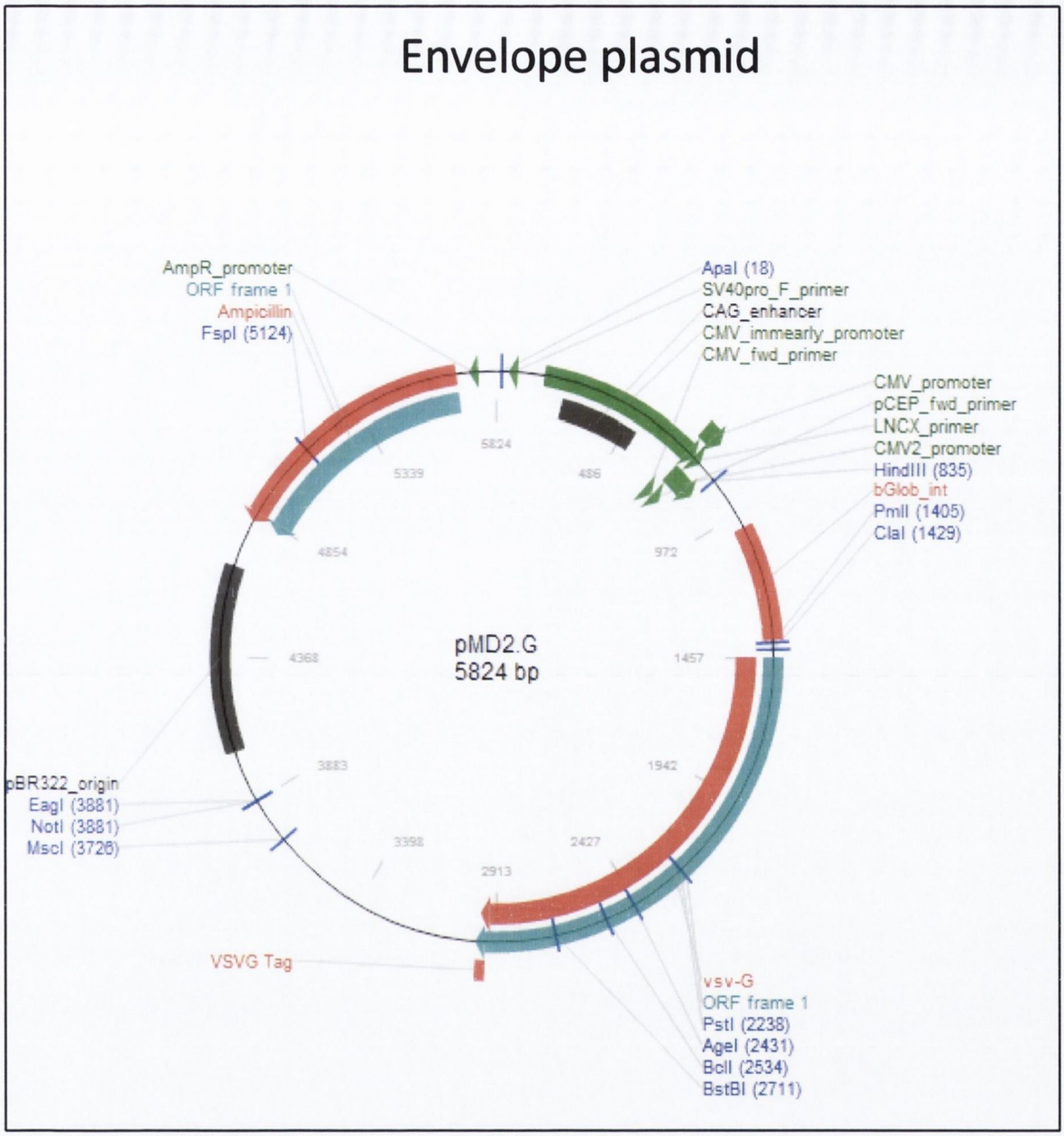

Figure A.2: Vector map of evelope plasmid.
The envelope plasmid was used for the generation of lentiviruses; this vector information was obtained from: http://www.addgene.org/12259/

B. Plasmids used for miR-630 knockdown and overexpression

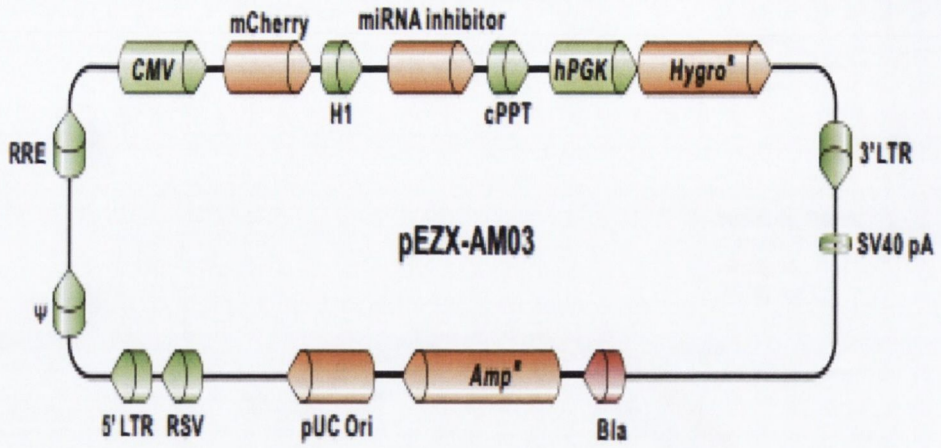

Figure B.1: Vector map for miR-630 and scrambled inhibitor plasmids.
The miR-630 inhibitor plasmid was used for the stable knockdown of miR-630 expression. The scrambled plasmid was used as a control for the experiments. The vector information was obtained from: http://www.genecopoeia.com/wp-content/uploads/oldpdfs/product/mirna/pEZX-AM03.pdf

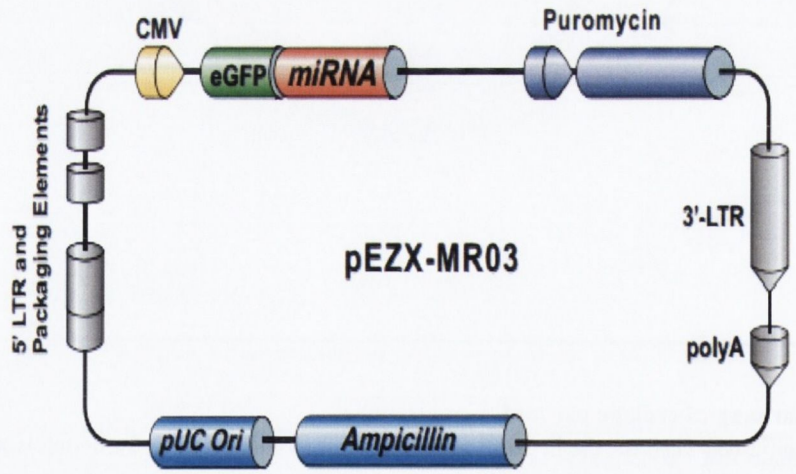

Figure B.2: Vector map for miR-630 and scrambled inhibitor plasmids.
The miR-630 precuror plasmid was used for the stable overexpression of miR-630. The scrambled plasmid was used as a control for the experiments. The vector information was obtained from: http://www.genecopoeia.com/wp-content/uploads/oldpdfs/product/mirna/pEZX-MR03.pdf

C. Sequencing of miR-630 and scrambled plasmids

In order to confirm that the plasmids obtained from genecopeia were correct and therefore appropriate for use for the miR-630 experiments. A sample of the commercially available plasmids was sent to Eurofins for sequencing. The readout obtained was aligned with the expected sequence using Multialign software. Blast software was used to determine that the miR-630 inhibitor/precursor plasmid sequences were specific to miR-630 and that the scrambled plasmids did not show similarity to any specific transcripts.

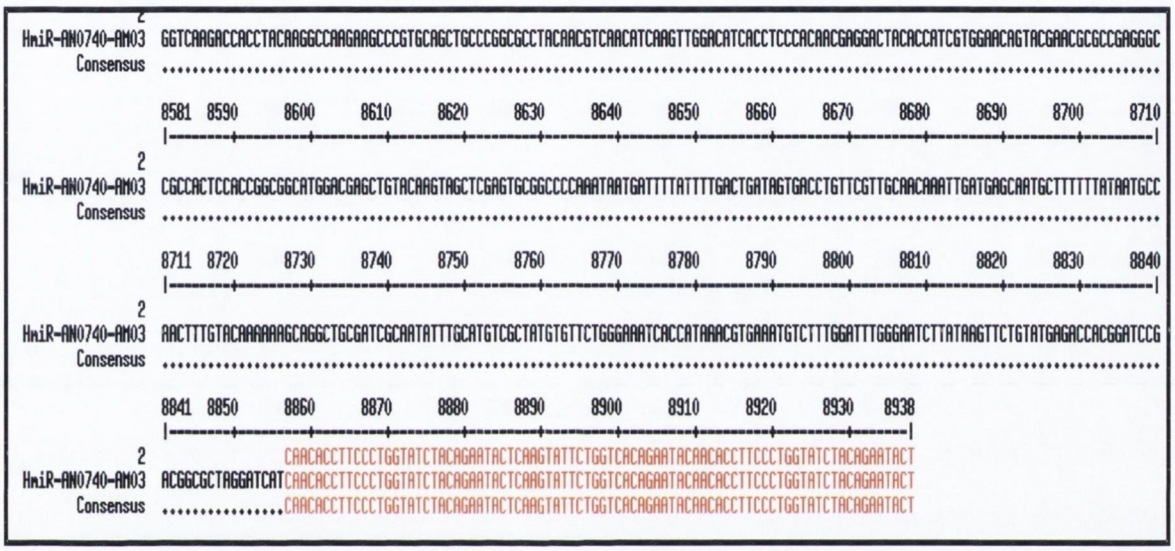

Figure C.1: Alignment of miR-630 inhibitor plasmid sequence
Alignment of miR-630 inhibitor (HmiR-AM0740-AM03) construct using MulitAlign software indicates that the expected insert sequence as given from the plasmid supplier (Genecopeia) aligns with the results after sequencing was performed. The label 'HmiR-AM0740-AM03' refers to the expected sequence given from Genecopeia while the label '2' refers to the sequence readout obtained after sample was sent to Eurofins for sequencing.

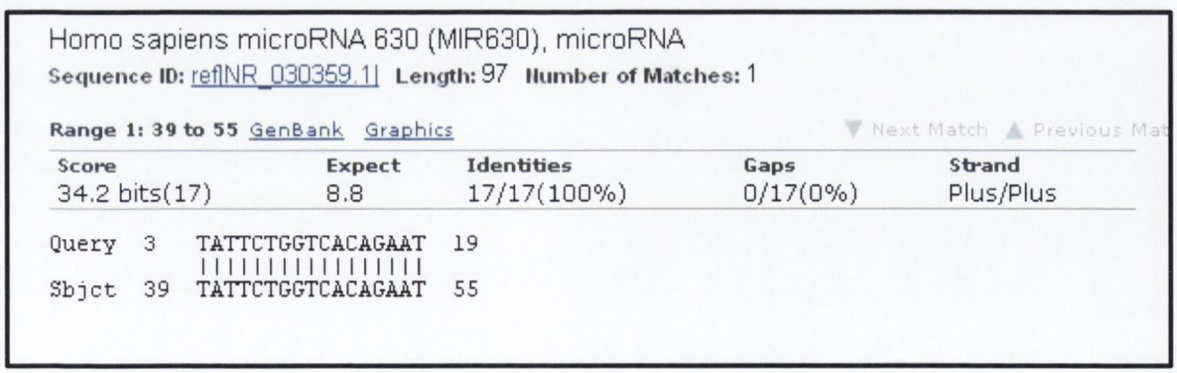

Figure C.2: miR-630 inhibitor is specific for miR-630.
Assessing the sequence on Blast Software confirms that the miR-630 inhibitor sequence is matched to miR-630



Figure C.3: Alignment of scrambled inhibitor plasmid sequence.
Alignment of scrambled inhibitor (CmiR-AM0001-AM03) construct using MulitAlign software indicates that the expected insert sequence as given from the plasmid supplier (Genecopeia) aligns with the results after sequencing was performed. The label 'CmiR-AM0001-AM03' refers to the expected sequence given from Genecopeia while the label '4' refers to the sequence readout obtained after sample was sent to Eurofins for sequencing.

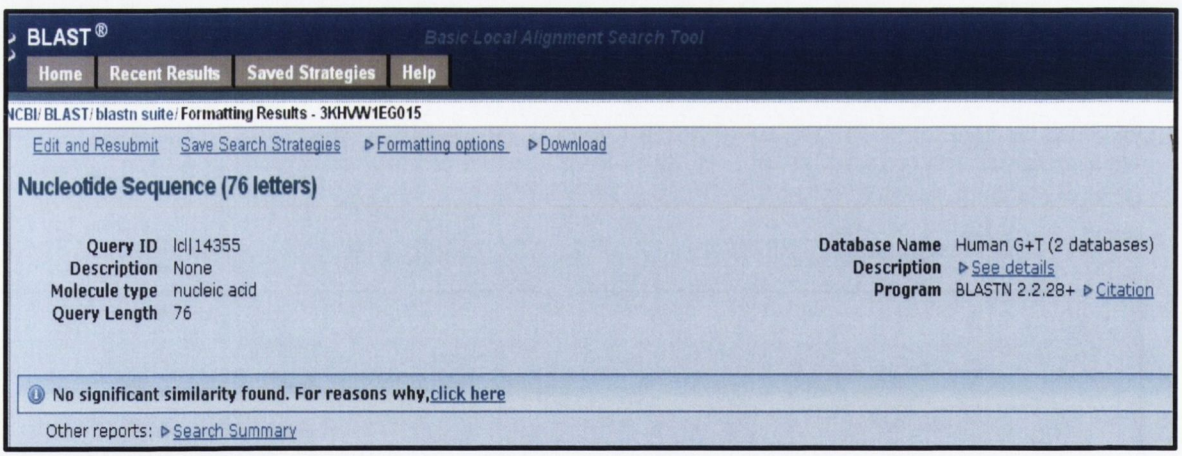

Figure C.4: Scrambled inhibitor is not specific for any transcript.
Assessing the sequence on Blast confirms that the scrambled inhibitor does not show any similarity to other transcripts

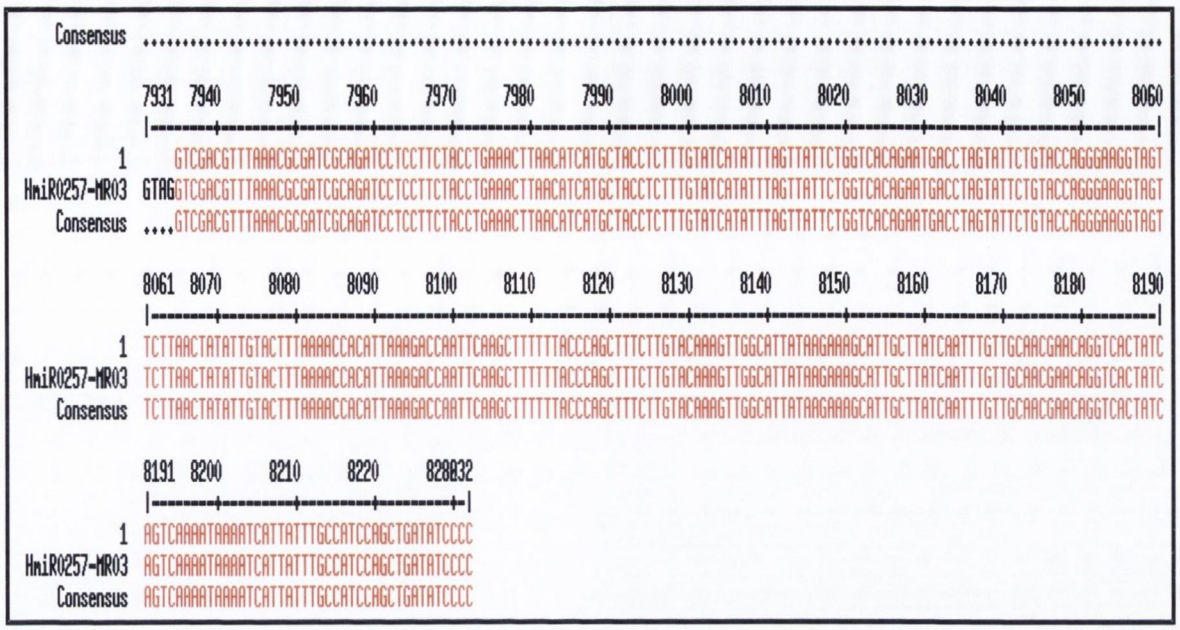

Figure C.5: Alignment of miR-630 precursor plasmid sequence.

Alignment of miR-630 precursor (HmiR-0257-MR03) construct using MulitAlign software indicates that the expected insert sequence as given from the plasmid supplier (Genecopeia) aligns with the results after sequencing was performed. The label 'HmiR-0257-MR03' refers to the expected sequence given from Genecopeia while the label '1' refers to the sequence readout obtained after sample was sent to Eurofins for sequencing.

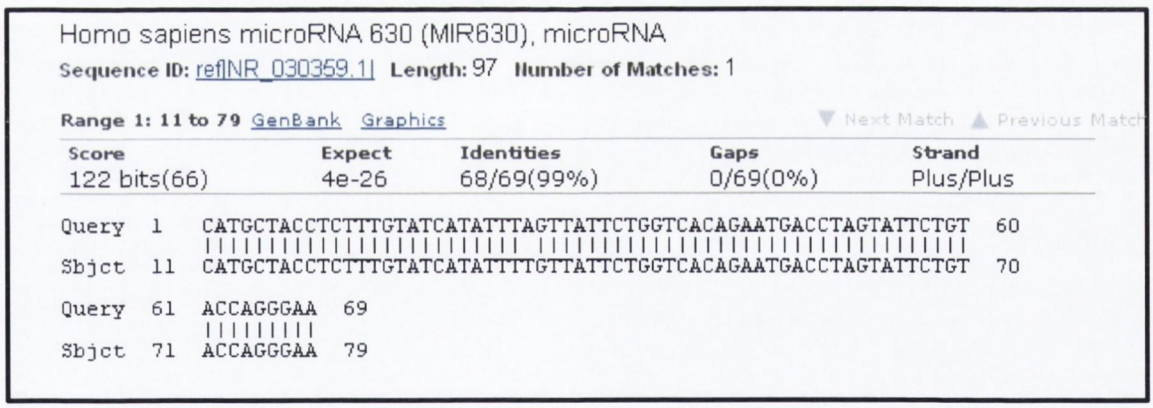

Figure C.6: miR-630 precursor is matched to miR-630.

Assessing the sequence on Blast confirms that the miR-630 precursor sequence matches to miR-630



Figure C.7: Alignment of scrambled precursor plasmid sequence.

Alignment of scrambled precursor (CmiR-00001-MR03) construct using MulitAlign software indicates that the expected insert sequence as given from the plasmid supplier (Genecopeia) aligns with the results after sequencing was performed. The label 'CmiR-00001-MR03' refers to the expected sequence given from Genecopeia while the label '3' refers to the sequence readout obtained after sample was sent to Eurofins for sequencing.

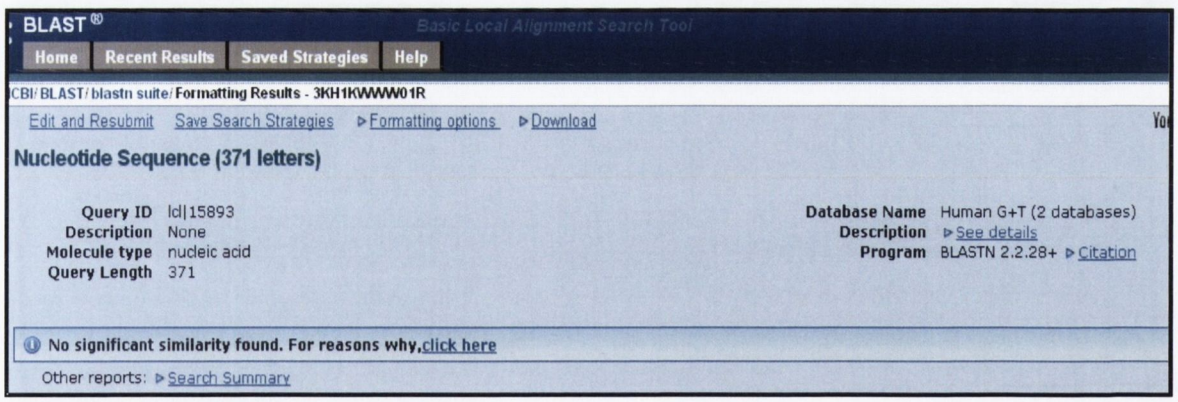

Figure C.8: Scrambled precursor is not matched for any transcript.

Assessing the sequence on Blast confirms that the scrambled precursor does not show any similarity to other transcripts

D. Generation of stable NmU-overexpressing cells

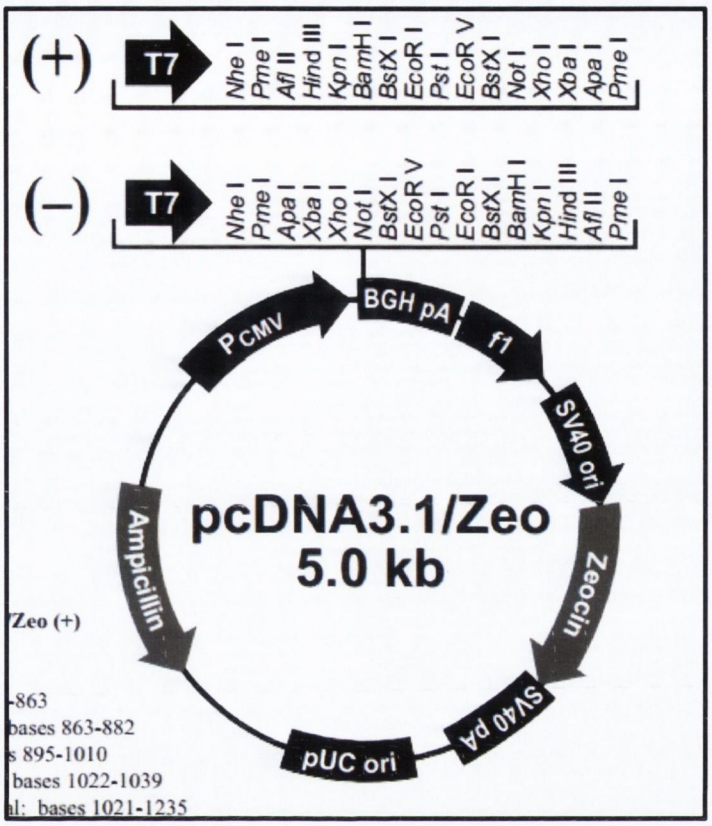

Figure D.1: Vector map for plasmid contruct used for NmU overexpression.
The pcDNA™3.1/Zeo (+) vectors contain the Zeocin resistance gene for selection of stable cell lines using Zeocin. Vector information was obtained from:
http://tools.lifetechnologies.com/content/sfs/manuals/pcdna3_1zeo_man.pdf

E. Generation of pcDNA3.1(+)zeo NmU construct

NmU (NM_006681) cDNA was bought from OpenBiosystems (Cat. No. IHS1380-97652453 clone ID LIFESEQ2498716) in pINCY vector.

The subcloning strategy involved cutting of NmU cDNA from the supposed to be pcDNA3 NMU construct (previously cloned EcoRV-NotI) with BamHI and NotI enzymes and cloning in the pcDNA3.1(+)zeo vector with the same enzymes.

One colony obtained from the ligation reaction was sent for sequencing with the primer pcDNA3_FOR (GGTCAACTAGAGAACCCACTG, 823-844)

Sequencing result:

```
> pcDNA3.1ZEO NMU_pcDNA3_for -- 7..975 of sequence
ATACGACTCACTATAGGGAGACCCAAGCTGGCTAGCGTTTAAACTTAAGCTTGGTACCGA
GCTCGGATCCACTAGTCCAGTGTGGTGGAATTCTGCAGATCACGCGTACGTAAGCTCGGA
ATTCGGCTCGAGGTCCTGTGTCCGGGCCCCGAGGCACAGCCAGGGCACCAGGTGGAGCAC
CAGCTACGCGTGGCGCAGCGCAGCGTCCCTAGCACCGAGCCTCCCGCAGCCGCCGAGATG
CTGCGAACAGAGAGCTGCCGCCCCAGGTCGCCCGCCGGACAGGTGGCCGCGGCGTCCCCG
CTCCTGCTGCTGCTGCTGCTGCTCGCCTGGTGCGCGGGCGCCTGCCGAGGTGCTCCAATA
TTACCTCAAGGATTACAGCCTGAACAACAGCTACAGTTGTGGAATGAGATAGATGATACT
TGTTCGTCTTTTCTGTCCATTGATTCTCAGCCTCAGGCATCCAACGCACTGGAGGAGCTT
TGCTTTATGATTATGGGAATGCTACCAAAGCCTCAGGAACAAGATGAAAAAGATAATACT
AAAAGGTTCTTATTTCATTATTCGAAGACACAGAAGTTGGGCAAGTCAAATGTTGTGTCG
TCAGTTGTGCATCCGTTGCTGCAGCTCGTTCCTCACCTGCATGAGAGAAGAATGAAGAGA
TTCAGAGTGGACGAAGAATTCCAAAGTCCCTTTGCAAGTCAAAGTCGAGGATATTTTTTA
TTCAGGCCACGGAATGGAAGAAGGTCAGCAGGGTTCATTTAAAATGGATGCCAGCTAATT
TTCCACAGAGCAATGCTATGGAATACAAAATGTACTGACATTTTGTTTTCTTCTGAAAAA
AATCCTTGCTAAATGTACTCTGTTGAAAATCCCTGTGTTGTCAATGTTCTCAGTTGTAAC
AATGTTGTAAATGTTCAATTTGTTGAAAATTAAAAAATCTAAAAATAAAAAAAAAAAAAA
AAGGGGCCG
```

Blast with pcDNA3.1(+)ZEO sequence:

```
>lcl|34603 pcDNA3.1/Zeo(+), 5015 bp
Length=5015

 Score =  185 bits (100),  Expect = 6e-50
 Identities = 100/100 (100%), Gaps = 0/100 (0%)
 Strand=Plus/Plus

Query  1    ATACGACTCACTATAGGGAGACCCAAGCTGGCTAGCGTTTAAACTTAAGCTTGGTACCGA  60
            ||||||||||||||||||||||||||||||||||||||||||||||||||||||||||||
Subject  865  ATACGACTCACTATAGGGAGACCCAAGCTGGCTAGCGTTTAAACTTAAGCTTGGTACCGA  924

Query  61   GCTCGGATCCACTAGTCCAGTGTGGTGGAATTCTGCAGAT  100
            ||||||||||||||||||||||||||||||||||||||||
Subject  925  GCTCGGATCCACTAGTCCAGTGTGGTGGAATTCTGCAGAT  964
```

Figure E.1: Alignment and confirmation of pcDNA3.1 (+) ZEO construct.

Assessing the sequence on Blast confirms that the pcDNA3.1(+)ZEO construct used for NmU overexpression studies matches to pcDNA3.1(+)ZEO sequence. 'Query' here represents the sequence read obtained after the sample of the plasmid was sent for sequencing at Eurofins, while 'Subject' represents the expected sequence for pcDNA3.1(+)ZEO

```
>lcl|25847 gi|195539393|ref|NM_006681.2| Homo sapiens neuromedin U (NMU),
mRNA
Length=818

 Score = 1509 bits (817),  Expect = 0.0
 Identities = 817/817 (100%), Gaps = 0/817 (0%)
 Strand=Plus/Plus

Query  133  GTCCTGTGTCCGGGCCCCGAGGCACAGCCAGGGCACCAGGTGGAGCACCAGCTACGCGTG  192
            ||||||||||||||||||||||||||||||||||||||||||||||||||||||||||||
Sbjct  2    GTCCTGTGTCCGGGCCCCGAGGCACAGCCAGGGCACCAGGTGGAGCACCAGCTACGCGTG  61

Query  193  GCGCAGCGCAGCGTCCCTAGCACCGAGCCTCCCGCAGCCGCCGAGATGCTGCGAACAGAG  252
            ||||||||||||||||||||||||||||||||||||||||||||||||||||||||||||
Sbjct  62   GCGCAGCGCAGCGTCCCTAGCACCGAGCCTCCCGCAGCCGCCGAGATGCTGCGAACAGAG  121

Query  253  AGCTGCCGCCCCAGGTCGCCCGCCGGACAGGTGGCCGCGGCGTCCCCGCTCctgctgctg  312
            ||||||||||||||||||||||||||||||||||||||||||||||||||||||||||||
Sbjct  122  AGCTGCCGCCCCAGGTCGCCCGCCGGACAGGTGGCCGCGGCGTCCCCGCTCCTGCTGCTG  181

Query  313  ctgctgctgctCGCCTGGTGCGCGGGCGCCTGCCGAGGTGCTCCAATATTACCTCAAGGA  372
            ||||||||||||||||||||||||||||||||||||||||||||||||||||||||||||
Sbjct  182  CTGCTGCTGCTCGCCTGGTGCGCGGGCGCCTGCCGAGGTGCTCCAATATTACCTCAAGGA  241

Query  373  TTACAGCCTGAACAACAGCTACAGTTGTGGAATGAGATAGATGATACTTGTTCGTCTTTT  432
            ||||||||||||||||||||||||||||||||||||||||||||||||||||||||||||
Sbjct  242  TTACAGCCTGAACAACAGCTACAGTTGTGGAATGAGATAGATGATACTTGTTCGTCTTTT  301

Query  433  CTGTCCATTGATTCTCAGCCTCAGGCATCCAACGCACTGGAGGAGCTTTGCTTTATGATT  492
            ||||||||||||||||||||||||||||||||||||||||||||||||||||||||||||
Sbjct  302  CTGTCCATTGATTCTCAGCCTCAGGCATCCAACGCACTGGAGGAGCTTTGCTTTATGATT  361

Query  493  ATGGGAATGCTACCAAAGCCTCAGGAACAAGATGAAAAAGATAATACTAAAAGGTTCTTA  552
            ||||||||||||||||||||||||||||||||||||||||||||||||||||||||||||
Sbjct  362  ATGGGAATGCTACCAAAGCCTCAGGAACAAGATGAAAAAGATAATACTAAAAGGTTCTTA  421

Query  553  TTTCATTATTCGAAGACACAGAAGTTGGGCAAGTCAAATGTTGTGTCGTCAGTTGTGCAT  612
            ||||||||||||||||||||||||||||||||||||||||||||||||||||||||||||
Sbjct  422  TTTCATTATTCGAAGACACAGAAGTTGGGCAAGTCAAATGTTGTGTCGTCAGTTGTGCAT  481

Query  613  CCGTTGCTGCAGCTCGTTCCTCACCTGCATGAGAGAAGAATGAAGAGATTCAGAGTGGAC  672
            ||||||||||||||||||||||||||||||||||||||||||||||||||||||||||||
Sbjct  482  CCGTTGCTGCAGCTCGTTCCTCACCTGCATGAGAGAAGAATGAAGAGATTCAGAGTGGAC  541

Query  673  GAAGAATTCCAAAGTCCCTTTGCAAGTCAAAGTCGAGGATATTTTTTATTCAGGCCACGG  732
            ||||||||||||||||||||||||||||||||||||||||||||||||||||||||||||
Sbjct  542  GAAGAATTCCAAAGTCCCTTTGCAAGTCAAAGTCGAGGATATTTTTTATTCAGGCCACGG  601

Query  733  AATGGAAGAAGGTCAGCAGGGTTCATTTAAAATGGATGCCAGCTAATTTTCCACAGAGCA  792
            ||||||||||||||||||||||||||||||||||||||||||||||||||||||||||||
Sbjct  602  AATGGAAGAAGGTCAGCAGGGTTCATTTAAAATGGATGCCAGCTAATTTTCCACAGAGCA  661

Query  793  ATGCTATGGAATACAAAATGTACTGACATTTTGTTTTCTTCTGaaaaaaaTCCTTGCTAA  852
            ||||||||||||||||||||||||||||||||||||||||||||||||||||||||||||
Sbjct  662  ATGCTATGGAATACAAAATGTACTGACATTTTGTTTTCTTCTGAAAAAAATCCTTGCTAA  721

Query  853  ATGTACTCTGTTGAAAATCCCTGTGTTGTCAATGTTCTCAGTTGTAACAATGTTGTAAAT  912
            ||||||||||||||||||||||||||||||||||||||||||||||||||||||||||||
Sbjct  722  ATGTACTCTGTTGAAAATCCCTGTGTTGTCAATGTTCTCAGTTGTAACAATGTTGTAAAT  781

Query  913  GTTCAATTTGTTGaaaattaaaaaatctaaaaataaa  949
            |||||||||||||||||||||||||||||||||||||
```

Figure E.2: Alignment and confirmation of pcDNA3.1 (+) ZEO construct.

Assessing the sequence on Blast confirms that the insert contained in the construct is effectively NMU cDNA and that it is inserted in the right orientation in pcDNA3.1(+) ZEO 'Query' here represents the sequence read obtained after the sample of the plasmid was sent for sequencing at Eurofins, while 'Subject' represents the expected sequence for NmU mRNA.

F. Stable knockdown of NmU by shRNAs

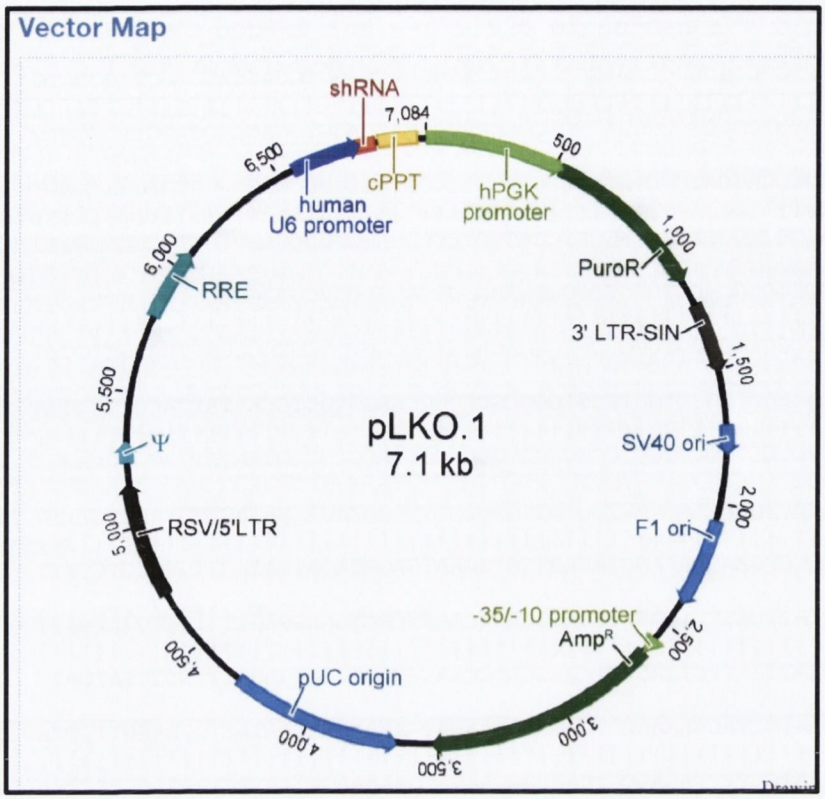

Figure F.1: Vector map for plasmid contruct used for NmU knockdown.

The pLKO.1 HIV-based lentiviral vector allows for transient and stable transfection of shRNA. Stable cell lines can be selected using the puromycin selectable marker. pLKO.1 Vector Information from Open Biosystems (Thermofischer) technical manual

G. Survival analysis of miR-630 in ER+ breast cancer

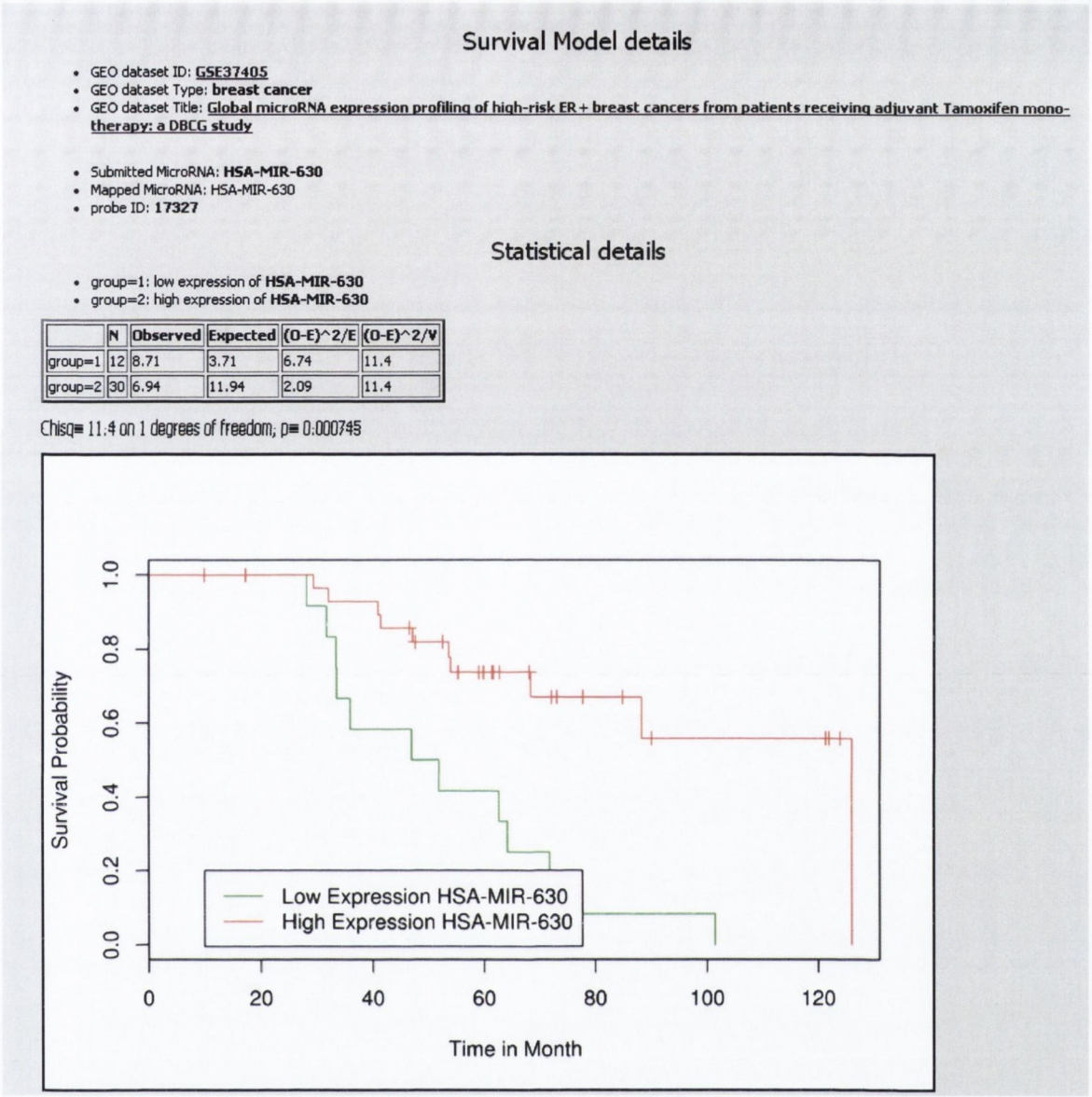

	N	Observed	Expected	(O-E)^2/E	(O-E)^2/V
group=1	12	8.71	3.71	6.74	11.4
group=2	30	6.94	11.94	2.09	11.4

Figure G.1: Survival analysis of miR-630 in ER+ breast cancer.

The online software, MIRUMIR, was used to assess the expression of miR-630 in association with survival in ER+ breast cancer patients receiving adjuvant tomoxifen treatment.

APPENDIX II

Publications, Achievements & Presentations

A. Publications

Research Articles

Exosomes from triple-negative breast cancer cells can transfer phenotypic traits representing their cells of origin to secondary cells
O'Brien K, Rani S, **Corcoran C**, Wallace R, Hughes L, Friel AM, McDonnell S, Crown J, Radomski MW, O'Driscoll L.
European Journal of Cance. 2013 May;49(8):1845-59.

Docetaxel-resistance in prostate cancer: evaluating associated phenotypic changes and potential for resistance transfer via exosomes
Corcoran C, Rani S, O'Brien K, O'Neill A, Prencipe M, Sheikh R, Webb G, McDermott R, Watson W, Crown J, O'Driscoll L
PLoS One. 2012;7(12):e50999. Epub 2012 Dec 10.

The use of LC-MS to identify differentially expressed proteins in docetaxel-resistant prostate cancer cell lines.
O'Connell K, Prencipe M, O'Neill A, **Corcoran C**, Rani S, Henry M, Dowling P, Meleady P, O'Driscoll L, Watson W, O'Connor R.
Proteomics. 2012 Jul;12(13):2115-26.

Characterisation and Manipulation of Docetaxel-resistant Prostate Cancer Cell lines
O'Neill A, Prencipe M, Dowling C, Fan Y, Mulrane L, Gallagher W, O'Connor D, O'Connor R, Devery A, **Corcoran C**, Rani S, O'Driscoll L, Fitzpatrick JM, Watson W.
Mol Cancer. 2011 Oct 7;10:126.

Reviews

Intracellular and extracellular microRNAs in breast cancer.
Corcoran C, Friel AM, Duffy MJ, Crown J, O'Driscoll L
Clin Chem. 2011 Jan;57(1):18-32. Epub 2010 Nov 8.

Relevance of circulating tumour cells, extracellular nucleic acids, and exosomes in breast cancer.
Friel AM, **Corcoran C,** Crown J, O'Driscoll L.
Breast Cancer Res Treat. 2010 Oct;123(3):613-25. Epub 2010 Jun 15.

Book Chapters

Isolation of Exosomes for Subsequent mRNA, MicroRNA, and Protein Profiling.
Rani S, O'Brien K, Kelleher FC, **Corcoran C**, Germano S, Radomski MW, Crown J, O'Driscoll L. *Methods Mol Biol.* 2011;784:181-95.

Published abstracts

The potential of miR-630, an IGF1R regulator, as a predictive biomarker for HER2-targeted drugs.
Corcoran C, Rani S, Breslin S, Ghobrial IM, Crown J and O'Driscoll L
J Clin Oncol 31, 2013 (suppl; abstr 620)

Assessment of neratinib-resistance and cross-resistance in HER2-overexpressing breast cancer cells. Breslin S, **Corcoran C**, Rani S, Crown J, O'Driscoll L
J Clin Oncol 31, 2013 (suppl; abstr e11520)

Generation and Characterisation of Neratinib-resistant Breast Cancer Cell Line Variants.
Breslin S, Rani S, **Corcoran C**, O'Brien K, O'Driscoll L
European Journal of Cancer 2012, 48:32-33.

The use of in vitro cell line models to investigate Docetaxel resistance in Prostate Cancer.
Corcoran C, Rani S, O'Brien K, Crown J, O'Driscoll L
Annual meeting of the Biomedical Sciences section of RAMI 2011; Trinity College Dublin. Irish Journal of Medical Science; 2011: S287.

Establishing and Characterising New in Vitro Models of Docetaxel-resistance in Prostate Cancer.
Corcoran C, Rani S, O'Brien K, Crown J, O'Driscoll L
European Journal of Cancer 2011, 47:S489.

Neuromedin U: A potential predictive biomarker for HER2-targeted drugs.
Rani S, Germano S, Madden SF, **Corcoran C**, Breslin S, O'Brien NA, McDermott M, Browne B, O'Donovan N, Crown J O'Driscoll L
Journal of Clinical Oncology 2012 30 (15)

Submitted papers

miR-630 targets IGF1R to regulate response to HER-targeting drugs and overall cancer cell progression in HER2 overexpressing breast cancer
Corcoran C, Rani S, Breslin S, Ghobrial IM, Crown J and O'Driscoll L
Submitted and under review

Neuromedin U: a potential predictive biomarker and a therapeutic target to overcome resistance to HER-tyrosine kinase inhibitors
Rani S , **Corcoran C**$^{\Omega}$, Germano S$^{\Omega}$, Madden SF, Breslin S, Mc Dermott MS, Browne BC , O'Donovan N, Crown J, O'Driscoll L
$^{\Omega}$ *authors contributed equally*
Submitted and under review

RTKs and drug-resistance –Development and characterisation of *in vitro* models of resistance to RTK inhibitors
Corcoran C, O'Driscoll L
Methods Mol Biol, expected publication date 2014

Manuscript in preparation

miR-34a is an intracellular and exosomal predictive biomarker for response to docetaxel with clinical relevance to prostate cancer progression
Corcoran C, Rani S, Prencipe M, O'Neill A, Watson W, O'Driscoll L
Manuscript in preparation

B. Awards, Honors & Other

- ***June 2013:*** Travel award to attend and present research at the American Society for Clinical Oncology (ASCO) Annual meeting, Chicago, Illinois (May 31st –June 4th , 2013)

- ***Sept 2012-Present:*** Peer reviewer for Clinical Chemistry

- ***March 2012: :*** Awarded Travel grant from Trinity College for poster presentation at the 103rd Annual meeting for the American Association of Cancer Research, Chicago, Illinois (March 31st –April 4th , 2012)

- ***January 2012:*** Awarded "Best Oral Presentation" at the Trinity College Post Graduate Research Symposium for presentation titled 'Intracellular and extracellular biomarkers predictive of response to anti-cancer treatments in breast and prostate cancer'

- ***December 2011:*** Awarded Science Foundation Ireland's Short Term Travel Fellowship award to conduct research at the Dana Farber Cancer Institute, Harvard.

- ***June 2011:*** Shortlisted for the Donegan Medal at the annual meeting of the Biomedical Sciences section of the Royal Academy of Medicine in Ireland (RAMI) for oral presentation titled 'The use of in vitro cell line models to investigate Docetaxel-resistance in Prostate Cancer' (June 22nd 2011)

- ***April 2011:*** Awarded 'Best Poster Prize' at the All Ireland Schools of Pharmacy Conference 2011 for poster titled 'The pursuit of miRNAs as minimally-invasive biomarkers predictive of response to anti-cancer treatment for HER2 positive breast cancer' (April 18th -19th, 2011)

- ***March 2011:*** Travel award to attend and present research at the 102nd Annual meeting for the American Association of Cancer Research, Orlando, Florida (April 2nd-6th, 2011)

- ***October 2010:*** Awarded registration fee waiver for poster presentation at the EMBO/EMBL Symposium: Non-Coding Genome Heidelberg, Germany (October 12th-16th, 2010)

- ***Sept 2010:*** Awarded Travel grant from Graduate Studies TCD to attend EMBO/EMBL Symposium: Non-Coding Genome, Heidelberg, Germany (October 12th-16th, 2010)

C. International and National conference presentations

Oral presentations

Corcoran C
Docetaxel-resistance in Prostate Cancer – A role for extracellular vesicles?
WG4: Diagnostic & therapeutic potential of microvesicles & exosomes
1st meeting for the European Network for Microvesicles and Exosomes in Health and Disease, 17th May 2013, Trinity Biomedical Sciences Institute, Dublin.

Corcoran C, O'Brien K, O'Driscoll L
MicroRNAs as Biomarkers & Therapeutics Targets for Cancer
Dublin microRNA Day, 29th May 2013, O'Callaghan Stephen's Green Hotel, 1-5 Harcourt, Dublin

Corcoran C, Rani S, O'Brien A, O'Neill A, O'Brien K, Prencipe M, Crown J, Watson W, O'Driscoll L
Exosomes – potential mediators of prostate cancer progression?
Irish Association for Cancer Research Annual meeting
Culloden Hotel, Belfast (February 29, March 1-2, 2012)

Corcoran C
Intracellular and extracellular biomarkers predictive of response to anti-cancer treatments in breast cancer and prostate cancer
Post Graduate Research Symposium 2012
Trinity College Dublin (January 12, 2012)

Corcoran C, Rani S, O'Brien K, Crown J, O'Driscoll L
The use of in vitro cell line models to investigate Docetaxel-resistance in Prostate Cancer
Annual meeting of the Biomedical Sciences section of RAMI 2011,
Trinity College Dublin (June 22, 2011)

Corcoran C, Rani S, O'Brien K, O'Neill A, Watson W, O'Driscoll L
Investigating the mechanisms of Docetaxel-resistance in prostate cancer
All Ireland Schools of Pharmacy Conference 2011,
Royal College of Surgeons, Dublin (April 18-19, 2011)

Poster Presentations

Corcoran C, Rani S, Breslin S, Ghobrial IM, Crown J and O'Driscoll L
The potential of miR-630, an IGF1R regulator, as a predictive biomarker for HER2-targeted drugs
American Society of Clinical Oncology Annual Meeding, McCormick Place Convention Centre, Chicago, Illinois (May 31-June 4, 2013)

Corcoran C, Rani S, O'Brien K, O'Neill A, Prencipe M, Watson W, Crown J, O'Driscoll L
Exosomes – potential regulators and biomarkers of prostate cancer progression
International Society for Extracellular Vesicles Annual Scientific Meeting 2012, Gothenburg, Sweden (April 18-21 2012)

Corcoran C, Rani S, O'Brien A, O'Neill A, O'Brien K, Prencipe M, Crown J, Watson W, O'Driscoll L
The relevance of exosome secretion in prostate cancer and their potential to confer docetaxel-resistance to secondary cells
103rd Annual Meeting of the American Association for Cancer Research
McCormick Place Convention Centre, Chicago, Illinois (March 31-April 4, 2012)

Corcoran C, Rani S, O'Brien K, O'Neill A, Prencipe M, Ray McDermott, Watson W, Crown J, O'Driscoll L
Prostate cancer progression: Do Exosomes play a role?
All Ireland Schools of Pharmacy Conference 2012,
University College Cork (April 1-2, 2012)

Corcoran C, Rani S, O'Brien K, Crown J, O'Driscoll L
Establishing and Characterising New in Vitro models of Docetaxel-resistance in Prostate Cancer
The European Multidisciplinary Cancer Congress, Stockholm (Sept 23-27, 2011)

Corcoran C, Rani S, Browne B, Crown J, O'Donovan N, O'Driscoll L
The pursuit of miRNAs as minimally-invasive biomarkers predictive of response to anti-cancer treatment for HER2 positive breast cancer
All Ireland Schools of Pharmacy Conference 2011,
Royal College of Surgeons, Dublin (April 18-19, 2011)

Corcoran C, Rani S, Browne B, Crown J, O'Donovan N, O'Driscoll L
Extracellular miRNAs have potential as minimally-invasive biomarkers for predicting response to HER2-targeted agents, including Trastuzumab, as used in breast cancer
102nd Annual Meeting of the AACR
Orlando Convention Centre, Florida (April 2-6, 2011)

Corcoran C, Rani S, Browne B, Crown J, O'Donovan N, O'Driscoll L
Identification of intracellular and extracellular miRNAs in SKBR3 and its Herceptin-resistant variant with potential as predictive biomarkers for breast cancer
EMBO|EMBL Symposium: Non-Coding Genome
EMBL Advanced Training Centre, Heidelberg, Germany (October 13-16, 2010)